TOWARDS TARGETED AND TUNABLE RELEASE OF HYDROGEN SULFIDE

A THESIS

SUBMITTED IN PARTIAL FULFILMENT OF THE

REQUIREMENTS

OF THE DEGREE OF

DOCTOR OF PHILOSOPHY

BY

PREETI CHAUHAN

20143331

INDIAN INSTITUTE OF SCIENCE EDUCATION AND RESEARCH PUNE – 411 008

2019

Dedicated to…

My Family

INDIAN INSTITUTE OF SCIENCE EDUCATION AND RESEARCH (IISER), PUNE
(An Autonomous Institution, Ministry of Human Resource Development, Govt. of India)
900 NCL Innovation Park Dr Homi Bhabha Road Pune 411008

Harinath Chakrapani, Ph.D.
Associate Professor – Chemistry
www.iiserpune.ac.in/~harinath/

CERTIFICATE

Certified that, the work incorporated in the thesis entitled, "***Towards Targeted and Tunable Release of Hydrogen Sulfide***" submitted by ***Preeti Chauhan*** was carried out by the candidate, under my supervision. The work presented here or any part of it has not been included in any other thesis submitted previously for the award of any degree or diploma from any other University or institution.

Date: 21st Dec, 2019 **Dr. Harinath Chakrapani**
Pune (MH), India.

DECLARATION

I declare that this written submission represents my ideas in my own words and where others' ideas have been included; I have adequately cited and referenced the original sources. I also declare that I have adhered to all principles of academic honesty and integrity and have not misrepresented or fabricated or falsified any idea/data/fact/source in my submission. I understand that violation of the above will be cause for disciplinary action by the Institute and can also evoke penal action from the sources which have thus not been properly cited or from whom proper permission has not been taken when needed.

Date: 21st Dec, 2019 **Preeti Chauhan**

Pune (MH), India. **20143331**

Table of Contents

CHAPTER 2: Esterase activated COS/H_2S donors

General remarks

- ^{1}H NMR spectra were recorded on JEOL ECX 400 MHz spectrometer using tetramethylsilane (TMS) as an internal standard. Chemical shifts are expressed in ppm units downfield to TMS.
- ^{13}C NMR spectra were recorded on JEOL ECX 100 MHz spectrometer.
- Mass spectra were obtained using HRMS-ESI-Q-Time of Flight LC-MS (Synapt G2, Waters) or MALDI TOF/TOF Analyser (Applied Biosystems 4800 Plus).
- FT-IR spectra were obtained using NICOLET 6700 FT-IR spectrophotometer as KBr disc or Bruker Alpha-FT-IR spectrometer and reported in cm^{-1}.
- All reactions were monitored by Thin-Layer Chromatography carried out on precoated Merck silica plates (F254, 0.25 mm thickness); compounds were visualized by UV light.
- All reactions were carried out under nitrogen or argon atmosphere with freshly dried solvents under anhydrous conditions and yields refer to chromatographically homogenous materials unless otherwise stated.
- All evaporators were carried out under reduced pressure on Büchi and Heildoph rotary evaporator below 45 °C unless otherwise specified.
- Silica gel (60-120) and (100-200) mesh were used for column chromatography.
- Materials were obtained from commercial suppliers and were used without further purification.
- Semi-preparative HPLC purification was performed using high performance liquid chromatography (HPLC), Dionex ICS-3000 model and preparative HPLC with C-18 preparative column (21.2 mm × 250 mm, 10 μm; Kromasil C18).
- HPLC analysis data was obtained using Agilent Technologies 1260 Infinity, C18 reversed phase column (4.6 mm × 250 mm, 5 μm).
- Spectrophotometric and fluorometric measurements were performed using Thermo Scientific Varioskan microwell plate reader.
- Scheme, Figure and Compound numbers in abstract and individual chapters are different.

Abbreviations

AAT - Asp aminotransferase

ACN – Acetonitrile

AcOH – Acetic acid

ADT-OH - 5-(4-hydroxyphenyl)-3H-1,2-dithiole-3-thione

AOAA - Aminooxyacetic acid

ARE - Antioxidant response element

ATP – Adenosine triphosphate

au – Arbitrary unit

BrdU - bromodeoxyuridine

bs – Broad singlet

^{t}BuOH – Tertiary-butanol

CA – Carbonic Anhydrase

Calcd – Calculated

CBS – Cystathionine-β-Synthase

$CDCl_3$ – Chloroform-D

$CHCl_3$ – Chloroform

Ctrl – Control

CO – Carbon Monoxide

COS – Carbonyl Sulfide

CSE - Cystathionine-γ-Lyase

Cys – Cysteine

DAS - Diallyl sulfide

DADS - Diallyl disulphide

DATS - Diallyl trisulfide

DBU - 1,8-Diazabicyclo[5.4.0]undec-7-ene

dd – Doublet of doublet

DCM – Dichloromethane

DMAP – *N*, *N*-Dimethylaminopyridine

DMEM – Dulbecco's Modified Eagle's Medium

DMF – *N*, *N*'-Dimethyl formamide

DMSO – Dimethyl sulfoxide

DNA – Deoxyribonucleic acid

Dn-N_3 – Dansyl azide

Dn-NH_2 – Dansyl amine

D_2O – Deuterium Oxide

DPBS – Dulbecco's Phosphate-Buffered Saline

DPPA - Diphenyl phosphoryl azide

dt – Doublet of triplet

DT-D – DT-Diaphorase

DTPA – Diethylene triamine pentaacetic acid

δ – Delta (in ppm)

E. coli – *Escherichia coli*

EDC.HCl - 1-Ethyl-3-(3-dimethylaminopropyl)carbodiimide Hydrochloride

eq. – Equivalents

ES – Esterase

ESI – Electron spray ionization

ESIPT - Excited-State Intramolecular Proton Transfer

Et_3N – Triethylamine

EtOH – Ethanol

EtOAc – Ethyl acetate

Et_2O – Diethyl ether

FAD – Flavin-adenine-dinucleotide

FBS – Fetal bovine serum

$FeCl_3$ – Ferric Chloride

FMN – Flavin-mononucleotide

g – Gram

GIT - Gastrointestinal tract

GSH – Glutathione

GS-T – Glutathione S-Transferase

h – Hours

HCl – Hydrochloric acid

HEPES - 2-[4-(2-hydroxyethyl)piperazin-1-yl]ethanesulfonic acid

H_2O – Water

H_2O_2 – Hydrogen peroxide

H_2S – Hydrogen Sulfide

HNO_3 – Nitric acid

HPLC – High performance liquid chromatography

HRMS – High-resolution mass spectrometry

Hz – Hertz

IBD - Inflammatory bowel disease

IC_{50} – Half maximal inhibitory concentration

IR – Infrared

J – Coupling constant

KEAP 1 - Kelch-like ECH- associated protein 1

KCl – Potassium Chloride

K_2CO_3 – Potassium carbonate

λ_{ex} – Excitation wavelength

λ_{em} – Emission wavelength

LDH – Lactate Dehydrogenase

LPS – Lipopolysaccharides

m – Multiplet

MALDI – Matrix-Assisted Laser Desorption Ionization

Me – Methyl

MeOH – Methanol

mg – Milligram

Min. – Minutes

MHz – Megahertz

mL – Millilitre

mM – Millimolar

mmol – Millimoles

m.p. – Melting point

MPO - Myeloperoxidase activity

MS – Mass spectrum

MSBT - Methyl sulfonyl benzathiazole

3-MST – 3-Mercaptopyruvate sulfur transferase

MTT – 3-(4,5-Dimethylthiazol-2-yl)-2,5-diphenyltetrazolium bromide

MW – Molecular weight

m/z – Mass to Charge ratio

µM – Micromolar

$NaBH_4$ – Sodium borohydride

NAC – *N*-acetyl cysteine

NADPH – Reduced nicotinamide-adenine-dinucleotide phosphate

NaH – Sodium hydride

$NaHCO_3$ – Sodium bicarbonate

NaI – Sodium iodide

NaOCl – Sodium hypochlorite

NaSH - Sodium hydrosulfide

Na_2S – Sodium sulfide

Na_2SO_4 – Sodium sulphate

$Na_2S_2O_5$ – Sodium metabisulfite

NBS – *N*-Bromosuccinimide

NH_4Cl – Ammonium chloride

NMR – Nuclear magnetic resonances

NO – Nitric oxide

NQO1 – NAD(P)H quinone oxidoreductase 1

nM – Nanomolar

NRF2 - nuclear factor erythroid 2-related factor 2

NSAID – Non-Steroidal Anti-inflammatory Drug

NTA - *N*-thiocarboxyanhydride

NTR – Nitroreductase

$^{\bullet}OH$ – Hydroxyl radical

$O_2^{\bullet-}$ – Superoxide radical

$ONOO^-$ – Peroxynitrite

PAG – Propargylglycine

PBS – Phosphate buffer saline

PBr_3 – Phosphorous tribromide

PBS – Phosphate buffered saline

PD - Parkinson's disease

$Pb(OAc)_2$ – Lead acetate

PbS – Lead sulfide

$Pd(dppf)Cl_2$ – [1,1′-Bis(diphenylphosphino)ferrocene]dichloropalladium(II)

pH – Potential of hydrogen

Ph – Phenyl

PPh_3 – Triphenyl phosphine

Py – Pyridine

ppm – Parts per million

% – Per cent

RNS − Reactive nitrogen species

ROS – Reactive oxygen species

RPMI Medium – Roswell Park Memorial Institute Medium

RT – Room temperature

rt – Retention Time

Ru(II) – Ruthenium (II)

s – Singlet

SiO_2 – Silica

SUR1 - sulfonylurea receptor 1

t – Triplet

TBDMSCl - *tert*-butyldimethylsilyl chloride

TBHP – *tert*-butyl hydroperoxide

TEA – Triethylamine

TFA – Trifluoroacetic acid

THF – Tetrahydrofuran

TLC – Thin layer chromatography

TMS – Tetramethylsilane

TST - Thiosulfate sulfurtransferase

UV – ultraviolet

µg – Microgram

µmol– Micromolar

µL – Microliter

µm – Micrometre

WT- MEF – Wild type mouse embryonic fibroblast cells

$Zn(OAc)_2$ – Zinc Acetate

Acknowledgements

Life of a PhD Scholar is a roller coaster ride. It has its own ups and downs. But, it's the support of our loved ones which help us through this journey.

First and foremost, I want to express my deepest gratitude to my supervisor Dr. Harinath Chakrapani (Hari). It was only because of his constant support, motivation, counselling and his faith in me that helped me to achieve this milestone. I find myself fortunate to be a part of his group. Thank you for inculcating in me the best of qualities that are required to be a good researcher. Thank you for bringing out the best in me and teaching me the most important lessons of life.

I would like to thank my RAC members Dr. Nithyanandhan (NCL Pune), Dr. Amrita Hazra and Dr. Jeet Kalia (IISER Bhopal) for their important suggestions, ideas and valuable feedback during RAC meetings. A special thanks to my lab mates: - Dr. Satish, Dr. Dharma, Dr. Kavita, Dr. Vinayak, Dr. Kundan, Dr. Ravikumar, Ajay, Amogh, Prerona, Pooja, Laxman, Anand, Farhan (Farah Ben), Gaurav, Suman, Swetha, Sushma, Aswin, MJ, Harshit, Suraj, Minhaj, Dr. Amol, Sharath, Abhishek, Komal, Dr. Viraj. Thank you all for your encouragement, support and patience. I want to thank Vinayak, my mentor, for teaching me the basics of research and basics of being a good researcher. I met people during my PhD who soon became the most important people in my life. I can never forget the time that I spent with these amazing people. Ajay (my lunch partner) and his famous jokes, Sharath, a very close friend, and my support system, I will always remember the time that I spent with you guys. Ravi and Kundan are more like my brothers – always ready to help. A special thanks to Kavita didi for being an elder sister to me. A big thanks to our seniors for creating a healthy and happy atmosphere in lab. I will always cherish the bitter sweet experiences that I had with Amogh. I will miss the long discussions on innumerable topics and subjects with Prerona (my chai partner), that soon became the most fun part of the day. She is supportive, helpful and a science enthusiast. It was fun discussing chemistry and other ascpects of life with her. I have earned a friend for life in her. I feel lucky to have juniors like Anand (calm and composed), Laxman (enjoy research), Pooja (her laughter), Suman (great ideas), Farhan (his jokes), Gaurav (trips), Harshit (GOT talks), Minhaj (sweetness).

I owe a special thanks to my friends Sucheta and Aakanksha for being by my side. You guys are special. Memorable moments, late night movies, theatre, weekly trip to the coffee shop, these moments have a special place in my heart. I would also like to thank Sugandha, for coming back into my life and making the last few months of my PhD, even more memorable. The days spent with you will be remembered for the lifetime.

Towards the end, I come to thank people who make my life worth living. I am nothing without you; my husband, my life partner, Yatharth Dixit. His constant encouragement, love, support and unwavering belief has helped me to complete this long journey. Thank you Yatharth, for helping me through all my troubles, bearing my tantrums, for being my joy and my guide in life. I also want to thank my in laws – 'you're the coolest mom and dad in laws in the world. Thank you for everything. Thank you Cheena and Siddharth bhaiya for all the fun and support. You guys are the best company to spend time with.

I also want to thank my brothers – Dhruv Bhaiya, Kuldeep Bhaiya and Rahul for their constant encouragement; Pink bhabhi and Bhavna bhabhi for always being there for me. Thank you Disha and Trisha, the cutest members of our family, for coming into our lives.

Last but not the least, I want to thank my mummy and papa for always being by my side. No words can ever describe your endless love and blessings that has helped me in the toughest times. It was their patience, trust, sacrifices and love that kept me going.

Preeti Chauhan

****

ABSTRACT

Hydrogen sulfide (H_2S) has emerged as an important gaseous signaling molecule with diverse physiological roles. Endogenously produced H_2S regulates the homeostasis of various physiological processes such as cardiovascular, neuronal, renal, gastrointestinal etc. Due to its increased physiological relevance, the role of H_2S as a potential therapeutic agent has been extensively studied. For example, diminished levels of H_2S are associated with various pathological conditions such as inflammation, gastrointestinal disorders, cardiovascular disorders etc. Exogenous administration of H_2S under these conditions has shown beneficial effects. However, the therapeutics of H_2S largely depends on the concentration and the rate at which it is produced. Therefore, methods for achieving controlled generation and dissipation of H_2S assume importance. Also, modulating the rate of H_2S release is needed for better understanding its implications in a diseased state. Due to its gaseous nature, reliable intracellular enhancement of H_2S is challenging. Although numerous methodologies for H_2S delivery have been reported in the past, but they suffer from limitations such as lack of specificity, no structural handle to tune the rate of release and lack of well-defined negative controls. Here we describe synthesis and evaluation of site directed and tunable H_2S donors with potential therapeutic applications.

Carbonyl sulfide (COS) is a naturally occurring gas that is hydrolyzed to H_2S by a widely prevalent enzyme, carbonic anhydrase (CA). This work focuses on controlled generation of COS in response to various biological stimuli. First, esterase activated COS/H_2S donors were designed and synthesized. In order to study the effects on rate of COS release after activation by esterase, carbonothioates (containing alcohols as leaving groups) and carbamothioates (with amines as leaving groups) were developed. The donors upon activation by esterase released COS which was further hydrolyzed to H_2S by CA. The rate of H_2S release from these donors was found to be dependent on the basicity of the amine. Due to the established roles of hydrogen sulfide as a protective agent against oxidative stress, the next class of COS donors were synthesized to be activated by elevated hydrogen peroxide, a condition that is frequently encountered during oxidative stress. In the presence of hydrogen peroxide these compounds decomposed and released H_2S. The half-lives of H_2S release from these donors ranged from 24 min to 208 min. Cellular assays revealed the anti-inflammatory effects of these donors by depletion of ROS levels. Gastrointestinal tract (GIT) is one of the most affected systems by excessive usage of non-steroidal anti-inflammatory drugs (NSAIDs) that cause erosions and further leads to peptic

ulcers. H_2S in conjugation with NSAIDs shows a remarkable increase in the efficacy of the drug and also protects the tissues against NSAID induced damage. Therefore, in the subsequent chapter, colon targeted delivery of H_2S and H_2S – NSAID hybrid donors was proposed. NAD(P)H quinone oxidoreductase (NQO1) is a 2e- reducing cytosolic enzyme over expressed in tissues such as colon epithelium which catalyzes the reduction of quinone to hydroquinone, thereby acting as a detoxifying agent in cells. Therefore, NQO1 activated H_2S and H_2S-NSAID hybrid donors were synthesized. The compounds were selective towards activation by NQO1 and showed cytoprotective effects against xenobiotic induced stress. The cytoprotective effects of H_2S were dependent on the extent of persulfidation induced by these donors. Thus, a correlation between the persulfidating ability and cytoprotective effects of the donors was established. Since the effects of H_2S were found to be dependent on the persulfidation ability of the donors, therefore, in the last chapter, NQO1 activated persulfide donors were synthesized and their cytoprotective effects were evaluated.

In summary, our results address important challenges associated with site directed delivery and tunable release of H_2S. Targeted delivery of H_2S, H_2S-NSAID hybrid and persulfide donors using the molecules that we have developed herein is possible.

CHAPTER 1: Introduction

1.1. Hydrogen Sulfide: History

The abundance of hydrogen sulfide (H_2S) in the prebiotic era points out to the likely involvement of this molecule towards the origin of life on earth. Samples obtained from Stanley Miller and Harold Urey's 1958 experiments supports the fact that H_2S originating from volcanic eruptions or other geothermal activities could be involved in the formation of basic sulfur containing molecules of life (such as cysteine or methionine).[1] It is presumed that the biomolecules such as RNA, lipid precursors or protein may have originated from cyanosulfidic protometabolism (the involvement of hydrogen cyanide and hydrogen sulfide in the chemical reactions of prebiotic system). Also, it is plausible to prepare nucleic acid precursors from the reaction of hydrogen cyanide and H_2S on a metal centre in the presence of UV light.[2] Therefore, H_2S may have played a crucial role in the origin of early life forms on earth. However, H_2S over the centuries has been considered as a poisonous gas with corrosive nature. The earliest mention of H_2S goes back to 1713 where an Italian physician Bernardino Ramazzini, in his publication *De Morbis Artificum Diatribes* described that the painful eye inflammation in the eyes of workers cleaning cesspits was caused due to unknown acidic vapours (H_2S) originating from the source.[3] However, the discovery of H_2S is credited to the Swedish pharmacist Carl Wilhelm Scheele, when he generated H_2S while reacting FeS_2 with mineral acid and reported it as "sulfur air".[4-6]

H_2S endured the historical reputation of a poisonous gas until 1996 when Kimura and co-workers for the first time demonstrated that endogenously produced H_2S acts a neuromodulator.[7] Although the propitious role of H_2S in blood vessels had been known for some time, the molecular target responsible for the vasodilatory effects was first identified by Zhao *et.al*. in 2001. The activation of ATP sensitive potassium (K_{ATP}) channels by H_2S mediates the vasodilatory effects induced by this gaseous species.[8] Yet another serendipitous discovery was made by Blackstone *et.al.* in 2005 where they observed that exposing mice to subtoxic levels of H_2S (20-80 ppm) induces suspended animation like state by the reduction of energy expenditure. Remarkably, the effects observed were found to be completely reversible which spurred interest towards developing H_2S based therapeutics for the treatment of trauma patients.[5,6,9,10] These observations catalysed the burgeoning literature on the physiological roles of H_2S and its potential to act as a therapeutic agent in various disease states.[5,6,10-12]

1.2. Biosynthesis of H_2S

The biosynthesis pathways responsible for the production of H_2S have been known for several decades. L-cysteine is a common substrate for the production of H_2S across many bacterial species.[13,14] Also, reduction of thiosulfate by the action of bacterial thiosulfate reductase produces H_2S in bacteria.[15,16] In mammals, the production of H_2S is catalysed by the action of three enzymes – cystathionine β-synthase (CBS), cystathionine-γ-lyase (CSE) and 3-mercaptopyruvate sulfur transferase (3-MST).[6,10,12,15,17,18] CBS and CSE are pyridoxal-5'-phosphate (PLP) dependent enzymes which metabolize L-cysteine to produce H_2S via transsulfuration pathway.[5,6,10,12,19] Methionine obtained from dietary sources, is converted to homocysteine which is further condensed with serine to form cystathionine in the presence of CBS enzyme.[20-22] Cystathionine, thus formed, is converted to cysteine by CSE enzyme. Cysteine so obtained is used as a substrate for the production of H_2S by CBS and CSE enzymes. Cysteine alone or in combination with homocysteine acts a substrate for CBS which produces serine or cystathionine respectively along with H_2S. Cysteine and homocysteine also act as a substrate for CSE which produces H_2S. Two moles of homocysteine are condensed together by CSE to produce homolanthionine and H_2S.[23] Homocysteine can also be converted to α -ketobutyrate by CSE and release H_2S in the process. Yet another pathway of H_2S production requires the reaction of α-ketoglutarate with cysteine in the presence of Asp aminotransferase (AAT) to form 3-mercaptopyruvate which acts as a substrate for 3-MST enzyme. 3-MST gets persulfidated in the process of converting 3-mercaptopyruvate to pyruvate. The persulfide then reacts with another reductant (RSH) to form a disulfide (MST-SSR) and release H_2S (Figure 1.1).[24,25] 3-MST is reduced back to its original form by thioredoxin redox system.[26] CSE acts as a dominant source of H_2S in peripheral tissues whereas CBS is a major H_2S producing enzyme in brain. CBS and CSE are mostly located in the cytosol whereas 3-MST is found in both the cytosol and the mitochondria.[27]

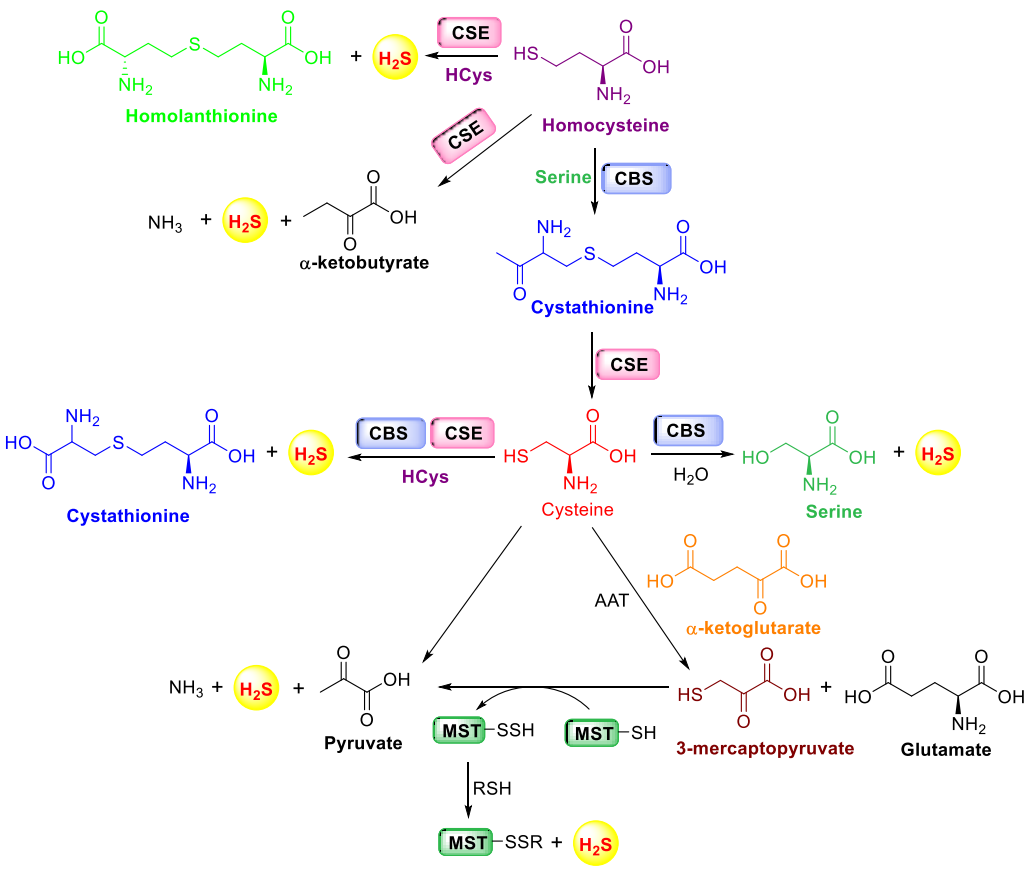

Figure 1.1. Biosynthetic pathways for H_2S production.

1.3. Physiological roles of H_2S

H_2S is involved in regulating the homeostasis of various systems in the human body which include neuronal, cardiovascular, respiratory, renal, gastrointestinal, liver and reproductive systems.[6,10] H_2S, being lipid soluble, can easily diffuse through the plasma membrane to reach its molecular targets either on the plasma membrane, cytosol or any intracellular organelle.[5] The ubiquitous nature of this gasotransmitter underscores the wide range of physiological roles played by H_2S (Figure 1.2). H_2S activates the ATP sensitive potassium (K_{ATP}) channels by persulfidating the Cys6 and Cys26 residues of the sulfonylurea receptor 1 (SUR1) subunit of K_{ATP} channel complex; thus leading to vasodilation.[10,28] H_2S also forms an important part of the anti-oxidant machinery of a cell and therefore helps in maintaining the redox homeostasis. H_2S induces persulfidation at Cys151 residue of Kelch-like ECH-associated protein 1 (KEAP1) which provokes the dissociation of nuclear factor erythroid 2-related factor 2 (NRF2) from KEAP1. This leads to nuclear translocation of NRF2 which binds to the antioxidant response element (ARE) and further increases the transcription of

genes involved in glutathione (GSH) synthesis. The subsequent increase in the GSH levels is likely responsible for the beneficial effects of H_2S.[29]

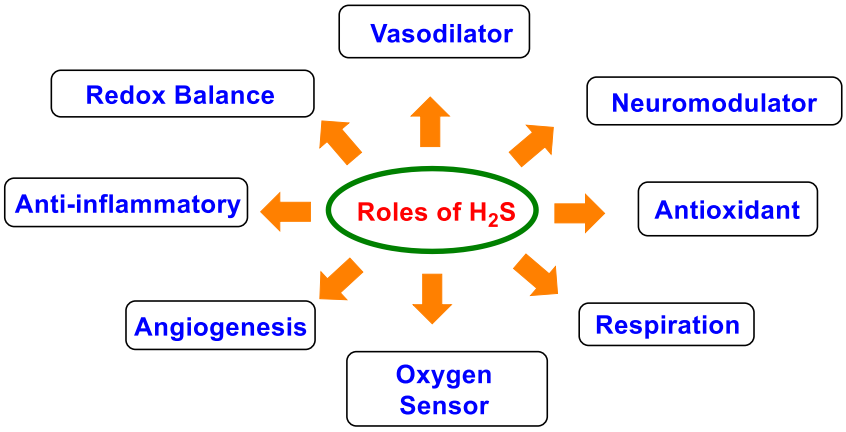

Figure 1.2. Physiological roles of H_2S.

Changes in the partial pressure of oxygen are managed differently by different tissues by altering the production or oxidation of H_2S. For example, dilation of systemic blood vessels by H_2S leads to angiogenesis which further increases the blood supply to hypoxic regions.[30] Also, under a state of hypoxia, the rate of mitochondrial H_2S oxidation is decreased which leads to enhancement in the H_2S levels. In vascular smooth muscle cells, CSE is translocated from cytosol to mitochondria where it uses L-cysteine to produce H_2S thereby increasing the concentration of H_2S in mitochondria. These are a few examples of the many physiological effects induced by H_2S. [31]

1.4. H_2S in disease and therapeutics:

An abnormal increase or decrease in the endogenously produced levels of H_2S is associated with various diseases such as cardiovascular, endocrinal, neurodegenerative disorders, gastrointestinal diseases, liver diseases, etc. Supplementing H_2S through an exogenous source under these conditions has proved to be beneficial. For example, Parkinson's disease (PD) is associated with elevated levels of reactive oxygen and nitrogen species. Parkin which is E3 ubiquitin ligase is known to ubiquitinase a wide range of substrates. High oxidative and nitrosative stress leads to nitrosylation of parkin. This post translational modification inactivates its catalytic activity which makes it a common cause in Parkinson's disease.[32,33] Snyder and group showed that exogenous administration of H_2S induces persulfidation of the cysteine residues of parkin which further stimulates its activity thereby acting as a neuroprotective agent (Figure 1.3). Beneficial roles of H_2S in rodent models of PD have also

been demonstrated previously.[34-36] This clearly states the importance of H_2S as a potential therapeutic agent.

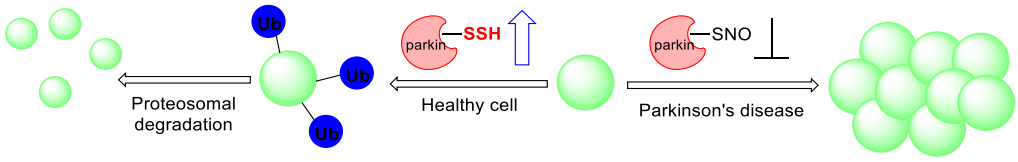

Figure 1.3. H_2S induced protein persulfidation in a model of Parkinson's disease.

H_2S plays an important role in diseases like ischemia reperfusion injury. A number of *in vitro* and *in vivo* studies have shown the beneficial effects of H_2S when administered at physiological concentrations.[37-40] Further, the therapeutic role of H_2S in gastrointestinal disorders cannot be ignored. H_2S-NSAID hybrids have been found to be effective towards treatment of various gastrointestinal diseases like Crohn's disease.[41] Thus, these reports pointing towards the potential therapeutic role of this highly reactive gaseous species quickly became the foundation for developing molecules for delivering H_2S.

1.5. H_2S as an anti-inflammatory agent

H_2S is a reducing agent and therefore it is not surprising to assume that H_2S can act as a potential anti-inflammatory agent. Interestingly, over the past few years H_2S has been observed to exert both pro and anti-inflammatory effects and thus can be put into the category of 'double edged' inflammatory mediators.[42] Although, there is still no clear consensus over the precise role H_2S in inflammatory signalling, recent observations suggest that the activity of H_2S in an inflammation model largely depended on the concentration and the rate of production of this gasotransmitter.[43-45] Sodium hydrosulfide (NaSH), which is an inorganic salt, when dissolved in water gives a bolus of H_2S that dissipates within seconds. On the other hand, endogenous production of H_2S in cells and tissues is relatively slow and sustained. It is very unlikely for cells to be exposed to such high concentrations of H_2S at any given time. Therefore, when NaSH was used as a source of sulfide, it was found to induce pro-inflammatory action as demonstrated by increased myeloperoxidase activity (MPO) and accumulated leukocytes presence in lungs and liver.[46] Also, DL-propargylglycine (PAG) which is an inhibitor of CSE revealed anti-inflammatory effects in an animal model of inflammation. Later in 2010, P.K. Moore and co-workers compared the effects of NaSH, fast releasing H_2S donor, with GYY4137, a slow releasing H_2S donor, in LPS induced inflammation in macrophages. Here they demonstrated opposite effects of the two donors

against inflammation. The apparent discrepancy is a testament to the pro- *versus* anti-inflammatory effects of H_2S (Figure 1.4).[43]

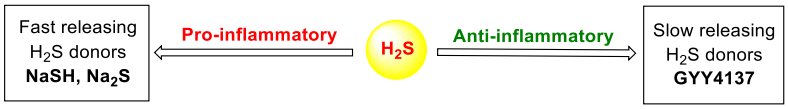

Figure 1.4. Pro and anti-inflammatory effects of H_2S.

H_2S can act through several pathways to resolve inflammation. It inhibits leukocyte adherence to the vascular endothelium at the site of injury thereby reducing edema formation. This is mainly due to its ability to induce vasodilation which therefore leads to the cytoprotective effects. H_2S suppresses the activity of NF-κB which is responsible for the production of pro-inflammatory cytokines. Resolving inflammation is also enhanced by promoting neutrophil apoptosis which further leads to their phagocytosis by macrophages. Also, H_2S can act as a source of ATP generation in many cells like gastrointestinal epithelial cells, by substituting oxygen in mitochondrial respiration. This contributes towards protecting and repairing tissues from injury (Figure 1.5).[42,44,47]

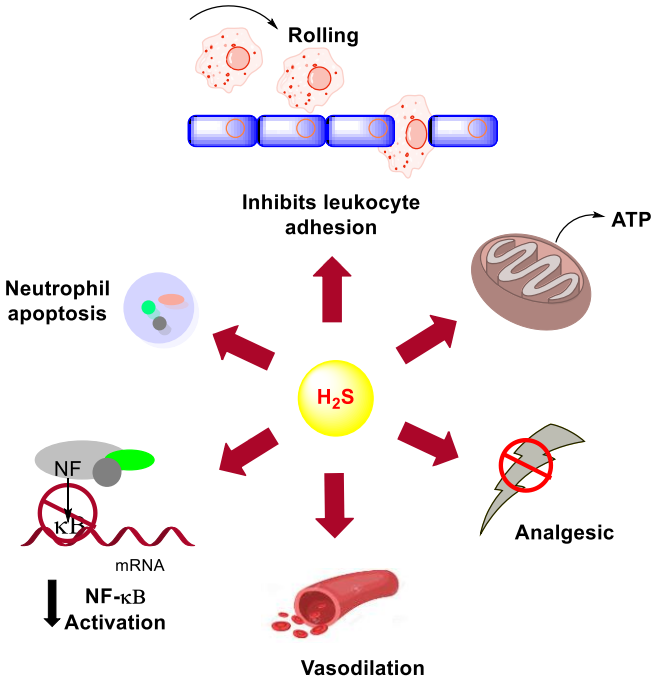

Figure 1.5. Anti-inflammatory and cytoprotective effects of H_2S.

The contribution of H_2S towards modulating inflammation has become clearer over the years but studies to elucidate the effects of this gaseous mediator and provide a better mechanistic understanding are limited due to lack of appropriate tools. GYY4137 although is a slow

releasing H_2S donor, provides limited scope for spatiotemporal control. Therefore, novel therapeutic agents are needed which could modulate the rate of H_2S release for exploiting the therapeutic value of H_2S against inflammation.

1.6. H_2S and cancer

The role of H_2S in cancer has again been very controversial. Literature reveals both pro and anti-cancer effects of H_2S. Several studies have indicated that H_2S producing enzymes (CBS or CSE) are over-expressed in cancer cells; therefore implying that endogenously produced H_2S is most likely related to pro-cancerous effects through regulation of mitochondrial bio-energetics, accelerating the process of cell cycle progression, angiogenesis or through other anti-apoptotic mechanisms. Szabo *et.al.* in 2007 showed that inhibiting enzymatic production of H_2S in colon cancer cells inhibits cell proliferation and therefore can act as a potential anti-cancer strategy.[48] In contrast, Moore and co-workers showed that cancer cells treated with relatively high concentrations of exogenously administered H_2S lead to uncontrolled intracellular acidification which suppressed the growth of cancer cells by inducing cell cycle arrest and thereby promoting apoptosis (Figure 1.6).[49,50] However higher concentration (higher µM range) of H_2S was required to observe these effects. This indicates that the effects of H_2S towards cancer are dependent on the concentration and rate of production. Therefore, designing a small molecule for cancer targeted delivery of H_2S with increased payload would be useful in analysing the therapeutic potential of the gas as an anti-cancer agent.[51]

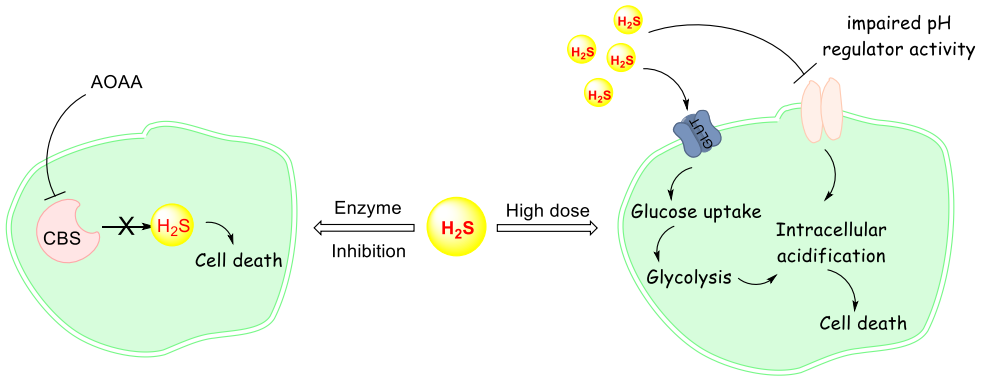

Figure 1.6. Role of H_2S in regulating tumor growth. Aminooxyacetic acid (AOAA) is CBS inhibitor.

1.7. H_2S in gastrointestinal disorders

The enteric bacteria or the microbiota present in the gut is one of the largest sources of H_2S within the human body which influences various physiological roles in the digestive tract.

Bacteria derived H_2S is responsible for mucosal defence and repair and contributes to the bioenergetics of the epithelial cells.[52,53] The use of drugs such as non-steroidal anti-inflammatory drugs (NSAIDs) can cause acute damage to the inner lining of the stomach which leads to gastric ulcers.[54] The expression of H_2S producing enzymes CBS and CSE have been found to be increased in the margins of the ulcers suggesting the potential role of H_2S in healing process. Therefore, it comes as no surprise that administration of H_2S donors such as NaSH have cytoprotective effects against gastric mucosal injury caused due to these exogenous or endogenous factors. The cytoprotective effects of H_2S are probably due to its ability to inhibit leukocyte adherence to the vascular endothelium which is a primary event in the induction of gastric mucosal damage by NSAIDs. H_2S being a vasodilator increases the blood flow thereby reducing the extent of injury caused by the NSAIDs.[55] The results obtained with H_2S-NSAID hybrids (developed in the recent past) are compelling in this regard as the extent of gastrointestinal damage is significantly reduced by these hybrid donors and are more effective than the parent NSAID. For example, molecules such as ATB-337 comprises of ADT-OH, a hydrolysis based H_2S donor coupled with diclofenac (NSAID) which was tested for its anti-inflammatory effects. The hybrid donor was found to be more effective towards inflammation compared to the parent NSAID. Similarly, ATB-429 which is a hybrid of ADT-OH with mesalamine (first in line therapy used for the treatment of colitis) was tested against animal model of colitis and was again found to be more effective towards the treatment of severe colitis compared to the parent drug.[56] Therefore designing molecules for tissue specific delivery of H_2S-NSAID hybrid donors for controlled generation of H_2S and NSAID would be desirable for therapeutic applications.

1.8. H_2S donors

Knowing the therapeutic importance of H_2S over the past few years, donors for achieving controlled and targeted delivery of H_2S are in development. Based on their ability to release H_2S, these donors can be divided into three categories – naturally occurring H_2S donors, hydrolysis based H_2S donors and triggerable H_2S donors.

1.8.1 Naturally occurring H_2S donors:

Organosulfur based polysulfides derived from allium plants such as garlic and onion provide a source for naturally occurring H_2S donors. These sources have been used for centuries for their beneficial health effects. Garlic has been known for its remarkable health effects such

as, consuming garlic reduces the risk of several cardiovascular disorders such as high blood pressure, high cholesterol etc. In 2007, Kraus and co-workers demonstrated that garlic crushing leads to the formation of a compound called allicin which then decomposes into diallyl based polysulfides which are diallyl sulfide (DAS), diallyl disulfide (DADS) and diallyl trisulfide (DATS) (Figure 1.7). These polysulfides upon reaction with biological thiols release H_2S.[57-59] However, uncontrolled release of H_2S from these donors and lack of appropriate negative controls limit their applicability in a biological system.

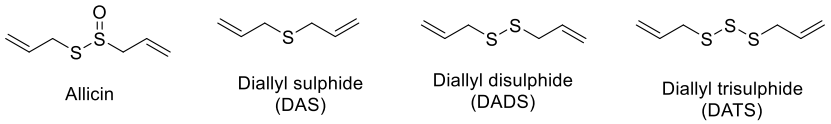

Figure 1.7. Structure of naturally occurring H_2S donors.

1.8.2. Hydrolysis based H_2S donors:

The most widely used source of H_2S for understanding its chemical biology are the inorganic salts – NaSH and Na_2S. These salts readily dissolve in water to form an aqueous solution of H_2S which rapidly dissipates within minutes. The salts release a bolus of H_2S which does not match the slow and consistent endogenous production of H_2S and therefore are not ideal for studying the biological effects of H_2S. Also, the high local concentration of H_2S produced from these donors could induce toxicity or might give ambiguous results. These donors are susceptible to auto-oxidation and therefore typically contain higher sulfur oxidation states such as polysulfides, thiosulfates or sulphites which limit their use for cellular studies.[60,61] Lawesson's reagent which is used as a sulfurization agent has also been used as a source of H_2S due to the slower rate of H_2S release obtained from this molecule. However, the compound is poorly soluble in aqueous solutions and lacks a handle for controlled release of H_2S, therefore cannot be used for site directed delivery of H_2S. Morpholin-4-ium (4-hydroxyphenyl)(morpholino)phosphinodithioate (GYY4137) is a derivative of lawesson's reagent which is widely used to achieve slow release of H_2S.[62] The molecule has good aqueous solubility and releases H_2S at a slow rate (1µmol/h) which has a half-life of days. The release of H_2S from GYY4137 is temperature and pH dependent. The molecule does not provide scope for controlled delivery as it lacks an appropriate structural handle. 5-(4-hydroxyphenyl)-3H-1,2-dithiole-3-thione (ADT-OH) which is a derivative of DTT, the core moiety responsible for H_2S production, also acts as a potent H_2S releasing agent (Figure 1.8). However, due to lack of appropriate negative controls, the results obtained using these

molecules could not be attributed to H_2S alone. Also, the mechanism of H_2S release from these donors still remains to be elucidated.[59,63]

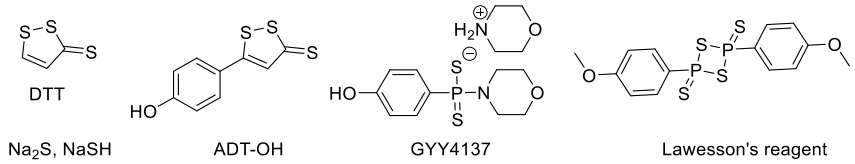

Figure 1.8. Structures of hydrolysis based H_2S donors

1.8.3. Triggerable donors

1.8.3.1. Thiol activated H_2S donors:

The concept of triggerable and controlled H_2S generation was first introduced by Ming Xian and group. They have reported a series of thiol activated H_2S donors which included *N*-(benzoylthio)benzamide derivatives which are activated by thiols to from perthiols and are further hydrolysed to cysteine.[64] Cysteine perthiols which are protected with an acyl group are also reported under this category.[65] Galardon and co-workers reported dithioperoxyanhydride based H_2S donors which are activated by thiols for controlled delivery of this gaseous species. Arylthioamides[66] and gem dithiols[67] are also reported in this category as thiol triggered H_2S donors (Figure 1.9).[68] Thiols are abundant in nearly all the cells, therefore, the donors mentioned above cannot be used for site directed delivery of H_2S. Also, thiols form a part of anti-oxidant machinery within cells, therefore using thiols as trigger may not be suitable for mechanistic understanding as the interpretation of the results obtained would be complicated.

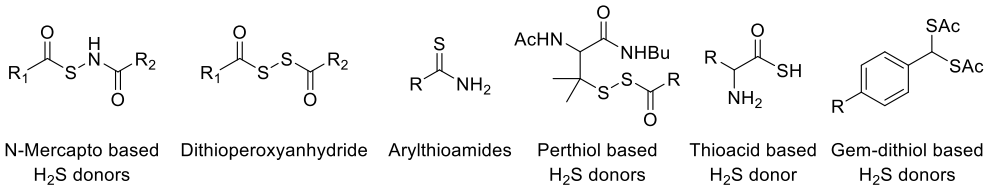

Figure 1.9. Representative structures of thiol activated H_2S donors.

1.8.3.2. Enzyme activated H_2S donors:

Enzyme activated delivery of H_2S has also been achieved in the recent past. Esterase activated H_2S donors were reported by Binghe Wang and co-workers where esterase trimethyl lock based thioacids were synthesized for the delivery of H_2S upon activation by

esterase (Figure 1.10a).[69] However, the ubiquitous nature of esterase enzyme limits its applicability. Species specific delivery of H_2S was reported for the first time by our lab wherein we reported bacteria targeted H_2S donors. The compounds get activated in the presence of nitroreductase enzyme (NTR), which is present in bacteria, to release H_2S(Figure 1.10b).[70] However, the donors do not provide a scope of modulating the rate of H_2S release.

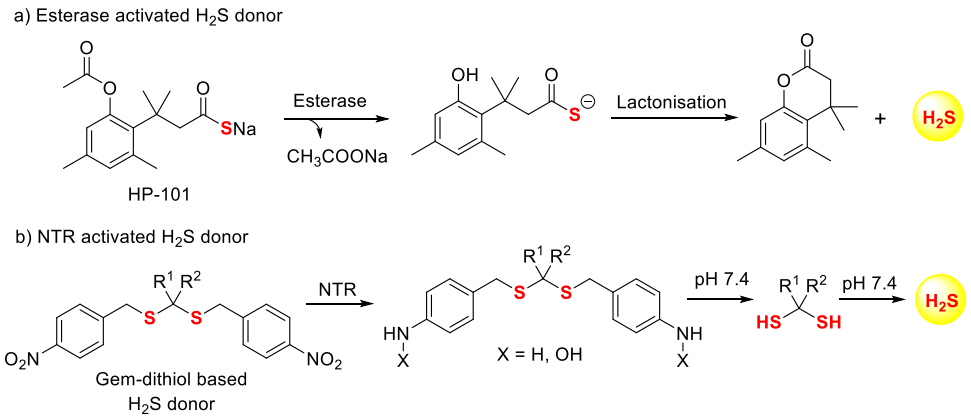

Figure 1.10. Examples of enzyme activated H_2S donors. a) Structure of HP-101 and mechanism of H_2S production upon activation by esterase enzyme. b) Representative structure of NTR activated H_2S donor and the mechanism of H_2S release upon activation by NTR.

1.8.3.3. pH controlled H_2S release:

Ming Xian and group have reported phosphonamidothioate-based pH controlled H_2S donors which is based on GYY4137 scaffold.[71] The compounds undergo intramolecular cyclisation to release H_2S in a pH dependent manner (Figure 1.11). But the compounds produce H_2S only under acidic conditions similar to GYY4137 and tuning the rate of H_2S release after activation could not be achieved from these donors.

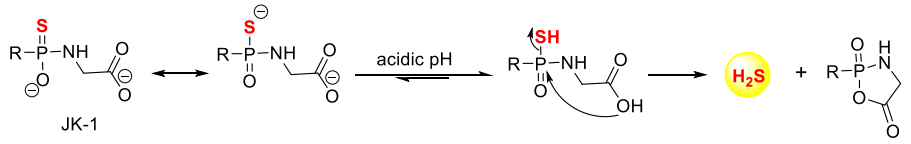

Figure 1.11. Representative example of pH sensitive H_2S donor and mechanism of release of H_2S.

1.8.3.4. Light activated H_2S donors:

Literature also includes the examples of light activated H_2S donors which fall under the category of triggerable H_2S donors. Gem dithiol based UV light activated H_2S donors are reported by Ming Xian and group. Also, ketoprofenate based UV light activated H_2S donors

have been reported by Nakagawa and co-workers. You and co-workers reported 1,3-diphenylbenzo[c]thiophene (DPBT) based donors which react with singlet oxygen to produce endoperoxide which further undergoes fragmentation to release H_2S. Connal and group have reported thio-benzaldehyde based H_2S donors which are activated in 355 nm light.[63] Pradeep Singh and co-workers have also reported Excited-State Intramolecular Proton Transfer (ESIPT) based H_2S donors by using *p*-hydroxyphenacyl as photo trigger which are activated with 410 nm light to produce H_2S. Most recent example includes Ru(II) based H_2S releasing agents which selectively get activated in the presence of red light (Figure 1.12).[72] Although the donors provide site directed delivery but the use of UV light limits their use in a cellular environment due to the toxicity induced by UV light. Also, use of light limits the scope of the donors from therapeutic point of view.

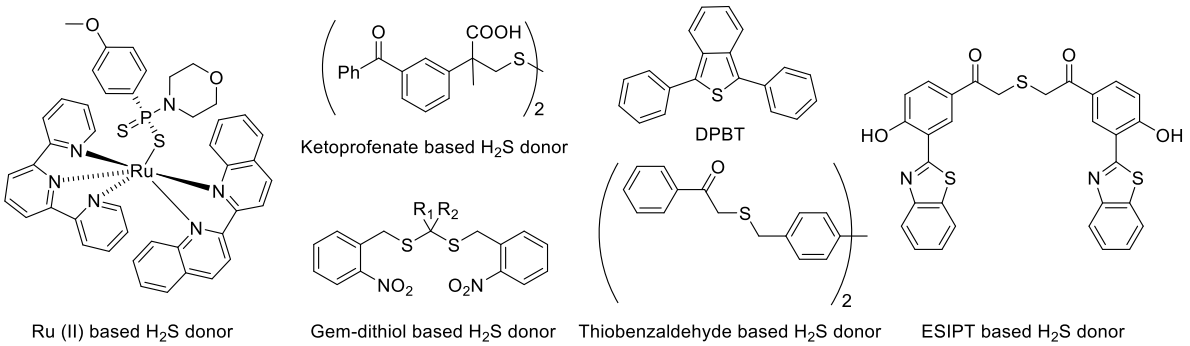

Figure 1.12. Structures of light activated H_2S donors.

1.9. Challenges:

The examples mentioned above clearly indicate that role of H_2S as a therapeutic agent largely depends on the concentration and the rate at which it is produced. Although a number of methodologies have been established for intracellular generation of H_2S; the aforementioned methods are associated with various limitations such as: a) non triggerable donors release H_2S spontaneously and provide limited scope to attain controlled release of this gaseous species; lack of well-defined negative controls complicate the conclusions drawn from the use of these donors and site directed delivery cannot be achieved using these scaffolds. b) Triggers like esterase and thiols which are ubiquitous in nature have been used to achieve controlled generation of H_2S and hence, cannot be utilized for site directed delivery. Also, the donors provide limited scope to modulate the rate of H_2S production. An ideal H_2S donor which has the capability to modulate the rate of production of H_2S once it is activated by an external stimulus is yet to be developed (Figure 1.13). Achieving site directed or tissue

specific delivery with simultaneous modulation of the rate of H_2S release is of utmost importance to understand the chemical biology of H_2S. Also, achieving targeted delivery of H_2S-NSAID hybrids would assume importance from a therapeutic and mechanistic stand point.

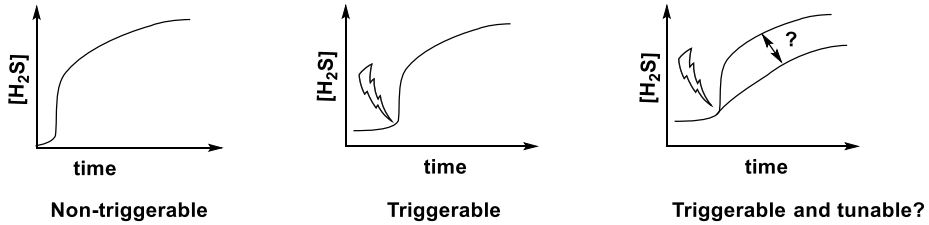

Figure 1.13. Categories of H_2S donors

1.10. Site directed delivery of H_2S

H_2S regulates the cellular homeostasis by maintaining the redox balance of a cell. However, under pathological conditions the redox balance of a cell is disturbed which leads to an increase in the levels of reactive oxygen species (ROS) resulting in oxidative stress. Most of the pathological conditions (such as ischemia reperfusion injury, neurological disorders, gastrointestinal diseases, inflammation etc.) are associated with increased levels of ROS. Exogenous administration of H_2S under these conditions protects the cells and tissues against oxidative stress induced damage. Thus, ROS induced delivery of H_2S would be important from therapeutic as well as mechanistic stand point. In order to address the challenge, we followed the work reported by our group. Nitroreducatse (NTR) activated gem-dithiol based H_2S donors have been reported previously to achieve bacteria targeted delivery of H_2S. The compounds were designed to study the role of H_2S in antibiotic resistance. The proposed mechanism of H_2S release from the scaffolds is as follows: the nitrobenzyl group upon reduction by NTR forms an intermediate **A** which further dissociates to release geminal dithiol **B**. The gem-dithiol so formed readily hydrolysis to release 2 moles of H_2S (Scheme 1.1).

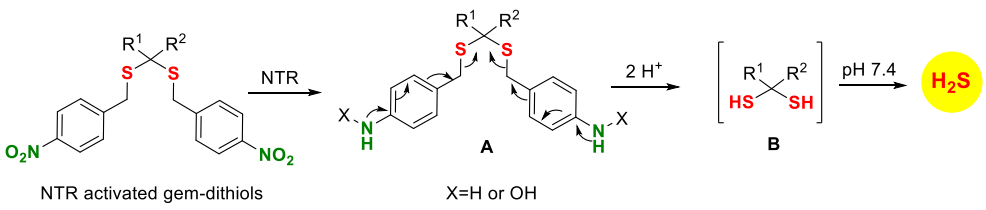

Scheme 1.1. Nitroreductase (NTR) activated gem-dithiol based H_2S donors

Nitro group in the scaffold can be replaced with a structural trigger which is selective towards activation by ROS. Therefore, in order to design ROS activated H_2S donors we used boronate esters as trigger for selective activation by H_2O_2. Boronate esters have been used as triggers for ROS activated delivery of latent fluorophores (imaging) or drugs. Boronate ester undergoes spontaneous hydrolysis to form boronic acid in pH 7.4 buffer. Upon reaction with H_2O_2 the boronic acid is converted to a free phenol (Scheme 1.2).

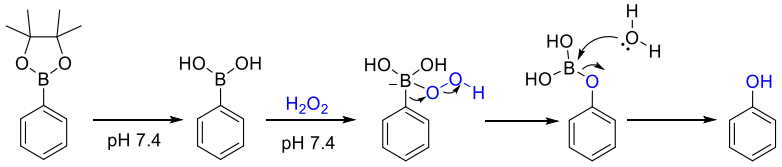

Scheme 1.2. Mechanism of boronate ester reaction with H_2O_2.

This strategy has been used to deliver drugs or for imaging intracellular H_2O_2. For example, Miller *et.al.* have reported H_2O_2 activated release of fluorophore for intracellular imaging of hydrogen peroxide (Scheme 1.3).

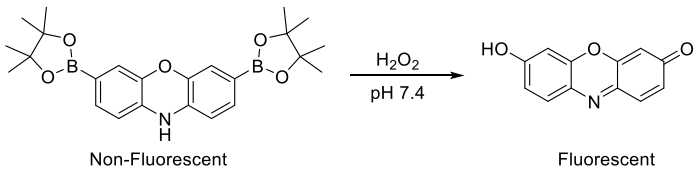

Scheme 1.3. Boronate ester based fluorophores for hydrogen peroxide.

Using this strategy, ROS activated gem-dithiol based H_2S donors were synthesized by our colleague Dr. Vinayak. It was proposed that the compounds upon activation by H_2O_2 would release an intermediate **C** which would further dissociate to release 2 moles of H_2S. However, the intermediate **C** formed after the reaction with H_2O_2 was found to be stable under the conditions and did not further dissociate to release H_2S (Scheme 1.4). The stability of intermediate **C** could be attributable to the poor leaving group ability of thiols (compared to phenols with lower pK_a such as *p*-nitrophenol) which prevents the cleavage of C-S bond. The high electronegativity of 'O' compared to 'N' might also be responsible for inhibiting the process of delocalisation of electrons to release thiol. Therefore, both the reasons may have contributed to the inefficient release of H_2S from boro-gem dithiol based H_2S donors.

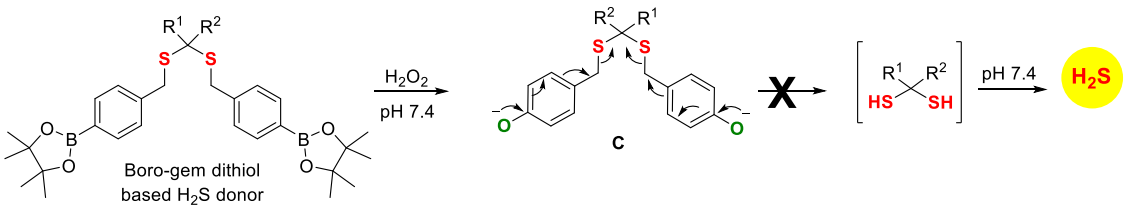

Scheme 1.4. ROS activated gem-dithiol based H_2S donor

1.11. Design

Two strategies were designed based on the above results. In approach 1, it was presumed that decreasing the pK_a of the thiol would increase its leaving group ability that would enable the process of self-immolation to release thiol. Thiols usually fall in the higher pK_a range (8-11) which makes them poor leaving groups. For example, pK_a of ethanethiol is 10.61 at 25 ^oC.[73] On the other hand, pK_a of thioacetic acid is 3.33[74] which is 7 units lower than ethanethiol due to the presence of an electron withdrawing carbonyl group (Figure 1.14). This indicates that introducing electron withdrawing group would greatly reduce the pK_a of the thiol thus making it a better leaving group.

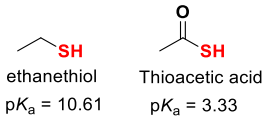

Figure 1.14. Effect of electron withdrawing group on the pK_a of thiol.

Therefore, in approach 1 we proposed to attach an electron withdrawing carbonyl group next to 'S' atom, with 'X' as a leaving group. Leaving group 'X' would serve as a structural handle to modulate the release of H_2S. In the second approach, introducing a self immolative linker that allows the formation of intermediate **A** (shown in Scheme 1.1), would help in achieving ROS triggered delivery of H_2S from gem-dithiol based scaffold (Scheme 1.5).

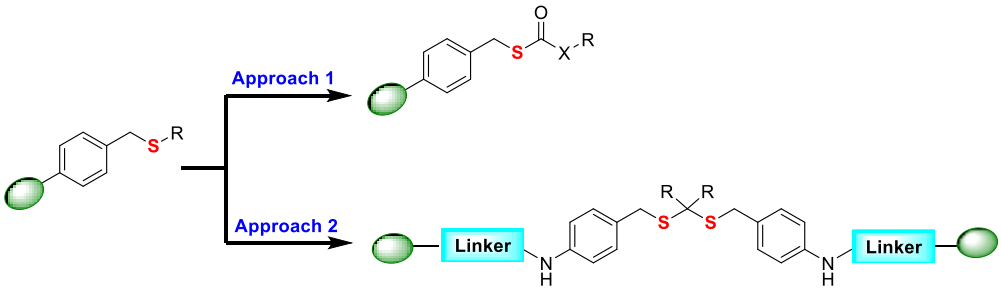

Scheme 1.5. Design of H_2S releasing scaffolds.

1.12. Direction of research

1.12.1. Carbonyl sulfide based H_2S donors

Utilising approach 1 for the delivery of H_2S, we designed scaffolds with 'X' as a leaving group. The scaffolds were termed as carbonothioates when alcohols were used as leaving group (X = O) and carbamothioates with amines as leaving group (X = NH) (Figure 1.15).

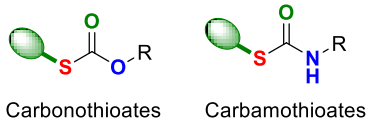

Figure 1.15. Structures of carbonothioates and carbamothioates.

The proposed mechanism of H_2S release from the scaffolds is as follows: compound upon activation by an external stimulus releases the trigger and forms an intermediate **I** which further dissociates to release carbonyl sulfide (COS) gas and the leaving group alcohol (X = O) or amine (X = NH) (Scheme 1.6)**.**

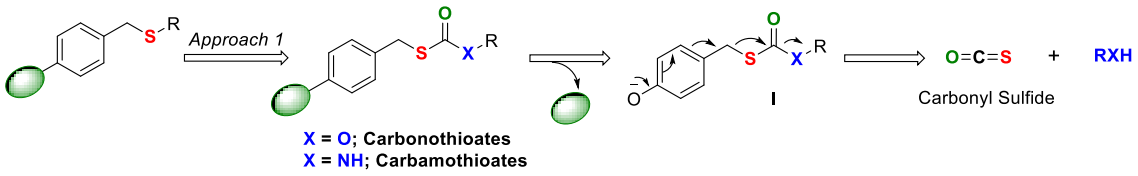

Scheme 1.6. General mechanism for the release of COS using approach 1.

Carbonyl sulfide (COS) is one of the most abundant sulfur containing gas in the earth's atmosphere with a concentration of 500 ppt. It is a linear molecule which is analogous to carbon dioxide and is originated from volcanoes, hot springs, deep sea vents and oceans. The production of COS is also reported in biological systems. Thiocyanate, $[SCN]^-$ which is produced during cyanide metabolism in bacteria, is converted to COS by the action of thiocyanate hydrolase enzyme.[75,76] COS thus produced is further hydrolysed to H_2S by carbonyl sulfide hydrolases. Similarly, higher plants act as a major sink for atmospheric COS where it is converted to H_2S by the action of carbonic anhydrase (CA) (Figure 1.16).[77,78] Although COS hydrolyzes in aqueous solutions to produce H_2S, the rate of hydrolysis is slow. However, the rate of hydrolysis is greatly accelerated in the presence of carbonic anhydrase (CA) enzyme (k_{cat} = 41 s^{-1}).[79] Carbonic anhydrase is a ubiquitous enzyme which is widely prevalent in nearly all the cells in a mammalian system. Thus, COS produced from

dissociation of carbonothioates or carbamothioates can be used as a surrogate for H_2S release in a cellular environment.

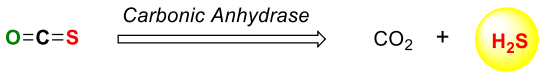

Figure 1.16. COS is hydrolysed to H_2S by carbonic anhydrase.

Using this approach, in chapter 2, esterase activated carbonothioates and carbamothioates based H_2S donors were synthesized. Esterase was considered for the preliminary studies due to the wide occurrence of the enzyme in nearly all the cells which would be useful in understanding the biology of H_2S (Scheme 1.7). Esterase would cleave the ester bond to release an intermediate which would further dissociate to generate COS and a leaving group. The nature of the leaving group X may affect the release of COS and hence could modulate the rate of H_2S release.

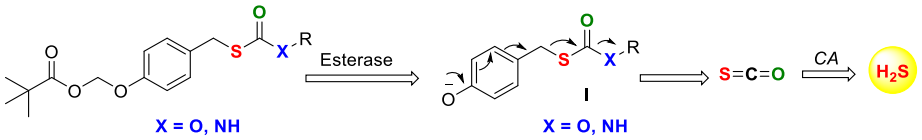

Scheme 1.7. Proposed mechanism of esterase triggered H_2S release.

1.12.2. ROS triggered H_2S release

After establishing the generation of H_2S from COS donor motifs, we proposed to achieve site directed delivery of H_2S. In chapter 3.1, boronate ester based COS scaffolds for ROS triggered delivery of H_2S were designed. Amine as the leaving group was affixed in this series of donors to modulate the release of H_2S and their cytoprotective effects were studied (Scheme 1.8). The versatility of the scaffold was studied by conjugating a non-steroidal anti-inflammatory drug (NSAID) with the COS scaffold for delivering H_2S-NSAID hybrid donors.

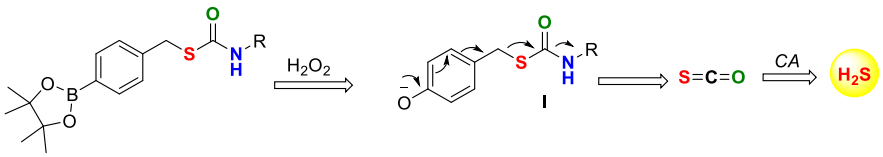

Scheme 1.8. Hydrogen peroxide induced release of H_2S.

In chapter 3.2, approach 2 was followed to design ROS triggered gem-dithiol based delivery tools with increased payload of H_2S. Anti-cancer effects of H_2S depend on the concentration of H_2S. Therefore, designing ROS activated release of H_2S from gem-dithiol based scaffold would be useful (Scheme 1.9). The scaffold allows the release of two moles of H_2S per mole of the donor and therefore can be utilized to study the anti-cancer effects of H_2S.

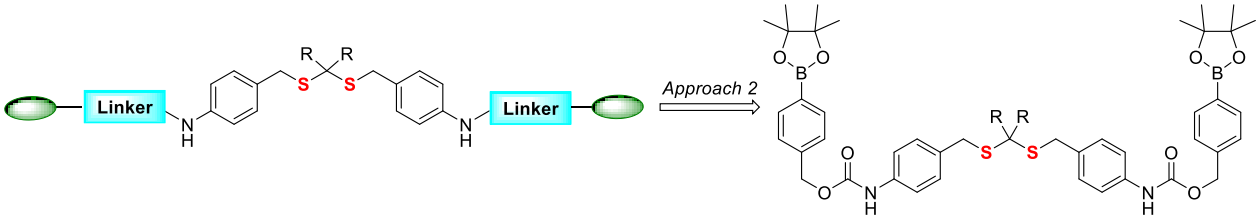

Scheme 1.9. ROS triggered delivery of H_2S with increased payload.

1.12.3. Colon targeted delivery of H_2S

Non-steroidal anti-inflammatory drugs (NSAIDs) are a class of clinically used drugs for the treatment of pain, arthritis, inflammation etc. However, extensive use of NSAIDs is associated with severe side effects such as inflammation which furthers leads to ulcers in the gastrointestinal tract (GIT). NSAIDs corrode the inner lining of the stomach thereby causing ulcers. H_2S in conjugation with NSAIDs have previously shown cytoprotective effects. H_2S-NSAID hybrid donors increase the efficacy of the drug and also reduce the side effects associated with the use of NSAIDs alone. For example, mesalamine (NSAID) is a clinically used drug for the treatment of colitis. However, it is ineffective towards severe forms of the disease. Wallace and co-workers demonstrated that H_2S-mesalamine hybrid donor (ATB-429) remarkably improves the efficacy of the parent drug towards treatment of severe forms of colitis is an animal model (Figure 1.17). Also, H_2S released protects the cells by inhibiting leukocyte adherence to the vascular epithelium. However, the uncontrolled release of H_2S from ATB-429 and lack of appropriate negative controls complicates the conclusions made from the study.

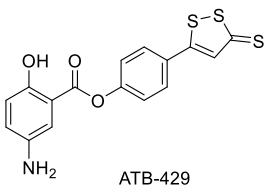

Figure 1.17. Structure of ATB-429.

Thus, in chapter 4, colon targeted delivery of H_2S and H_2S-NSAID hybrid donors is proposed. NAD(P)H quinone oxidoreductase (NQO1) is a 2 e^- reducing cytosolic enzyme which is over expressed in colon epithelium. The expression of NQO1 increases under oxidative stress and electrophilic stress. Cell utilizes NQO1 as a detoxification strategy by reducing quinones to hydroquinones which are then excreted out. This strategy has been taken advantage off in the past for delivery of drugs and latent fluorophores (Scheme 1.10). Keeping this in mind, bioreductively activated H_2S and H_2S-mesalamine hybrid molecules for targeted delivery towards colon were designed (Scheme 1.11).

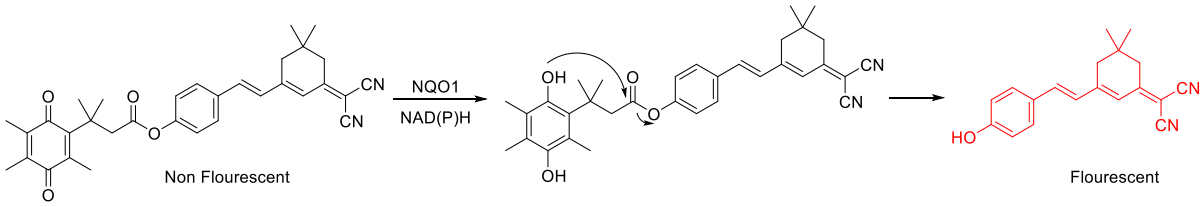

Scheme 1.10. NQO1 activated release of fluorophore.

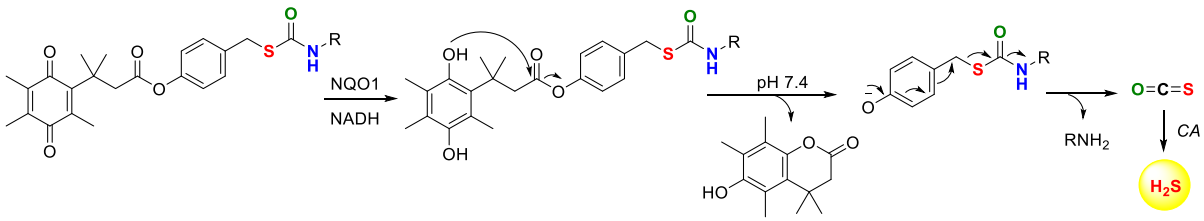

Scheme 1.11. NQO1 responsive COS/ H_2S donors.

Finally, in chapter 4.2 the effect of pK_a of thiols on their leaving group ability is further evaluated. Perthiols or persulfides (RSSH) are reactive sulfur species containing each sulfur in -1 oxidation state. It is proposed that the mechanism by which H_2S acts as a signalling molecule is by persulfidating the cysteine residues (Cys-SSH) of a protein which is regarded as a post translational modification. Therefore, targeted and controlled delivery of persulfides assume importance. The bond dissociation energy of S-H bond in perthiols (70 kcal mol^{-1}) is lower than that of the corresponding thiol (92 kcal mol^{-1}); thus, making perthiols more acidic than their corresponding thiols. Therefore, the pK_a of perthiols is approximately 2 units lower than thiols.[5] Thus, the capability of the scaffold to release perulfides under these conditions is demonstrated in this chapter. Also, achieving targeted delivery of perthiols is useful to investigate their biological implications from a therapeutic stand point.

Matson and co-workers have recently reported ROS induced delivery of persulfides and demonstrated its cytoprotective effects (Scheme 1.12). Therefore, in chapter 4.2, NQO1 activated persulfide donors to study the cytoprotective effects against xenobiotic induced stress is established in this chapter (Scheme 1.13).

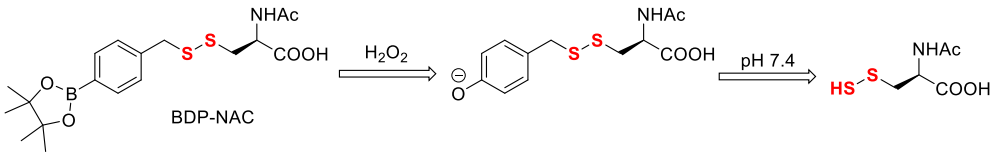

Scheme 1.12. ROS activated persulfide donor.

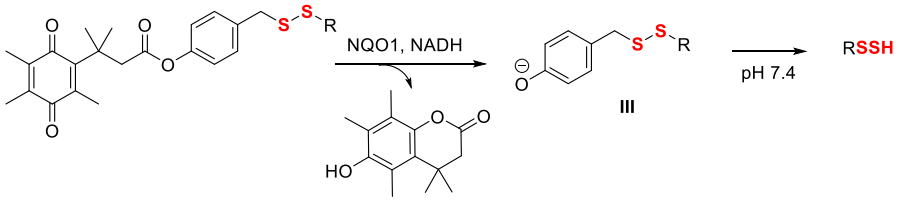

Scheme 1.13. NQO1 activated persulfide donors

Collectively, this thesis comprises of results which address important problems associated with the delivery of H_2S in a physiological system. Site directed delivery and tunable release of H_2S may help in understanding the mechanism of H_2S in cellular stress responses and may also serve as tools for exploiting the therapeutic potential of the gas. The leaving group ability of sulfur containing species based on their pK_a values have also been evaluated.

1.15. References:

(1) Parker, E. T.; Cleaves, H. J.; Dworkin, J. P.; Glavin, D. P.; Callahan, M.; Aubrey, A.; Lazcano, A.; Bada, J. L. *Proc. Natl. Acad. Sci. U. S. A.* **2011**, *108*, 5526.

(2) Patel, B. H.; Percivalle, C.; Ritson, D. J.; Duffy, C. D.; Sutherland, J. D. *Nat. Chem.* **2015**, *7*, 301.

(3) Ramazzini, B. **1713**.

(4) Scheele, C. W. **1777**.

(5) Filipovic, M. R.; Zivanovic, J.; Alvarez, B.; Banerjee, R. *Chem. Rev.* **2018**, *118*, 1253.

(6) Wang, R. *Physiological Reviews* **2012**, *92*, 791.

(7) Abe, K.; Kimura, H. *J. Neurosci.* **1996**, *16*, 1066.

(8) Zhao, W.; Zhang, J.; Lu, Y.; Wang, R. *EMBO J.* **2001**, *20*, 6008.

(9) Blackstone, E.; Morrison, M.; Roth, M. B. *Science* **2005**, *308*, 518.

(10) Wallace, J. L.; Wang, R. *Nat. Rev. Drug. Discov.* **2015**, *14*, 329.

(11) Li, L.; Rose, P.; Moore, P. K. *Annu. Rev. Pharmacol. Toxicol.* **2011**, *51*, 169.

(12) Szabo, C. *Nat Rev Drug Discov* **2007**, *6*, 917.

(13) Basic, A.; Blomqvist, S.; Carlén, A.; Dahlén, G. *J. Oral Microbiol.* **2015**, *7*, 28166.

(14) Dubois, T.; Dancer-Thibonnier, M.; Monot, M.; Hamiot, A.; Bouillaut, L.; Soutourina, O.; Martin-Verstraete, I.; Dupuy, B. *Infect. immun.* **2016**, *84*, 2389.

(15) Szabo, C. *Biochem. Pharmacol.* **2018**, *149*, 5.

(16) Kaji, A.; McElroy, W. D. *J. bacteriol.* **1959**, *77*, 630.

(17) Kabil, O.; Banerjee, R. *J. biol. chem.* **2010**, *285*, 21903.

(18) Gadalla, M. M.; Snyder, S. H. *J. neurochem.* **2010**, *113*, 14.

(19) Kabil, O.; Vitvitsky, V.; Xie, P.; Banerjee, R. *Antioxid. redox signal.* **2011**, *15*, 363.

(20) Stipanuk, M. H.; Ueki, I. *J. inherit. metab. dis.* **2011**, *34*, 17.

(21) Linden, D. R.; Sha, L.; Mazzone, A.; Stoltz, G. J.; Bernard, C. E.; Furne, J. K.; Levitt, M. D.; Farrugia, G.; Szurszewski, J. H. *J. neurochem.* **2008**, *106*, 1577.

(22) Kery, V.; Bukovska, G.; Kraus, J. P. *J. Biol. Chem.* **1994**, *269*, 25283.

(23) Chiku, T.; Padovani, D.; Zhu, W.; Singh, S.; Vitvitsky, V.; Banerjee, R. *J. Biol. Chem.* **2009**, *284*, 11601.

(24) Jarabak, R.; Westley, J. *Arch. Biochem. Biophys.* **1978**, *185*, 458.

(25) Yadav, P. K.; Yamada, K.; Chiku, T.; Koutmos, M.; Banerjee, R. *J. Biol. Chem.* **2013**, *288*, 20002.

(26) Nagahara, N.; Yoshii, T.; Abe, Y.; Matsumura, T. *J. Biol. Chem.* **2007**, *282*, 1561.

(27) Nagahara, N.; Ito, T.; Kitamura, H.; Nishino, T. *Histochem. Cell Biol.* **1998**, *110*, 243.

(28) Jiang, B.; Tang, G.; Cao, K.; Wu, L.; Wang, R. *Antioxid. Redox Signal.* **2010**, *12*, 1167.

(29) Yang, G.; Zhao, K.; Ju, Y.; Mani, S.; Cao, Q.; Puukila, S.; Khaper, N.; Wu, L.; Wang, R. *Antioxid. Redox Signal.* **2013**, *18*, 1906.

(30) Yang, G.; Wu, L.; Jiang, B.; Yang, W.; Qi, J.; Cao, K.; Meng, Q.; Mustafa, A. K.; Mu, W.; Zhang, S.; Snyder, S. H.; Wang, R. *Science* **2008**, *322*, 587.

(31) Fu, M.; Zhang, W.; Wu, L.; Yang, G.; Li, H.; Wang, R. *Proc. Natl. Acad. Sci. U. S. A.* **2012**, *109*, 2943.

(32) Hatano, T.; Kubo, S.-i.; Sato, S.; Hattori, N. *J. Neurochem.* **2009**, *111*, 1075.

(33) Vandiver, M. S.; Paul, B. D.; Xu, R.; Karuppagounder, S.; Rao, F.; Snowman, A. M.; Ko, H. S.; Lee, Y. I.; Dawson, V. L.; Dawson, T. M.; Sen, N.; Snyder, S. H. *Nat. Commun.* **2013**, *4*, 1626.

(34) Kida, K.; Yamada, M.; Tokuda, K.; Marutani, E.; Kakinohana, M.; Kaneki, M.; Ichinose, F. *Antioxid. redox signal.* **2011**, *15*, 343.

(35) Hu, L.-F.; Lu, M.; Tiong, C. X.; Dawe, G. S.; Hu, G.; Bian, J.-S. *Aging Cell* **2010**, *9*, 135.

(36) Lu, M.; Zhao, F.-F.; Tang, J.-J.; Su, C.-J.; Fan, Y.; Ding, J.-H.; Bian, J.-S.; Hu, G. *Antioxid. redox signal.* **2012**, *17*, 849.

(37) Calvert, J. W.; Coetzee, W. A.; Lefer, D. J. *Antioxid. Redox Signal.* **2010**, *12*, 1203.

(38) Elrod, J. W.; Calvert, J. W.; Morrison, J.; Doeller, J. E.; Kraus, D. W.; Tao, L.; Jiao, X.; Scalia, R.; Kiss, L.; Szabo, C.; Kimura, H.; Chow, C.-W.; Lefer, D. J. *Proc. Natl. Acad. Sci. U S A* **2007**, *104*, 15560.

(39) Mard, S. A.; Neisi, N.; Solgi, G.; Hassanpour, M.; Darbor, M.; Maleki, M. *Dig. Dis. Sci.* **2012**, *57*, 1496.

(40) Polhemus, D. J.; Lefer, D. J. *Circ. res.* **2014**, *114*, 730.

(41) Fiorucci, S.; Orlandi, S.; Mencarelli, A.; Caliendo, G.; Santagada, V.; Distrutti, E.; Santucci, L.; Cirino, G.; Wallace, J. L. *Br. J. Pharmacol.* **2007**, *150*, 996.

(42) Li, L.; Moore, P. K. *Expert rev. clin. pharmacol.* **2013**, *6*, 593.

(43) Whiteman, M.; Li, L.; Rose, P.; Tan, C.-H.; Parkinson, D. B.; Moore, P. K. *Antioxid. Redox Signal.* **2010**, *12*, 1147.

(44) Bhatia, M. *Scientifica* **2012**, *2012*, 12.

(45) Whiteman, M.; Winyard, P. G. *Expert Rev. Clin. Pharmacol.* **2011**, *4*, 13.

(46) Li, L.; Bhatia, M.; Zhu, Y. Z.; Zhu, Y. C.; Ramnath, R. D.; Wang, Z. J.; Anuar, F. B. M.; Whiteman, M.; Salto-Tellez, M.; Moore, P. K. *FASEB J.* **2005**, *19*, 1196.

(47) Wallace, J. L.; Ferraz, J. G. P.; Muscara, M. N. *Antioxid. Redox Signal.* **2012**, *17*, 58.

(48) Szabo, C.; Coletta, C.; Chao, C.; Módis, K.; Szczesny, B.; Papapetropoulos, A.; Hellmich, M. R. *Proc. Natl. Acad. Sci. U.S.A.* **2013**, *110*, 12474.

(49) Lee, Z. W.; Teo, X. Y.; Tay, E. Y. W.; Tan, C. H.; Hagen, T.; Moore, P. K.; Deng, L. W. *Br. J. Pharmacol.* **2014**, *171*, 4322.

(50) Lee, Z. W.; Zhou, J.; Chen, C.-S.; Zhao, Y.; Tan, C.-H.; Li, L.; Moore, P. K.; Deng, L.-W. *PloS one.* **2011**, *6*, e21077.

(51) Wu, D.; Si, W.; Wang, M.; Lv, S.; Ji, A.; Li, Y. *Nitric oxide* **2015**, *50*, 38.

(52) Shen, X.; Carlström, M.; Borniquel, S.; Jädert, C.; Kevil, C. G.; Lundberg, J. O. *Free radic. biol. med.* **2013**, *60*, 195.

(53) Flannigan, K. L.; McCoy, K. D.; Wallace, J. L. *Am. J. Physiol. Gastrointest. Liver Physiol.* **2011**, *301*, G188.

(54) Wallace, J. L. *Best Pract. Res. Clin. Gastroenterol.* **2000**, *14*, 147.

(55) Zanardo, R. C. O.; Brancaleone, V.; Distrutti, E.; Fiorucci, S.; Cirino, G.; Wallace, J. L. *FASEB J.* **2006**, *20*, 2118.

(56) Stefano, F.; Luca, S. *Inflamm. Allergy Drug Targets.* **2011**, *10*, 133.

(57) Benavides, G. A.; Squadrito, G. L.; Mills, R. W.; Patel, H. D.; Isbell, T. S.; Patel, R. P.; Darley-Usmar, V. M.; Doeller, J. E.; Kraus, D. W. *Proc. Natl. Acad. Sci.* **2007**, *104*, 17977.

(58) Zhao, Y.; Biggs, T. D.; Xian, M. *Chem. Commun.* **2014**, *50*, 11788.

(59) Zheng, Y.; Ji, X.; Ji, K.; Wang, B. *Acta. Pharm. Sin. B.* **2015**, *5*, 367.

(60) Ono, K.; Akaike, T.; Sawa, T.; Kumagai, Y.; Wink, D. A.; Tantillo, D. J.; Hobbs, A. J.; Nagy, P.; Xian, M.; Lin, J.; Fukuto, J. M. *Free Radic. Biol. Med.* **2014**, *77*, 82.

(61) Li, Q.; Lancaster, J. R., Jr. *Nitric oxide.* **2013**, *35*, 21.

(62) Li, L.; Whiteman, M.; Guan Yan, Y.; Neo Kay, L.; Cheng, Y.; Lee Shiau, W.; Zhao, Y.; Baskar, R.; Tan, C.-H.; Moore Philip, K. *Circulation* **2008**, *117*, 2351.

(63) Bora, P.; Chauhan, P.; Pardeshi, K. A.; Chakrapani, H. *RSC Adv.* **2018**, *8*, 27359.

(64) Zhao, Y.; Wang, H.; Xian, M. *J. Am. Chem. Soc.* **2011**, *133*, 15.

(65) Zhao, Y.; Bhushan, S.; Yang, C.; Otsuka, H.; Stein, J. D.; Pacheco, A.; Peng, B.; Devarie-Baez, N. O.; Aguilar, H. C.; Lefer, D. J.; Xian, M. *ACS chem. biol.* **2013**, *8*, 1283.

(66) Martelli, A.; Testai, L.; Citi, V.; Marino, A.; Pugliesi, I.; Barresi, E.; Nesi, G.; Rapposelli, S.; Taliani, S.; Da Settimo, F.; Breschi, M. C.; Calderone, V. *ACS Med. Chem. Lett.* **2013**, *4*, 904.

(67) Zhao, Y.; Kang, J.; Park, C.-M.; Bagdon, P. E.; Peng, B.; Xian, M. *Org. Lett.* **2014**, *16*, 4536.

(68) Szabo, C.; Papapetropoulos, A. *Pharmacol. Rev.* **2017**, *69*, 497.

(69) Zheng, Y.; Yu, B.; Ji, K.; Pan, Z.; Chittavong, V.; Wang, B. *Angew.Chem. Int.Ed.* **2016**, *55*, 4514.

(70) Shukla, P.; Khodade, V. S.; SharathChandra, M.; Chauhan, P.; Mishra, S.; Siddaramappa, S.; Pradeep, B. E.; Singh, A.; Chakrapani, H. *Chem. Sci.* **2017**, *8*, 4967.

(71) Kang, J.; Li, Z.; Organ, C. L.; Park, C.-M.; Yang, C.-t.; Pacheco, A.; Wang, D.; Lefer, D. J.; Xian, M. *J. Am. Chem. Soc.* **2016**, *138*, 6336.

(72) Woods, J. J.; Cao, J.; Lippert, A. R.; Wilson, J. J. *J. Am. Chem. Soc.* **2018**, *140*, 12383.

(73) International Union of, P.; Applied, C.; Commission on Equilibrium, D.; Serjeant, E. P.; Dempsey, B.; International Union of, P.; Applied, C.; Commission on Electrochemical, D.; Pergamon Press: Oxford; New York, 1979.

(74) Janssen, M. J. In *Carboxylic Acids and Esters (1969)*; Patai, S., Ed. 1969, p 705.

(75) Sorokin, D. Y.; Tourova, T. P.; Lysenko, A. M.; Kuenen, J. G. *Appl. Environ. Microbiol.* **2001**, *67*, 528.

(76) Luque-Almagro, V. M.; Cabello, P.; Sáez, L. P.; Olaya-Abril, A.; Moreno-Vivián, C.; Roldán, M. D. *Appl. Microbiol. Biotechnol.* **2018**, *102*, 1067.

(77) Protoschill-Krebs, G.; Wilhelm, C.; Kesselmeier, J. *Atmos. Environ.* **1996**, *30*, 3151.

(78) Maseyk, K.; Berry, J. A.; Billesbach, D.; Campbell, J. E.; Torn, M. S.; Zahniser, M.; Seibt, U. *Proc. Natl. Acad. Sci. U. S. A.* **2014**, *111*, 9064.

(79) Haritos, V. S.; Dojchinov, G. *Comp. Biochem. Physiol. Part C: Toxicol. Pharmacol.* **2005**, *140*, 139.

CHAPTER 2: Esterase activated COS/H_2S donors

2.1. Introduction

H_2S acts as a protective agent against diseases like myocardial ischemia injury[1,2], neuronal[3-6] or gastrointestinal disorders[7,8] suggesting that modulating the levels of H_2S within cells would have tremendous impact on disease biology. [9-12] Ubiquitous targets of H_2S demands localized delivery of the gas for a better mechanistic understanding.[13-20] Also, previous reports suggest that the therapeutic potential of H_2S depends on the rate of release of the gaseous species. [20-22] Therefore, methods for achieving controlled generation and dissipation of H_2S assume utmost importance. [23]

Carbonyl sulfide (COS) is the most abundant sulfur containing gas present in the earth's atmosphere. COS is absorbed by the higher plants and is hydrolysed to H_2S using carbonic anhydrase (CA) enzyme.[24] COS is also produced in bacteria during cyanide metabolism where it is converted to H_2S by the action of carbonyl sulfide hydrolases.[25] The rate of COS hydrolysis by carbonic anhydrase (CA) is extremely fast (k_{cat} = 41 s^{-1}) suggesting that COS can act as a surrogate for H_2S release.[26] CA is a widely prevalent enzyme in mammalian cells required for catalysing the interconversion between carbon dioxide and carbonic acid.

Therefore, based on approach 1 (as shown in Chapter 1, Scheme 1.6), COS mediated H_2S delivery was proposed to attain controlled and targeted release of H_2S. Esterase (ES) was considered as trigger for our first set of studies due to the wide occurrence of the enzyme in all the cells that would find broad use in understanding the H_2S biology. Esterase has been extensively used in the past to deliver latent fluorophores (for imaging), drugs[27] and other biologically relevant species (Scheme 2.1).[28,29]

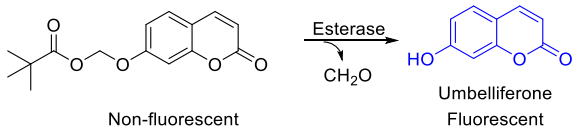

Scheme 2.1. Esterase activated release of fluorophores.

Thus, following approach 1 (as shown in Chapter 1, Scheme 1.6), esterase activated carbonothioates (X = O) and carbamothioates (X = NH) scaffolds are considered for H_2S release. The nature of leaving group X may act as a structural handle to modulate the rate of H_2S generation (Figure 2.1).

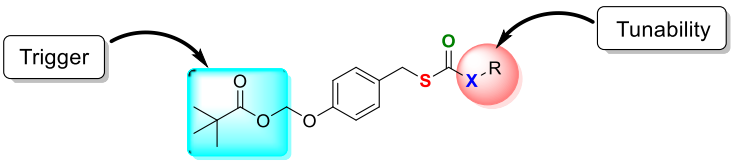

Figure 2.1. Design of esterase activated COS/H_2S donors

During the progress of this work, Pluth and co-workers reported azide based COS/H_2S donors which are triggered by H_2S.[30] Azide upon reduction by endogenous H_2S releases COS, which is further hydrolysed to H_2S by CA (Scheme 2.2a). The reported thiocarbamates can be used as analytical tools for the detection of H_2S and also aid in analyte homeostasis. However, azide is a chemical trigger that requires H_2S for its activation. Thus, the donors cannot be used for therapeutic applications. A subsequent report on COS based H_2S donors was reported by Matson and co-workers where they showed *N*-thiocarboxyanhydride (NTA) based COS donors activated by nucleophiles such as thiols.[31] Nucleophile reacts with NTA to generate COS/H_2S which is further hydrolysed to H_2S (Scheme 2.2b). However, the ubiquitous nature of thiols greatly compromises the selectivity of the donors. Therefore, new and improved tools to generate COS are needed.

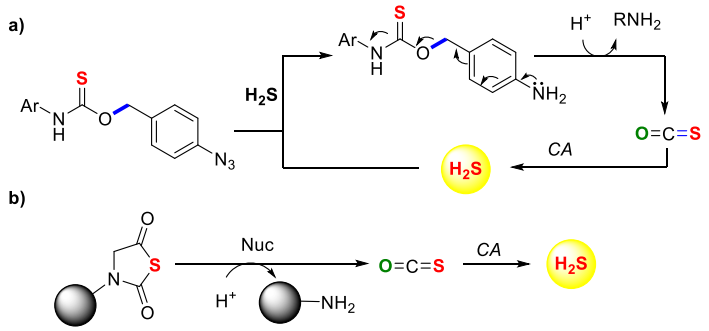

Scheme 2.2. a) H_2S triggered generation of COS/H_2S. b) nucleophile activated COS/H_2S donors.

Hence, esterase activated COS/H_2S donors are prepared. The proposed mechanism of H_2S release from the scaffolds is as follows: esterase hydrolysis the ester bond which is followed by a rapid release of formaldehyde to generate intermediate **I**. The intermediate formed further dissociates to generate COS which is then hydrolysed to produce H_2S by carbonic anhydrase (CA) (Scheme 2.3).

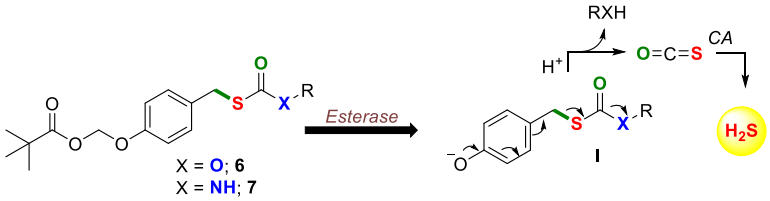

Scheme2.3. Proposed mechanism for esterase activated COS/H_2S donors.

2.2. Results and Discussion

2.2.1. Synthesis of esterase activated COS/H_2S donors

In order to test the hypothesis, esterase activated COS/H_2S donors were synthesized in 6 steps. Chloromethyl pivalate was treated with sodium iodide (NaI) in ACN at room temperature for 5 h to give **1** in 74% yield. Compound **1** was further reacted with *p*-hydroxybenzyl alcohol in the presence of NaH at 0 ^oC and allowed to reach room temperature over a period of 6 h to give **2** in 83% yield which was purified by column chromatography. Compound **2** was converted to thiol, **3**, in three steps. First, **2**, was reacted with tribromophosphine at 0 ^oC in DCM for 1 h. The product obtained was further reacted with thiourea in THF at room temperature for 12 h to give a thiourea salt adduct. The thiourea adduct was then hydrolyzed in the presence of sodium metabisulfite ($Na_2S_2O_5$) to obtain thiol **3** in 58% overall yield (Scheme 2.4).

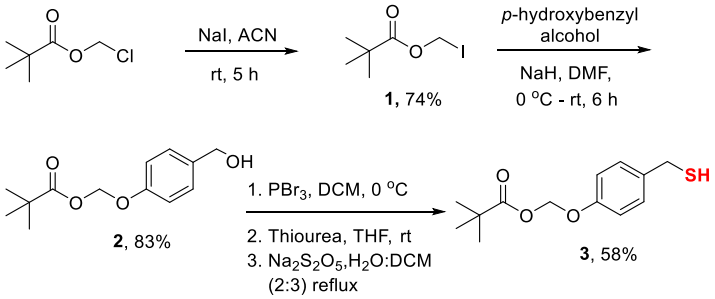

Scheme 2.4. Synthesis of thiol **3**.

Compound **3** was independently reacted with *p*-nitrophenyl chloroformate, phenyl chloroformate and benzyl chloroformate to give the desired carbonothioates **6a**, **6b** and **6c** respectively (Scheme 2.6). In order to synthesize carbamothioates, the respective carbamates (**5a**-**5c**) were first synthesized by reacting *p*-nitrophenyl chloroformate with respective amines (Scheme 2.5). Carbamothioates **7a**, **7b** and **7c** were then synthesized from the reaction of **3** with respective carbamates **5a**, **5b** and **5c** (Scheme 2.6).

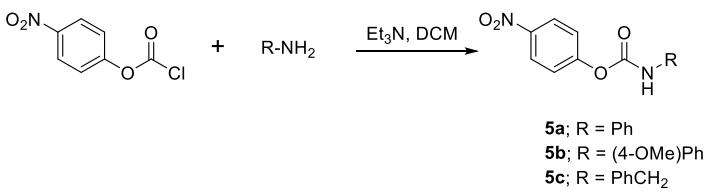

Scheme 2.5. Synthesis of carbamates **5a**-**5c**

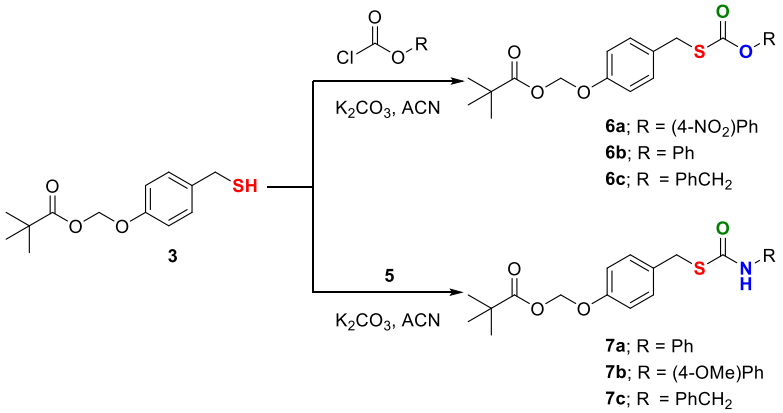

Scheme 2.6. Synthesis of carbamates **6a-6c** and **7a-7c**.

Table 2.1: Carbonothioates (**6a-6c**) and carbamothioates(**7a-7c**).

Entry	R	product	yield (%)[a]
1.	4-NO_2Ph	**6a**	77
2.	Ph	**6b**	64
3.	$PhCH_2$	**6c**	16
4.	Ph	**7a**	11
5.	4-OMePh	**7b**	44
6.	$PhCH_2$	**7c**	37

Compound **4** was synthesized as a negative control by reacting compound **2** with tribromophosphine followed by reaction with *p*-nitrophenol to give **4** in 10% yield (Scheme 2.7).

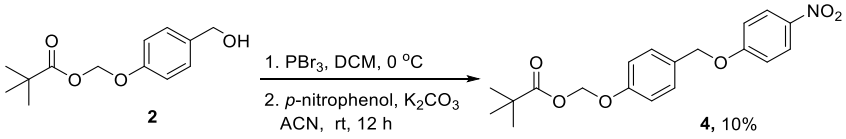

Scheme 2.7. Synthesis of negative control, **4**.

2.2.2. Detection of COS by mass spectrometry:

First, the ability of the donors to generate COS in the presence of ES was evaluated using mass spectrometry. Reaction was performed in a closed vial where compound **6a** was incubated in pH 7.4 buffer containing ES at 37 ^{o}C for 30 min. The absence of CA slowed

down the rate of COS hydrolysis in buffer and therefore making it available for detection. ESI- MS spectra was recorded by direct injection of the reaction mixture in Agilent 6540 UHD QTOF MS with Dual Jet Stream ESI source. A peak corresponding to the protonated form of COS was recorded which was in accordance with the previous reports (Figure 2.2).[32]

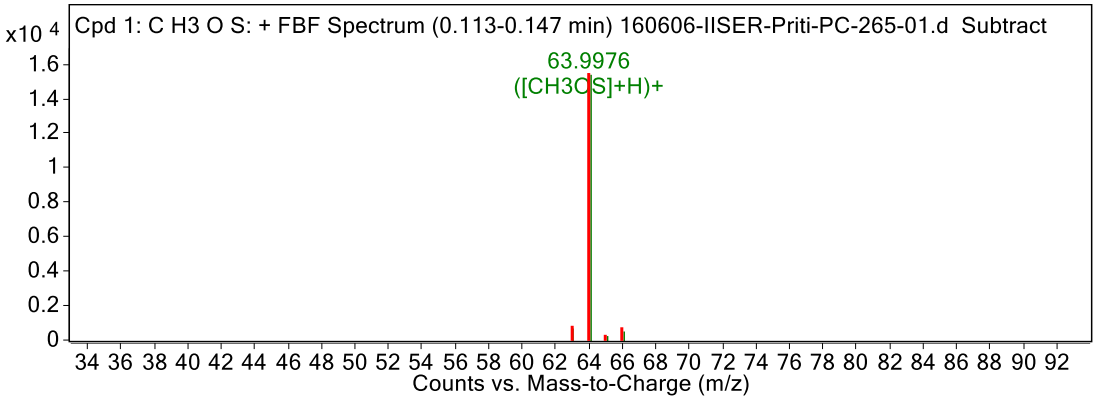

Figure 2.2. Detection of COS by mass spectrometry.

2.2.3. Detection of H_2S:

Detection of H_2S is challenging due to its high reactivity and volatility. Therefore, generation of H_2S from the COS/H_2S donors was validated using multiple independent techniques.

2.2.3.1. Evaluating the formation of H_2S by dansyl azide method:

Formation of H_2S was first assessed by using dansyl azide (Dn-N_3), a H_2S sensitive fluorogenic dye. The probe reacts with H_2S to form dansylamine (Dn-NH_2) which shows a distinct fluorescent signal at 535 nm with excitation at 340 nm (Scheme 2.8).[33]

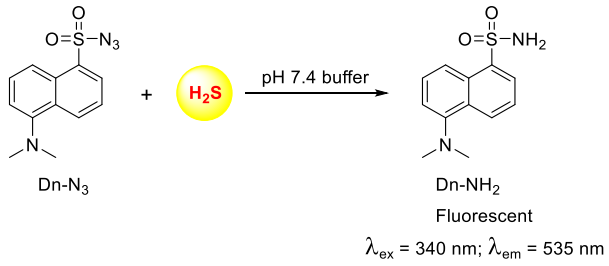

Scheme 2.8. Reduction of weakly fluorescent Dn-N_3 to fluorescent Dn-NH_2 by H_2S.

All the compounds were independently incubated in phosphate buffer (pH 7.4) containing esterase (ES) and carbonic anhydrase (CA) for 60 min. Next, Dn-N_3 was added and the reaction mixture was further incubated for 15 min. Thereafter, fluorescence signal corresponding to the formation of Dn-NH_2 was measured at 535 nm using a microtiter plate reader. Fluorescence signal corresponding to Dn-NH_2 formation was observed from all the

donors indicating that the compounds produced H_2S in the presence of ES and CA. No significant fluorescence signal was observed from compound **4** which lacked the ability to produce H_2S (Figure 2.3).

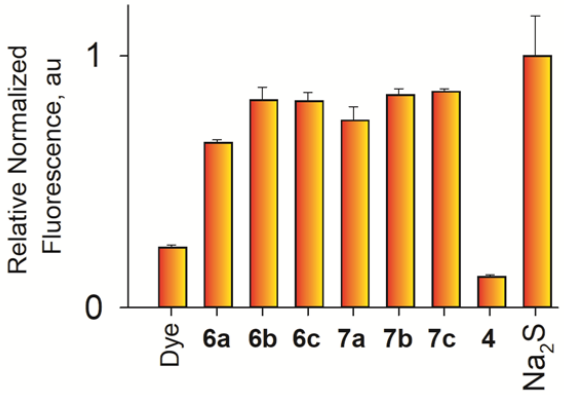

Figure 2.3. Yields of H_2S measured using Dn-N_3 assay upon incubating compounds in pH 7.4 buffer in the presence of ES and CA for 60 min. Fluorescence intensity measured at 535 nm (excitation 340 nm).

Formation of Dn-NH_2 from H_2S in the aforementioned assay was further confirmed by HPLC analysis. Compound **6c** was incubated in buffer (pH 7.4) containing ES, CA and Dn-N_3 for 40 min at 37 ^oC and injected in HPLC. Dn-NH_2 formation was monitored by using a fluorescence detector with excitation 340 nm and emission at 535 nm. Peak corresponding to Dn-NH_2 was observed at retention time of 15.3 min which was also observed from the reaction of Na_2S with Dn-N_3. No fluorescence signal was observed from compound **6c** alone (Figure 2.4).

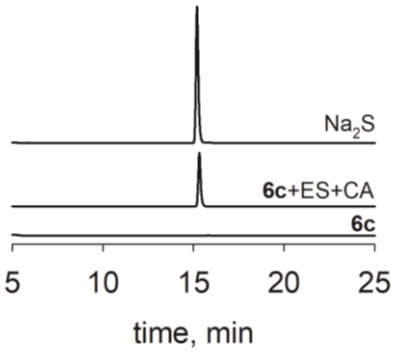

Figure 2.4. HPLC analysis to monitor the formation of Dn-NH_2 from compound **6c** in the presence of ES and CA. Fluorescence detector used; excitation 340 nm and emission 535 nm.

2.2.3.2. Detection of H_2S using electrode:

Formation of H_2S from the scaffolds was further evaluated by using sulfide selective electrode. Compound **6a** was incubated in phosphate buffer (pH 7.4) containing CA at 37 ^oC. After 5 min of incubation, esterase was added to the reaction mixture as indicated by the arrow. Soon after the addition of esterase, signal attributable to the release of H_2S was observed indicating that the compound was activated in the presence of esterase to generate H_2S (Figure 2.5).

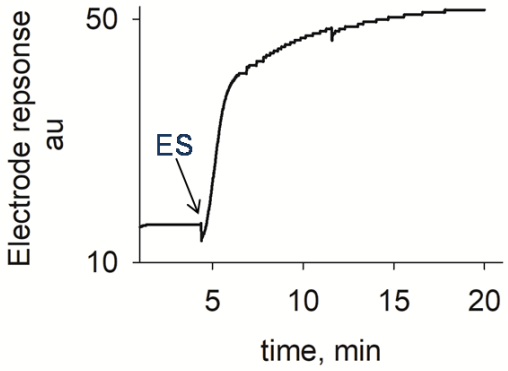

Figure 2.5. Trace for H_2S detection using sulfide selective electrode; **6a** was incubated in pH 7.4 buffer containing CA. Esterase was added to the reaction mixture after 5 min as shown by the arrow.

2.2.3.3. Lead acetate paper test for H_2S detection:

Lead acetate paper test is yet another method which is extensively used for the rapid detection of H_2S.[34] It is a qualitative method wherein H_2S reacts with lead acetate to form a dark coloured precipitate of lead sulfide which indicates the presence of H_2S (Scheme 2.9).

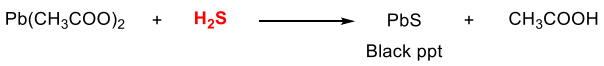

Scheme 2.9. Reaction of lead acetate with H_2S to form lead sulfide (PbS).

In order to conduct this experiment lead acetate paper strips were made by cutting Whatman filter paper into rectangular strips which were then dipped in a saturated solution of lead acetate. Once completely soaked, the paper strips were dried in the oven at 65 ^oC for 1 day to form lead acetate paper strips. These strips were then used for the experiment. Compound **6c** was incubated in phosphate buffer pH 7.4 in the presence of ES and CA at 37 ^oC. An aliquot of the reaction mixture was added to the lead acetate paper which showed a distinct dark

coloration corresponding to the formation of lead sulfide. Ctrl represents the incubation of **6c** alone (Figure 2.6).

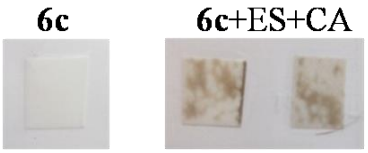

Figure 2.6. Dark coloration of lead acetate paper indicative of the formation of lead sulfide from **6c**. Ctrl represents incubation of **6c** alone.

2.2.3.4. Detection of H_2S using methylene blue assay:

Methylene Blue is a well established method used for the detection of H_2S both in chemical and biological systems.[35] It is based on the formation of methylene blue complex from the reaction of H_2S with *N*,*N*-dimethyl-*p*-phenylene diamine in the presence of $FeCl_3$ under acidic conditions (Scheme 2.10). $Zn(OAc)_2$ is added to trap the H_2S formed in the reaction mixture. Methylene blue is a coloured complex which can be monitored by measuring the absorbance at 676 nm.

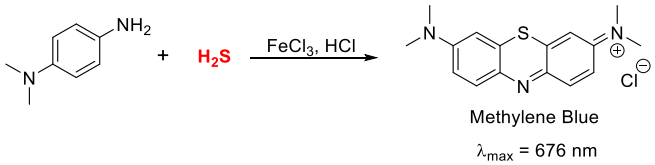

Scheme 2.10. Methylene blue formation from H_2S.

In order to establish the release of H_2S from the donors, formation of methylene blue complex was monitored. Compound **7b** (representative donor) was incubated in the presence of ES, CA and $Zn(OAc)_2$ in pH 7.4 buffer for 2 h. After 2 h of incubation, an aliquot from the reaction mixture was treated with methylene blue reagents (*N*,*N*-dimethyl-*p*-phenylene diamine and $FeCl_3$) and incubated for 30 min to allow the formation of methylene blue complex. Next, the reaction mixture was transferred to a 96 well plate and the absorbance profile was measured from 500 nm to 800 nm using a microtiter plate reader.[31] Compound **7b** in the presence of ES and CA showed a signal for the formation of methylene blue complex. However, no signal for the methylene blue complex was observed from compound **7b** in the absence of ES and CA, suggesting that the compounds were stable and selective towards activation by esterase (Figure 2.7).

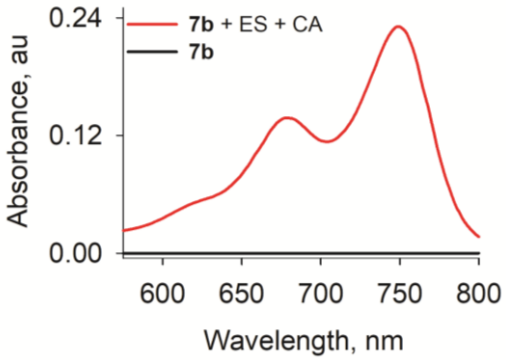

Figure 2.7. H_2S formation was determined by methylene blue assay using spectrophotometry after incubating compound **7b** in pH 7.4 buffer with ES and CA.

2.2.4. Kinetics of H_2S generation from carbonothioates (6a-6c):

2.2.4.1. Dansyl azide method:

Next, the kinetics of H_2S generation was evaluated to establish the dependence of the rates of H_2S formation on the leaving group. Dn-N_3 method was used to follow the formation of H_2S. The time course of Dn-NH_2 formation would act as a proxy for H_2S release. Compounds were incubated with ES, CA and Dn-N_3 in pH 7.4 buffer at 37 ^oC. The formation of Dn-NH_2 was followed at excitation 340 nm and emission 535 nm. H_2S generation profiles for carbonothioates are shown below (Figure 2.8). The rate constants for H_2S release were calculated by fitting the initial rate data into first order kinetics (Table 2.2). Although, there was a large difference in the pK_a values of the leaving group alcohols, however, the rates of H_2S release from carbonothioates were not significantly different in magnitude. Thus, rate of H_2S production could not be modulated by changing the leaving group alcohol.

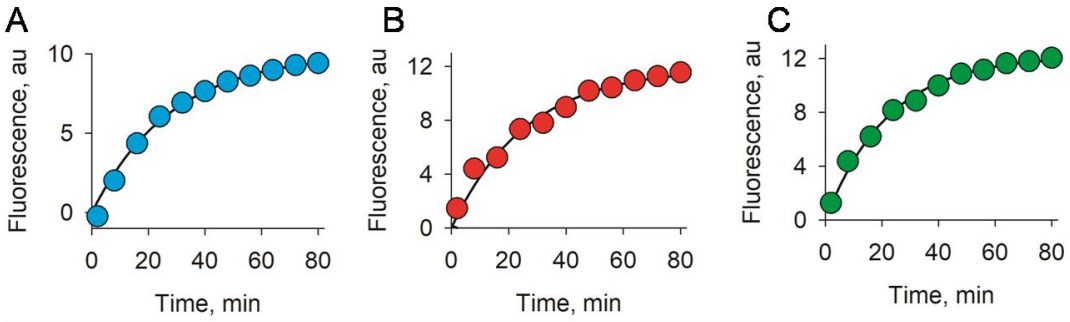

Figure 2.8. H_2S generation profile for carbonothioates (**6a** – **6c**) by following the formation of Dn-NH_2 from Dn-N_3. a) H_2S release profile for compound **6a**. b) H_2S release profile for compound **6b**. c) H_2S release profile for compound **6c**.

Table 2.2. Rates of H_2S production from carbonothioates (**6a - 6c**) using Dn-N_3 method.

Compd	R	k, min^{-1}	Rel. Rate	pK_a
6a	4-NO_2Ph	0.042	1	7.2
6b	Ph	0.040	0.95	9.9
6c	$PhCH_2$	0.039	0.93	14.4

2.2.4.2. Measuring the release of *p*-nitrophenol:

Previous results suggested that the rate of H_2S release could not be modulated with alcohols as leaving group. This was independently confirmed by following the time course of *p*-nitrophenol formation from compound **6a** and compound **4**. Compound **4** upon activation by ES would release *p*-nitrophenol without producing COS. Formation of *p*-nitrophenol from both the compounds was followed by measuring the absorbance at 405 nm using varioskan microtiter plate reader (Figure 2.9). The rate constant for *p*-nitrophenol formation was calculated to be 0.14 min^{-1} for **6a** and a comparable rate constant of 0.15 min^{-1} was recorded for compound **4**. Collectively these results suggested that the intermediate formed was short lived and readily decomposed to release COS and the leaving group. Although the rate of *p*-nitrophenol formation was found to be faster than the rate of H_2S release, the differences observed were small and did not support substantial accumulation of the intermediate.

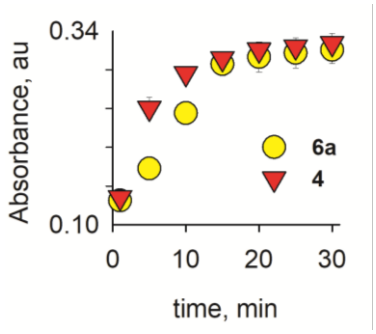

Figure 2.9. *p*-nitrophenol measurement from **6a** and **4** using microtiter plate reader.

2.2.4.3. *p*-nitrophenol formation using HPLC:

The release of *p*-nitrophenol was also monitored by HPLC analysis by following the decomposition of compound **6a** in the presence of ES. **6a** was incubated in pH 7.4 buffer containing ES at 37 ^{o}C and injected into HPLC. A complete disappearance of the compound peak was observed within 15 min of incubation in buffer indicating its fast reactivity towards ES. Concomitant formation of *p*-nitrophenol was recorded during this study which was confirmed by injecting an authentic sample of the compound (λ_{max} = 405 nm) (Figure 2.10).

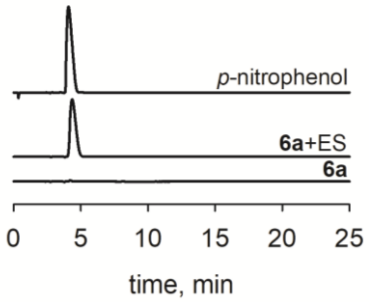

Figure 2.10. Representative HPLC plots for the formation of *p*-nitrophenol from compound **6a**.

2.2.4.4. Limitations of carbonothioates:

Carbonothioates were incapable of modulating the rate of H_2S release which was possibly due to the instability of the carbonothioate core towards ES. This was confirmed by a separate experiment where compound **6a** was incubated in two sets in the presence of ES and Dn-N_3 in pH 7.4 buffer at 37 ^{o}C and the formation of Dn-NH_2 was followed using a microtiter plate reader (λ_{ex} = 340 nm and λ_{em} = 535 nm). CA was added after 10 min of incubation to one of the sets (as marked by the arrow) (Figure 2.11). A fluorescence signal for the formation of Dn-NH_2 was observed from both the sets even in the absence of CA. However, an enhancement in the signal was observed upon addition of CA. This experiment indicated that carbonothioate core was cleaved by esterase to release free thiol which also reduced the Dn-N_3 to DN-NH_2 (Scheme 2.11). Thus, carbonothioates synthesized in this study were incapable of modulating the release of H_2S due to a competing reaction that was playing a role.

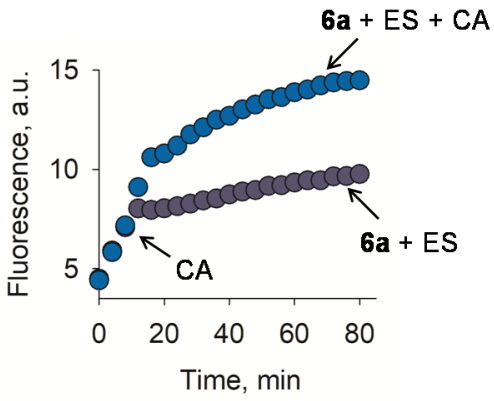

Figure 2.11. Dn-NH_2 formation from compound **6a** in the presence and absence of CA.

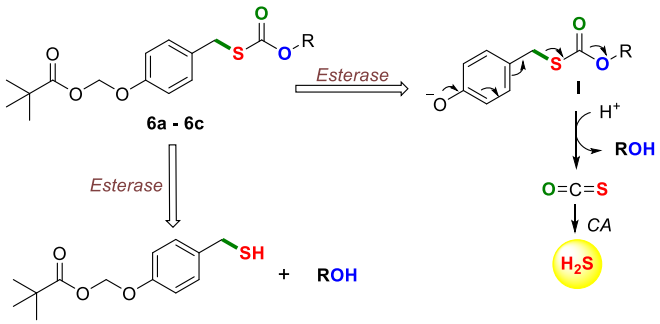

Scheme 2.11. Formation of thiol from carbonothioates upon reaction with ES.

2.2.5. Kinetics of H_2S generation from carbamothioates (7a-7c):

2.2.5.1. Dansyl azide method:

Next, the kinetics of H_2S release from carbamothioates (**7a-7c**) was examined using Dn-N_3 method. H_2S generation from the compounds was recorded after incubating the donors in buffer (pH 7.4) containing ES, CA and Dn-N_3 (Figure 2.12). The rate constants for H_2S release were calculated by fitting the initial rate data into first order kinetics. The relative rates for the formation of H_2S from compounds **7a** and **7b** were found to be comparable. However, the rate of H_2S release from compound **7c** was found to be slightly lower as compared to **7a** or **7b** (Table 2.3). Compounds **7a** (aniline as leaving group) and **7b** (*p*-anisidine as leaving group) with amines of lower pK_aH value showed a slightly higher rate of H_2S production compared to compound **7c** (with benzyl amine as leaving group) which had a higher pK_aH value. This indicated that the rate of H_2S release from carbamothioates based donors may be dependent on the basicity of the amine.

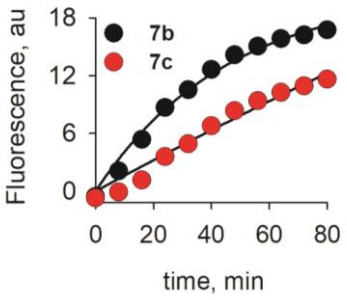

Figure 2.12. H_2S release profile from **7b** and **7c** using Dn-N_3.

Table 2.3. Rates of H_2S production from carbamothioates (**7a** – **7c**) using Dn-N_3 method.

Compd	**R**	k, min^{-1}	Rel. Rate	pK_aH
7a	Ph	0.031	0.97	4.6
7b	4-OMePh	0.032	1	5.2
7c	$PhCH_2$	0.014	0.44	9.1

2.2.5.2. Methylene Blue assay:

The difference in the rates of H_2S release obtained in the case of carbamothioates was further investigated using methylene blue assay. Formation of methylene blue complex from compounds **7b** and **7c** was followed over a period of time. Compounds were incubated in pH 7.4 buffer in the presence of ES, CA and $Zn(OAc)_2$ at 37 ^oC. At predetermined time points, an aliquot was taken from the reaction mixture and treated with methylene blue reagents and incubated for 30 min at 37 ^oC to allow the formation of the complex. After methylene blue formation the reaction mixture was transferred to a 96 well plate and an absorbance profile was measured from 500- 800 nm (Figure 2.13). H_2S production from **7b** and **7c** was monitored for a period of 4 h. Saturation in the signal corresponding to H_2S release was observed from compound **7b** after 1 h of incubation (Figure 2.13a insight) whereas the signal for H_2S release from **7c** kept on increasing even after 4 h of incubation (Figure 2.13b insight). The results obtained were in accordance with the rates observed with Dn-N_3 experiment. Collectively, the data suggested that carbamothioates could be used to modulate the rate of H_2S release.

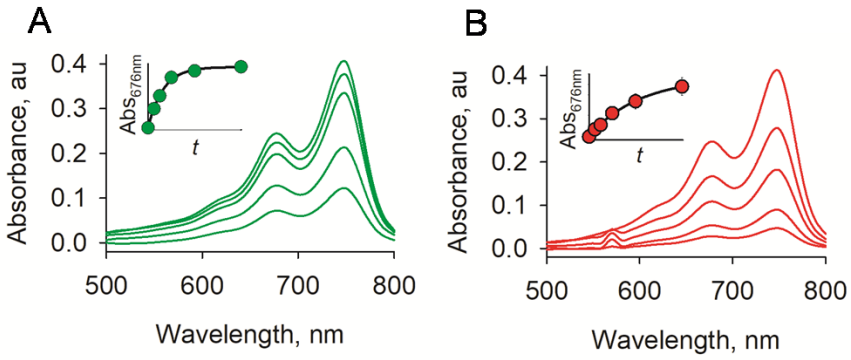

Figure 2.13. a) Methylene blue profile for compound **7b** obtained over a period of 4 h at different time intervals – 15 min, 30 min, 60 min, 120 min and 240 min. b) Methylene blue profile obtained for compound **7c** over a period of 4 h.

2.2.6. Methylene blue assay with CA inhibitor:

The production of COS in the reaction mixture was further validated by using acetazolamide, **8**, a known CA inhibitor (Figure 2.14a). The signal for H_2S release from compounds was expected to go down in the presence of CA inhibitor. Compound **7b** when incubated in the presence of **8**, showed a significant decrease in the formation of methylene blue complex compared to the untreated sample (Figure 2.14b). Ctrl represents **7b** treated with ES in the absence of CA. No methylene blue formation was observed in the absence of CA suggesting that the carbamothioates were stable towards hydrolysis and produced H_2S only upon activation by esterase. The experiment supported the hypothesis that H_2S was produced from the COS/H_2S donors via generation of COS.

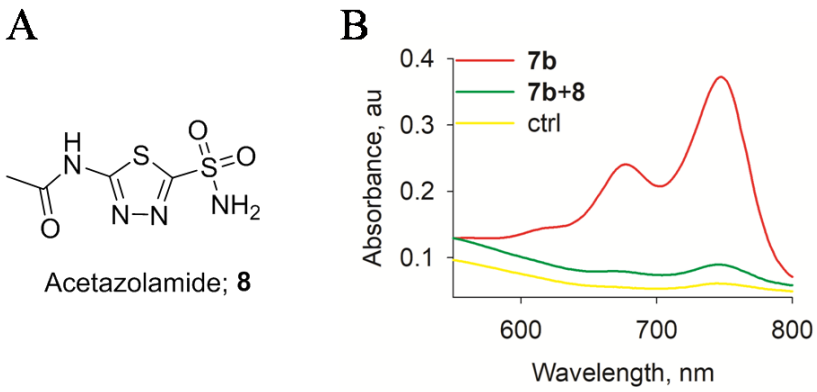

Figure 2.14. a) Structure of acetazolamide. b) Methylene blue assay for the detection of H_2S from compound **7b** in the presence of acetazolamide, **8.**

2.2.7. HPLC Analysis:

In order to understand the mechanism of generation of COS, decomposition of compounds **7b** and **7c** were followed by HPLC**.** Compounds were incubated in buffer containing ES at 37 ^{o}C and injected in HPLC at different time points. A complete disappearance of peak corresponding to compound **7b** was observed after 15 min of incubation in the presence of ES (Figure 2.15a). A new peak was formed in the process which decomposed over a period of 60 min (Figure 2.15b) and led to the formation of *p*-anisidine (Figure 2.16). The new peak formed was attributable to the formation of an intermediate. Thus, pivaloyloxymethyl group undergoes a rapid cleavage in the presence of esterase to generate an intermediate which further dissociates to release COS.

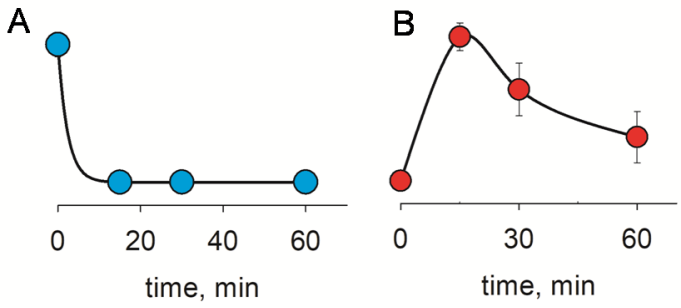

Figure 2.15. a) Area under the curve for the decomposition of compound **7b**. b) Dissociation of the intermediate formed in the course of reaction.

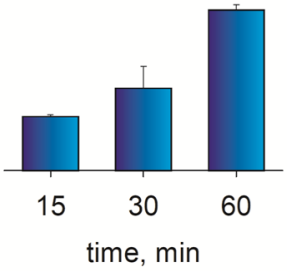

Figure 2.16. Area under the curve corresponding to the formation of *p*-anisidine.

Decomposition profile of compound **7c** showed a rapid disappearance of the compound in 15 min as observed in the case of **7b** (Figure 2.17, 2.18a). However, the intermediate formed in this case was comparatively long lived and gradually decomposed over a period of 6 h (Figure 2.18b). This clearly established the fast reactivity of the trigger towards the stimulus. Although we were unable to characterize the intermediate, it seemed that the rate of COS

release was dependent on the decomposition of the intermediate formed. Hence, the carbamothioates developed herein could offer distinct advantage in modulating the rates of H_2S production through stereoelectronic effects of the nitrogen.

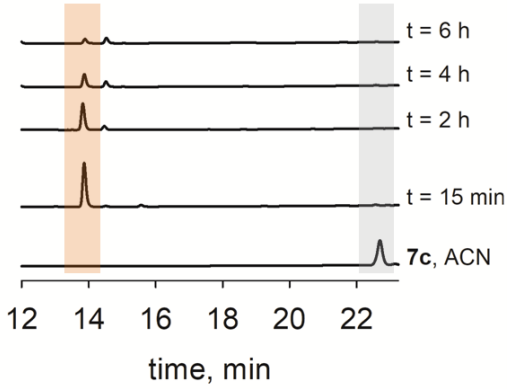

Figure 2.17. Representative HPLC traces for decomposition of compound **7c** in the presence of ES.

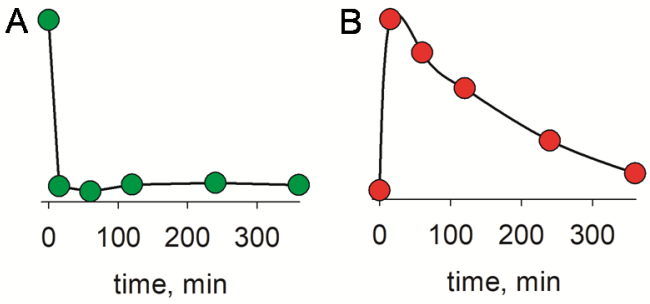

Figure 2.18. a) Area under the curve corresponding to the decomposition of **7c**. b) Area under the curve corresponding to the dissociation of the intermediate formed during the course of the reaction.

2.2.8. Mechanism:

Based on the results obtained, the mechanism of COS release from the donors was proposed. The pivaloyl ester cleavage was rapid with esterase which was demonstrated by HPLC analysis suggesting that the first step was not the rate determining step. Compounds upon reaction with esterase formed an intermediate which further decomposed to release COS. The rate of COS release was found to be dependent on the decomposition of the intermediate. Therefore, based on the observations the mechanism of COS release was proposed.

Reaction of compound with ES forms intermediate **I** which may further dissociate to form intermediate **II**. The rate of H_2S release may be dependent on the decomposition of intermediate **II**. However, in case of carbonothioates, the rate of decomposition of

intermediate **II** is fast which is partly due to the competing pathway of thiol release. In case of carbamothioates, the rate of COS release is dependent on the decomposition of intermediate which is further dependent on the basicity of the leaving group amine (Scheme 2.12).

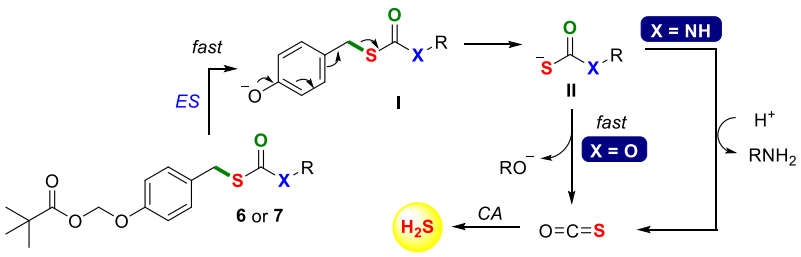

Scheme 2.12. Mechanism of COS release from the donors.

2.2.9. Cell viability assay:

Cell viability from the H_2S donors was demonstrated in human breast cancer, MCF-7 cells using standard MTT assay. Cells were treated with varying concentrations of H_2S donors and incubated for 24 h. No significant cytotoxicity from 50 µM concentration of the compounds was observed indicating that the H_2S donor motifs were well tolerated by the cells and can be used for further biological assays (Figure 2.19).

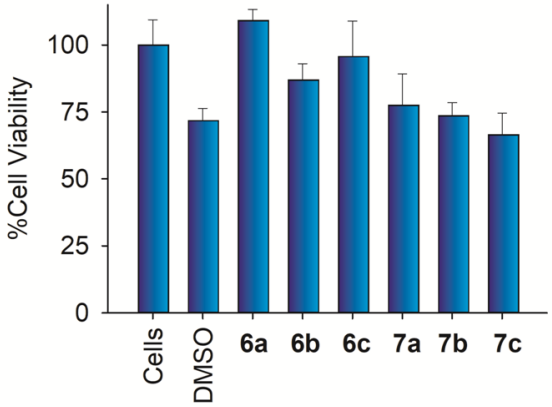

Figure 2.19. Cell Viability assay for cytotoxicity of H_2S donor motifs in MCF-7 cells.

2.2.10. Detection of H_2S in cells

The ability of compounds to generate H_2S within cells was tested by using NBD-Fluorescein, a H_2S sensitive dye (Figure 2.20).[36] H_2S upon reaction with NBD-Fluorescein releases free flourescein which can be visualized using fluorescence microscopy. The cells were co-incubated with H_2S donor (**7b**) and NBD-Fluorescein dye (10 µM) for 40 min. A dose

dependent increase in the fluorescence signal was observed from compound **7b** (Figure 2.21). Thus, compounds were capable of producing H_2S within cells.

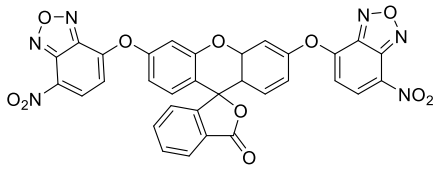

NBD-Fluorescein

Figure 2.20. Structure of NBD-Flourescein dye used for H_2S detection in cells

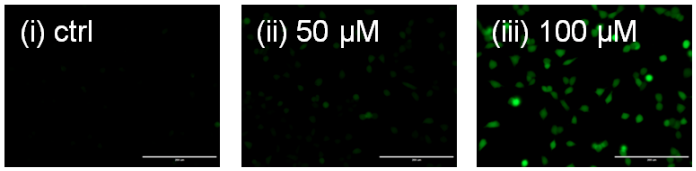

Figure 2.21. Detection of H_2S from compound **7b** in cells using NBD-Fluorescein. Ctrl represents dye alone.

2.3. Other reports

Pluth and co-workers have also reported esterase activated COS/H_2S donors. They demonstrated rapid decomposition of the compounds to release COS (Scheme 2.13). However, the compounds reported were toxic and reduced cellular respiration and ATP synthesis in BEAS 2B human lung epithelial cells. Also, no tunable release of H_2S was reported from these donors.

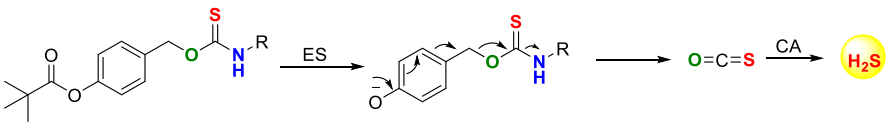

Scheme 2.13. Esterase activated thiocarbamate based COS/H_2S donors.

2.4. Summary

In summary, we have synthesized a series of carbonothioates and carbamothioates based COS/H_2S which generate H_2S under physiologically relevant conditions. H_2S produced from these donors was validated via four independent methods. We observed a rapid cleavage of these compounds in the presence of esterase to generate COS which was further hydrolysed

by CA to produce H_2S. The rate of H_2S release from these scaffolds was studied. Carbonothioates (with alcohols as leaving group) were unable to modulate the rate of H_2S release. Carbamothioates, on the other hand, showed a slight difference in the rates of H_2S production. Although the difference observed was small but it laid a strong foundation to further investigate the effects of basicity of amines on the rates of H_2S production. The H_2S donor motifs were found to be well tolerated by the cells and were capable of producing H_2S within cells. The donors provide tools for wide range of biological applications.

2.5. Experimental and characterization of data:

2.5.1. Experimental section:

Compound **2**[37] was synthesized using a previously reported procedure and the analytical data that we collected were consistent with the reported values: ^{1}H-NMR spectra are included below. Compounds **5a**, 5**b** and 5**c** were synthesised using a reported procedure and were taken further for the next step without purification.[38]

(4-(mercaptomethyl)phenoxy)methyl pivalate (3):

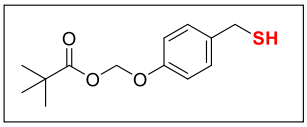

To a well stirred ice cold solution of **2 (**2.08g, 8.2mmol)in dry DCM (15 mL), PBr_3 (0.9 mL, 9.9mmol) was added slowly under N_2 atmosphere. The reaction was allowed to stir for 1 h at 0 °C (progress of the reaction was monitored by TLC). Reaction was quenched by adding 15 mL of saturated $NaHCO_3$. Aqueous layer was extracted using DCM (3 × 10 mL). The combined organic layer was dried over Na_2SO_4, filtered and concentrated. The compound was obtained as light yellow oil. This was further dissolved in dry THF (15 mL) and thiourea salt (0.9 g, 12.7 mmol) was added at room temperature and the reaction mixture was stirred overnight. After completion of the reaction, solvent was removed under reduced pressure and the salt obtained was dissolved in water (20 mL) followed by the addition of DCM (30 mL). The reaction mixture was purged with N_2 for 5 min. To this heterogeneous solution, 4 equivalents of sodium metabisulfite salt ($Na_2S_2O_5$, 4.82 g, 25.4mmol) were added. The resulting mixture was refluxed for 6 h under N_2 atmosphere. The solution was cooled to room temperature and washed twice with DCM (20 mL). The combined organic layer was dried over Na_2SO_4, filtered and concentrated. The crude obtained was purified using silica gel column chromatography (2% EtOAc/ hexane). Compound **3** was obtained as a colorless liquid with pungent smell (1.3 g, 58%). FT-IR (ν_{max}, cm^{-1}): 1745; ^{1}H NMR (400 MHz, $CDCl_3$): δ 7.26 (d, *J* = 8.6 Hz, 2H), 6.98 (d, *J* = 8.7 Hz, 2H), 5.75 (s, 2H), 3.72 (d, *J* = 7.4 Hz, 2H), 1.75 (t, *J* = 7.4 Hz, 1H), 1.21 (s, 9H); ^{13}C NMR (100 MHz, $CDCl_3$): δ 177.4, 156.0, 135.4, 129.2, 116.4, 85.9, 38.9, 28.3, 26.9; HRMS (ESI) for $C_{13}H_{18}O_3S$ $[M+Na]^+$: Calcd., 291.1030, Found., 291.1610.

(4-((((4-nitrophenoxy)carbonyl)thio)methyl)phenoxy)methyl pivalate (6a):

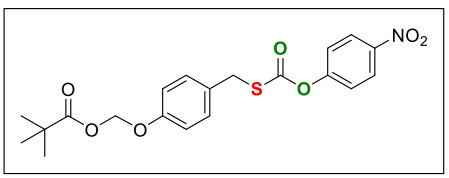

To a well stirred solution of **3** (0.05 g, 0.2 mmol) in dry ACN, *p*-nitrophenylchloroformate (0.04 g, 0.2 mmol)

was added followed by the addition of K_2CO_3 (0.08 g, 0.6 mmol). The reaction mixture was stirred for 17 h at room temperature and the progress of the reaction was monitored by TLC. To the resulting mixture was then added 10 mL of water and washed twice with DCM (5 mL). The combined organic layer was dried over Na_2SO_4, filtered and concentrated. The resulting crude was purified using silica gel chromatography (4% EtOAc / hexane) to give compound **6a** in (0.064g, 77%) as a white solid. FT-IR (ν_{max}, cm^{-1}): 1746, 1709, 1518, 1345, 1154; ^{1}H NMR ($CDCl_3$, 400 MHz): δ 8.27 (d, *J* = 9.2 Hz, 2H), 7.36 - 7.30 (m, 4H), 7.00 (d, *J* = 8.7 Hz, 2H), 5.76 (s, 2H), 4.17 (s, 2H), 1.21 (s, 9H); ^{13}C NMR ($CDCl_3$, 100 MHz): δ 177.4, 169.3, 156.7, 155.6, 145.4, 130.3, 125.3, 122.0, 116.5, 85.8, 38.9, 35.3, 26.9; HRMS (ESI) for $C_{20}H_{21}NO_7S$ $[M+Na]^+$: Calcd., 442.0936, Found, 442.0946.

(4-(((phenoxycarbonyl)thio)methyl)phenoxy)methyl pivalate (6b):

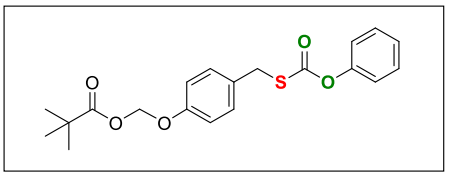

Compound **6b** was prepared according to the procedure outlined for **6a**: Yield (0.184g, 64%); FT-IR (ν_{max}, cm^{-1}): 1724, 1156; ^{1}H NMR ($CDCl_3$, 400 MHz): δ 7.38 (t, *J* = 8.0 Hz, 2H), 7.31 (d, *J* = 8.6 Hz, 2H), 7.26 – 7.22 (m, 1H), 7.14 (d, *J* = 7.6 Hz, 2H), 6.99 (d, *J* = 8.6 Hz, 2H), 5.75 (s, 1H), 4.14 (s, 1H), 1.21 (s, 9H); ^{13}C NMR ($CDCl_3$, 100 MHz): δ 177.4, 170.0, 156.5, 151.1, 130.9, 130.3, 129.5, 126.2, 121.3, 116.3, 85.8, 38.9, 35.1, 26.9; HRMS (ESI) for $C_{20}H_{22}O_5S$ $[M+Na]^+$: Calcd., 397.1085, Found, 397.1086.

(4-((((benzyloxy)carbonyl)thio)methyl)phenoxy)methyl pivalate (6c):

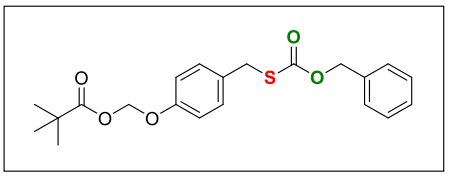

Compound **6c** was prepared according to the procedure outlined for **6a**: Yield (0.071g, 16%); FT-IR (ν_{max}, cm^{-1}): 1747, 1711, 1128; ^{1}H NMR ($CDCl_3$, 400 MHz): δ7.37 – 7.34 (m, 5H), 7.27 (d, *J* = 8.8 Hz, 2 H), 6.96 (d, *J* = 8.7 Hz, 2H), 5.74 (s, 2H), 5.24 (s, 2H), 4.08 (s, 2H), 1.20 (s, 9H); ^{13}C NMR ($CDCl_3$, 100 MHz): δ 177.5, 170.9, 156.5, 135.2, 131.4, 130.2, 128.7, 128.6, 128.5, 116.4, 85.9, 69.2, 39.0, 34.9, 27.0; HRMS (ESI) for $C_{20}H_{24}O_5S$ $[M+Na]^+$: Calcd., 411.1241, Found, 411.1250.

(4-(((phenylcarbamoyl)thio)methyl)phenoxy)methyl pivalate (7a):

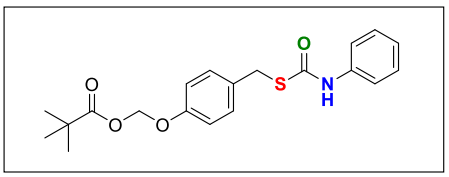

To a solution of compound **3** (0.2 g, 0.8 mmol) in THF (5 mL) was added Et_3N (0.2 mL, 1.6 mmol) at 0 ^oC. The reaction mixture was stirred for 2- 3 h and the progress was monitored by TLC. The reaction was quenched by adding 10 mL of water and the aqueous layer was washed with EtOAc (2 × 10 mL). The combined organic layer was dried over Na_2SO_4, filtered and concentrated under reduced pressure. Purification was done using prep HPLC and ACN- water as the eluant. Compound **7a** was obtained as a white solid (0.034 g, 11%). FT-IR (ν_{max}, cm^{-1}): 3323, 1738, 1671, 1151; ^1H NMR ($CDCl_3$, 400 MHz): δ 7.41 (d, *J* = 7.7 Hz, 2H), 7.33 – 7.29 (m, 4H), 7.11 (t, *J* = 7.3 Hz, 1H), 7.07 (bs, 1H), 6.97 (d, *J* = 7.8 Hz, 2H), 5.74 (s, 2H), 4.19 (s, 2H), 1.20 (s, 9H); ^{13}C NMR ($CDCl_3$, 100 MHz): δ 177.4, 165.2, 156.3, 137.6, 132.2, 130.1, 129.2, 124.6, 119.9, 116.3, 85.9, 38.9, 33.9, 26.9; HRMS (ESI) for $C_{20}H_{23}NO_4S$ $[M+Na]^+$: Calcd., 396.1245, Found, 396.1245.

(4-((((4-methoxyphenyl)carbamoyl)thio)methyl)phenoxy)methyl pivalate (7b):

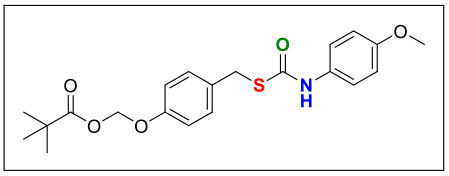

Compound **7b** was synthesised using procedure outlined for **7a**: Yield (0.14g, 44%); FT-IR (ν_{max}, cm^{-1}): 3319, 1740, 1676, 1152; ^1H NMR ($CDCl_3$, 600 MHz): δ7.30 – 7.28 (m, 4H), 7.02 (s, 1H), 6.96 (d, *J* = 8.5 Hz, 2 H), 6.85 (d, *J* = 9.0 Hz, 2H), 5.73 (s, 2H), 4.16 (s, 2H), 3.78 (s, 3H), 1.20 (s, 9H); ^{13}C NMR ($CDCl_3$, 150 MHz): δ 177.4, 165, 156.3, 150.2, 132.3, 130.1, 129.9, 121.6, 116.3, 114.3, 85.9, 55.5, 38.9, 33.8, 26.9; HRMS (ESI) for $C_{21}H_{25}NO_5S$ $[M+Na]^+$: Calcd., 426.1350, Found, 426.1350.

(4-(((benzylcarbamoyl)thio)methyl)phenoxy)methyl pivalate (7c):

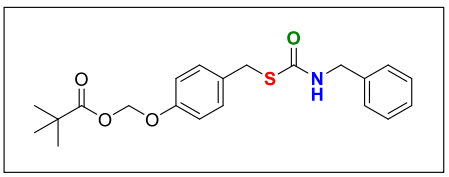

Compound **7c** was synthesised using procedure outlined for **7a**: Yield (0.139g, 37%); FT-IR (ν_{max}, cm^{-1}): 3328, 1744, 1658, 1156; ^1H NMR ($CDCl_3$, 400 MHz): δ 7.34 – 7.26 (m, 7H), 6.96 (d, *J* = 8.7 Hz, 2H), 5.74 (s, 2H), 5.60 (bs, 1H), 4.49 (d, *J* = 5.3 Hz, 2H), 4.15 (s, 2H), 1.21 (s, 9H); ^{13}C NMR ($CDCl_3$, 100 MHz): δ 177.4, 166.9, 156.2, 137.5, 132.5, 130.3, 130.1, 128.8, 127.8, 121.6, 116.3, 85.9, 45.5, 38.9, 33.7, 26.9; HRMS (ESI) for $C_{21}H_{25}NO_4S$ $[M+Na]^+$: Calcd., 410.1401, Found, 410.1398.

(4-((4-nitrophenoxy)methyl)phenoxy)methyl pivalate (4):

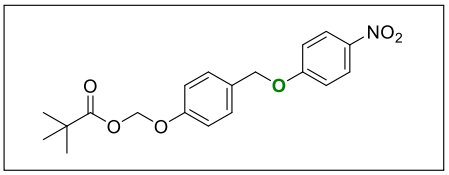

To a well stirred ice cold solution of **2** (0.2 g, 0.8 mmol) in dry DCM (5 mL), PBr_3 (0.09 mL, 0.9 mmol) was added slowly under N_2 atmosphere. The reaction was allowed to stir at 0 ^oC for 1 h. After completion, the reaction was quenched by adding 10 mL of saturated $NaHCO_3$ solution. Aqueous layer was extracted using DCM (3 × 5 mL). The combined organic layer was dried over Na_2SO_4, filtered and concentrated. The oily liquid so obtained was dissolved in ACN (5 mL) followed by the addition of *p*- nitrophenol (0.17 g, 1.25 mmol) and K_2CO_3 (0.26 g, 1.9 mmol). The mixture was allowed to stir at room temperature for 12 h. The reaction mixture was then quenched with water (10 mL) and extracted with DCM (10 mL). The organic layer was dried over Na_2SO_4, filtered and concentrated under reduced pressure. Purification was done using silica gel chromatography and EtOAc/ hexane as the eluents. Compound **4** was obtained as a white solid (0.023 g, 10% overall yield).FT-IR (ν_{max}, cm^{-1}): 1745, 1512, 1339; ^1H NMR ($CDCl_3$, 400 MHz): δ 8.21 (d, *J* = 9.3 Hz, 2H), 7.37 (d, *J* = 8.8 Hz, 2H), 7.07 (d, *J* = 8.3 Hz, 2H), 7.03 (d, *J* = 9.3 Hz, 2H), 5.78 (s, 2H), 5.10 (s, 2H), 1.21 (s, 9H); ^{13}C NMR ($CDCl_3$, 100 MHz): δ 177.4, 163.6, 157.2, 141.7, 129.6, 129.3, 128.7, 125.9, 116.4, 114.8, 85.6, 70.3, 38.9, 26.9; HRMS (ESI) for $C_{19}H_{21}NO_6$ $[M+Na]^+$: Calcd., 382.1266, Found, 382.1275.

2.5.2 H_2S detection using Dansyl Azide:

A 10 mM stock solution of dansyl azide and a 5 mM stock solution of COS/H_2S donors were independently prepared in DMSO. The stock solutions of porcine liver esterase (2 U/mL, pH 7.4 PBS buffer) and carbonic anhydrase from bovine erythrocytes (67 μM in HEPES buffer pH 7.4, 100 mM KCl) were prepared. The experiment was done in a 96 well plate. For the experiment described in Figure 2.1, the reaction mixture consisted of COS/ H_2S donors or **4** (50 μM), esterase 1 U/mL and 2 μL of carbonic anhydrase from bovine erythrocytes enzyme in pH 7.4 buffer and Dn-N_3 (100 μM) was added after 60 min. The fluorescence was measured using microtiter plate reader (λ_{ex} = 340 nm and λ_{em} = 535 nm). For the kinetics experiment described below, Dn-N_3 was co-incubated with the donors and the enzymes and the fluorescence of the Dn-NH_2 formed was measured.

2.5.3 Detection of dansyl amine formation using HPLC:

A stock solution of **6c** (5 mM) and dansyl azide (10 mM) were prepared in DMSO. The reaction mixture contained **6c** (2 μL, 5 mM), Dn-N_3 (2 μL, 10 mM), 100 μL of esterase enzyme solution (2 U/mL in PBS) and 2 μL of CA enzyme solution (1% in HEPES buffer) in

96 μL of PBS buffer and incubated at 37 ^{o}C for 40 min. The resulting mixture was filtered (0.22 micron filter) and injected (50 μL) in a high performance liquid chromatography (HPLC Agilent Technologies 1260 Infinity). The mobile phase was H_2O/ CH_3CN. The stationary phase was C-18 reverse phase column (Phenomenex, 5 μm, 4.6 x 250 mm). CH_3CN concentration was increased linearly from 30% to 80% over 20 min and maintained at 80% for another 10 min at a flow rate of 1 mL/min. The formation of dansyl amine was monitored by a fluorescence detector with excitation at 340 nm and emission at 535 nm. Authentic Na_2S solution (50 μM) was reacted with Dn-N_3 (100 μM) in phosphate buffer and used as a positive control. Under these conditions Dn-NH_2 eluted at 15.3 min.

2.5.4. Lead Acetate Paper Test:

A strip of Whatman filter paper was taken and dipped into a saturated aqueous solution of lead(II) acetate.[39] The paper strip was dried by keeping it in the oven for 3-4 h at 65 ^{o}C and then cut into small strips to be used for the test. To compound **6c** (1 mM), porcine liver esterase (0.01 U/μL) and carbonic anhydrase from bovine erythrocytes (3.3 μM) was added in pH 7.4 buffer followed by the addition of a (1 cm^2) piece of lead acetate paper into the reaction mixture. It was incubated for 2 h at 37 ^{o}C. The brown coloration of the lead acetate paper confirmed the production of H_2S. Compound **6c** alone was taken as a control.

2.5.5. Methylene Blue method for H_2S detection:

Each assay described was done in triplicate in vials with closed lids, containing 470 μL of PBS, 10 μL of compound **7b** (10 mM stock in DMSO), 500 μL of esterase (2U/mL stock in PBS), 10 μL carbonic anhydrase (1% stock in HEPES buffer) and 10 μL $Zn(OAc)_2$ (10 mM stock in H_2O) . The reaction mixture was incubated at 37 ^{o}C. At predetermined time points 100 μL aliquot was removed from each reaction vial and diluted with 100 μL of $FeCl_3$ (30 mM stock in 1.2 M HCl) and 100 μL of *N*,*N*–dimethyl-*p*-pheneylenediamine sulfate (20 mM stock in 7.2 M HCl). The aliquots were stored until the final aliquot had been taken to allow the formation of methylene blue complex. After completion of the reaction, aliquots were transferred to a 96 well plate (250 μL/ well) and the absorbance spectra were collected from 500 to 800 nm on a plate reader. The analysis was done by subtracting the absorbance of the control experiment. Calibration curve was obtained using similar conditions (Figure 2.22b). Based on the calibration curve, 74% of H_2S is obtained from **7c** and 55% of H_2S was obtained from **7b** after 4h.

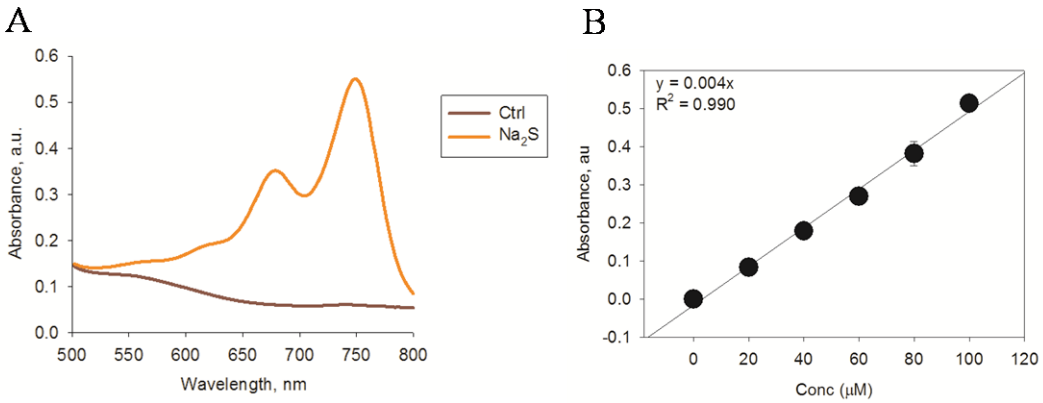

Figure 2.22. a) Methylene blue assay for H_2S detection with Na_2S. b) Calibration curve with $Na_2S.9H_2O$.

2.5.6. Methylene Blue assay with CA Inhibitor:[31]

Each assay described was done in triplicate in vials with closed lids, containing 92 µL of PBS, 2 µL of compound **7b** (10 mM stock in DMSO), 100 µL of esterase (2U/mL stock in PBS), 2 µL carbonic anhydrase (1% stock in HEPES buffer), 2 µL acetazolamide (5 mM stock in PBS pH 7.4 buffer) and 2 µL of Zn $(OAc)_2$ (40 mM stock in H_2O). The reaction was allowed to stir at 37 ^oC for 60 min. 100 µL of the reaction aliquot was taken out and diluted with 100 µL of $FeCl_3$ (30 mM stock in 1.2 M HCl) and 100 µL of N,N–dimethyl-p-pheneylenediamine sulfate (20 mM stock in 7.2 M HCl). The reaction was again stirred for 30 min and the aliquots were transferred to a 96 well plate (250 µL/ well). The absorbance spectra were collected from 600 to 800 nm.

2.5.7. H_2S detection using an electrode:

The calibration of the electrode (Lazar Research Laboratories, Inc.) was done using a freshly prepared $Na_2S.\ 9H_2O$ solution in antioxidant buffer. The manufacturer's protocol was followed. The reaction was carried out in a closed vial containing a small magnetic bead for stirring the solution. Compound **6a** (100 µM) was dissolved in phosphate buffer pH 7.4 along with carbonic anhydrase (0.6 µM) and incubated 37^oC for 5 min. To this, esterase enzyme solution (1 U/ mL) was added and the reaction was followed.

2.5.8. Detection of COS by mass spectrometry:

The reaction was performed in a closed vial with compound **6a** (50 µM) and esterase (0.5 U/mL) in pH 7.4 buffer. The reaction mixture was incubated at 37^oC for 30 min. ESI- MS spectra was recorded by direct injection of the reaction mixture in Agilent 6540 UHD QTOF MS with Dual Jet Stream ESI source. The gas temperature was 325 ^oC with gas flow rate being 5L/ min. The spectra was acquired in positive mode with specific conditions being as

follows: sheath gas temperature 295 ^{o}C, capillary voltage 3500 V, fragmentor 270, scan rate 2 Hz, and the mass range from 50–500 a.m.u. The spectra were acquired using Mass Hunter software.

2.5.9. Formation of 4-nitrophenol:

A stock solution of **6a** (10 mM) was prepared in DMSO. The reaction mixture contained **6a** (2 μL, 10 mM), 100 μL of esterase enzyme solution in 98 μL of pH 7.4 PBS buffer and incubated at 37^{o}C for 40 min. The resulting mixture was filtered (0.22 micron filter) and injected (50 μL) in a high performance liquid chromatography (HPLC Agilent Technologies 1260 Infinity).The mobile phase was H_2O/ CH_3CN. The stationary phase was C-18 reverse phase column (Phenomenex, 5 μm, 4.6 x 250 mm). A linear increase in the CH_3CN concentration from 30% to 80 % over 20 min and then keeping 80% for another 10 min at a flow rate of 1 mL/ min. 4- nitrophenol release was monitored by UV detector at 405 nm. Authentic 4-nitrophenol solution (100 μM) was used as a positive control. Under these 4-nitrophenol was eluted at 4.3 min retention time.

2.5.10. Microwell assay for 4-nitrophenol release:

A 5 mM stock solution of compound **6a** in DMSO and a 2 U/mL stock solution of procrine liver esterase enzyme (Sigma Aldrich) were prepared using pH 7.4 buffer. The experiment was performed in a 96 well plate. The reaction mixture consisted of compound **6a** (50 μM) and esterase 1 U/mL in pH 7.4 buffer. In the control set only compound **6a** (50 μM) was added. Absorbance was measured using microtiter plate reader (Abs = 405 nm).

2.5.11. Cell viability Assay:

Human breast cancer cells MCF-7 were seeded at a concentration of 1×10^3 cells/well overnight in a 96-well plate in complete DMEM media. Cells were exposed to varying concentrations of the test compounds prepared as a DMSO stock solution so that the final concentration of DMSO was 0.5%. The cells were incubated for 24 h at 37 ^{o}C. A stock solution of 3-(4, 5-dimethylthiazol-2-yl)-2, 5-diphenyl tetrazolium bromide (MTT) was prepared 3.5 mg in 700 μL DMEM. This stock was diluted with 6.3 mL DMEM and 100 μL of the resulting solution was added to each well. After 4 h incubation, the media was removed carefully and 100 μL of DMSO was added. Spectrophotometric analysis of each well using a microplate reader (Thermo Scientific Varioscan) at 570 nm was carried out to estimate cell viability.

2.5.12. Detection of H_2S in cells:

MCF-7 cells were seeded at 1×10^5 cells/well in 6-well corning plate for overnight in DMEM medium supplemented with 10% FBS (fetalbovin serum) and 1% antibiotic solution in an atmosphere of 5% CO_2 at 37 °C. After incubation, media was removed and the cells were washed with 1 mL of PBS (1X) buffer. Then 1 mL of fresh DMEM media was added along with compound (50 µM, 100µM) and NBD Fluorescein dye (10µM, Figure 2.9c). The cells were incubated for 40 minutes at 37 °C. After 40 minutes, old media was removed, cells were washed with 1mL of PBS (1X) and then were imaged on an EVOS fluorescence microscopy with 20 X GFP filter.

2.5.13. H_2S Detection using NBD- fluorescein:

A 1 mM stock solution of NBD- fluorescein and a 5 mM stock solution of COS/H_2S donors were independently prepared in DMSO. The stock solutions of porcine liver esterase (2 U/mL, pH 7.4 PBS buffer) and carbonic anhydrase from bovine erythrocytes (67 µM in HEPES buffer pH 7.4, 100 mM KCl) were prepared. The experiment was done in closed vials. The reaction mixture consisted of **7b** or **4** (50 µM), esterase 1 U/mL, NBD- fluorescein (10 µM) and 2 µL of carbonic anhydrase from bovine erythrocytes enzyme in pH 7.4 buffer. The reaction mixture was incubated at 37 ^oC for 60 min following which 200 µL of the aliquot was transferred to the 96 well plate. The fluorescence was measured using microtiter plate reader (λ_{ex} = 490 nm and λ_{em} = 514 nm) (Figure 2.23).

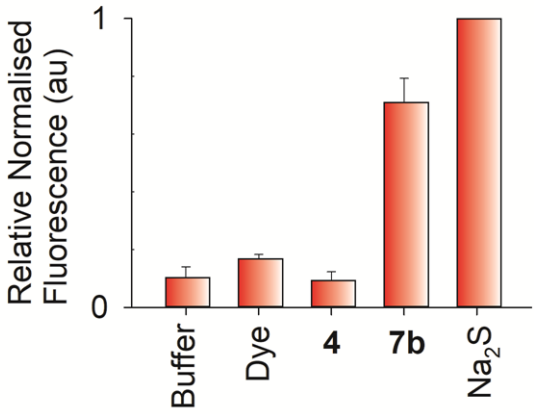

Figure 2.23. Selectivity data with NBD Fluorescein

2.6. Spectral Charts:

^{1}H-NMR ($CDCl_3$, 400 MHz) for Compound **3**:

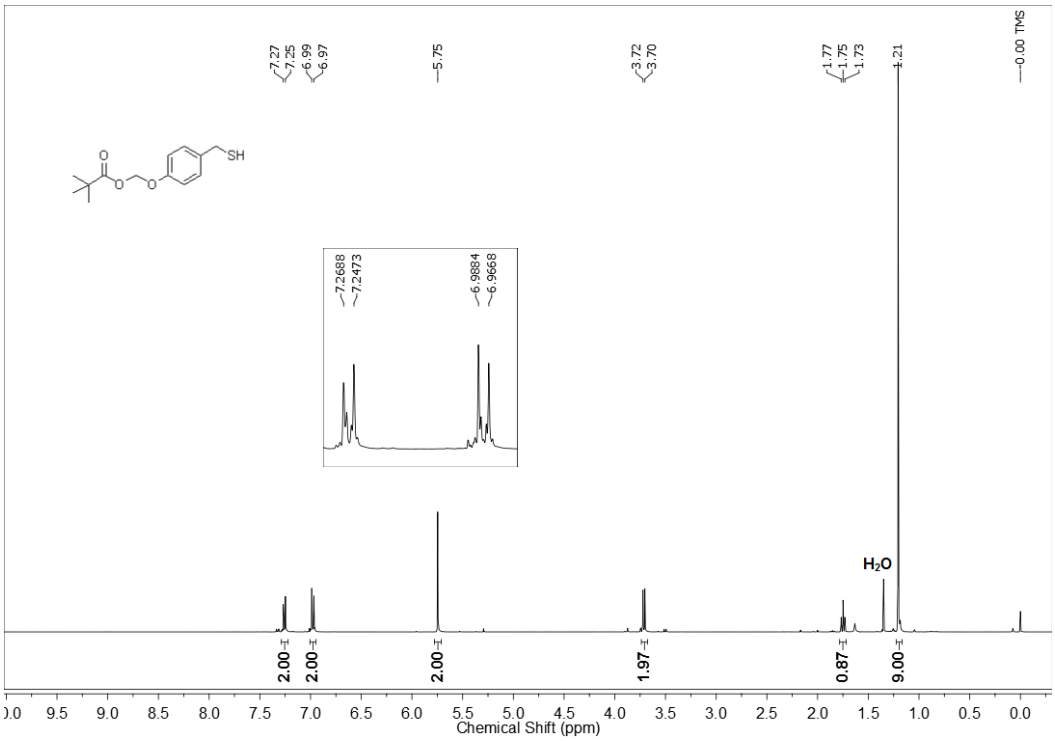

^{13}C-NMR ($CDCl_3$, 100 MHz) for Compound **3**:

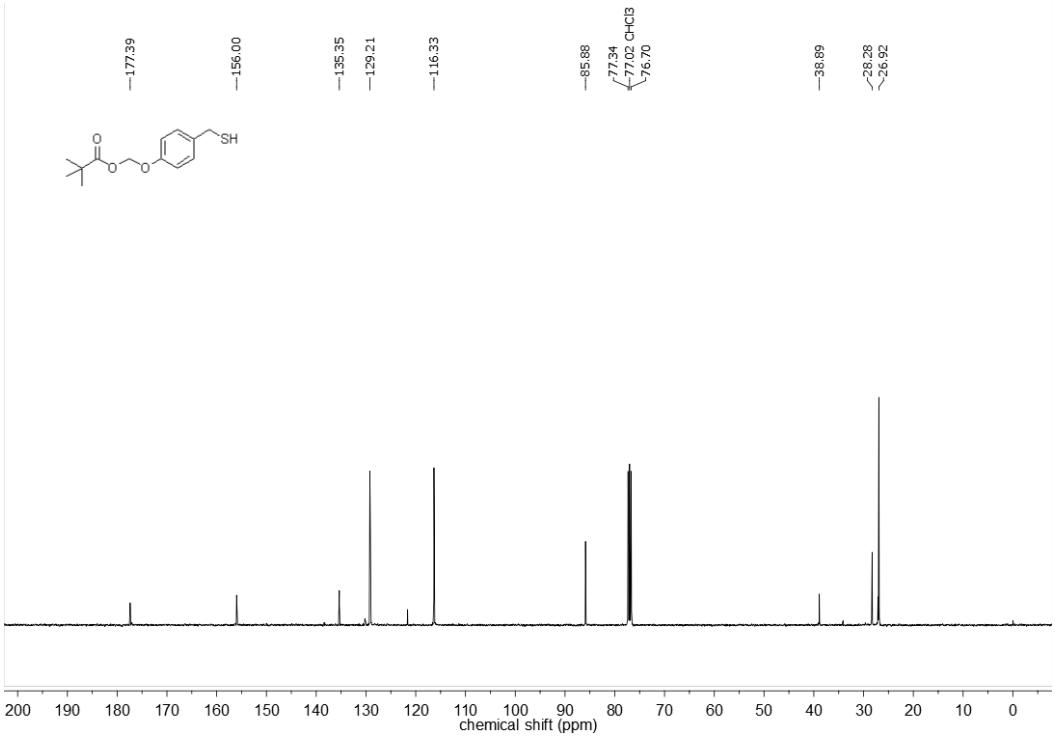

^{1}H-NMR ($CDCl_3$, 400 MHz) for Compound **6a**

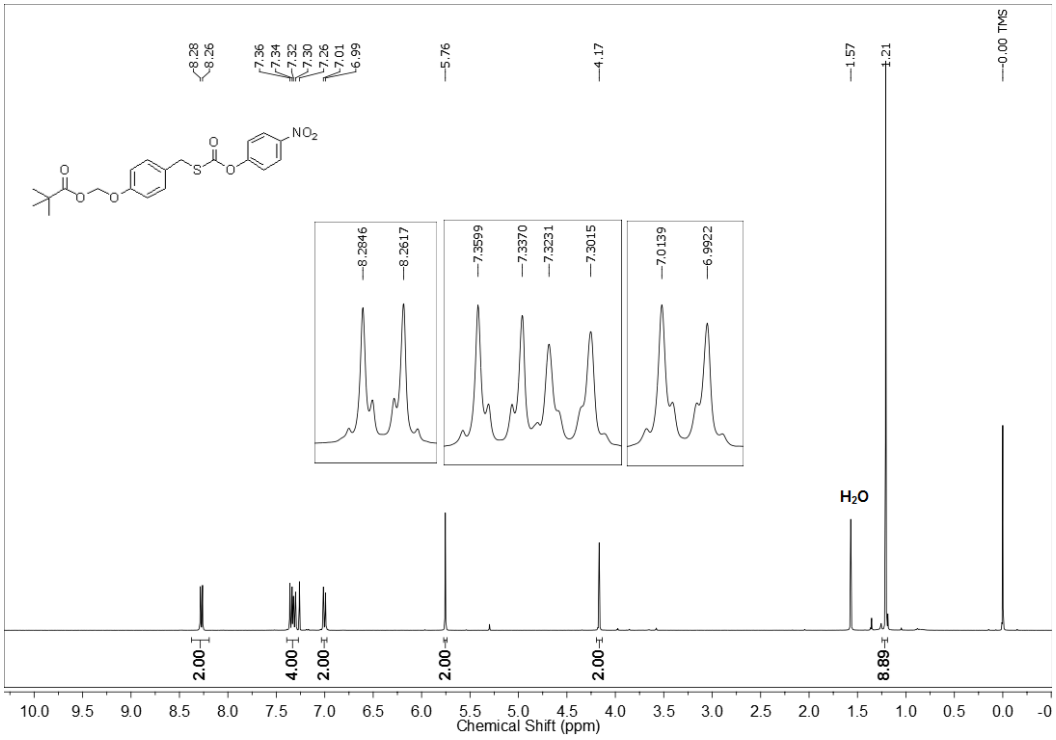

^{13}C-NMR ($CDCl_3$, 100 MHz) for Compound **6a**

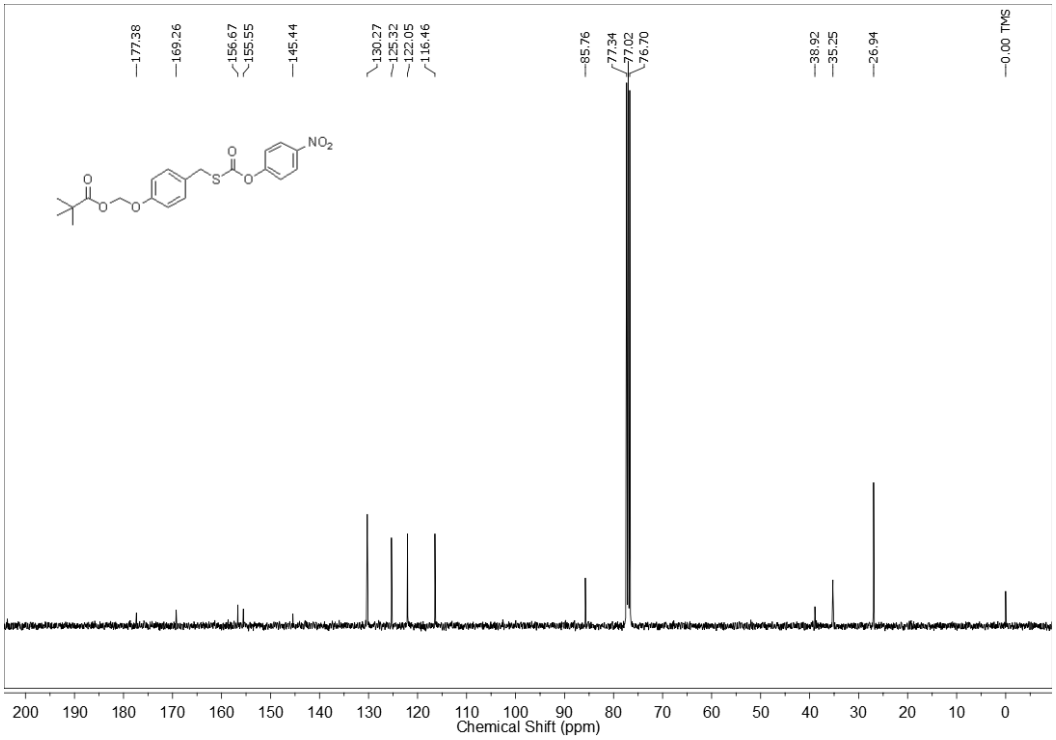

^{1}H-NMR ($CDCl_3$, 400 MHz) for Compound **6b**

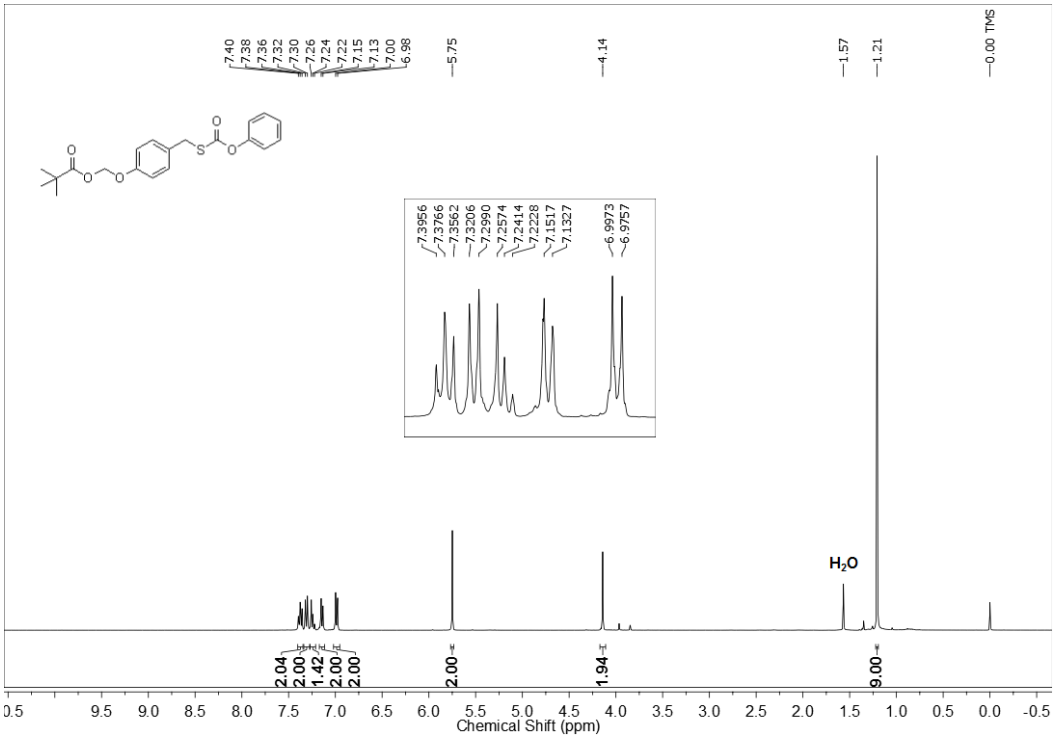

^{13}C-NMR ($CDCl_3$, 100 MHz) for Compound **6b**

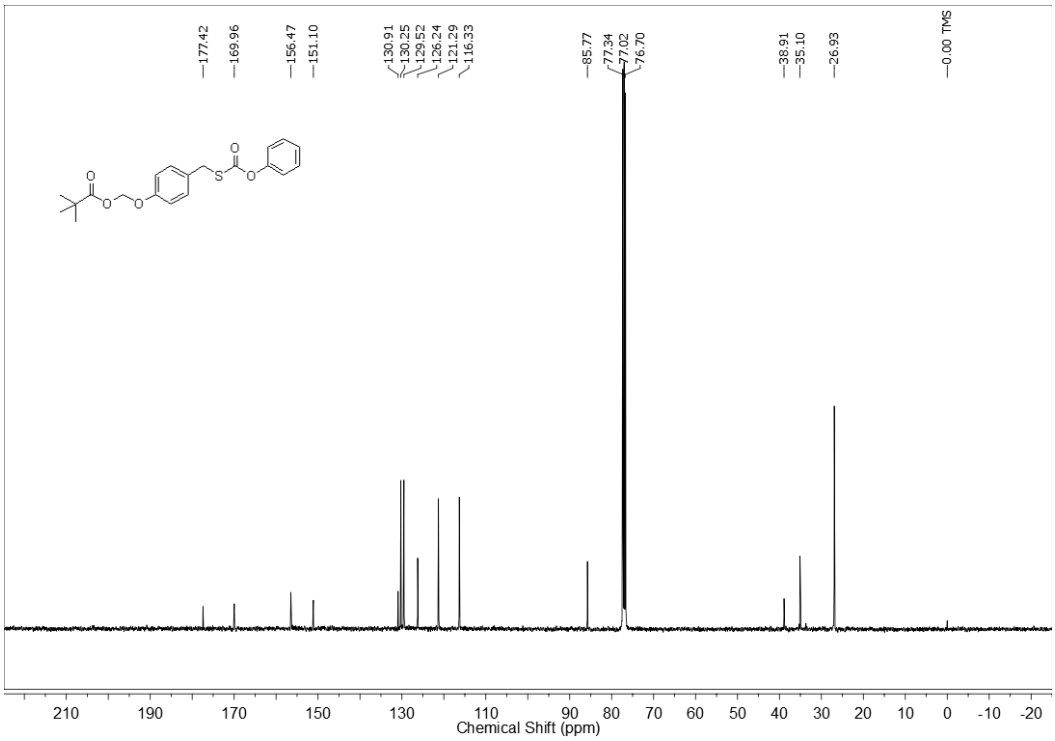

^{1}H-NMR ($CDCl_3$, 400 MHz) for Compound **6c**

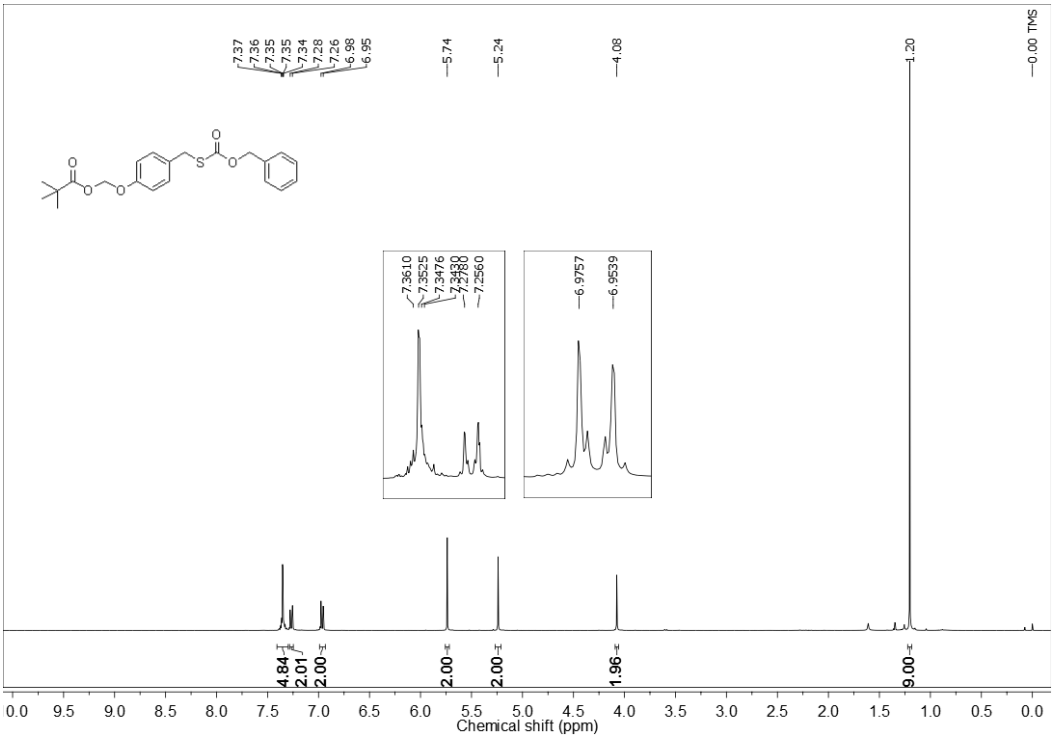

^{13}C-NMR ($CDCl_3$, 100 MHz) for Compound **6c**

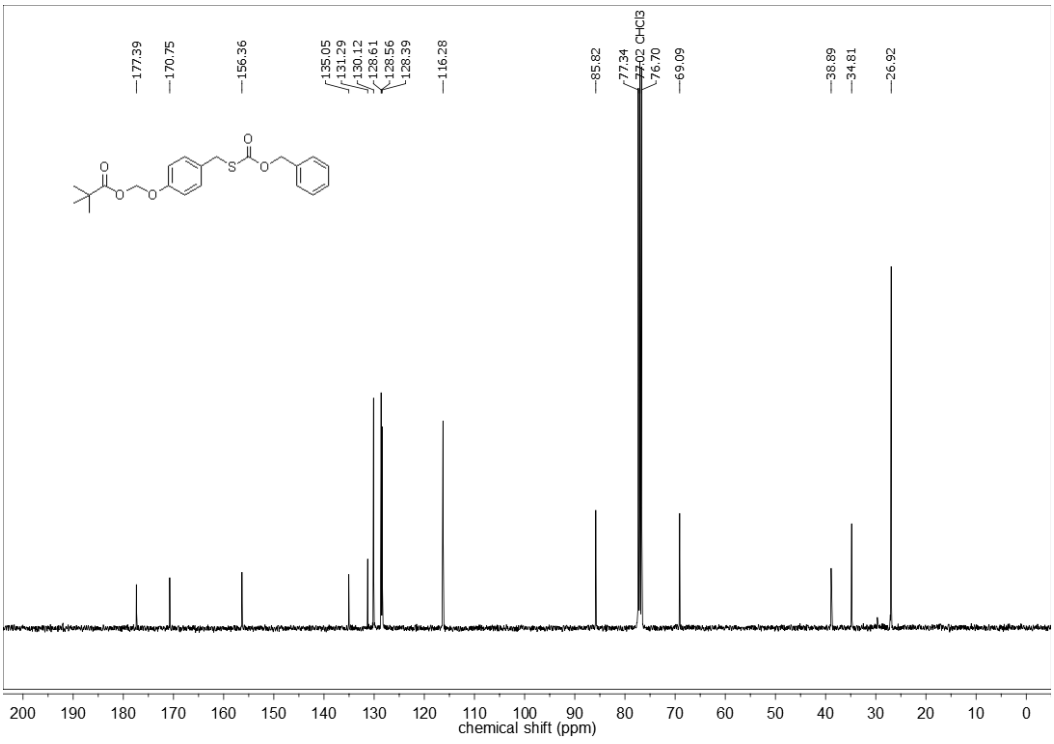

^{1}H-NMR ($CDCl_3$, 400 MHz) for Compound **7a**

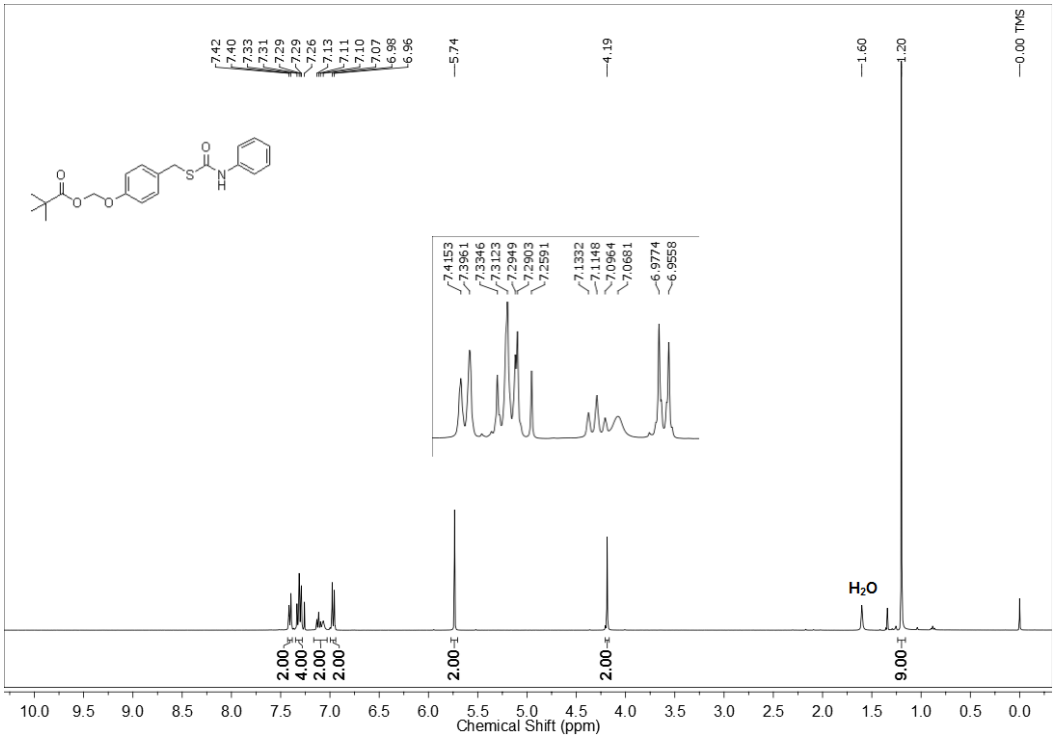

^{13}C-NMR ($CDCl_3$, 100 MHz) for Compound **7a**

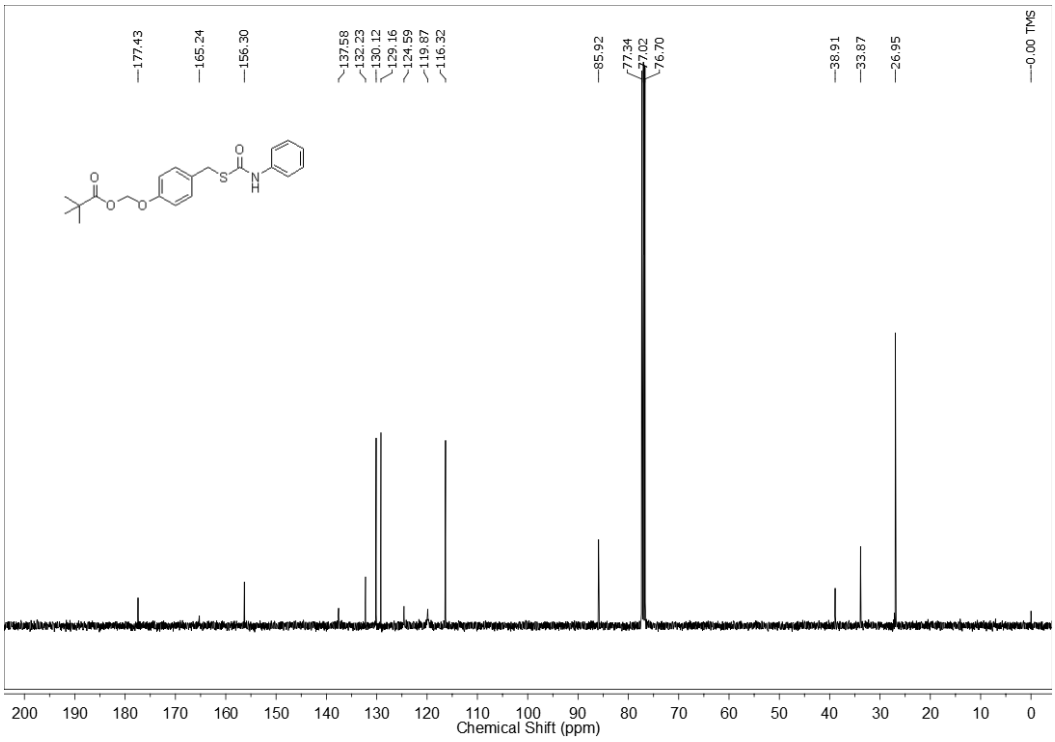

^{1}H-NMR ($CDCl_3$, 400 MHz) for Compound **7b**

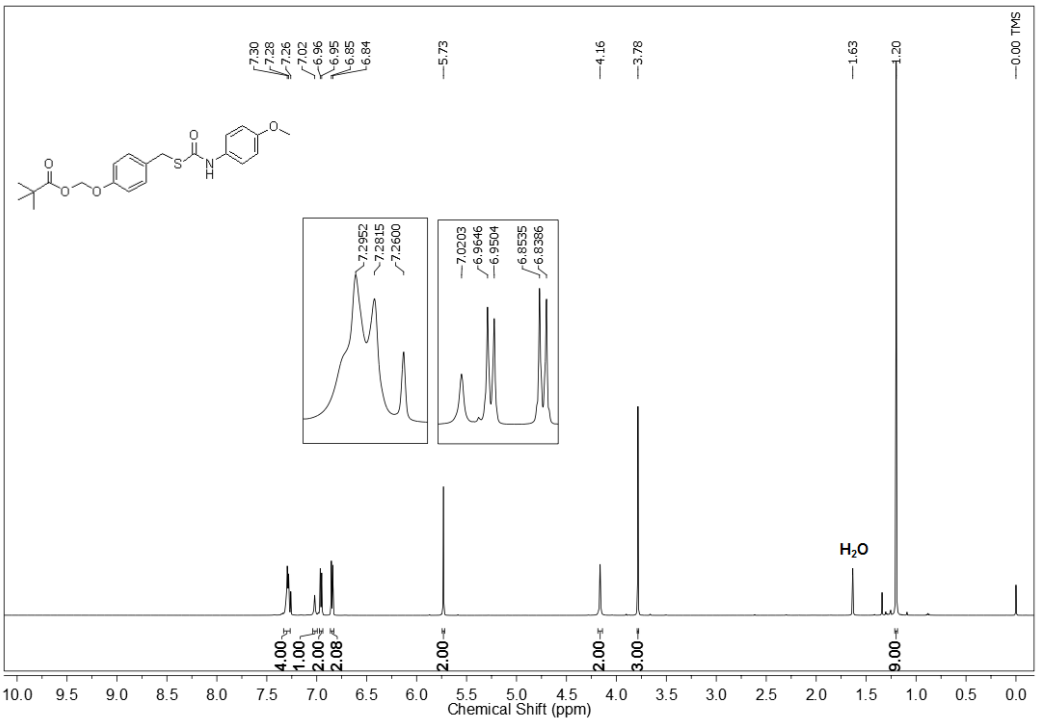

^{13}C-NMR ($CDCl_3$, 100 MHz) for Compound **7b**

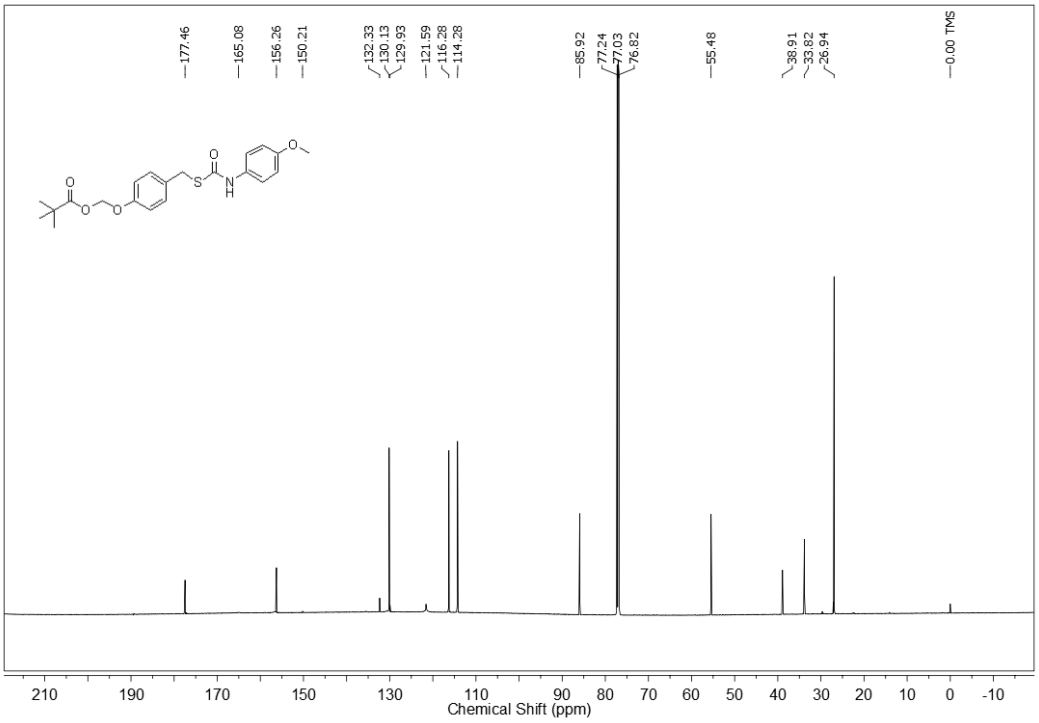

^{1}H-NMR ($CDCl_3$, 400 MHz) for Compound **7c**

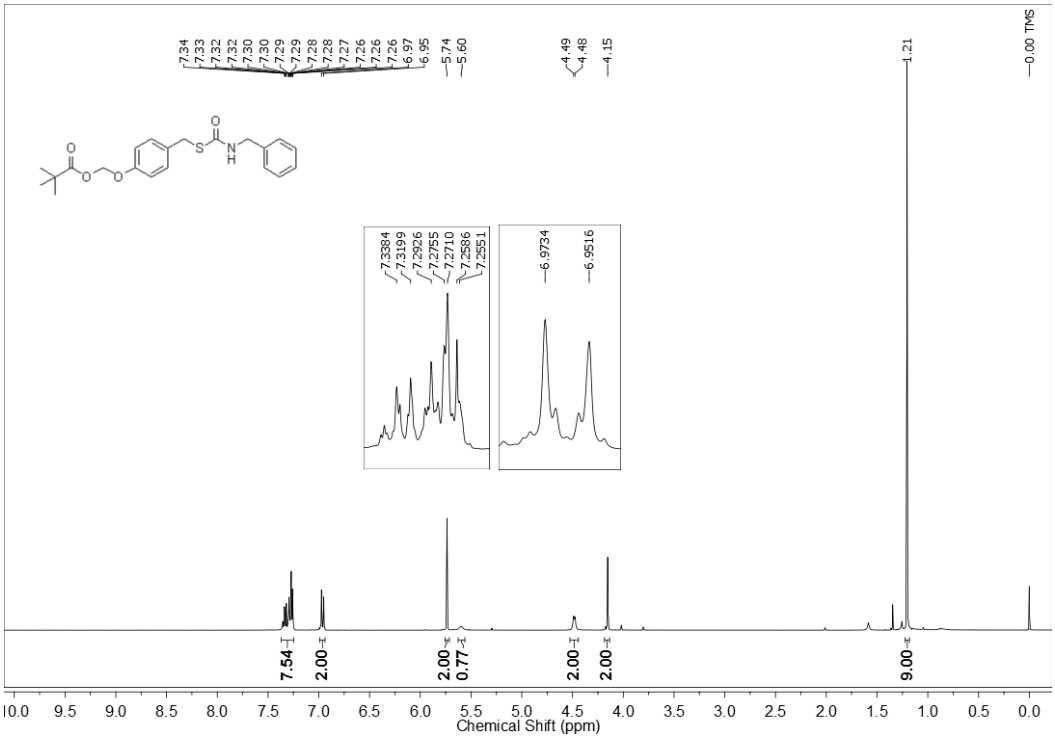

^{13}C-NMR ($CDCl_3$, 100 MHz) for Compound **7c**

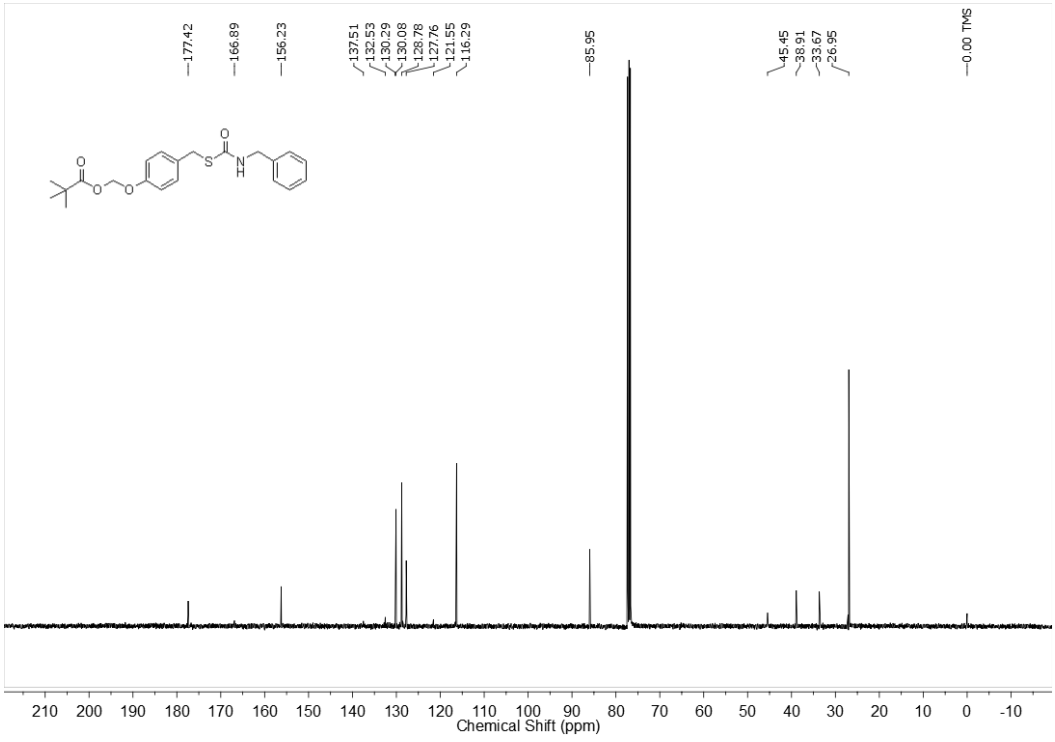

^{1}H-NMR ($CDCl_3$, 400 MHz) for Compound 4

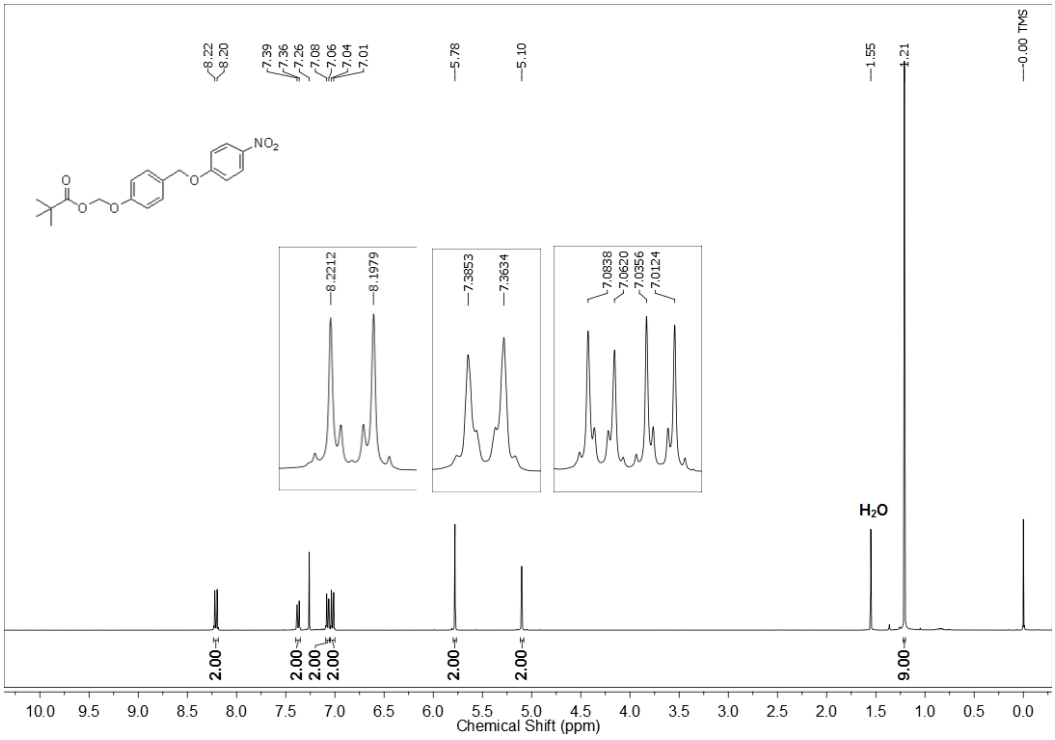

^{13}C-NMR ($CDCl_3$, 100 MHz) for Compound **4**

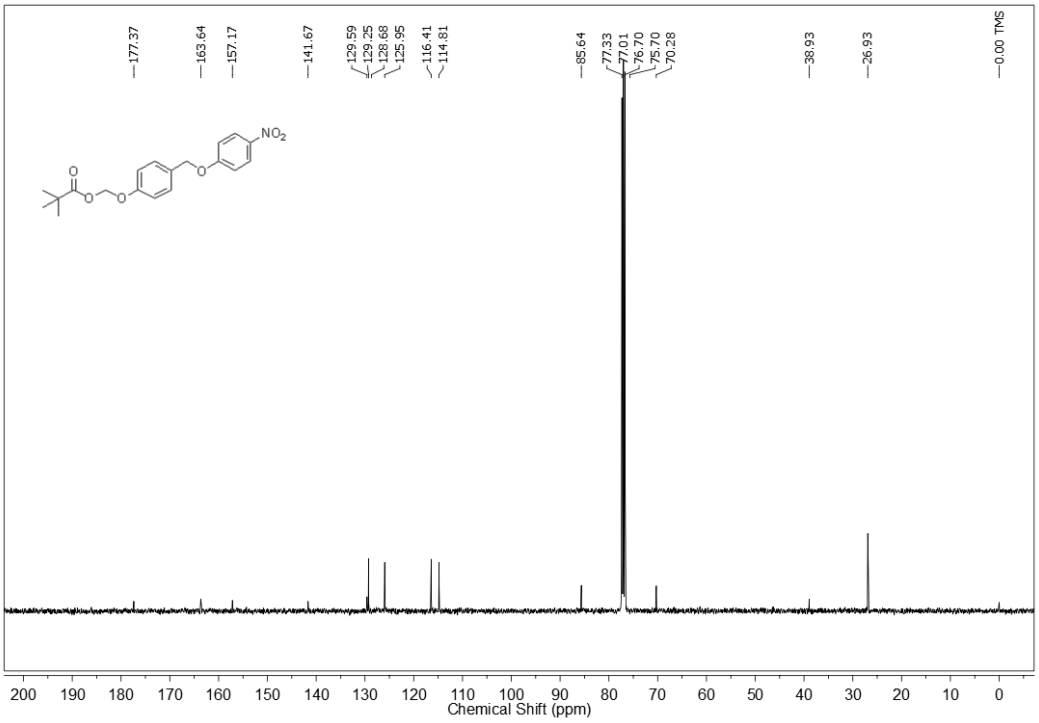

^{1}H-NMR ($CDCl_3$, 400 MHz) for Compound **2**

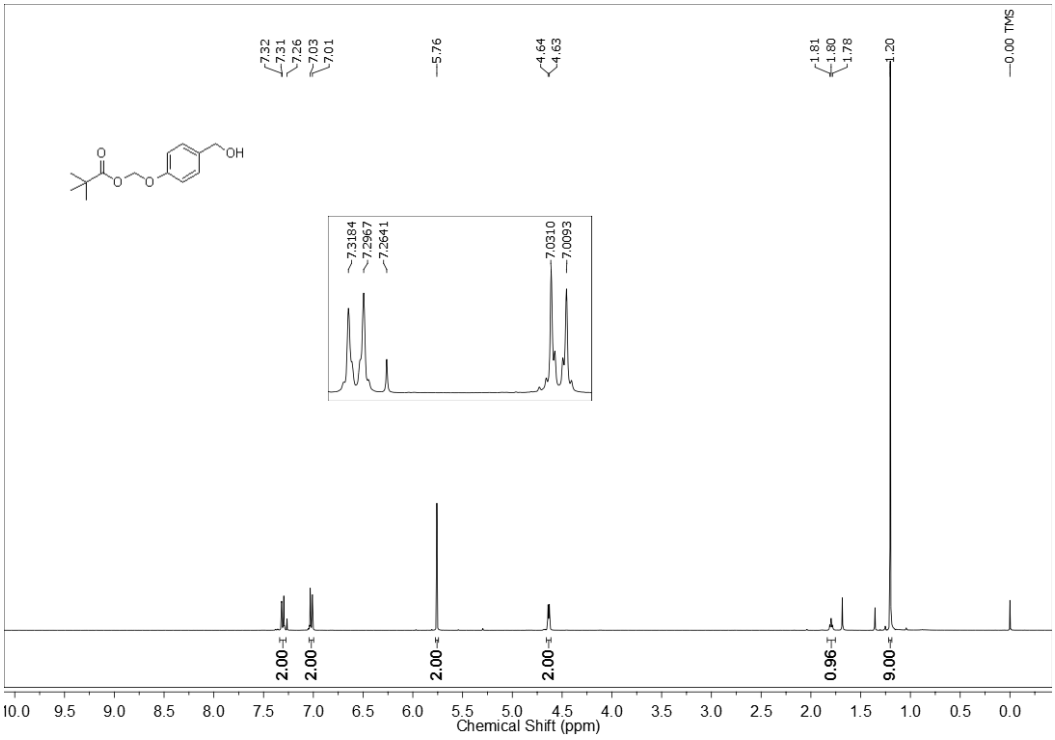

2.7. References:

(1) Elrod, J. W.; Calvert, J. W.; Morrison, J.; Doeller, J. E.; Kraus, D. W.; Tao, L.; Jiao, X.; Scalia, R.; Kiss, L.; Szabo, C.; Kimura, H.; Chow, C.-W.; Lefer, D. J. *Proc. Natl. Acad. Sci. U S A* **2007**, *104*, 15560.

(2) Polhemus David, J.; Lefer David, J. *Circ. Res.* **2014**, *114*, 730.

(3) Kimura, H.; Shibuya, N.; Kimura, Y. *Antioxid. redox signal.* **2012**, *17*, 45.

(4) Kimura, Y.; Dargusch, R.; Schubert, D.; Kimura, D. H. *Antioxid. Redox Signal.* **2006**, *8*, 661.

(5) KIMURA, Y.; KIMURA, H. *FASEB J.* **2004**, *18*, 1165.

(6) Paul, B. D.; Snyder, S. H. *Biochem. Pharmacol.* **2018**, *149*, 101.

(7) Fiorucci, S.; Distrutti, E.; Cirino, G.; Wallace, J. L. *Gastroenterology* **2006**, *131*, 259.

(8) Linden, D. R. *Antioxid. redox signal.* **2014**, *20*, 818.

(9) Wallace, J. L.; Wang, R. *Nat. Rev. Drug. Discov.* **2015**, *14*, 329.

(10) Wang, R. *Physiological Reviews* **2012**, *92*, 791.

(11) Filipovic, M. R.; Zivanovic, J.; Alvarez, B.; Banerjee, R. *Chem. Rev.* **2018**, *118*, 1253.

(12) Szabo, C. *Nat Rev Drug Discov* **2007**, *6*, 917.

(13) Devarie-Baez, N. O.; Bagdon, P. E.; Peng, B.; Zhao, Y.; Park, C.-M.; Xian, M. *Org. Lett.* **2013**, *15*, 2786.

(14) Kang, J.; Li, Z.; Organ, C. L.; Park, C.-M.; Yang, C.-t.; Pacheco, A.; Wang, D.; Lefer, D. J.; Xian, M. *J. Am. Chem. Soc.* **2016**, *138*, 6336.

(15) Li, L.; Salto-Tellez, M.; Tan, C.-H.; Whiteman, M.; Moore, P. K. *Free Rad. Biol. Med.* **2009**, *47*, 103.

(16) Zhao, Y.; Kang, J.; Park, C.-M.; Bagdon, P. E.; Peng, B.; Xian, M. *Org. Lett.* **2014**, *16*, 4536.

(17) Zhao, Y.; Pluth, M. D. *Angew. Chem. Int. Ed.* **2016**, *55*, 14638.

(18) Zhao, Y.; Wang, H.; Xian, M. *J. Am. Chem. Soc.* **2011**, *133*, 15.

(19) Zheng, Y.; Ji, X.; Ji, K.; Wang, B. *Acta. Pharm. Sin. B.* **2015**, *5*, 367.

(20) Zheng, Y.; Yu, B.; Ji, K.; Pan, Z.; Chittavong, V.; Wang, B. *Angew.Chem. Int.Ed.* **2016**, *55*, 4514.

(21) Fiorucci, S.; Orlandi, S.; Mencarelli, A.; Caliendo, G.; Santagada, V.; Distrutti, E.; Santucci, L.; Cirino, G.; Wallace, J. L. *Br. J. Pharmacol.* **2007**, *150*, 996.

(22) Bhatia, M. *Scientifica* **2012**, *2012*, 12.

(23) Shatalin, K.; Shatalina, E.; Mironov, A.; Nudler, E. *Science* **2011**, *334*, 986.

(24) Protoschill-Krebs, G.; Wilhelm, C.; Kesselmeier, J. *Atmos. Environ.* **1996**, *30*, 3151.

(25) Sorokin, D. Y.; Tourova, T. P.; Lysenko, A. M.; Kuenen, J. G. *Appl. Environ. Microbiol.* **2001**, *67*, 528.

(26) Haritos, V. S.; Dojchinov, G. *Comp. Biochem. Physiol. C Pharmacol. Toxicol. Pharmacol.* **2005**, *140*, 139.

(27) Shin, W. S.; Han, J.; Verwilst, P.; Kumar, R.; Kim, J.-H.; Kim, J. S. *Bioconjugate Chem.* **2016**, *27*, 1419.

(28) Sharma, K.; Iyer, A.; Sengupta, K.; Chakrapani, H. *Org. Lett.* **2013**, *15*, 2636.

(29) Sharma, K.; Sengupta, K.; Chakrapani, H. *Bioorg. Med. Chem. Lett.* **2013**, *23*, 5964.

(30) Steiger, A. K.; Pardue, S.; Kevil, C. G.; Pluth, M. D. *J. Am. Chem. Soc.* **2016**, *138*, 7256.

(31) Powell, C. R.; Foster, J. C.; Okyere, B.; Theus, M. H.; Matson, J. B. *J. Am. Chem. Soc.* **2016**, *138*, 13477.

(32) Tanc, M.; Carta, F.; Scozzafava, A.; Supuran, C. T. *ACS Med. Chem. Lett.* **2015**, *6*, 292.

(33) Peng, H.; Cheng, Y.; Dai, C.; King, A. L.; Predmore, B. L.; Lefer, D. J.; Wang, B. *Angew.Chem. Int.Ed.* **2011**, *50*, 9672.

(34) Haydt, D.; Hornberger, R. *Galvanic Applied Sciences.* **2001**.

(35) Moest, R. R. *Anal. Chem.* **1975**, *47*, 1204.

(36) Wei, C.; Zhu, Q.; Liu, W.; Chen, W.; Xi, Z.; Yi, L. *Org. Biomol. Chem.* **2014**, *12*, 479.

(37) Bensel, N.; Reymond, M. T.; Reymond, J.-L. *Chem. Euro. J.* **2001**, *7*, 4604.

(38) Sankar, R. K.; Kumbhare, R. S.; Dharmaraja, A. T.; Chakrapani, H. *Chem. Commun.* **2014**, *50*, 15323.

(39) Haydt, D.; Hornberger, R. *Galvanic Appl. Sci.* **2001**.

Title: Esterase Activated Carbonyl Sulfide/Hydrogen Sulfide (H2S) Donors

Author: Preeti Chauhan, Prerona Bora, Govindan Ravikumar, et al

Publication: Organic Letters

Publisher: American Chemical Society

Date: Jan 1, 2017

PERMISSION/LICENSE IS GRANTED FOR YOUR ORDER AT NO CHARGE

This type of permission/license, instead of the standard Terms & Conditions, is sent to you because no fee is being charged for your order. Please note the following:

- Permission is granted for your request in both print and electronic formats, and translations.
- If figures and/or tables were requested, they may be adapted or used in part.
- Please print this page for your records and send a copy of it to your publisher/graduate school.
- Appropriate credit for the requested material should be given as follows: "Reprinted (adapted) with permission from (COMPLETE REFERENCE CITATION). Copyright (YEAR) American Chemical Society." Insert appropriate information in place of the capitalized words.
- One-time permission is granted only for the use specified in your request. No additional uses are granted (such as derivative works or other editions). For any other uses, please submit a new request.

BACK CLOSE WINDOW

CHAPTER 3.1: ROS triggered COS/H_2S donors for targeted and tunable release

3.1.1. Introduction

Hydrogen sulfide forms a part of the antioxidant machinery of a cell which helps in maintaining the redox homeostasis.[1,2] Diminished levels of H_2S have been associated with various diseases like cardiovascular diseases, neurodegenerative disorders, inflammation etc. Most of these pathological conditions have increased levels of reactive oxygen species (ROS) thereby causing oxidative stress.[3,4] Exogenous administration of H_2S under such conditions acts as a cytoprotective agent.[5] Thus, delivering H_2S to areas associated with inflammation is of great therapeutic value. However, the anti-oxidant properties of H_2S are largely dependent on the concentration and the rate of release.[6] Moore and coworkers in 2010 have evaluated the anti-inflammatory activities of fast (NaSH) and slow (GYY4137) releasing H_2S donors.[7] GYY4137 significantly reduced the concentration of pro-inflammatory cytokines like TNF-a and IL-6 in lipoploysaccharide (LPS) treated murine RAW264.6 macrophages whereas NaSH exacerbated the condition and increased the levels of these pro-inflammatory mediators.[8] This clearly indicates that the complex effects of H_2S on inflammatory responses depend both on the concentration and the rate at which H_2S is generated. Wang and coworkers have also shown the superior cardioprotective effects of diallyl trisulfide based nanoparticle over NaSH in a myocardial ischemia model.[9] These studies highlight the significance of modulating the release of hydrogen sulfide. Thus, small molecule based H_2S donors for targeted and tunable release of H_2S is highly desirable.

Since enhanced levels of ROS are associated with various disorders, therefore, designing ROS triggered H_2S donors is useful. Furthermore, modulating the rates of H_2S release to study its effects in a physiological system is highly desirable.

Boronate esters have been extensively used in the past to deliver drugs, reactive species and latent fluorophores (for imaging) to regions under oxidative stress. For example, ROS triggered delivery of nitric oxide (NO) has been reported previously by Chakrapani and co-workers (Scheme 3.1.1).[10]

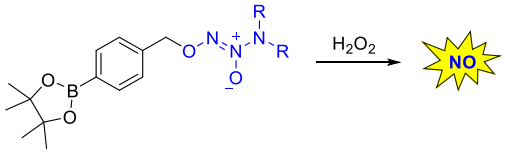

Scheme 3.1.1. ROS activated NO donors

Therefore, carbamothioate based ROS responsive H_2S donors, for targeted and tunable release of H_2S, have been developed. The scaffolds reported in the previous chapter have been modified by replacing ester moiety with the boronate ester to achieve ROS triggered delivery of H_2S (Scheme 3.1.2). Also, carbamothioate was chosen as the scaffold of interest as changing the stereoelectronics on the nitrogen could modulate the rate of H_2S release. Amines with varying pK_aH values were selected to study the effect of the basicity of the amine on the rate of H_2S release.[11]

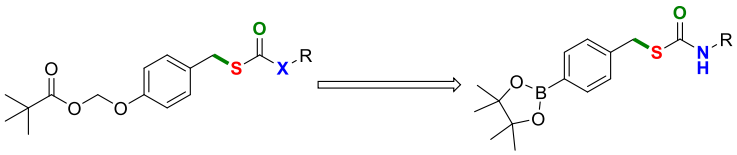

Scheme 3.1.2. Design of ROS activated H_2S donors

Carbamothioate based H_2S donors are versatile and provide scope for conjugation with drug to prepare H_2S-drug hybrids. Non-steroidal anti-inflammatory drugs (NSAIDs) have been previously conjugated with H_2S to form H_2S-NSAID hybrids which have shown enhanced activity compared to the parent drug.[12,13] Thus, this strategy can potentially be adapted to prepare ROS triggered H_2S-NSAID hybrid donors (Scheme 3.1.3).

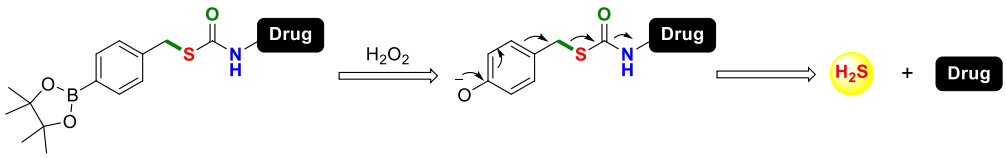

Scheme 3.1.3. ROS triggered H_2S-Drug hybrids

The mechanism of H_2S release from ROS activated H_2S donors is as follows: boronate ester moiety is first hydrolysed to boronic acid in buffer (pH 7.4) which upon reaction with H_2O_2 forms a phenolate intermediate. The phenolate thus formed self immolates to release COS which is further hydrolysed to H_2S in the presence of carbonic anhydrase (CA) (Scheme 3.1.4).

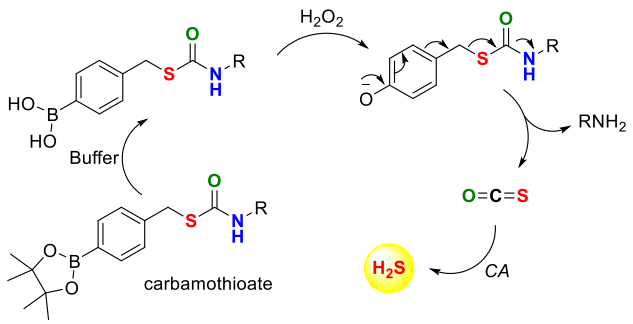

Scheme 3.1.4. Mechanism of H_2S release from ROS activated COS/H_2S donors

3.1.2. Results and Discussion

3.1.2.1 Synthesis

A series of ROS activated COS/H_2S donors (**13a-13g**) were synthesized to test the hypothesis. Following synthetic scheme was used to synthesize the donors: *p*-bromo banezaldehyde was converted to 4-(4,4,5,5-tetramethyl-1,3,2-dioxaborolan-2-yl)benzaldehyde, **9**, using Pd(dppf)Cl_2 catalyst in the presence of $B_2(pin)_2$, KOAc in a quantitative yield. Compound **9** was unstable on silica and therefore was taken forward without further purification. Aldehyde group in **9** was reduced to an alcohol in the presence of $NaBH_4$ to give compound **10** in 81% overall yield. Compound **10** was further reacted with tribromophosphine in dry DCM at 0 ^oC. The product formed was unstable and therefore was taken further to react with thiourea to give a thiourea adduct. The salt obtained was hydrolyzed to give thiol, **11**, using sodium metabisulfite ($Na_2S_2O_5$) in 83% overall yield (Scheme 3.1.5).

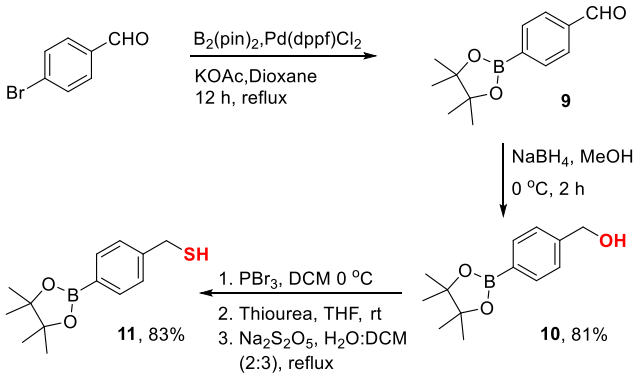

Scheme 3.1.5. Synthesis of thiol, **11**.

Next, carbamates (**12a-12i**) of the respective amines were synthesized by reacting with *p*-nitrophenyl chloroformate (Scheme 3.1.6). The carbamates so formed were taken further without purification.

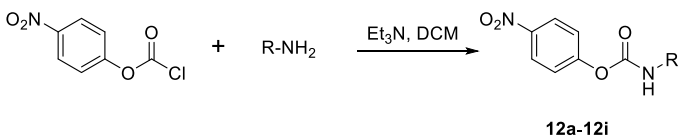

Scheme 3.1.6. Synthesis of carbamates (**12a-12i**)

Finally, carbamothioates were prepared by reacting compound **11** with respective carbamates to give compounds (**13a-13g**) in varying yields (Scheme 3.1.7). The yields of the carbamothioates synthesized are reported in Table 3.1.1. Carbamate **12g** with *tert*-butylamine was found to decompose under these conditions and therefore corresponding carbamothioate

could not be prepared. Carbamate of pyrrolidine **12h** was synthesized to have a secondary carbamothioate in the series. However, no reaction of **11** with **12h** (carbamate of pyrrolidine) was observed which could possibly be due to the low reactivity of secondary amines. Compounds shown in the entry 1,2 and 5-7 were synthesized by Ms Swetha Jos.

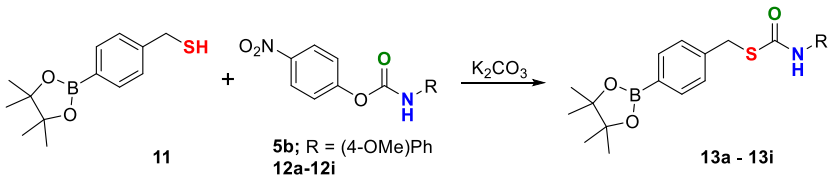

Scheme 3.1.7. Synthesis of ROS responsive COS/H_2S donors.

Table 3.1.1. ROS activated COS/H_2S donors

entry	R	pK_a RNH_2[a]	carbamate	prod	% yield
1	(3-COOMe)Ph	4.75	**12a**	**13a**	28[c]
2	4-OCH_2CH_2OHPh	5.03[b]	**12b**	**13b**	32[c]
3	(4-OMe)Ph	5.34	**5b**	**13c**	27
4	(4-NO_2)PhCH_2	8.36[b]	**12d**	**13d**	23
5	4-(O-Propargyl)-PhCH_2	9.18[b]	**12e**	**13e**	41[c]
6	PhCH_2	9.34	**12f**	**13f**	21[c]
7	$CH_3CH_2CH_2$	10.53	**12g**	**13g**	27[c]
8	*t*-butyl	10.45	**12h**	**13h**	-
9	pyrrolidine	11.27	**12i**	**13i**	-

[a]pK_a values were used from Ref 23; [b]Scifinder was used for pK_a values; [c]Compounds were synthesized by Ms Swetha Jos.

Compound **14** was synthesized as a negative control which would cleave in the presence of H_2O_2 but would not produce COS (Scheme 3.1.8). Compound **10** was reacted with carbamate **5b** in the presence of K_2CO_3 to give compound **14** in 40% yield.

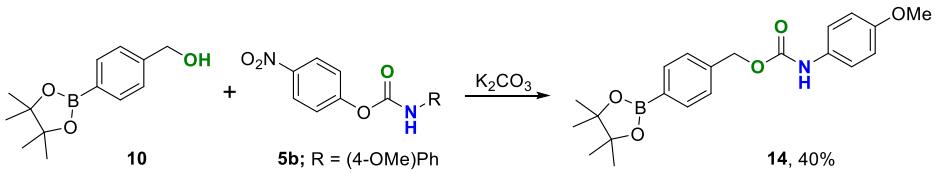

Scheme 3.1.8. Synthesis of negative control **14**.

3.1.2.2. H_2S detection using methylene blue

H_2S generation from the scaffolds was demonstrated by using methylene blue formation assay.[14] Briefly, the donors were incubated in phosphate buffer (pH 7.4, 10 μM DTPA, 50 mM) containing CA and 10 eq of H_2O_2 at 37 ^oC. After 2 h of incubation an aliquot of the reaction mixture was treated with the methylene blue reagents (*N*,*N*-dimethyl-*p*-phenylene diamine, $FeCl_3$) and further incubated for 30 min at 37 ^oC. After the formation of methylene blue complex, the reaction mixture was transferred to a 96 well plate and absorbance was measured at 676 nm. Compounds showed a signal corresponding to H_2S generation in the presence of H_2O_2. Although the yields obtained from the donors were different, which was possibly due to the difference in the rates of H_2S generation. As expected, no signal for H_2S release was observed from compound **14** which lacked the ability to produce COS (Figure 3.1.1).

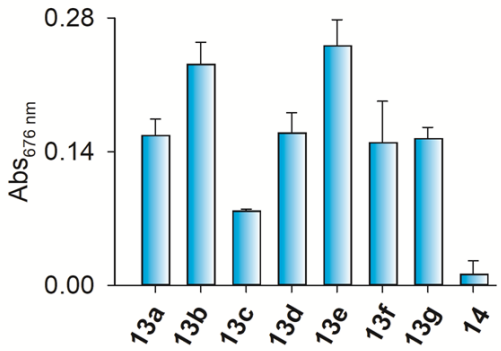

Figure 3.1.1. Measurement of H_2S from the donors (**13a** – **13g**) after 2 h incubation in the presence of H_2O_2 using methylene blue assay.

3.1.2.3. Kinetics of H_2S generation

After establishing H_2S release from the donors, next, the effect of the pK_aH of the amines on the rates of H_2S generation was investigated. Methylene blue assay was used to monitor the H_2S release. The experiment was conducted by Ms Swetha Jos. Briefly, compounds were incubated in buffer pretreated with CA in the presence of 10 eq of H_2O_2 at 37 ^oC. At predetermined time points, an aliquot from the reaction mixture was treated with methylene blue cocktail and incubated at 37 ^oC for another 30 min. After the formation of methylene blue complex, the mixture was transferred to a 96 well plate and absorbance was measured at 676 nm. Absorbance measured was plotted against time in a pseudo first order kinetics plot (Figure 3.1.2). Compounds **13a**, **13b** and **13c** with aniline derivatives as the leaving groups lying in the range of lower pK_aH values (4.75 – 5.34) had a faster rate of H_2S production. H_2S

releasing profiles for these compounds were found to get saturated within 1 -2 h time point. On the other hand, compounds **13d -13g** with amines falling in the range of higher pK_aH values (8.36 – 10.53) were found to have slower rate of H_2S generation. A consistent increase in the signal for H_2S production was observed even after 6 h of incubation.

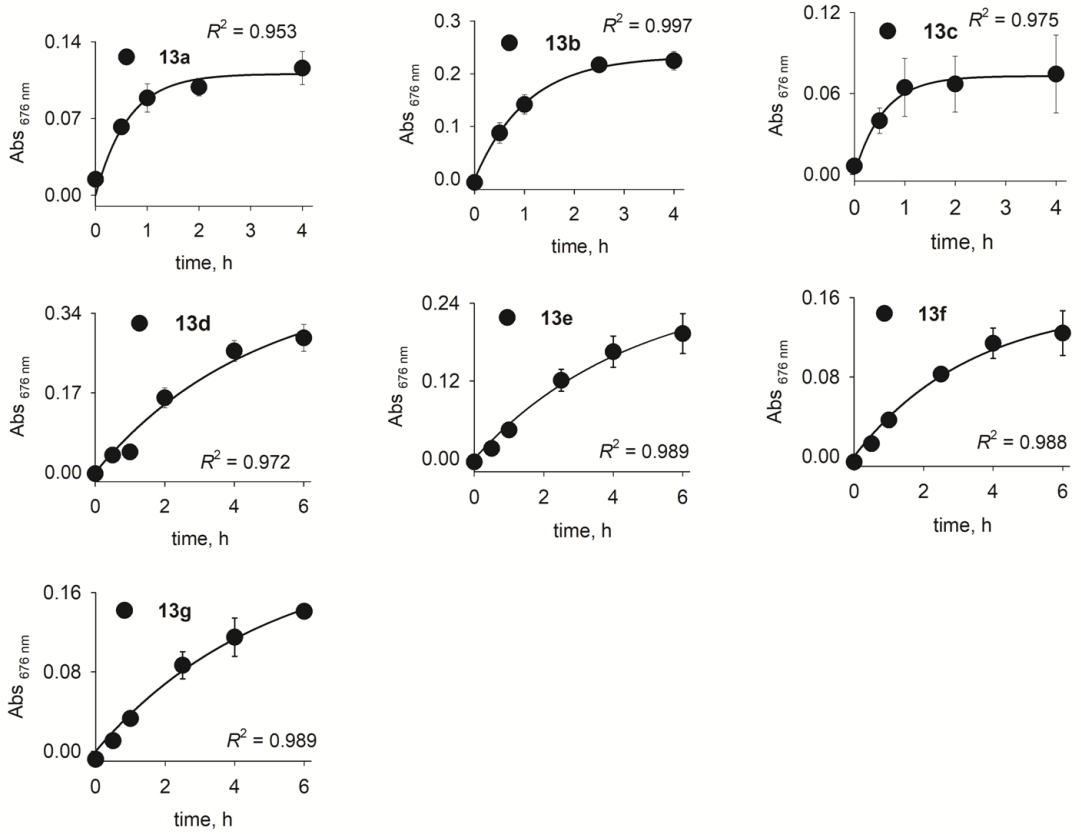

Figure 3.1.2. Representative plots for the H_2S release from ROS activated H_2S donors.

Pseudo first order rate constants and respective half-lives were calculated for all the donors (Table 3.1.2). Compound **13c** (Table 3.1.2. entry 3) with *p*-anisidine as a leaving group was found to be the fastest donor for H_2S. Half-life of H_2S release for compound **13c** was calculated to be 23.9 min. Interestingly, compound **13g** (Table 3.1.2, entry 7) with propylamine as the leaving group showed the slowest rate of H_2S release with half-life of 203.8 min. The results obtained were in accordance with our hypothesis that aniline based derivatives with pK_aH values in the range 4.75 to 5.34 showed faster rate of H_2S release compared to the derivatives with pK_aH values falling in the range of 8.36 to 10.53. We calculated the relative rates with respect to **13c** (fastest rate of H_2S release) and a difference of 8- fold in the rate of H_2S release from the donors was recorded.

Table 3.1.2. Kinetics of H_2S release.

entry	compd	pK_aH	k, min^{-1}	$t_{1/2}$, min	relative rate
1.	**13a**	4.75	0.026	26.7	0.90
2.	**13b**	5.03	0.017	40.8	0.59
3.	**13c**	5.34	0.029	23.9	1.00
4.	**13d**	8.36	0.004	173.3	0.14
5.	**13e**	9.18	0.0045	154.0	0.16
6.	**13f**	9.34	0.0049	141.4	0.17
7.	**13g**	10.53	0.0034	203.8	0.12

3.1.2.4 Linear Regression Analysis Plot

In order to establish a correlation between the observed relative rates and the pK_aH values of the amines, a linear regression analysis plot was created. The analysis showed a good correlation between the relative rates obtained and the pK_aH of the corresponding amines which clearly indicated that modulating the rate of H_2S release was possible by changing the basicity of the amine (Figure 3.1.3).

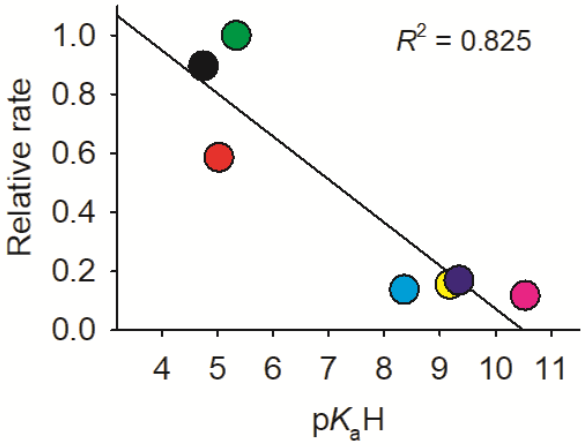

Figure 3.1.3. Linear regression analysis of relative rates of H_2S generation upon reaction with H_2O_2 with pK_aH of the amines.

3.1.2.5. HPLC plots

Dissociation of the compound **13c** (fast H_2S donor) and **13g** (slow H_2S donor) in the presence of H_2O_2, was followed by HPLC to understand the mechanism involved in the release H_2S

from the donors. The HPLC experiment was conducted by Ms Swetha Jos. Compound **13c** when injected in ACN was eluted at retention time 17.63 min. Upon incubation in buffer the boronate ester was readily converted to boronic acid which eluted at 9.85 min (Figure 3.1.4). A complete disappearance of the compound was observed when treated with H_2O_2 in buffer after 30 min incubation. A new peak attributable to formation of an intermediate was observed which gradually decomposed in 2 h to generate *p*-anisidine (Figure 3.1.5a). The rate of *p*-anisidine formation was calculated to be 0.04 min^{-1} which was in accordance with the rate of H_2S release 0.03 min^{-1} (Figure 3.1.5b).

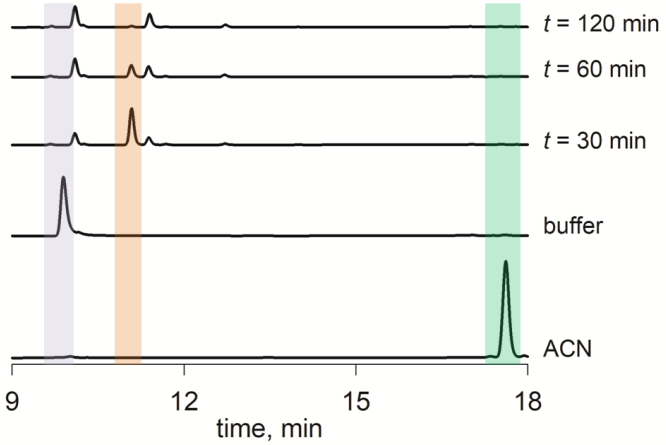

Figure 3.1.4. Representative HPLC plots for the decomposition of **13c**.

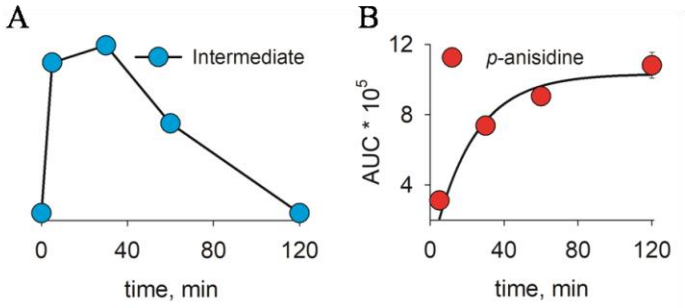

Figure 3.1.5. a) Dissociation of the intermediate formed over the time. b) Area under the curve corresponding to the formation of *p*-anisidine followed by HPLC.

Similar observations were made in the case of compound **13g**. The boronate ester was readily converted to boronic acid in buffer which upon reaction with H_2O_2 completely disappeared within 30 min of incubation (same as **13c**) (Figure 3.1.6). The reaction with H_2O_2 led to the appearance of new peak corresponding to the formation of an intermediate. This indicated that the intermediate formed from reaction of **13g** (aliphatic amine based donor; propylamine as leaving group) with H_2O_2 had UV absorbance property. Intermediate formed was comparatively long lived and decomposed over a period of 6 h (Figure 3.1.6c). Thus, the rate

of H_2S release from carbamothioate based COS donors was dependent on the dissociation of the intermediate formed.

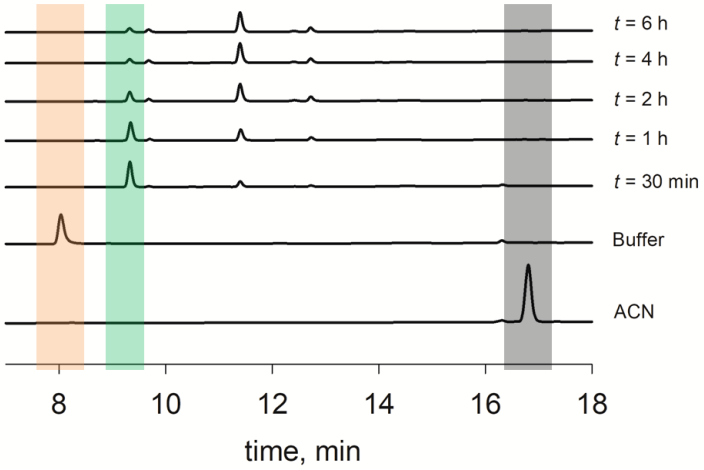

Figure 3.1.6. Representative HPLC plots for the decomposition of **13g**.

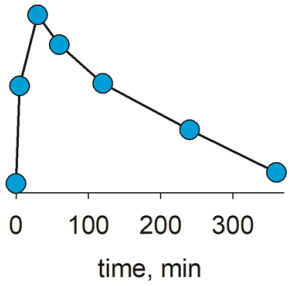

Figure 3.1.7. Dissociation of the intermediate formed from **13g** over time.

Next, the stability of the donors in buffer was tested. Compound **13g** was incubated in buffer at 37 ^{o}C and injected in HPLC at different time points. Nearly quantitative recovery of the compound was made even after 6 h of incubation suggesting that the compounds were stable towards hydrolysis in buffer (Figure 3.1.8).

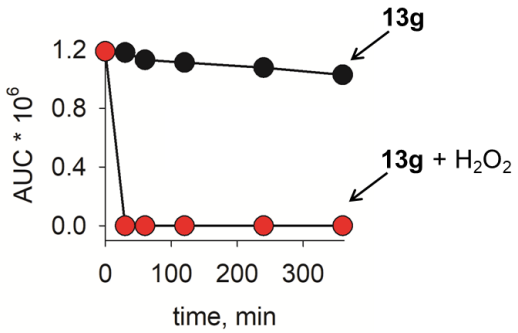

Figure 3.1.8. Area under the curve corresponding to the decomposition of compound **13g** with and without H_2O_2.

3.1.2.6. Mechanism

Based on these observations, mechanism for the release H_2S from the donor motifs is proposed. Boronate ester based carbamothioates first hydrolyse to form boronic acid in buffer (pH 7.4). The rate of hydrolysis is extremely fast as reported previously[15,16] and also observed by the HPLC analysis. Boronic acid then reacts with H_2O_2 (10 eq) to form an intermediate **I**; the rate constant for the reaction of boronic esters/ acids with 10 eq of hydrogen peroxide has been previously reported as 0.09 min^{-1}.[16] The higher rate constant (compared to rate constants for H_2S release) suggests that this step could not be the rate determining step. Intermediate **I** can follow two pathways for the release of COS. In pathway 1, intermediate **I** can undergo dissociation to form an intermediate **II** which upon subsequent protonation of the amine releases COS. COS thus formed is readily hydrolyzed to H_2S in the presence of carbonic anhydrase (k = 109.2 min^{-1}).[17] Intermediate **I** can also follow pathway 2 wherein a concerted mechanism is followed for the release of COS (Scheme 3.1.9).

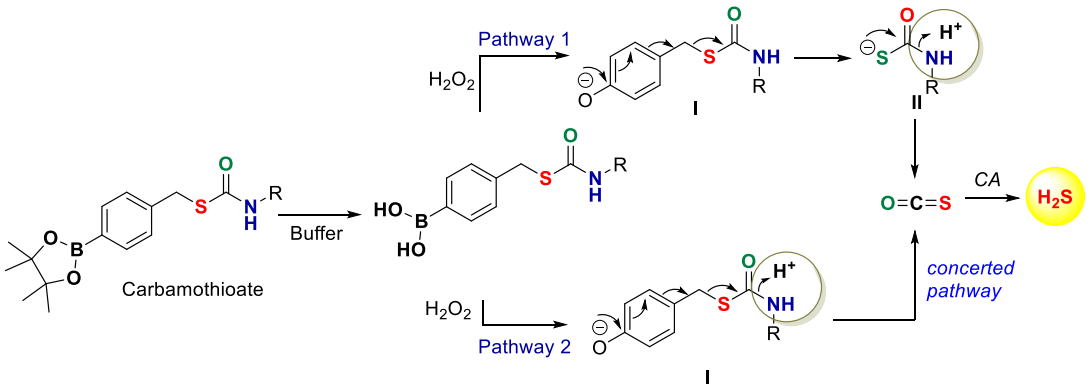

Scheme 3.1.9. Proposed mechanism of H_2S production from carbamothioates

In order to differentiate between the two pathways the following points were considered.

3.1.2.6.1. HPLC Analysis for compound 13g:

It was evident from the aforementioned HPLC experiments that the intermediate formed had UV absorbance property. In case of compound **13g** (aliphatic amine based donor) formation of an intermediate was observed by HPLC which decomposed over a period of 6 h. Since the rate of decomposition of intermediate correlates well with that of H_2S release, it is more likely that pathway 2 is operational in release of H_2S from these scaffolds i.e. the slow step may be the decomposition of intermediate **I** by a concerted mechanism (Scheme 3.1.6).

3.1.2.6.2. ^{1}H NMR Experiment:

In order to further validate the nature of the intermediate formed, ^{1}H NMR experiment was performed wherein the decomposition of compound **13g** in the presence of H_2O_2 in DMSO:

D_2O (9:1) was followed over a period of time. Compound **13g** upon reaction with H_2O_2 formed an intermediate in DMSO:D_2O mixture within 30 minute of reaction when incubated at 37 ^oC. Peaks corresponding to the formation of intermediate **I** were observed in the NMR experiment (Scheme 3.1.10). The intermediate formed was stable even after 30 h of incubation in the DMSO:D_2O mixture at 37 ^oC. No peaks corresponding to the formation of free *p*-hydroxybenzyl alcohol or propylamine were observed after 30 h of incubation (Figure 3.1.9). Thus, the experiment suggests that the reaction follows pathway 2 for the release of COS in the reaction mixture. Intermediate **I** formed upon reaction with H_2O_2 determines the rate of H_2S release from the donors.

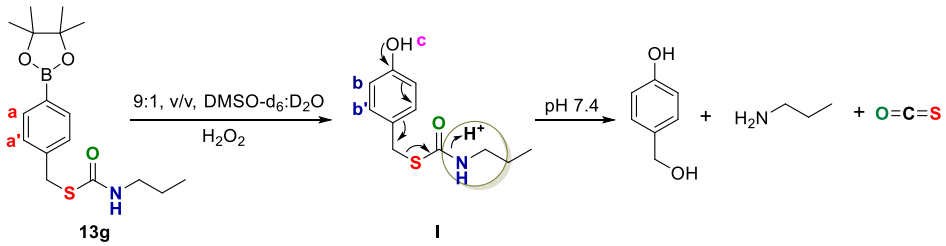

Scheme 3.1.10. Proposed mechanism of COS release from compound **13g** in the presence of H_2O_2.

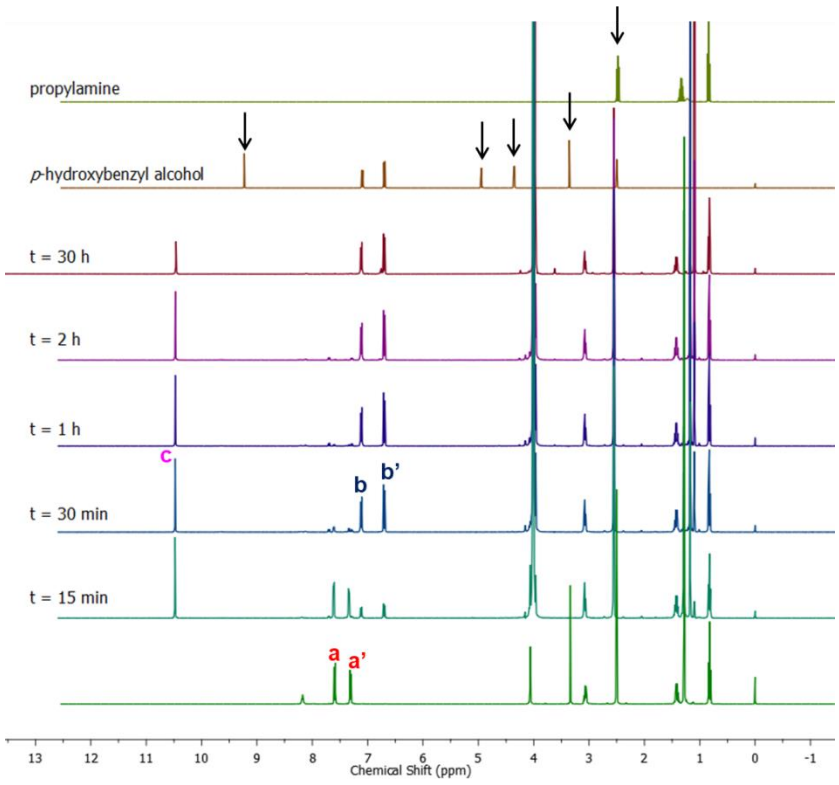

Figure 3.1.9. ^1H NMR experiment to follow the decomposition of compound **13g** in the presence of H_2O_2.

3.1.2.7. Cell viability experiment

Next, cytotoxicity of the compounds was tested in human breast cancer, MCF-7 cell line using MTT assay. The cells were treated with varying concentrations of compound **13g** for 24 h following which the cell viability was monitored. No significant cytotoxicity at 25 µM concentration of the compound was observed suggesting that the compounds were well tolerated by the cells and could be used for further biological studies (Figure 3.1.10).

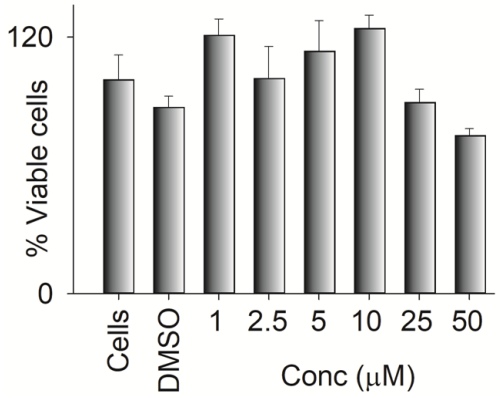

Figure 3.1.10. Cell viability assay for compound **13g** was conducted using human breast cancer cells, MCF-7 cells for 24 h.

3.1.2.8. ROS depletion assay:

H_2S being an anti-oxidant, protects the cells against damage induced by oxidative stress by depleting the levels of ROS within cells. Ageing is a natural process through which cells lose their function over time due to accumulation of oxidative damage.[18] However, exogenous administration of H_2S may have protective effects towards oxidative damage caused during ageing process. In a cellular model, treating cells with (bromodeoxyuridine) BrDU ceases the cell division process and turns them into senescent cells. This increases the levels of ROS within the cells, thereby inducing oxidative stress.[19] Therefore, the ability of the COS/H_2S donors reported in this study, to deplete the levels of ROS within cells was evaluated.

The data was provided by Ms. Kavya Gupta from Dr. Deepak Saini's lab in IISc Bangalore. Human lung carcinoma, A549 cells were treated with (BrdU) to induce senescence. ROS levels were measured using DCF-DA dye; a probe extensively used for the detection of ROS within cells.[20] As can be seen in Figure 3.1.11b, senescent cells showed a higher fluorescence signal for ROS production compared to the control cells. Senescent cells were then treated with fast (**13a**) and slow donors (**13g**) to observe the effects of the rates of H_2S release on depletion of oxidative stress. A slight decrease in the ROS levels was observed in the case of cells treated with compound **13a** (fast H_2S donor). Interestingly, the slow donor (**13g**) showed a significant decrease in the levels of ROS compared to the fast donor (**13a**). Na_2S, on the

other hand, was not effective against depleting ROS levels. Compound **15** was used as a negative control and showed no decrease in the ROS levels (Figure 3.1.11c). Therefore, the results obtained were in accordance with the hypothesis that the rate of H_2S release determines the protective effects of this gaseous signaling molecule.

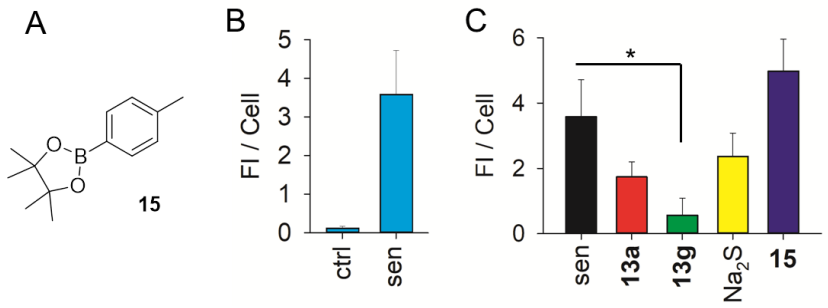

Figure 3.1.11. a) Structure of the negative control, 15 used for the study. b) ROS levels in A549 control cells and senescent cells measured by DCF-DA dye. c) Comparison of ROS depletion by fast and slow donor with respect to Na_2S in senescent cells.

3.1.2.9. ROS activated H_2S-NSAID donor

Conjugating drugs with similar therapeutic applications is gaining a lot of attention in the field of hybrid drugs.[13] The idea of conjugating non-steroidal anti-inflammatory drugs (NSAIDs) which are extensively used for the treatment of pain or inflammation, with H_2S donors has especially attracted great deal of recognition.[12] NSAIDS have been found to be associated with side effects such as corrosion of the inner stomach lining which ultimately leads to stomach ulcers, also liver and kidney problems. However, Wallace and coworkers reported that conjugating H_2S with NSAIDs markedly improves the anti-inflammatory properties of the parent drug and also increases the tolerability compared to NSAID alone.[21] H_2S contributes to gastric mucosal defense by inhibiting the leukocyte adherence to the vascular endothelium, which is the major cause of the pathogenesis of the NSAIDs.[1] Mesalamine (NSAID) is a clinically used drug for the treatment of colitis. The presence of an amine functionality in mesalamine can be utilized to conjugate with thiol to form respective carbamothioate (Scheme 3.1.11). This strategy can be effectively adapted to conjugate any drug with amine functionality which complements the properties of H_2S to form H_2S-drug hybrids.

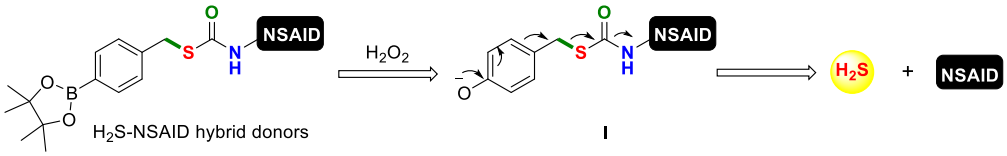

Scheme 3.1.11. Design of H_2S-NSAID hybrid donor

Mesalamine was chosen as the drug of interest due to the presence of amine functionality through which it can be conjugated to make the respective carbamothioate. First, the acid functionality was protected to form methyl ester derivative of mesalamine, **16**. Compound **16** was converted into respective carbamate by reacting with *p*-nitrophenyl chloroformate to give compound **17** (Scheme 3.1.12). Compound **17** was taken further without purification. Finally, H_2S-NSAID hybrid donor was synthesized by reacting compound **17** with the thiol, **11** to give compound **18** in 52% yield (Scheme 3.1.13).

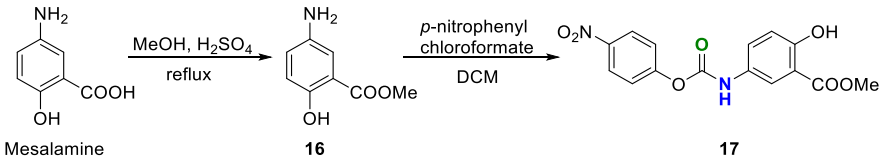

Scheme 3.1.12. Synthesis of compound **17**.

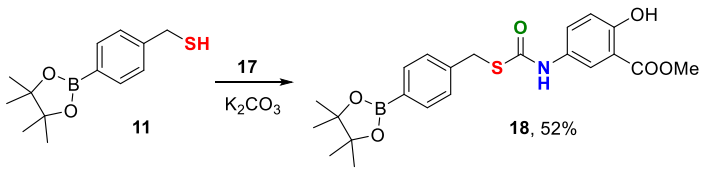

Scheme 3.1.13. Synthesis of compound **18**.

3.1.2.10. H_2S release profile for compound 18

H_2S production from compound **18** was monitored by using methylene blue formation assay. Compound **18** was incubated in buffer containing CA and 10 eq of H_2O_2 at 37 ^oC. An aliquot was removed at pre-determined time points and treated with methylene blue reagents. The formation of methylene blue was monitored by measuring the absorbance at 676 nm. Compound produced H_2S upon reaction with H_2O_2 as shown in Figure 3.1.12a. Pseudo first order rate constant for compound **18** (pK_aH of **16**; 4.13) was calculated to be 0.0145 min^{-1} which was comparable to that of compound **13b** of similar pK_aH value (pK_aH 5.03). The rate constant for H_2S generation from compound **18** followed the trend of linear regression

analysis. This further strengthened the fact that the rate of H_2S generation from crabamothioates was dependent on the pK_aH of the respective amines.

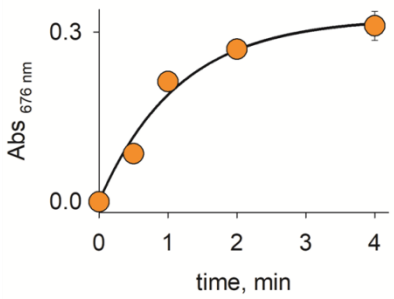

Figure 3.1.12. H_2S release profile obtained for compound **18** in the presence of H_2O_2.

3.1.2.11. Selectivity assay:

The ability of donors to generate H_2S in the presence of other reactive oxygen and sulfur species was also evaluated. Compound **18** was incubated in buffer at 37 ^oC in the presence of various reactive species for 2 h. The compound was found to be selective towards activation by H_2O_2 alone (Figure 3.1.10b) and did not produce H_2S in the presence of either glutathione, hypochlorite or *tert*-butyl hydroperoxide.

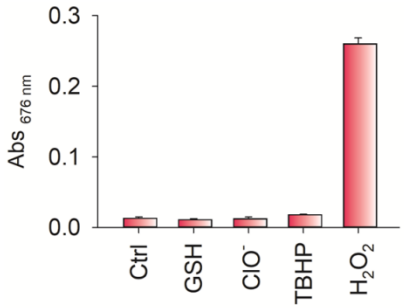

Figure 3.1.13. H_2S release response of compound **18** in the presence of various reactive oxygen and sulfur species. Ctrl represents compound alone.

3.1.2.12. TLC experiment to show mesalamine formation

In order to demonstrate the formation of **16**, upon reaction of compound **18** with H_2O_2, a TLC experiment was performed. Compound **18** was incubated in phosphate buffer (pH 7.4, 50 mM) containing H_2O_2 for 2 h. The reaction mixture was then extracted with ethyl acetate and the organic layer was spotted on a TLC plate. Formation of **16** was visualized using ninhydrin solution stain (Figure 3.1.11a). Next the hydrolysis of compound **16** to form mesalamine in the presence of esterase was demonstrated. Compound **16** was incubated in buffer containing ES at 37 ^oC for 12 h. A complete disappearance of compound **16** and formation of mesalamine was observed after completion of the reaction. Formation of meslamine was

visualized using ninhydrin stain (Figure 3.1.11b). The experiment suggested that compound **18** upon activation by ROS within cells would release COS and compound **16** which would further be converted to mesalamine upon action by esterase present in the cells. COS released would be hydrolysed to H_2S by CA.

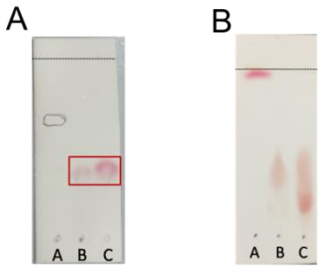

Figure 3.1.14. a) Formation of compound **16** as monitored by TLC. b) Formation of mesalamine from compound **16** upon reaction with esterase enzyme.

3.1.2.13. Cytotoxicity study of compound 18

The ability of compound **18** to inhibit proliferation of human breast cancer cell line, MCF-7 cells was evaluated by using standard MTT assay. MCF-7 cells were incubated with varying concentrations of **18** for 24 h following which the cell viability was monitored. No significant cytotoxicity was observed with 50 μM concentration of the compound suggesting that the compound was well tolerated by the cells and could be used for further biological applications (Figure 3.1.12).

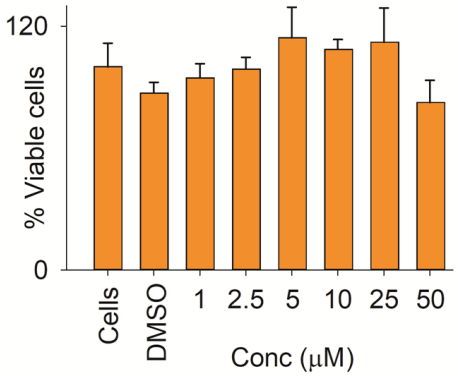

Figure 3.1.15. Cell viability assay with compound **18** in human breast carcinoma cell line, MCF-7 cells for 24 h.

3.1.3. Other Reports:

While this work was in progress, Pluth and coworkers synthesized scaffolds to understand the kinetics of H_2S delivery using isomers of the caged carbonyl sulfide.[22] Although the work reported by Pluth and co-workers was thorough, but there were certain points that differed

from the analysis reported in this study. Firstly, the molecules synthesized in the study were found to follow trigger independent pathways for the generation of H_2S and therefore a clear correlation between the rates of H_2S obtained with the electronics of leaving group amine could not be made (Scheme 3.1.14).

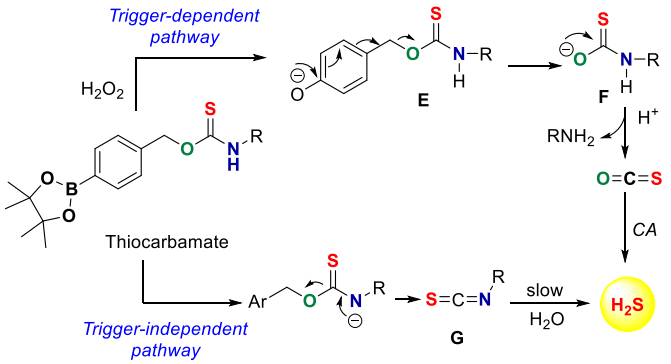

Scheme 3.1.14. Pathways of H_2S production from thiocarbamates.

Also, the pK_aH range (1.01 – 5.08) tested by Pluth and coworkers was small. We sampled a broader range of pK_aH values for a comprehensive analysis. Interestingly, 4-fluoroaniline based carbamothioate derivative (**SA-PeroxyTCM-1**) was also reported in this study and the rate of H_2S release when exposed to H_2O_2 was measured (Figure 3.1.3a). The rate of H_2S production from 4-fluororaniline with pK_aH value of 4.66 was calculated to be 0.01 $M^{-1}s^{-1}$. The pseudo first constant rate constant for the same was calculated to be 0.016 min^{-1} (data from Figure S3, Supporting Information, Ref 22) which followed the trend shown in the linear regression analysis. This is a testament to the robustness of our model that predicts the H_2S release from carbamothioates. Finally, the study reported the decomposition of intermediate **F** as the rate determining step which was unlikely based on our analysis. Also, this meant that the rate constants for both the thiocarbamate and the carbamothioate of a respective amine should be same which was not found to be the case.

3.1.4. Summary

In conclusion, carbamothioate based ROS triggered COS/H_2S donors for targeted delivery of H_2S towards areas under oxidative stress have been reported. In this chapter it is demonstrated that modulating the rate of H_2S release is possible by varying the basicity of the amine leaving group. A 8-fold in the rates of H_2S production from the H_2S donor motifs have been achieved with the donors. Compound **13c** with *p*-anisidine as the leaving group is the fastest (half-life of 23.9 min) and compound **13g** with propylamine as the leaving group is the slowest (half-life of 203.8 min) amongst all. ROS activated H_2S-NSAID hybrid donor with a

derivative of mesalamine (clinically used drug for the treatment of colitis) have also been reported. This is the first example of achieving targeted delivery of H_2S-NSAID hybrid drugs. The donors are well tolerated by the cells and therefore can be used for further cellular analysis. Also, compounds are capable of depleting ROS levels within cells as demonstrated by the ROS depletion assay.

3.1.5. Experimental Section

3.1.5.1 Synthesis and characterization:

Compound **10**[23] and **16**[24] were synthesized using a previously reported procedure and the analytical data collected was consistent with the reported values.

(4-(4,4,5,5-tetramethyl-1,3,2-dioxaborolan-2-yl) phenyl) methanethiol (11):

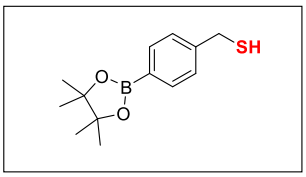

To a well- stirred solution of **10** (1.2 g, 5.13 mmol) in dry DCM (10 mL), PBr_3 (481 µL, 5.13 mmol) was added slowly under N_2 atmosphere. The reaction was allowed to stir for 1 h at 0 ^oC. Progress of the reaction was monitored by TLC. After completion the reaction mixture was quenched by adding 15 mL of saturated $NaHCO_3$ solution. The aqueous layer was extracted using DCM (3 x 10 mL). The combined organic layer was dried over Na_2SO_4, filtered and concentrated. The residue obtained was slightly brown in colour. This was further dissolved in dry THF (15 mL) and thiourea salt(1 g, 13 mmol) was added at room temperature. Reaction was allowed to stir overnight at room temperature. After completion of the reaction (as monitored by TLC), solvent was removed under reduced pressure and salt obtained was dissolved in water (20 mL) followed by the addition of DCM (30 mL). The reaction was purged with N_2 for 5 min. To this heterogenous solution, 4 equivalents of sodium metabisulfite salt ($Na_2S_2O_5$) were added. The resulting mixture was refluxed for 4 h under N_2 atmosphere. The solution was then cooled to room temperature and washed twice with DCM (20 mL). The organic layer was combined and dried over Na_2SO_4, filtered and concentrated. The crude obtained was purified using silica gel column chromatography (1% EtOAc/hexane). The compound was obtained as a white color crystalline solid with pungent smell (1.1 g, 82%). NMR obtained matched with the reported spectra. FT-IR (υ_{max} , cm^{-1}) 2924; ^1H NMR (400MHz, $CDCl_3$): δ 7.77 (d, *J*=8.0 Hz, 2H), 7.33 (d, *J*=8.0 Hz, 2H), 3.74 (d,*J* = 7.6 Hz, 2H), 1.74 (t, *J* = 7.6 Hz, 1H), 1.34(s, 12H);^{13}C NMR (100 MHz, $CDCl_3$) δ 144.3, 135.2, 127.4, 83.8, 29.1, 24.8; HRMS for $C_{13}H_{19}BO_2S$ $(M+H)^+$: Calculated: 251.1277, Found: 251.1279.

Synthesis of carbamates (12a-12i, 17):

To a well-stirred solution of the methyl 3-aminobenzoate (0.20 g, 1.32 mmol) in dry THF at 0 ^oC, pyridine (110 µL, 1.32 mmol) was added. To this *p*-nitrophenylchloroformate (0.27 g,

1.32 mmol) was added. The reaction was stirred for reported time point and the completion of reaction was monitored by TLC. To the resulting mixture was then added 10 mL of water and washed twice with DCM (2 x 10 ml). The combined organic layer was dried over Na_2SO_4, filtered and concentrated. The crude was taken forward for next step without purification. Similar protocol was used for the synthesis of other carbamates. No base was required for the synthesis of **17**.

S-(4-(4,4,5,5-tetramethyl-1,3,2-dioxaborolan-2-yl) benzyl) (4methoxyphenyl) carbamothioate (13c):

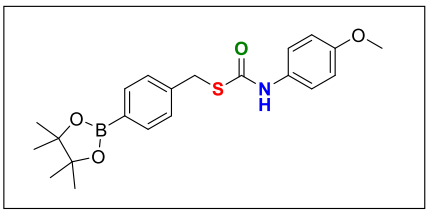

To the well-stirred solution of **11** (0.20g, 0.80 mmol) in dry ACN under the N_2 atmosphere, K_2CO_3 (0.30 g, 2.16 mmol) was added. The reaction was allowed to stir 5 min followed by addition of **5c** (0.23 g, 0.70 mmol). Reaction mixture was then stirred for 3 h and the progress was monitored by TLC. After completion of the reaction, it was quenched by adding 10 mL of water and washed thrice with DCM (10 mL). The organic layer was combined and dried over Na_2SO_4, filtered and concentrated. Purification was done using prep HPLC and ACN-water as the eluents. **13c** was obtained as white solid (86 mg, 27 %). FT-IR (υ_{max} , cm^{-1}) 3294, 1662, 1609; ^{1}H NMR (400 MHz, $CDCl_3$): δ 7.75 (d, *J* = 7.9 Hz, 2H), 7.35 (d, *J* = 7.8 Hz, 2H), 7.29 (d, *J* = 8.7 Hz, 2H), 6.95 (s, 1H), 6.84 (d, *J* = 8.9 Hz, 2H), 4.20 (s, 2H), 3.79 (s, 2H), 1.33 (s, 12H); ^{13}C NMR (100 MHz, $CDCl_3$) δ 165.3, 157.0, 141.3, 135.2, 128.4, 115.9, 83.9, 55.6, 34.6, 24.9; HRMS for $C_{21}H_{26}BNO_4S$ $(M+H)^+$: Calculated: 400.1754, Found: 400.1763.

S-(4-(4,4,5,5-tetramethyl-1,3,2-dioxaborolan-2-yl)benzyl) (4-nitrobenzyl)carbamothioate (13d):

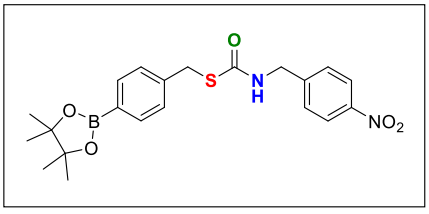

Compound **13d** was synthesized using protocol outlined for **13c**. Compound **11** (0.18g, 0.72 mmol), K_2CO_3(0.30 g, 2.16 mmol) and **12d** (0.23g, 0.72 mmol) were taken. **13d** was obtained as white solid (70 mg, 23 %). FT-IR (υ_{max} , cm^{-1}) 3054, 2926, 1671, 1520, 1355; ^{1}H NMR (400 MHz, $CDCl_3$): δ 8.18 (d, *J*=8.0 Hz, 2H), 7.76 (d, *J*=8.0 Hz, 2H), 7.41 (d, *J*=8.0 Hz, 2H), 7.34 (d, *J*=8.0 Hz, 2H), 5.77 (s, 1H), 4.58 (d, *J*=4.0 Hz, 2H), 4.19 (s, 2H), 1.34 (s, 12 H); ^{13}C NMR (100 MHz, $CDCl_3$) 147.4, 145.1, 141.1,

135.1, 128.2, 128.1, 124.0, 83.8, 44.5, 34.5, 24.9; HRMS for $C_{22}H_{25}BN_2O_5S$ $(M+H)^+$: Calculated: 429.1655, Found: 429.1664.

Methyl 2-hydroxy-5-((((4-(4,4,5,5-tetramethyl-1,3,2-dioxaborolan-2-yl)benzyl)thio)carbonyl)amino)benzoate (18):

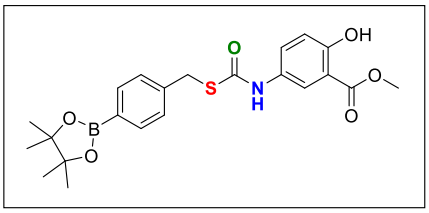

Compound **18** was synthesized using protocol outlined for compound **13c**. Compound **11** (0.10g, 0.39mmol), K_2CO_3 (0.17g, 1.20 mmol) and **17** (0.13 g, 0.39mmol) were added in DMF and stirred for 30 min. Compound **18** was obtained as a white solid (92 mg , 52%).FT-IR ($\upsilon_{max,}$ cm^{-1}): 3472, 3293, 2979, 1680, 1615; ^1H NMR (400 MHz, $CDCl_3$): δ 10.65 (s, 1H), 7.92 (d, *J* = 2.1 Hz, 1H), 7.75 (d, *J* = 8.0 Hz, 2H), 7.40 (dd, *J* = 8.9, 2.7 Hz, 1H), 7.35 (d, *J* = 8.0 Hz, 2H), 6.97 (s, 1H), 6.94 (d, *J* = 8.9 Hz, 1H), 4.21 (s, 2H), 3.94 (s, 3H), 1.33 (s, 12H); ^{13}C NMR (100 MHz, $CDCl_3$) 170.0, 158.9, 141.0, 135.1, 128.2, 118.2, 112.2, 83.8, 52.5, 34.5, 24.8; HRMS(ESI) for $C_{22}H_{26}BNO_6S$: Calculated $(M+H)^+$:444.1652, Found :444.1662.

4-(4,4,5,5-tetramethyl-1,3,2-dioxaborolan-2-yl)benzyl (4-methoxyphenyl)carbamate (14):

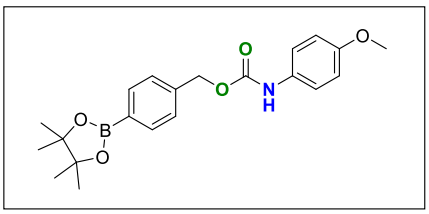

To a well stirred solution of **10** (0.25 g, 1.07 mmol) in dry ACN, K_2CO_3 (0.44 g, 3.20 mmol) was added. To this **5c** (0.31 g, 1.07 mmol) was added after 5 min. The reaction was allowed to stir at room temperature for 1 h. Progress of the reaction was monitored by TLC. After completion, the reaction was quenched by adding water (10 mL) and extracted with DCM (3 × 10 mL). The combined organic layer was dried over Na_2SO_4, filtered and concentrated.The crude obtained was purified using prep HPLC with ACN-water as the eluents. Product was obtained as off white solid (165 mg, 40.31%). %). FT-IR ($\upsilon_{max,}$ cm^{-1}) 3346, 2969, 1693; ^1H NMR (400 MHz $CDCl_3$):δ 7.80 (d, *J* = 7.9 Hz, 2H), 7.38 (d, *J* = 7.9 Hz, 2H), 7.27 (d, *J* = 7.2 Hz, 2H), 6.83 (d, *J* = 9.0 Hz, 2H), 6.57 (s, 1H), 5.18 (s, 2H), 3.77 (s, 3H), 1.33 (s, 12H); ^{13}C NMR ($CDCl_3$, 100 MHz): δ 139.2, 135.0, 130.8 127.3, 120.7, 114.3, 84.0, 66.8, 55.5, 24.9; HRMS(ESI) for $C_{21}H_{26}BNO_5$: Calculated $(M+H)^+$: 384.1982, Found :384.1981.

3.1.5.2. Methylene Blue assay for H_2S detection:

Each assay described herein was done in triplicate in vials with closed lids, containing 249 µL of PBS (pH 7.4, 50 mM, 10µM DTPA), 3 µL of compound (10 mM stock in DMSO), 3 µL of carbonic anhydrase (1% stock in PBS buffer),15µL of $Zn(OAc)_2$ (40mM stock in H_2O) and 30 µL of H_2O_2 (10 mM stock in buffer) was added. The reaction was allowed to stir at 37 ^oC for 2 h. 100µL of the reaction aliquot was taken out and diluted with 100 µL of $FeCl_3$ (30 mM stock in 1.2 M HCl) and 100 µL of N,N-dimethyl-*p*-phenylenediamine sulfate (20 mM stock in 7.2 M HCl). The reaction was again allowed to stir for 30 min. The aliquots were transferred to a 96 well plate (250 µL/well) and the absorbance was measured at 676 nm using a microtiter plate reader.[25]

3.1.5.3. Kinetics of H_2S release using methylene blue:

This experiment was conducted by Ms Swetha Jos. Briefly, each assay described was done in triplicate in vials with closed lids, containing 664 µL of PBS (pH 7.4, 50 mM, 10µM DTPA), 8 µL of compound (10 mM stock in DMSO), 8 µL of carbonic anhydrase (1% stock in PBS buffer), 40 µL of $Zn(OAc)_2$ (40 mM stock in H_2O) and 80 µL of H_2O_2(10 mM stock in buffer) was added. The reaction was allowed to stir at 37 ^oC for 6 h. At predetermined time points, 100 µL of the reaction aliquot was removed and diluted with 100 µL of $FeCl_3$ (30 mM stock in 1.2 M HCl) and 100 µL of *N*,*N*-dimethyl-*p*-phenylenediamine sulfate (20 mM stock in 7.2 M HCl). The reaction was again allowed to stir for 30 min. The aliquots were transferred to a 96 well plate (250 µL/well) and the absorbance spectra were collected from 500 to 800 nm wavelength. The H_2S release kinetics plots for the compounds are shown in Figure 3.1.2.

3.1.5.4. HPLC based kinetics study:

This experiment was conducted by Ms Swetha Jos. A stock solution of **13c** (10 mM) was prepared in DMSO. The reaction mixture contained **13c** (10 µL, 10 mM), 100 µL of H_2O_2 (10 mM in H_2O) in 890 µL of buffer and stirred at 37 ^oC. Aliquots of 100 µL were taken at reported time points, filtered (0.22-micron filter) and injected (50 µL) in a high-performance liquid chromatography (HPLC Agilent Technologies 1260 Infinity). The mobile phase was H_2O/ACN. The stationary phase was C-18 reverse phased column (Phenomenex, 5 µm, 4.6 x 250 mm). A multistep gradient was used with a flow rate of 1 mL/min starting with → 0 - 5 min, 70:30 to 50:50 → 5 - 15 min, 50:50 to 10:90 → 15 - 17 min, 10:90 to 40:60 → 17- 22

min, 70:30. A similar protocol was followed for the decomposition of **13g**. **13c** and **13g** were taken as representative compounds since the difference in rate constants for the release of H_2S were significant under the activation by H_2O_2. Figure 3.1.4 shows the representative plot for the intermediate formation from compound **13c** and its dissipation in 2 h. In Acetonitrile (ACN) **13c** has a retention time (rt) of 17.62 min and with incubation in the buffer for 5 minutes, it shifts to 9.85 min. This is due to hydrolysis of boronate ester group to boronic acid in buffer. The boronic acid so formed decomposes to form an intermediate within 30 min which dissipates over a period of 2 h. Similar observations were made in the case of **13g**, however the intermediate formed decomposed over a period of 6 h.

3.1.5.5. Selectivity study:

Compound **18** was tested for its ability to produce H_2S in the presence of thiol and reactive oxygen species like hypochlorite and TBHP. Each assay described was done in triplicate in vials with closed lids, containing 368 µL of PBS (pH 7.4, 50 mM, 10µM DTPA), 4 µL of compound (10 mM stock in DMSO), 4 µL of carbonic anhydrase (1% stock in PBS buffer), 20µL of $Zn(OAc)_2$ (40mM stock in H_2O) and 4 µL of H_2O_2 (100 mM stock in H_2O) was added at the end. The reaction was allowed to stir at 37 ^oC for 2 h. 100µL of the reaction aliquot was taken and diluted with 100 µL of $FeCl_3$ (30 mM stock in 1.2 M HCl) and 100 µL of *N*,*N*-dimethyl-*p*-phenylenediamine sulfate (20 mM stock in 7.2 M HCl). The reaction was again allowed to stir for 30 min. The aliquots were transferred to a 96 well plate (250µL/well) and the absorbance was measured at 676 nm.

3.1.5.6. Detection of 16 by TLC:

Compound **18** (1mM) was incubated with H_2O_2 (10 mM) in PBS (pH 7.4, 50 mM, 10µM DTPA) at 37 ^oC for 2 h, after which the reaction mixture was extracted with ethyl acetate and spotted on a TLC plate. The eluant used was 30% ethyl acetate- hexane; ninhydrin stain solution was used to visualize the formation of compound **16** on the TLC plate.

3.1.5.7. Detection of mesalamine by TLC:

Compound **16** (2 mM) was incubated with esterase (0.01 U/µL) in PBS (pH 7.4, 50 mM) at 37 ^oC for overnight. The reaction mixture was extracted with ethyl acetate and spotted on a TLC plate. The eluant used was 30% methanol – chloroform and ninhydrin stain was used to visualize the formation of mesalamine.

3.1.5.8. Cytotoxicity assay:

Human breast cancer MCF-7 cells, were seeded at a concentration of 1 x 10^4/well overnight in a 96-well plate in complete DMEM media. Cells were exposed to varying concentrations of the test compound prepared as DMSO stock solution to make the final concentration of DMSO as 0.5%. The cells were incubated for 24 h at 37^{o}C. A concentration of 0.5 mg/mL solution of 3-(4,5-dimethylthiazol-2-yl)-2,5-diphenyl tetrazolium bromide (MTT) was prepared (3.5 mg in 7 mL of DMEM). 100 µL of the resulting solution was added to each well. Media was removed after 4 h and 100 µL of DMSO was added. Spectrophotometric analysis of each well was performed using a microplate reader (Thermo Scientific Varioskan) at 570 nm.

3.1.5.9. ROS depletion assay:

Human lung carcinoma, A549 cells were seeded (50x10^3 cells/well) in 24 well plate and incubated at 37^o C with 5% CO_2. Next day, cells were treated with 200µM bromodeoxyuridine (BrdU) and incubated for 96 h at 37^o C with 5% CO_2. Cells were then washed twice with 1x PBS and treated with 10µM of ROS activated H_2S donors (**13a** and **13g**) and incubated for 4 h. Cells were again washed twice with 1x PBS and treated with 10µM DCFDA in only DMEM for 40 minutes at 37^o C with 5% CO_2 followed by washing twice with 1x PBS. Fluorescence was measured at 492 nm (excitation) and 515 nm (emission). Fluorescence was normalized to per cell and fold change was plotted.

3.1.6. Spectra Analysis

^{1}H NMR spectrum (400 MHz, $CDCl_3$) of compound **11**

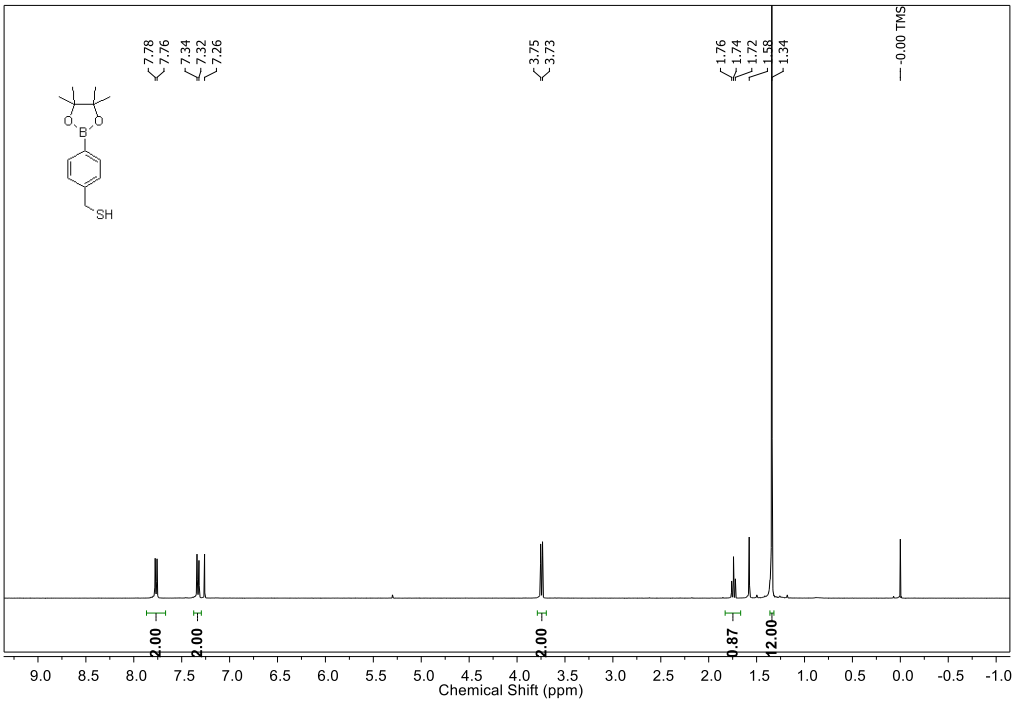

^{13}C NMR spectrum (100 MHz, $CDCl_3$) of compound **11**

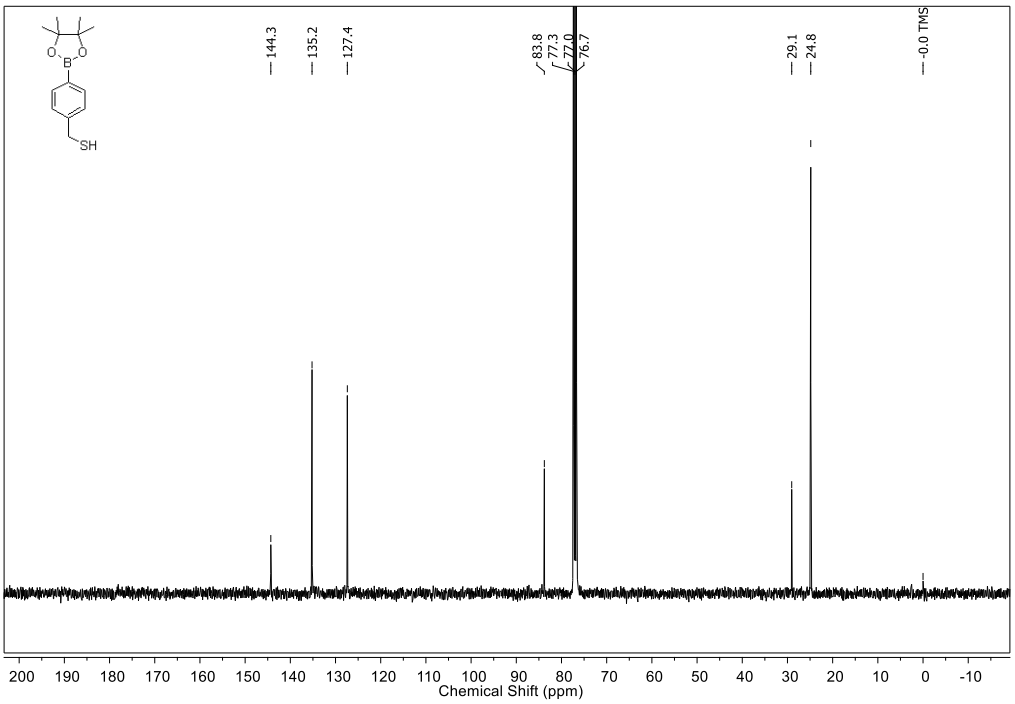

^{1}H NMR spectrum (400 MHz, $CDCl_3$) of compound **13a**

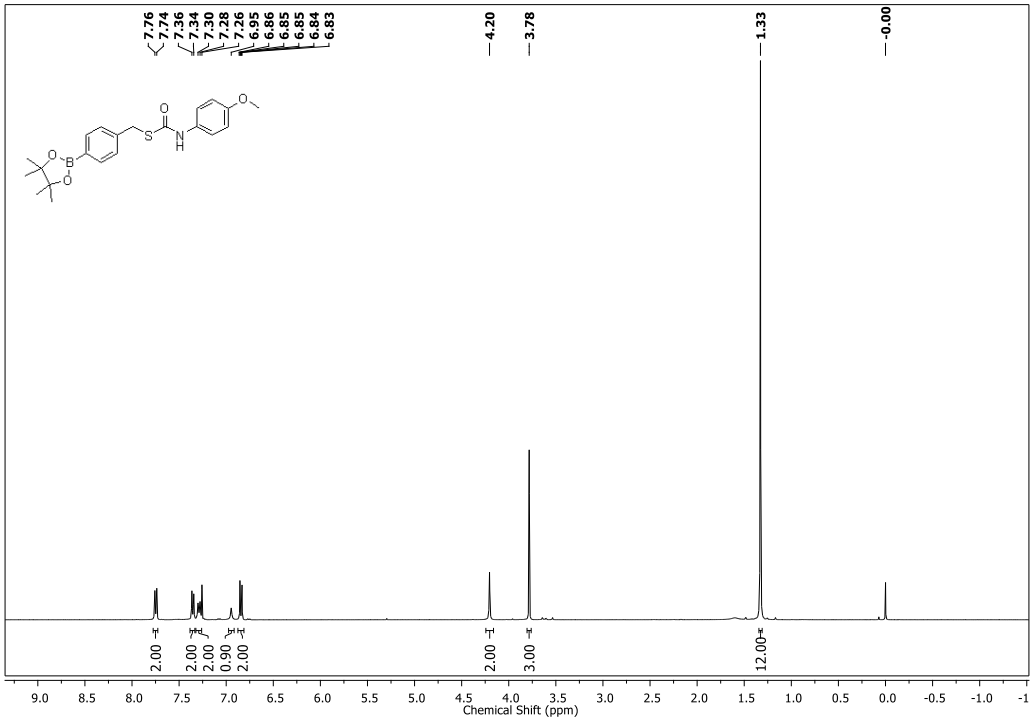

^{13}C NMR spectrum (100 MHz, $CDCl_3$) of compound **13a**

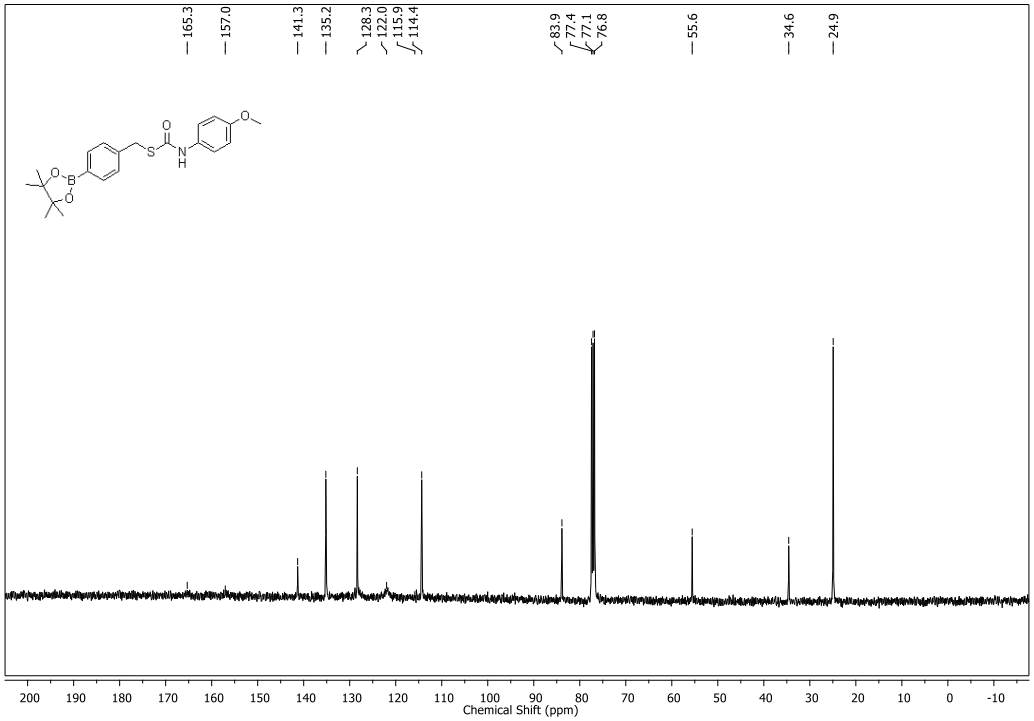

^{1}H NMR spectrum (400 MHz, $CDCl_3$) of compound **13d**

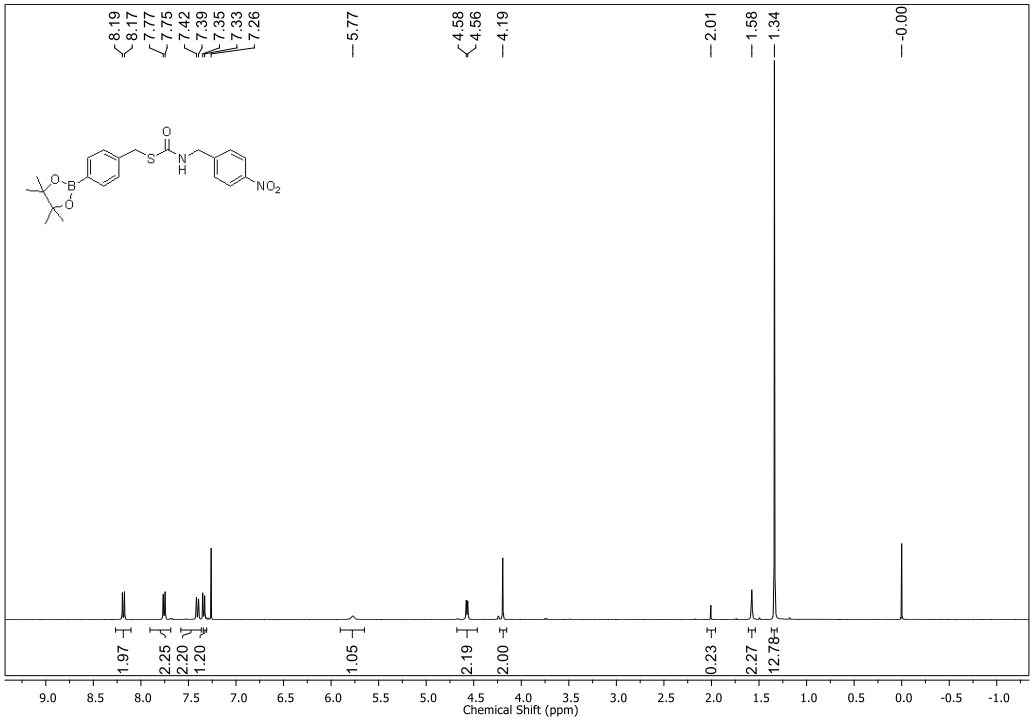

^{13}C NMR spectrum (100 MHz, $CDCl_3$) of compound **13d**

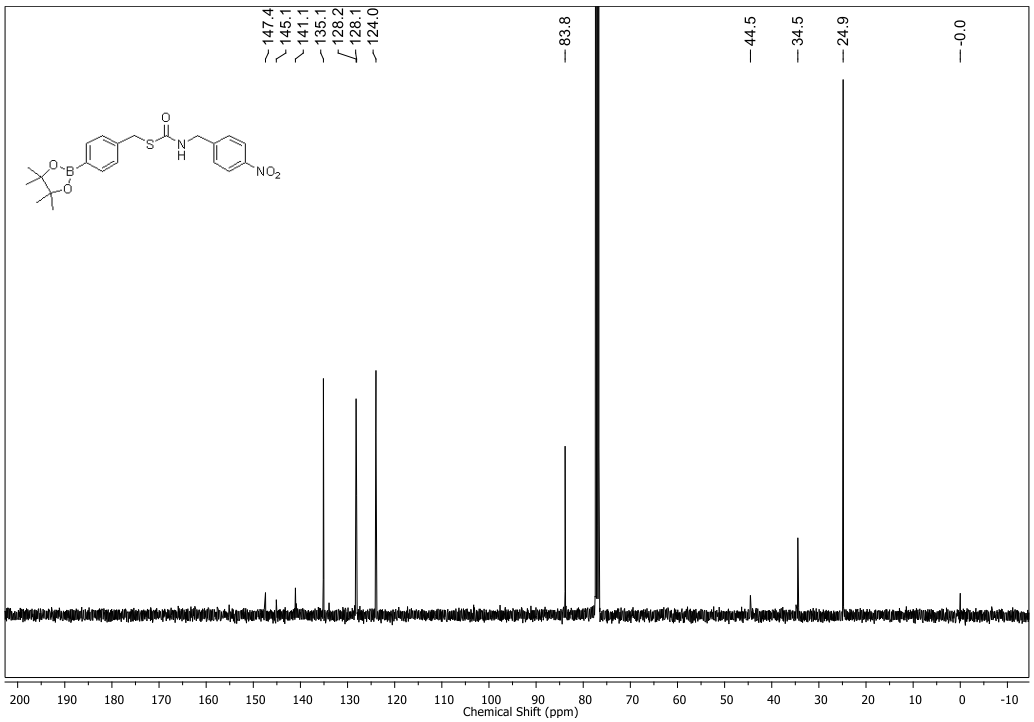

^{1}H NMR spectrum (400 MHz, $CDCl_3$) of compound **18**

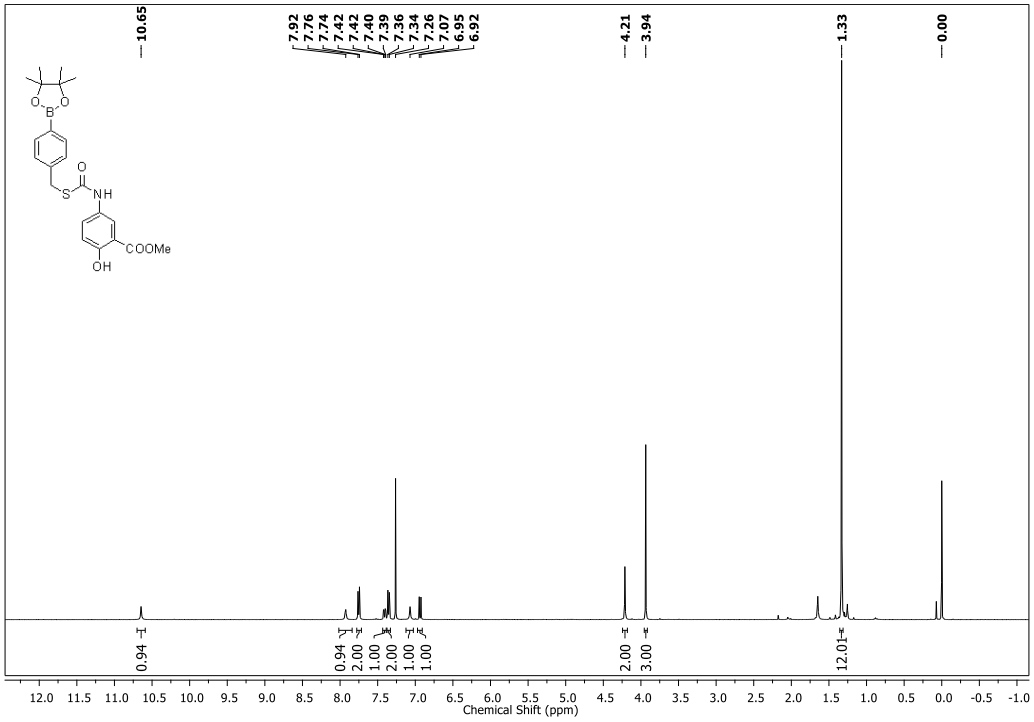

^{13}C NMR spectrum (100 MHz, $CDCl_3$) of compound **18**

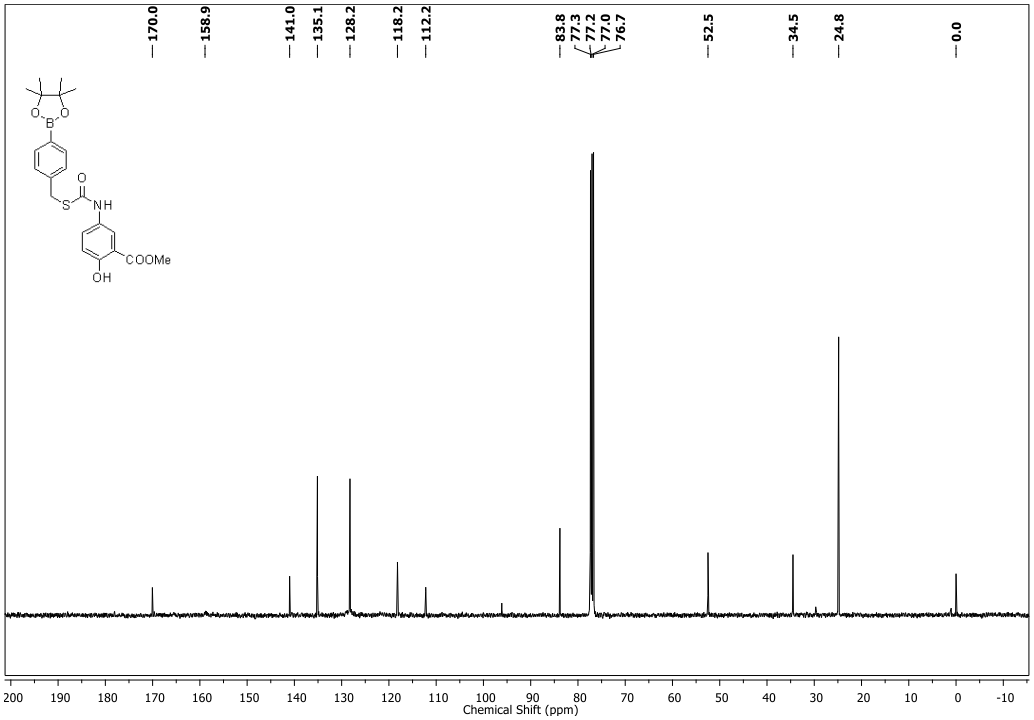

^{1}H NMR spectrum (400 MHz, $CDCl_3$) of compound **14**

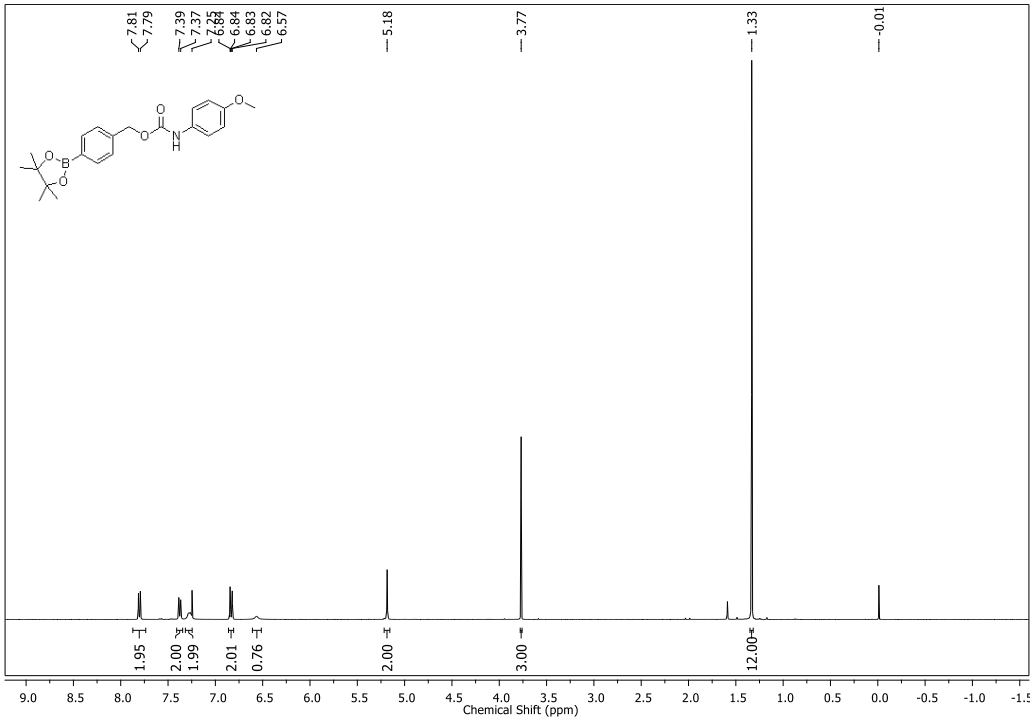

^{13}C NMR spectrum (100 MHz, $CDCl_3$) of compound **14**

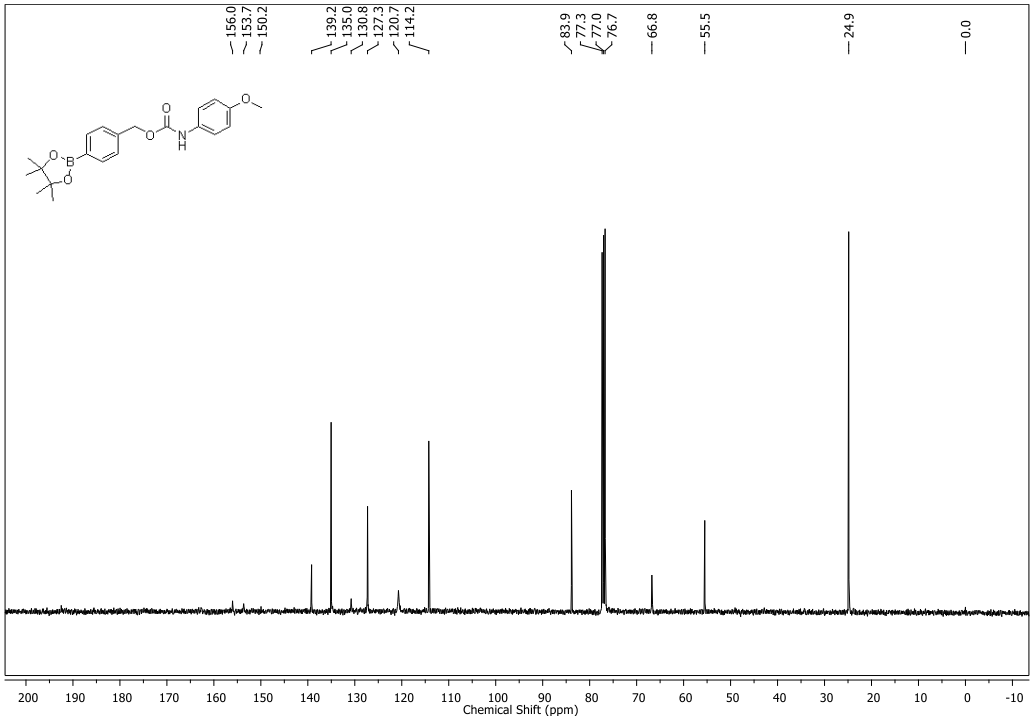

3.1.7. References

(1) Wallace, J. L.; Wang, R. *Nat. Rev. Drug. Discov.* **2015**, *14*, 329.

(2) Szabo, C. *Nat Rev Drug Discov* **2007**, *6*, 917.

(3) Wang, R. *Physiological Reviews* **2012**, *92*, 791.

(4) Elrod, J. W.; Calvert, J. W.; Morrison, J.; Doeller, J. E.; Kraus, D. W.; Tao, L.; Jiao, X.; Scalia, R.; Kiss, L.; Szabo, C.; Kimura, H.; Chow, C.-W.; Lefer, D. J. *Proc. Natl. Acad. Sci. U S A* **2007**, *104*, 15560.

(5) Vacek, T. P.; Gillespie, W.; Tyagi, N.; Vacek, J. C.; Tyagi, S. C. *Amino Acids.* **2010**, *39*, 1161.

(6) Bhatia, M. *Scientifica* **2012**, *2012*, 159680.

(7) Li, L.; Whiteman, M.; Guan Yan, Y.; Neo Kay, L.; Cheng, Y.; Lee Shiau, W.; Zhao, Y.; Baskar, R.; Tan, C.-H.; Moore Philip, K. *Circulation* **2008**, *117*, 2351.

(8) Whiteman, M.; Li, L.; Rose, P.; Tan, C.-H.; Parkinson, D. B.; Moore, P. K. *Antioxid. Redox Signal.* **2010**, *12*, 1147.

(9) Sun, X.; Wang, W.; Dai, J.; Jin, S.; Huang, J.; Guo, C.; Wang, C.; Pang, L.; Wang, Y. *Sci. rep.* **2017**, *7*, 3541.

(10) Dharmaraja, A. T.; Ravikumar, G.; Chakrapani, H. *Org. Lett.* **2014**, *16*, 2610.

(11) Hall, H. K. *J. Am. Chem. Soc.* **1957**, *79*, 5441.

(12) Li, L.; Rossoni, G.; Sparatore, A.; Lee, L. C.; Del Soldato, P.; Moore, P. K. *Free Radic. Biol. Med.* **2007**, *42*, 706.

(13) Sparatore, A.; Santus, G.; Giustarini, D.; Rossi, R.; Del Soldato, P. *Expert rev. clin. pharmacol.* **2011**, *4*, 109.

(14) Moest, R. R. *Anal. Chem.* **1975**, *47*, 1204.

(15) Kalyanaraman, B.; Darley-Usmar, V.; Davies, K. J. A.; Dennery, P. A.; Forman, H. J.; Grisham, M. B.; Mann, G. E.; Moore, K.; Roberts, L. J.; Ischiropoulos, H. *Free. Radic. Biol. Med.* **2012**, *52*, 1.

(16) Sikora, A.; Zielonka, J.; Lopez, M.; Joseph, J.; Kalyanaraman, B. *Free radic. biol. med.* **2009**, *47*, 1401.

(17) Steiger, A. K.; Pardue, S.; Kevil, C. G.; Pluth, M. D. *J. Am. Chem. Soc.* **2016**, *138*, 7256.

(18) Liguori, I.; Russo, G.; Curcio, F.; Bulli, G.; Aran, L.; Della-Morte, D.; Gargiulo, G.; Testa, G.; Cacciatore, F.; Bonaduce, D.; Abete, P. *Clin. Interv. Aging* **2018**, *13*, 757.

(19) Zhang, Y.; Unnikrishnan, A.; Deepa, S. S.; Liu, Y.; Li, Y.; Ikeno, Y.; Sosnowska, D.; Van Remmen, H.; Richardson, A. *Redox Biol.* **2016**, *11*, 30.

(20) Dharmaraja, A. T.; Chakrapani, H. *Org. Lett.* **2014**, *16*, 398.

(21) Fiorucci, S.; Orlandi, S.; Mencarelli, A.; Caliendo, G.; Santagada, V.; Distrutti, E.; Santucci, L.; Cirino, G.; Wallace, J. L. *Br. J. Pharmacol.* **2007**, *150*, 996.

(22) Zhao, Y.; Henthorn, H. A.; Pluth, M. D. *J. Am. Chem. Soc.* **2017**, *139*, 16365.

(23) Hopper, D. W.; Vera, M. D.; How, D.; Sabatini, J.; Xiang, J. S.; Ipek, M.; Thomason, J.; Hu, Y.; Feyfant, E.; Wang, Q.; Georgiadis, K. E.; Reifenberg, E.; Sheldon, R. T.; Keohan, C. C.; Majumdar, M. K.; Morris, E. A.; Skotnicki, J.; Sum, P.-E. *Bioorg. Med. Chem. Lett.* **2009**, *19*, 2487.

(24) Agharbaoui, F. E.; Hoyte, A. C.; Ferro, S.; Gitto, R.; Buemi, M. R.; Fuchs, J. R.; Kvaratskhelia, M.; De Luca, L. *Eur. J. Med. Chem.* **2016**, *123*, 673.

(25) Powell, C. R.; Foster, J. C.; Okyere, B.; Theus, M. H.; Matson, J. B. *J. Am. Chem. Soc.* **2016**, *138*, 13477.

Title: Reactive Oxygen Species-Triggered Tunable Hydrogen Sulfide Release

Author: Preeti Chauhan, Swetha Jos, Harinath Chakrapani

Publication: Organic Letters

Publisher: American Chemical Society

Date: Jul 1, 2018

PERMISSION/LICENSE IS GRANTED FOR YOUR ORDER AT NO CHARGE

This type of permission/license, instead of the standard Terms & Conditions, is sent to you because no fee is being charged for your order. Please note the following:

- Permission is granted for your request in both print and electronic formats, and translations.
- If figures and/or tables were requested, they may be adapted or used in part.
- Please print this page for your records and send a copy of it to your publisher/graduate school.
- Appropriate credit for the requested material should be given as follows: "Reprinted (adapted) with permission from (COMPLETE REFERENCE CITATION). Copyright (YEAR) American Chemical Society." Insert appropriate information in place of the capitalized words.
- One-time permission is granted only for the use specified in your request. No additional uses are granted (such as derivative works or other editions). For any other uses, please submit a new request.

CHAPTER 3.2: ROS activated gem-dithiol based H_2S donors

3.2.1. Introduction

In chapter 3.2, we propose to follow approach 2 to synthesize ROS activated gem-dithiol based H_2S donor for studying the anti-cancer effects of this gaseous species. The role of hydrogen sulfide in cancer is controversial with both pro and anti-cancer activities reported.[1-3] H_2S producing enzymes (CBS or CSE) are found to be over expressed in various cancers[4,5] and therefore inhibiting the production of H_2S within cells has shown anti-cancer effects. For example, inhibition of CSE by propargylglycine or CSE knockdown by shRNA inhibits the proliferation and migration of human colon cancer SW480 cells.[6] In contrast to this, increasing the dose of H_2S through exogenous administration can also act as a potential anti-cancer strategy. H_2S is reported to induce cell cycle arrest through uncontrolled intracellular acidification; thus, promoting apoptosis.[3] Moore and coworkers, have shown that treatment of HepG2 and MCF-7 cancer cells with increasing dose of GYY4137 for 5 days lead to a substantial increase in the rate of glycolysis which resulted in excess lactate production. H_2S suppressed the activities of the anion exchanger and Na/H exchanger without affecting the pH regulators. Therefore, enhanced acid production and defect in pH regulation lead to an uncontrolled intracellular acidification which resulted in cancer cell death. However, GYY4137 lacks spatiotemporal control over the release of H_2S. Also, the conclusions drawn from the study are ambiguous due to the lack of negative control. Thus, achieving cancer targeted delivery with increased payload of H_2S would be useful in this regard.

Figure 3.2.1. H_2S as an anti-cancer agent

Cancer is associated with higher levels ROS which induces oxidative stress; thus designing ROS triggered gem-dithiol based H_2S donors would be useful. Previous results showed that intermediate **A** decomposed to produce intermediate **B** which further hydrolyzed to give 2 moles of H_2S. On the other hand, no H_2S formation was observed from intermediate **C** which was found to be stable in pH 7.4 buffer (Scheme 3.2.1).

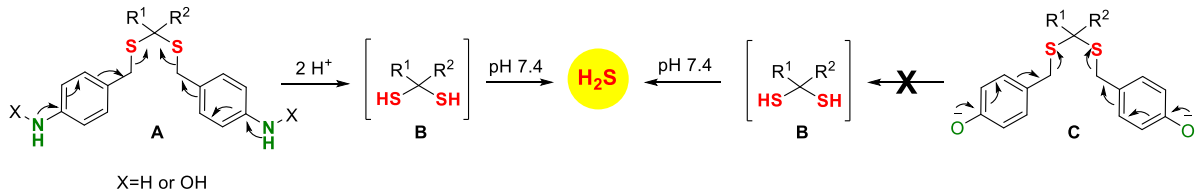

Scheme 3.2.1. Proposed mechanism of H_2S release from intermediates **A** and **C**.

Therefore, in approach 2 we propose to introduce a self immolative linker between boronate ester trigger and intermediate **A** through a carbamate bond (Scheme 3.2.2). The proposed mechanism of H_2S release is as follows: Compound upon reaction with H_2O_2 releases an intermediate **D** which further dissociates to generate geminal dithiol, **B**. Being labile under buffer conditions intermediate **B** would rapidly hydrolyse to generate 2 moles of H_2S. Compound also generates 4 equivalents of quinone methide upon decomposition (Scheme 3.2.3).

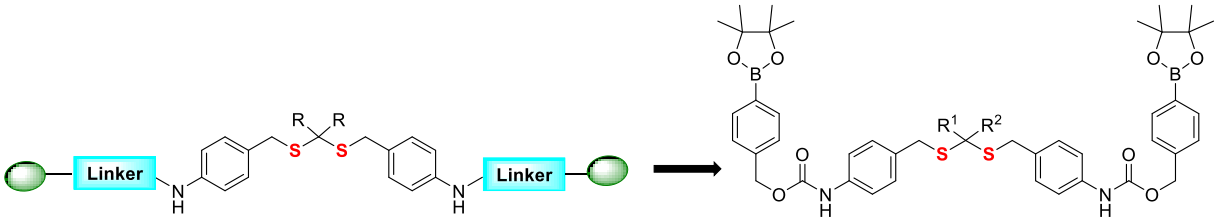

Scheme 3.2.2. Design of ROS triggered gem-dithiol based H_2S donors.

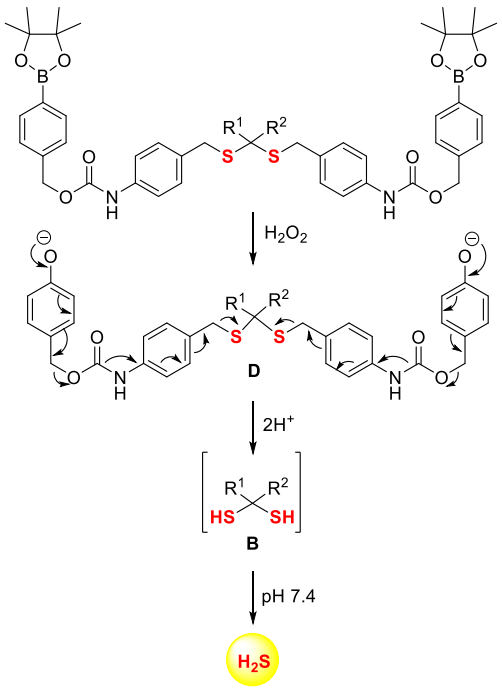

Scheme 3.2.3. Modified design of ROS activated H_2S donors.

3.2.2. Results and Discussion

3.2.2.1. Synthesis:

Compound **24** was synthesized in eight steps using the scheme shown below (scheme 3.2.4). *p*-bromobenzaldehyde was reacted with $B_2(pin)_2$ in the presence of $Pd(dppf)Cl_2$ catalyst and potassium acetate base for 12 h to give compound **9** in a quantitative yield. Compound **9** was then reduced in the presence of $NaBH_4$ to give compound **10** in 81% yield. Compound **10** was further reacted with 4-formylbenzoic acid in the presence diphenyl phosphoryl azide (DPPA) to form compound **20** in 58% yield via curtius rearrangement. The aldehyde group in compound **20** was further reduced to an alcohol in the presence of $NaBH_4$ to form compound **21** with 80% yield. The alcohol moiety was converted to a bromide group by reacting with tribromophosphine for 1 h at 0 ^oC. Compound **22** so formed was unstable and therefore was taken further without purification to react with thiourea salt and form a thiourea adduct. The thiourea salt was then hydrolysed in the presence of $Na_2S_2O_5$ to produce thiol **23** in 66% overall yield (Scheme 3.2.4). Thiol **23** was coupled with cyclopentanone in the presence of Lewis acid $TiCl_4$ to form geminal dithiol group and give compound **24** in 17% yield. The reaction does not go to completion and also the compound formed was unstable on silica which may be contributing the low yield of the final product (Scheme 3.2.5).

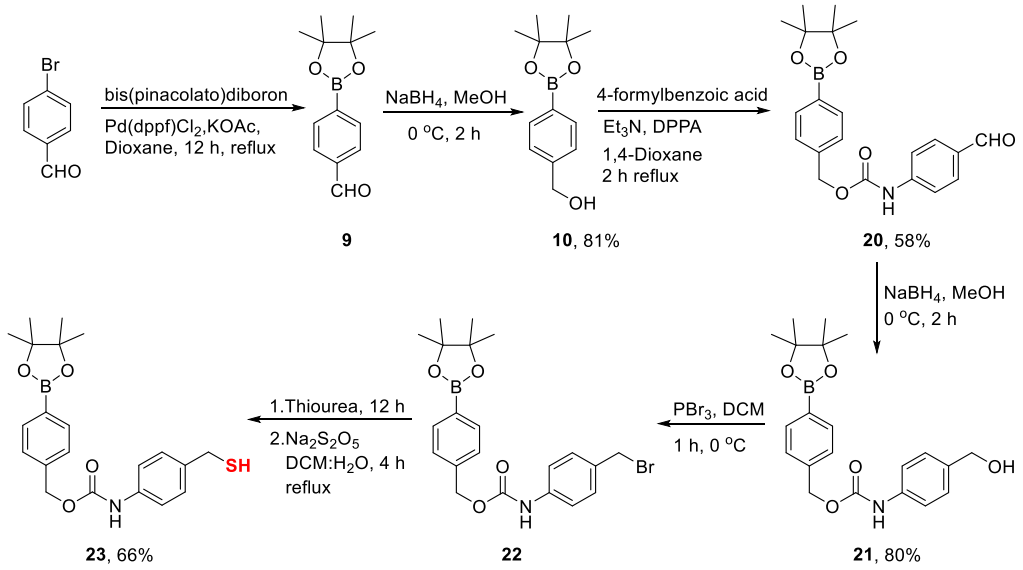

Scheme 3.2.4. Synthesis of thiol **22**.

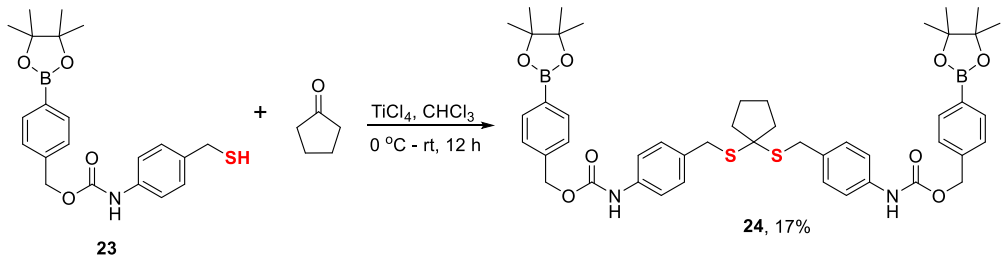

Scheme 3.2.5. Synthesis of H_2S donor **24**.

3.2.2.2. Detection of H_2S using NBD-Fluorescein:

H_2S release from compound **24** was tested by using NBD-Fluorescein dye. Compound was incubated in pH 7.4 buffer (10% ACN) with NBD-Fluorescein dye and H_2O_2 at 37 ^oC. Fluorescence was measured at excitation 490 nm and emission 514 nm. The enhancement in the fluorescence signal was found to be extremely slow which could be due to the poor solubility of the donor. Therefore the data presented here was taken after 21 h of incubation. Dye showed a slight increase in the fluorescence signal when treated with H_2O_2 compared to the dye alone control. An enhancement in the signal was observed with compound **24** upon treatment with H_2O_2 which indicated towards the release of H_2S. However, compound **15**, which served as a negative control also showed a fluorescence signal (Figure 3.2.2). Therefore, the data presented here could not confirm the production of H_2S from compound **24**. Also, due to the poor solubility of the donor, generation of H_2S from **24** could not be confirmed through any other method.

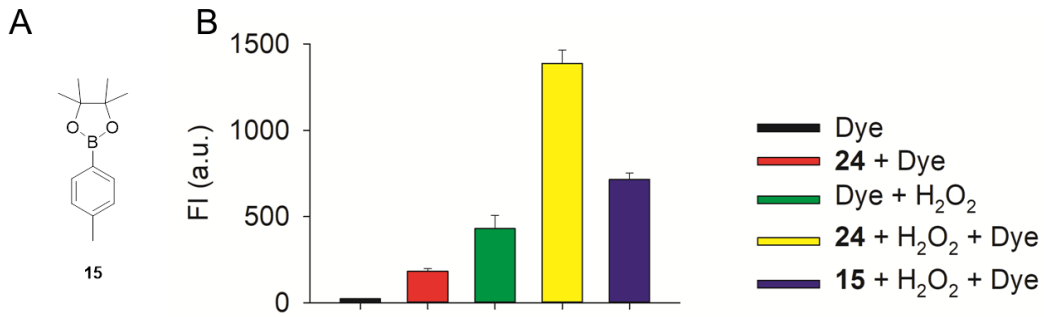

Figure 3.2.2. Detection of H_2S using NBD-Fluorescein.

3.2.2.3. HPLC plots:

The purity of the compound was tested by HPLC analysis. Compound **24** was injected in HPLC which eluted at 23.22 min (Figure 3.2.3). The decomposition studies could not be followed due to the poor solubility of the donor.

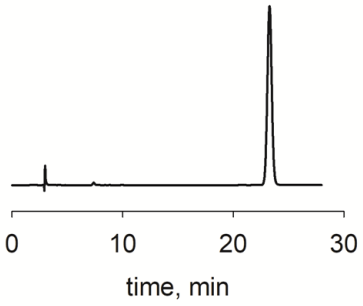

Figure 3.2.3. HPLC plot for compound **24**.

3.2.3. Summary

ROS activated gem-dithiol based H_2S donors was synthesized for cancer targeted delivery of H_2S. The compound was synthesized in eight steps with 17% yield. However, the compound was poorly soluble in buffer and therefore H_2S release could not be established from the scaffold. Making a water soluble derivative in the series would be useful for further evaluation.

3.2.4. Experimental Section:

3.2.4.1. Synthesis and Characterization: Compounds **9**[7], **10**[8], **20**[9], **21**[9] were synthesized using reported procedure. The analytical data was collected for each compound which matched with the reported values.

Synthesis of 4-(4,4,5,5-tetramethyl-1,3,2-dioxaborolan-2-yl)benzyl (4-(mercaptomethyl)phenyl)carbamate (23):

To a well stirred ice cold solution of **21** (0.2 g, 0.5 mmol) in dry DCM (10 mL), PBr_3 (0.5 mL, 0.6 mmol) was added slowly under N_2 atomosphere. The reaction was allowed to stir for 1h at 0 ^oC (progress of the reaction was monitored by TLC). Reaction was quenched by adding 10 mL of saturated $NaHCO_3$. Aqueous layer was extracted using DCM (3 X 10 mL). The combined organic layer was dried over Na_2SO_4, filtered and concentrated. Compound **22** was found to be unstable and therefore was taken as such to the next step. **22** (0.2 g, 0.5 mmol) was dissolved in 10 mL of dry THF followed by the addition of thiourea (1.2 g, 0.65 mmol) under N_2 atmosphere. The reaction was allowed to stir at room temperature for 12 h. After completion of the reaction, solvent was removed under vacuum. The thiourea salt (0.25 g, 0.48 mmol) was dissolved in water (15 mL) and purged with N_2 for 5 min. To the reaction mixture 20 mL of DCM was added under N_2 atmosphere followed by the addition of $Na_2S_2O_5$ (2.6 g, 13.29 mmol). The reaction was refluxed for 4-6 h. Progress of the reaction was monitored by TLC. Reaction was quenched by adding 10 mL of water. The aqueous layer was extracted by DCM (3 X 10 mL). The combined organic layer was dried over Na_2SO_4, filtered and concentrated. The crude obtained was purified using silica gel by column chromatography. The crude obtained was purified using Silica gel column chromatography. Hexane and ethyl acetate were used as eluents. **23** was obtained as pungent smelling liquid with 66% overall yield in two steps: FT-IR (ν_{max}, cm^{-1}) 2298, 1734, 1526; ^1H NMR (400 MHz, $CDCl_3$) δ 7.82 (d, *J* = 8.1 Hz, 2H), 7.39 (d, *J* = 8.1 Hz, 2H), 7.33 (d, *J* = 8.3 Hz, 2H), 7.28 – 7.23 (m, 2H), 6.70 (s, 1H), 5.21 (s, 2H), 3.70 (d, *J* = 7.5 Hz, 2H), 1.73 (t, *J* = 7.5 Hz, 1H), 1.35 (s, 12H); ^{13}C NMR (100 MHz, $CDCl_3$): δ 153.3, 139.1, 136.7, 136.4, 135.1, 128.8, 127.4, 119.0, 84.0, 67.0, 28.5, 24.9; HRMS (ESI) $C_{21}H_{26}BNO_4S$ $[M+Na]^+$: Calcd., 422.1573, Found., 422.1593.

bis(4-(4,4,5,5-tetramethyl-1,3,2-dioxaborolan-2-yl)benzyl) (((cyclopentane-1,1-diylbis(sulfanediyl))bis(methylene))bis(4,1-phenylene))dicarbamate (24): The reported procedure was followed with slight modifications.[10] Compound **23** (0.2 g, 0.6 mmol) and

pentanone (0.02 mL, 0.23 mmol) were dissolved chloroform under N_2 atmosphere at 0 ^oC. The reaction was allowed to stir at 0 ^oC for 10 min followed by the addition of $TiCl_4$ (0.026 mL, 0.23 mmol). The reaction was allowed to warm to room temperature and stirred for 12 h. Reaction mixture was quenched by addition of 10 mL of water. The aqueous layer was extracted with DCM (3 X 10 mL). The combined organic layer was dried over Na_2SO_4, filtered and concentrated under vacuum. The crude was first passed through silica column using hexane and ethyl acetate as eluents. The crude was further dissolved in acetonitrile (3 mL) and filtered through a 0.2 micron filter to obtain a clear solution. The solution was then injected into Dionex HPLC. Acetonitrile and water were used as eluents. Compound **24** was obtained as a white powder, 17% yield: mp 165-166 ^oC; FT-IR (ν_{max}, cm^{-1}) 2974, 2299, 1718, 1528; ^1H NMR (400 MHz, $CDCl_3$): δ 7.82 (d, *J* = 8.0 Hz, 4H), 7.39 (d, *J* = 8.0 Hz, 4H), 7.33 – 7.26 (m, 8H), 6.67 (s, 2H), 5.21 (s, 4H), 3.83 (s, 4H), 1.89 (d, *J* = 6.5 Hz, 4H), 1.79 – 1.72 (m, 4H), 1.34 (s, 24H); ^{13}C NMR (100 MHz, $CDCl_3$): δ 153.3, 139.1, 136.5, 135.1, 133.3, 129.9, 127.4, 118.8, 83.9, 66.9, 41.5, 35.2, 24.9, 24.3; MALDI- TOF peak for $C_{47}H_{58}B_2N_2O_8S_2$ $[M+Na]^+$: Calcd., 887.37, Found., 887.39.

3.2.4.2. Detection of H_2S using NBD-Fluorescein:

Stock solution (10 mM) of the compound was prepared in DMSO. Compound **24** (50 µM) was incubated in phosphate buffer (pH 7.4, 50 mM, 10µM DTPA) containing H_2O_2 (10 eq) and NBD-Fluorescein (10 µM) in a 96 well plate. The reaction mixture was incubated at 37 ^oC for 21 h. Fluorescence was measured at excitation 490 nm and emission 514 nm using a thermofischer varioskan microtiter plate reader.

3.2.4.3. HPLC for purity:

A 10 mM stock solution of **24** was prepared in DMSO. The compound (50 µM) was injected into high-performance liquid chromatography (HPLC Agilent Technologies 1260 Infinity) in ACN to monitor the purity of the compound. The mobile phase was H_2O/ACN. The stationary phase was C-18 reverse phased column (Phenomenex, 5 µm, 4.6 x 250 mm). An isocratic method was followed to monitor compound **24** with a flow rate of 1 mL/min starting with → 90:10 to 10:90 for 28 min. Compound was eluted at retention time of 23.22 min.

3.2.5. Spectra

^{1}H NMR spectrum (400 MHz, $CDCl_3$) of compound **23**

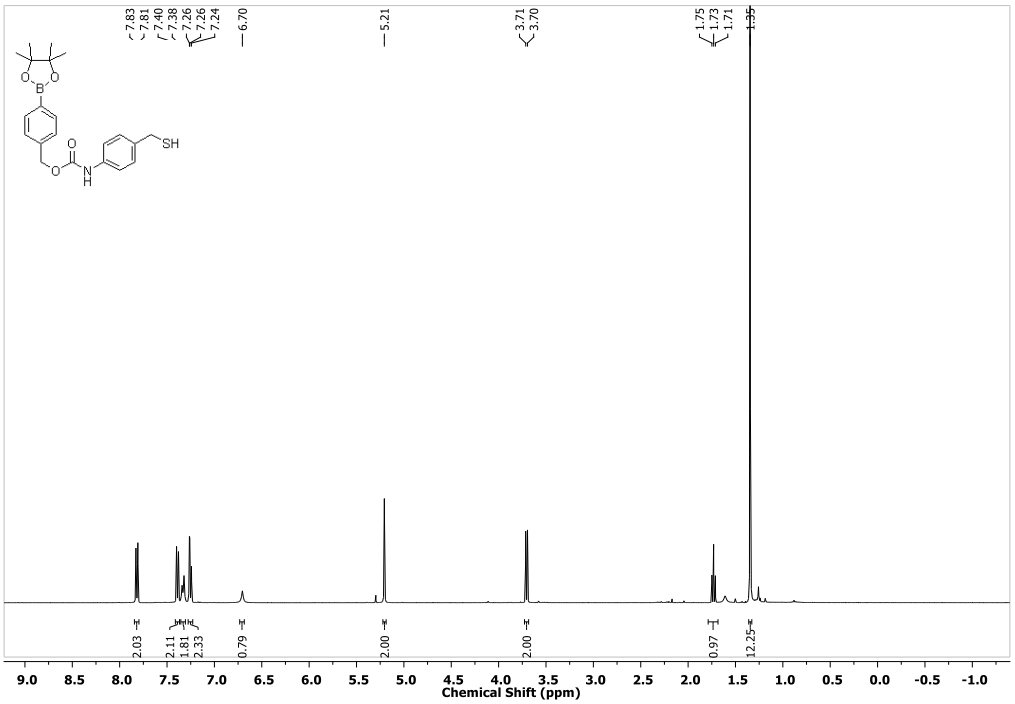

^{13}C NMR spectrum (100 MHz, $CDCl_3$) of compound **23**

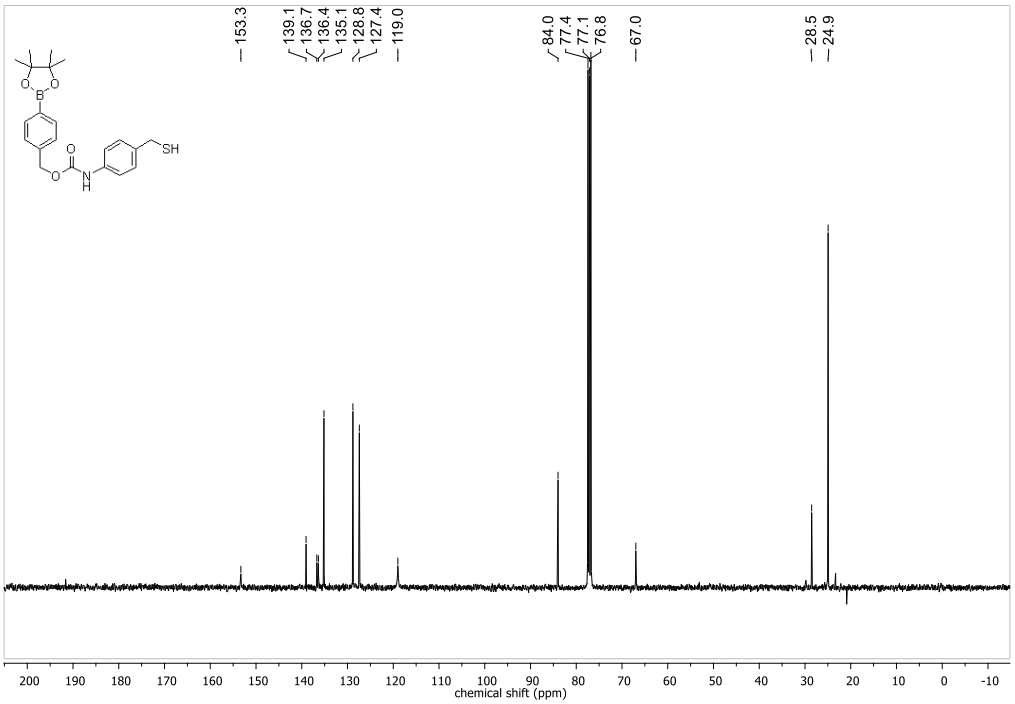

^{1}H NMR spectrum (400 MHz, $CDCl_3$) of compound **24**

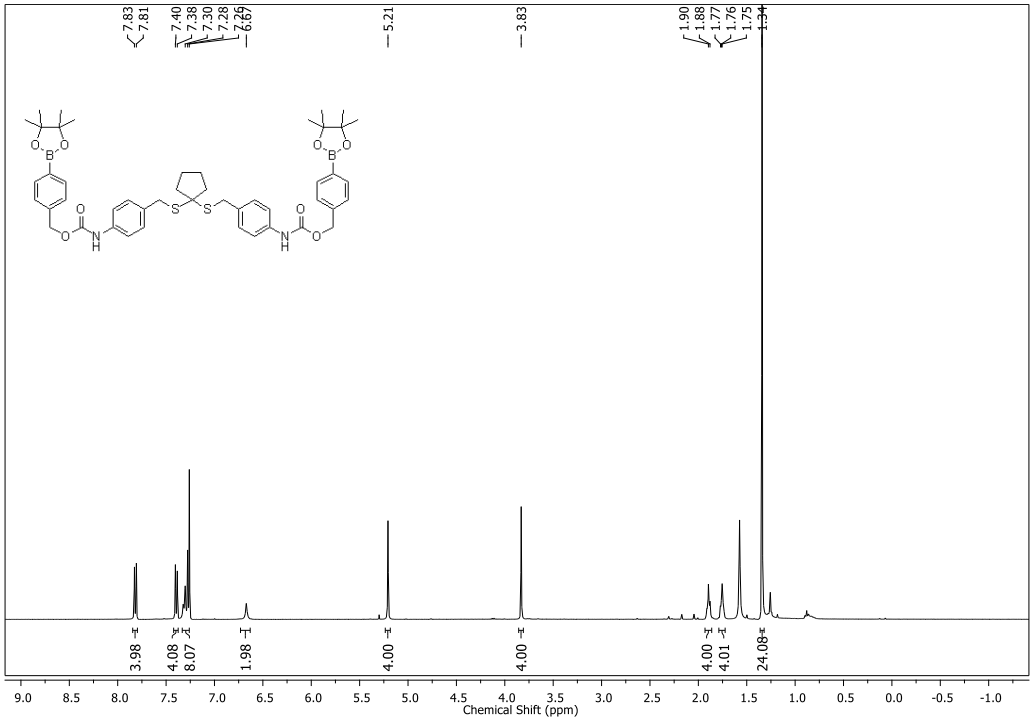

^{13}C NMR spectrum (100 MHz, $CDCl_3$) of compound **24**

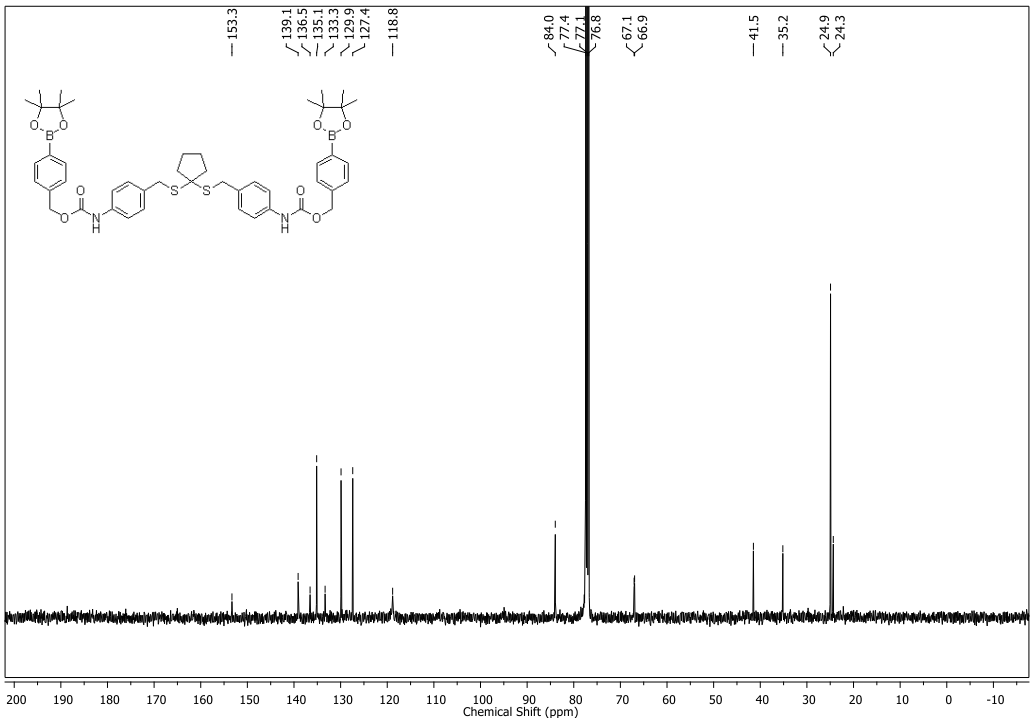

3.2.6. References

(1) Lee, Z. W.; Teo, X. Y.; Tay, E. Y. W.; Tan, C. H.; Hagen, T.; Moore, P. K.; Deng, L. W. *Br. J. Pharmacol.* **2014**, *171*, 4322.

(2) Ma, Z.; Bi, Q.; Wang, Y. *Oral Dis.* **2015**, *21*, 156.

(3) Wu, D.; Si, W.; Wang, M.; Lv, S.; Ji, A.; Li, Y. *Nitric oxide* **2015**, *50*, 38.

(4) Szabo, C.; Coletta, C.; Chao, C.; Módis, K.; Szczesny, B.; Papapetropoulos, A.; Hellmich, M. R. *Proc. Natl. Acad. Sci. U.S.A.* **2013**, *110*, 12474.

(5) Cai, W.-J.; Wang, M.-J.; Ju, L.-H.; Wang, C.; Zhu, Y.-C. *Cell Biol. Int.* **2010**, *34*, 565.

(6) Fan, K.; Li, N.; Qi, J.; Yin, P.; Zhao, C.; Wang, L.; Li, Z.; Zha, X. *Cell. Signal.* **2014**, *26*, 2801.

(7) Dharmaraja, A. T.; Ravikumar, G.; Chakrapani, H. *Org. Lett.* **2014**, *16*, 2610.

(8) Chung, S.-H.; Lin, T.-J.; Hu, Q.-Y.; Tsai, C.-H.; Pan, P.-S. *Molecules.* **2013**, *18*, 12346.

(9) Nuñez, S. A.; Yeung, K.; Fox, N. S.; Phillips, S. T. *J. org. chem.* **2011**, *76*, 10099.

(10) Devarie-Baez, N. O.; Bagdon, P. E.; Peng, B.; Zhao, Y.; Park, C.-M.; Xian, M. *Org. Lett.* **2013**, *15*, 2786.

CHAPTER 4.1: NQO1 responsive COS/H_2S donors

4.1.1. Introduction:

In the fourth chapter we propose to achieve tissue specific delivery of H_2S and H_2S-NSAID hybrid donors.[1-3] Mesalamine (also known as 5- aminosalicyclic acid) is a non-steroidal anti-inflammatory drug (NSAID) extensively used for the treatment of ulcerative colitis which is an inflammatory bowel disease (IBD) and is associated with extensive ulceration and inflammation. [4-6] However, the drug is effective only against mild to moderate forms of colitis and is ineffective against the severe forms of disease.[7] In 2007, Wallace and co-workers investigated the possibility of H_2S acting in synergism with other NSAIDs to enhance the anti-inflammatory properties of the drug. ATB-429 is a H_2S-NSAID hybrid donor reported in this regard, where ADT-OH is conjugated with mesalamine through an ester bond (Figure 4.1.1). The compound produces H_2S upon hydrolysis in buffer. ATB 429 has been shown to be effective in reducing the severity of colitis in a mouse model compared to the parent drug and a significant decrease in the mucosal injury and disease activity are also reported. The mRNA expression of several pro-inflammatory cytokines such as TNF-α and IL-6 are also reduced upon treatment with ATB-429.[3] However, the H_2S release from the donor is spontaneous and provides limited scope for site directed delivery. Also, lack of appropriate controls complicate the conclusions drawn from the experiments.

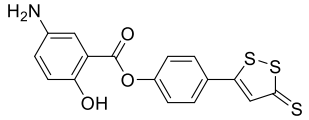

ATB-429

Figure 4.1.1. Structure of ATB-429.

NAD(P)H quinone oxidoreductase 1 (NQO1) also referred to as DT-Diaphorase, is predominantly a two electron reducing cytosolic enzyme encoded in human by NQO1 gene. It is an FAD binding protein which forms homodimers and is used by the cell for reduction of quinones to hydroquinones.[8,9] Cell specific expression of NQO1 as detected by immunohistochemistry has shown its expression in tissues like respiratory epithelium, thyroid follicle, colonic epithelium and corneal and lens epithelium.[10] NQO1 is a highly inducible protein and its expression levels go up in oxidative stress and electrophilic stress.[11,12] Over expression of NQO1 is a strategy adapted by the cell for detoxification and removal of quinone based xenobiotics.[8] The over expression of NQO1 in certain cell types has been extensively taken advantage in the past for delivering drugs or latent fluorophores (imaging)

(Scheme 4.1.1). Quinones upon entering into the cells are reduced by NQO1 to form corresponding hydroquinones which initiate a rapid lactonization of the trimethyl lock moiety thereby releasing the payload (drug or fluorophore).[13,14]

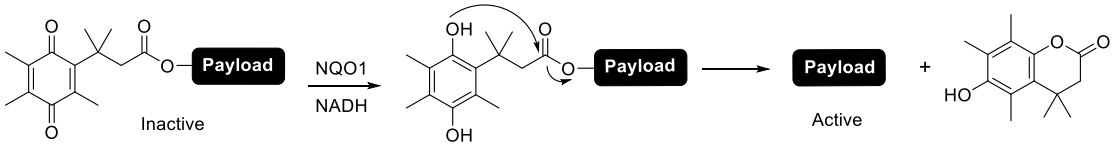

Scheme 4.1.1. NQO1 activated delivery of prodrugs or fluorophores.

Based on this strategy we proposed to design NQO1 activated H_2S (fast and slow donor) and H_2S-mesalamine hybrid donors. The proposed mechanism of H_2S release from the scaffold is as follows: Compound upon entering into cells is reduced by NQO1 in the presence of NAD(P)H cofactor to give the corresponding hydroquinone which further undergoes rapid lactonization to release the intermediate **I**. The intermediate formed dissociates to release COS and mesalamine derivative (Scheme 4.1.2). COS is further hydrolysed to H_2S by carbonic anhydrase (CA).

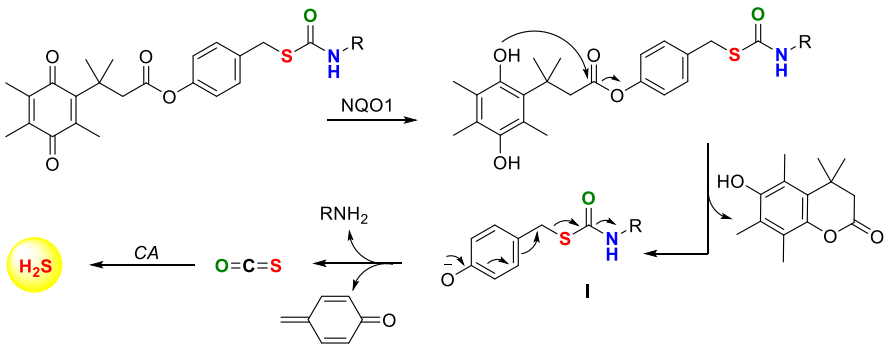

Scheme 4.1.2. NQO1 responsive COS/H_2S donors.

4.1.2. Results and Discussion

4.1.2.1. Synthesis of NQO1 responsive COS/H_2S donors

In order to test the hypothesis compounds **31a**, **31b** and **31c** were synthesized as NQO1 activated COS/H_2S donors (Scheme 4.1.5). Compound **31a** was conjugated with mesalamine which served as an H_2S-NSAID hybrid; compound **31b** with *p*-anisidine as a leaving group served as fast COS/H_2S donor and **31c** with propylamine as a leaving group served as slow COS/H_2S donor. The compounds were synthesized in seven steps starting with the reaction of *p*-hydroxybenzyl alcohol with *tert*-butyldimethylsilyl chloride (TBDMSCl) in the presence of imidazole to give compound **25** (Scheme 4.1.3).

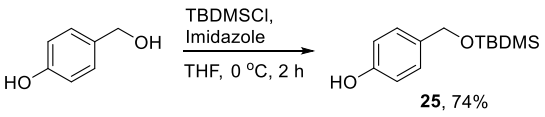

Scheme 4.1.3. Synthesis of compound **25**.

2,3,5-trimethylbenzene-1,4-diol was reacted with 3-methylbut-2-enoic acid to give compound **26** which was further oxidized to **27** in the presence of *N*-bromosuccinimide (NBS). Compound **27** was coupled with compound **25** to form an ester, **28** in the presence of EDC.HCl and DMAP in 71% yield. This was followed by deprotection of *tert*-butyl dimethylsilyl (TBDMS) group in the presence of acetic acid in THF and water to give compound **29** in 97% yield, which was further reacted with tribromophosphine to prepare compound **30** in 43% yield. Compound **30** was reacted with thiourea to form an adduct which was hydrolysed to form the thiol in the presence of $Na_2S_2O_5$. The thiol prepared was extremely unstable and was readily reacted with respective carbamates (**17**, **5b** and **12g**) to give compound **31a** in 43% yield, **31b** in 65% yield and **31c** in 34% yield respectively (Scheme 4.1.4).

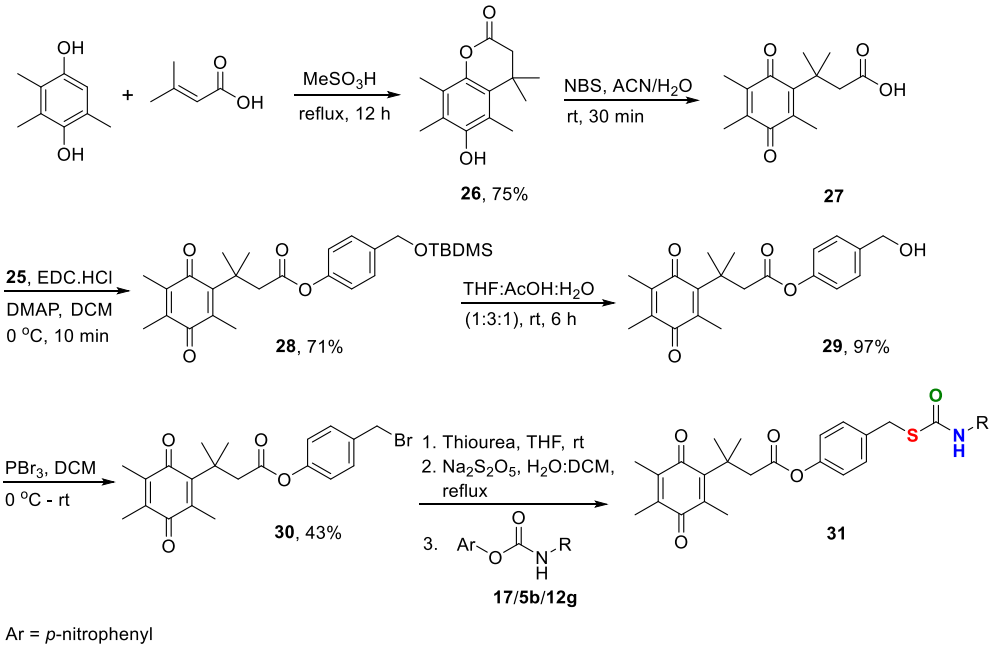

Scheme 4.1.4. Synthesis of NQO1 responsive COS/ H_2S donors.

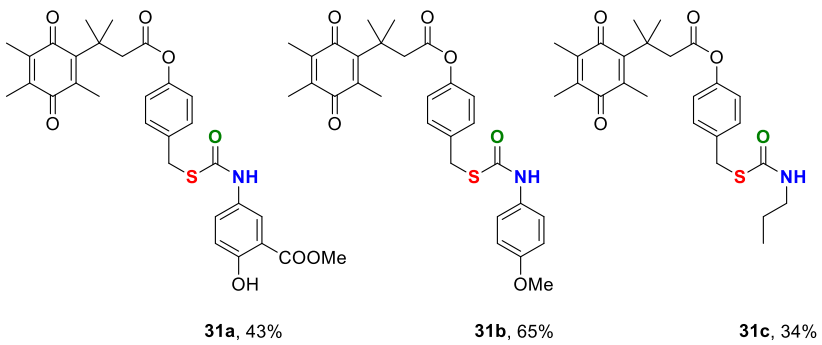

Scheme 4.1.5. Structures of NQO1 responsive COS/H_2S donors.

4.1.2.2. Detection of hydrogen sulfide using electrode

The formation of H_2S from COS/H_2S donors was first evaluated by using sulfide selective electrode ISO-H2S 100. Compound **31a** was added to phosphate buffer (pH 7.4, 50 mM) containing NQO1, NADH and CA at 37 ^oC. The reaction was stirred continuously at 37 ^oC. An increase in the current corresponding to the formation of sulfide was observed which continued for a period of 1 h (Figure 4.1.2). Further, stability of the compound in buffer was tested by incubating compound **31a** in buffer containing CA and monitoring the generation of H_2S. No significant increase in the current attributable to formation of H_2S was observed indicating that the compound was stable towards hydrolysis. Furthermore, stability of the compound towards plasma proteins was investigated by incubating **31a** in media containing 10% FBS. Again, no signal for H_2S generation was observed. Thus, the compounds reported herein were found to be selective towards activation by NQO1 and were stable towards hydrolysis (Figure 4.1.2).

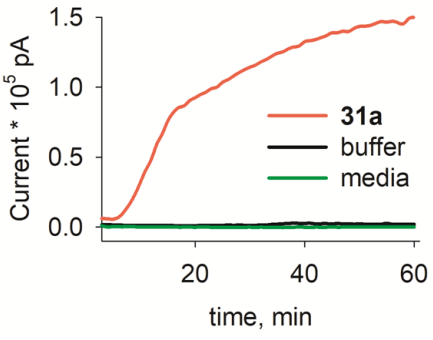

Figure 4.1.2. Detection of H_2S using sulfide selective electrode.

4.1.2.3. Detection of H_2S using methylene blue

The generation of H_2S from these donors was also shown via methylene blue complex formation assay.[15] Compounds were incubated in buffer in the presence of NQO1, NADH

and CA at 37 ^{o}C for 4 h following which the aliquots were removed and diluted with methylene blue reagents. The reaction mixture was further incubated for 30 min to allow the formation of methylene blue complex. The reaction mixture was then transferred to a 96 well plate and the formation of methylene blue complex was monitoreed by measuring absorbance from 500 nm to 800 nm. All the compounds showed a signal corresponding to the formation of H_2S (Figure 4.1.3b). However, compound **31a** gave a comparatively lower yield of H_2S due to poor solubility. Methylene blue complex was not formed in the case of compound **29** which served as a negative control. Also, no signal was observed upon incubating compound **31a** alone in buffer. This further validated the fact that the compounds were stable towards hydrolysis in buffer. In order to further validate the proposed mechanism, H_2S generation from compound **31a** was monitored in the presence of dicoumarol, **32**, a known inhibitor of NQO1 (Figure 4.1.3a). As expected a diminished signal for H_2S release from compound **31a** was observed in the presence of dicoumarol, indicating that the compounds are selective towards activation by NQO1.

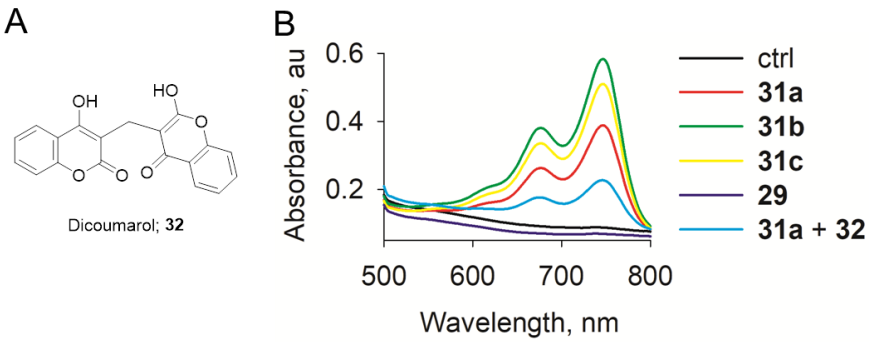

Figure 4.1.3. a) Structure of dicoumarol, **32**. b) Methylene blue complex formation from COS/H_2S donors.

The kinetics of H_2S release from these donors was also monitored using methylene blue assay. Compounds were incubated in pH 7.4 buffer containing NQO1, NADH and CA (Figure 4.1.4). An aliquot was removed at pre-determined time points and treated with methylene blue reagents. The reaction mixture was further stirred for another 30 min followed by measuring the absorbance at 676 nm. The rate constants for H_2S generation were obtained by fitting the initial rate data into first order kinetics. The rate constants for compounds **31a**, **31b** and **31c** were calculated to be 0.012 min^{-1}, 0.016 min^{-1} and 0.008 min^{-1} respectively. The rate of H_2S production from compound **31c** was only slightly lower than that for compound **31b**. The observed difference in the rate constants for the fast donor and slow donor was less which could be due to the poor aqueous solubility of the donors. This

was found to be one of the limitations of the reported set of donors. However, it was assumed that the compounds would produce H_2S at different rates in a cellular environment when used at lower concentrations.

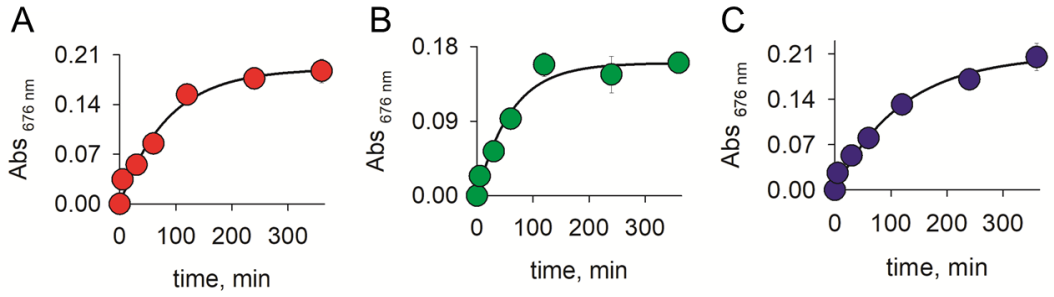

Figure 4.1.4 a) H_2S generation plot from **31a** using methylene blue. b) H_2S generation from compound **31b**. c) H_2S generation from compound **31c**.

4.1.2.4. HPLC studies

Next HPLC experiments were performed to demonstrate the formation of lactone upon reaction with NQO1 enzyme. In order to do so, the dissociation of compound **31b** was monitored to follow the release of lactone and *p*-ansidine. Compound **31b** when injected in ACN was eluted at retention time 16.59 min. (Figure 4.1.5a). A complete disappearance of the compound was observed when treated with NQO1 and NADH in pH 7.4 buffer after 30 min of incubation. A new peak corresponding to the formation of an intermediate was observed at retention time 7.76 min, which gradually decomposed in 2 h to generate *p*-anisidine with retention time of 4.84 min. Peak corresponding to the formation of lactone was observed at 8.29 min. The rate constant for the decomposition of compound **31b** was found to be 0.063 min^{-1} which was found to be in accordance with the rate constant for the formation of lactone i.e. 0.066 min^{-1} (Figure 4.1.6a, 4.1.6b). This indicated that the reduction of quinone by NQO1 in the presence of NADH was a fast step which was in accordance with the previous reports.

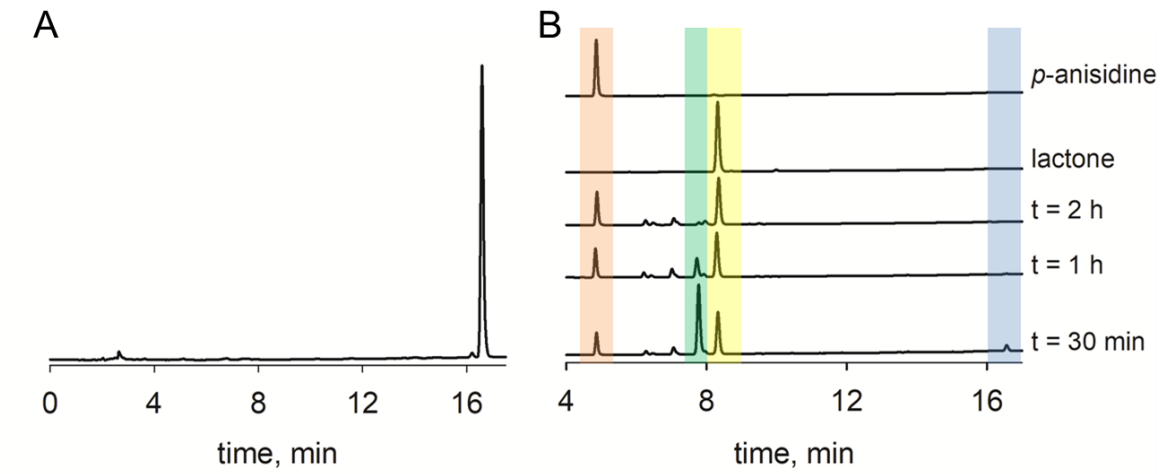

Figure 4.1.5. a) Representative HPLC trace for compound **31b** in ACN. b) HPLC traces for the decomposition of compound **31b** in the presence of NQO1 and NADH in phosphate buffer (pH 7.4).

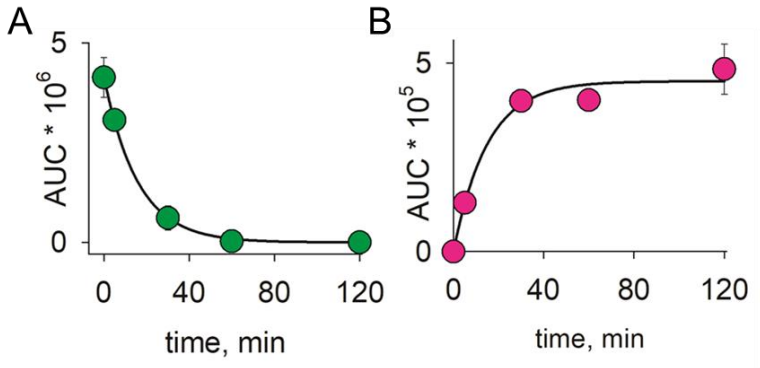

Figure 4.1.6. a) Area under the curve representing decomposition of the compound **31b**. b) Area under the curve representing the formation of lactone.

Formation of mesalamine was also followed by HPLC using a similar protocol. An intermediate was formed upon reaction of compound **31a** in the presence of NQO1 and NADH in buffer which gradually decomposed over a period of 2 h to give compound **16** (methyl ester form of mesalamine) as the product. The rate constant for the formation of compound **16** was calculated to be 0.02 min^{-1} (Figure 4.1.7) which was similar to the rate of formation of H_2S (0.012min^{-1}).

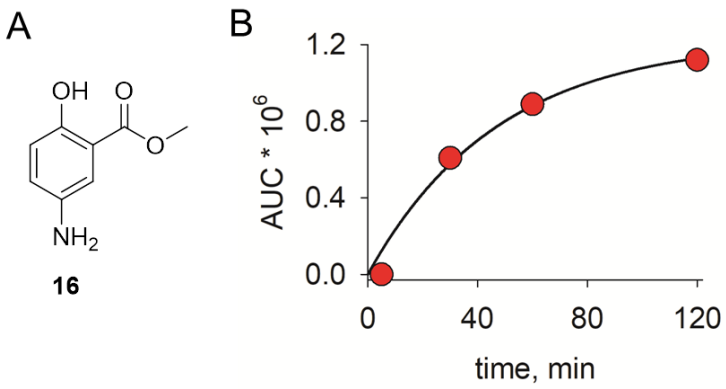

Figure 4.1.7. a) Structure of compound **16**. b) Area under the curve corresponding to the formation of compound **16**.

4.1.2.5. MTT assay for cell viability

Recent reports have pointed towards the toxicity associated with the accumulation of COS within cells. Pluth and co-workers have reported that donors with higher rate of COS release lead to the accumulation of this gaseous species which induces toxicity.[16]

Thus before evaluating the biological applicability of the H_2S donors, we first investigated the cytotoxicity of the compounds using standard cell viability assays – MTT assay and LDH assay. The cytotoxicity of NQO1 based H_2S donors was tested against multiple cell lines (shown later). Human breast carcinoma, MCF-7 cells were treated with varying concentrations of compound **31a** for 72 h following which the cell viability was measured using MTT assay. No significant toxicity at 50 µM concentration of compound **31a** was observed after 72 h incubation. This indicated that the compound was well tolerated by the cells even for 72 h (Figure 4.1.8).

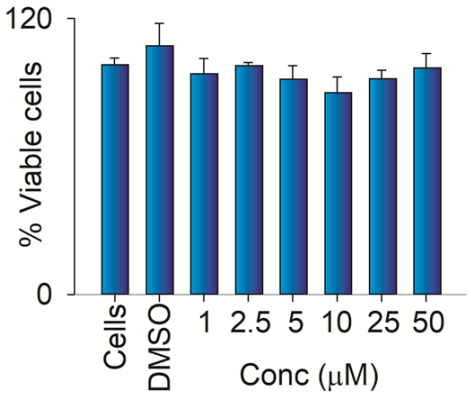

Figure 4.1.8. Compound **31a** was tested for cytotoxicity in human breast carcinoma MCF-7 cells using MTT assay.

4.1.2.6. LDH assay for cell viability

The cytotoxicity of the compounds was further evaluated through LDH assay. MCF-7 cells were treated with varying concentration of **31a** for 24 h following which the cell viability was monitored. Again, no significant toxicity was observed with 50 µM concentration of the compound (Figure 4.1.9). Thus, H_2S donors reported herein were non-toxic and can be taken further for biological studies.

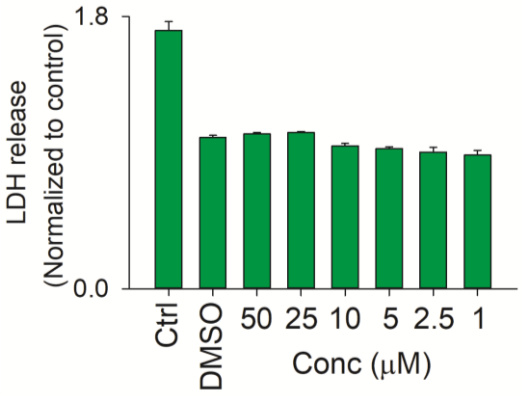

Figure 4.1.9. LDH assay for cell viability in MCF-7 cells after 24 h treatment of compound **31a**.

4.1.2.7. Persulfidation

The mechanism by which H_2S signals is by persulfidating the cysteine residues of a protein which is considered as an oxidative posttranslation modification.[17] For example, H_2S induces persulfidation of Kelch-like-ECH-associated protein 1 (KEAP 1) at Cys 151 residue which allows the dissociation of KEAP1 from nuclear factor erythroid 2-related factor 2 (NRF2) which thereby leads to enhancement in the antioxidant responses mediated by NRF2 (Figure 4.1.10).[18,19]

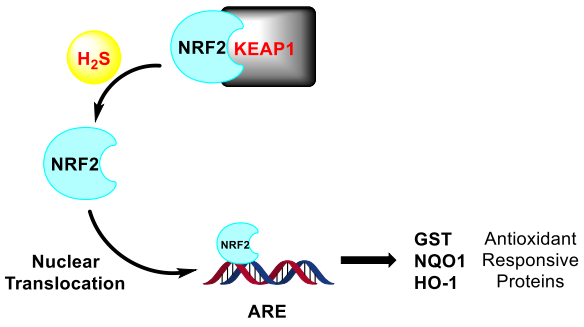

Figure 4.1.10. Activation of NRF2-KEAP1 pathway by H_2S.

Thus, we evaluated the ability of the H_2S donor motifs to induce protein persulfidation within cells using improved tag switch method.[20] Protein persulfides produced within cells are trapped by using methyl sulfonyl benzathiazole, MSBT, (an aromatic thiol blocking agent) to form mixed disulfides (Figure 4.1.11). This results in the formation of a reactive mixed disulfide.[21] The mixed disulfide thus formed is further reacted with BODIPY-tagged cyanoacetic acid based nucleophile (BODIPY acts as a fluorescent reporter) to form a thioether bond tagged with a fluorescent reporter which can be imaged using a microscope (Scheme 4.1.6). Thus, the technique allows the detection of protein persulfides formed in the cells. We used this strategy to monitor protein persufidation induced by the H_2S donors within cells.

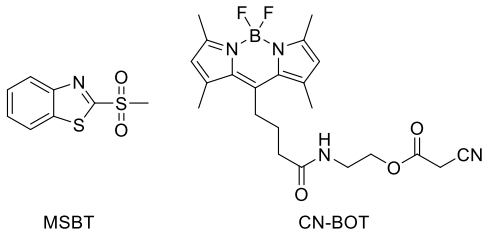

Figure 4.1.11. Structures of persulfidating agents.

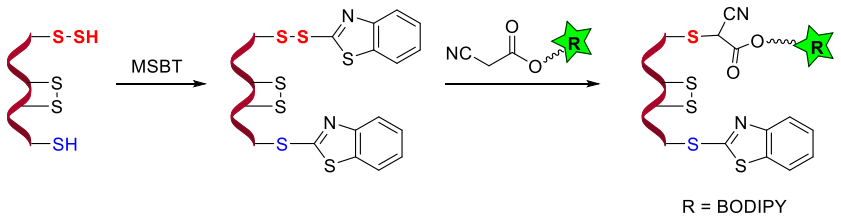

Scheme 4.1.6. Improved tag switch method for imaging persulfides in fixed cells.

Persulfidation data was provided by Kavya Gupta, from Dr. Deepak Saini's Lab in IISc Bangalore. Human colon carcinoma, DLD-1 cells were incubated with H_2S donors (10 µM) and Na_2S (200 µM) for 1 h. The cells were fixed using ice cold methanol followed by permeabilization of the cell membrane using ice cold acetone. Cells were further treated with MSBT for 12 h to block the persulfides. Finally cells were incubated with CN-BOT for 1 h at room temperature to tag the persulfides with a fluorescent reporter (the persulfidation detection reagents). Cells were then imaged using IX83 microscope from Olympus. Cells treated with H_2S donors **31a** (H_2S-NSAID hybrid) and **31b** (fast donor) showed enhanced fluorescence signal compared to the untreated control. Interestingly, compound **31c**, a slow releasing H_2S donor showed less fluorescence compared to **31a** and **31b** suggesting that the compound was activated within the cells and produced H_2S at a slower rate which was in

accordance with our hypothesis. Na_2S was used as a positive control which showed diminished signal in comparison to the H_2S donors (Figure 4.1.12). This may due to the fact that Na_2S gives a burst of H_2S which dissipates at a faster rate and therefore the effective concentration of H_2S is low to induce persulfidation. The fluorescence signal obtained was quantified and plotted for all the donors to give corrected total cell fluorescence. A significant increase in the fluorescence per cell was observed in the case of **31a** and **31b** compared to the untreated control (Figure 4.1.13). Compound **31c** showed enhanced fluorescence which was comparable to Na_2S but was less compared to **31a** and **31b**. Collectively, the data confirmed that the compounds were capable of inducing protein persulfidation in cells. The extent of persufidation was dependent on the rate of H_2S release.

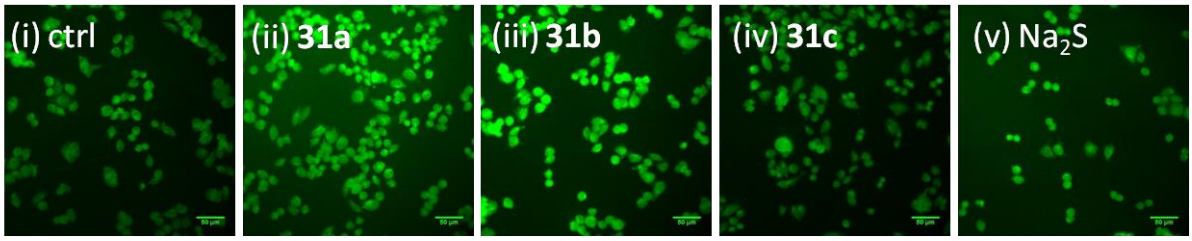

Figure 4.1.12. Representative images of DLD-1 cells. Persulfidation induced by H_2S donors (**31a**, **31b** and **31c**) within DLD-1 cells imaged using IX83 microscope from Olympus. Scale bar is 50 µm.

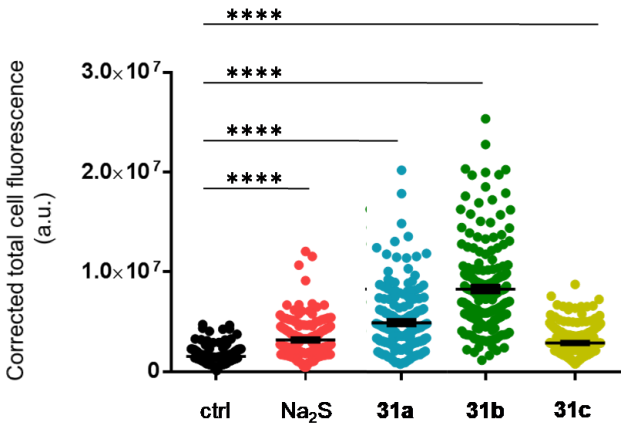

Figure 4.1.13. Corrected total cell fluorescence in DLD-1 cells. Persulfidation induced by H_2S donors (**31a**, **31b**, **31c** and Na_2S) within DLD-1 cells imaged using IX83 microscope from Olympus.

4.1.2.8. Protection against JCHD induced stress in DLD-1 cells

Next, the ability of H_2S donor motifs to protect the cells against oxidative stress induced toxicity was evaluated. JCHD, a derivative of juglone and a superoxide generator, was used to stimulate oxidative stress within cells.[22,23] First, DLD-1 cells were treated with varying

concentrations of JCHD for 24 h and the cell viability was evaluated. EC 50 value for JCHD was calculated by plotting percentage cell viability obtained against the log (concentration) of the compound (Figure 4.1.14). The EC50 value was calculated to be 9.65 µM. Thus, 15 µM concentration of JCHD was used for further set of experiments to induce 80% cytotoxicity.

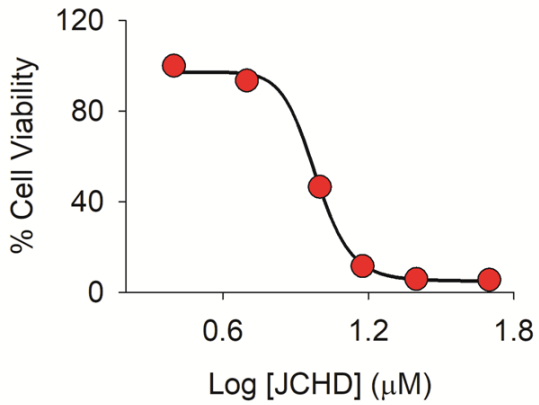

Figure 4.1.14. Induction of cell death of human colon carcinoma, DLD-1 cells using JCHD after 24 h.

The ability of H_2S donors to protect cells against xenobiotic induced oxidative stress was tested. DLD-1 cells were co-incubated with H_2S donors and JCHD (15 µM) for 24 h and then the cell viability was measured using MTT. Compound **31a** and **31b** at 50 µM concentration showed protection against JCHD induced toxicity. On the other hand, compound **31c** at 50 µM concentration (slow H_2S donor) showed no significant increase in the cell viability under these conditions (Figure 4.1.15) which could be correlated with the lower extent of persulfidation observed with **31c**. Although a clear mechanistic understanding could not be made, however, it seemed likely that the extent of persulfidation determined the cytoprotective effects of the donor. Also, no significant difference in the cell viability was observed from H_2S-NSAID donor (**31a**) when compared with **31b**, suggesting that the obtained effects were attributable to the release of COS within cells. Compound **29** which lacked the ability to produce COS showed no enhancement in the cell viability. Mesalamine alone was also found to be ineffective in protecting the cells against JCHD induced toxicity which could be due to the poor cell permeability of the molecule. Significant cell viability was observed when the cells were treated with compounds alone. Thus, compounds were found to be non-toxic at the reported concentration of 50 µM. Therefore, the observations suggested that the compounds were capable of protecting cells against JCHD induced oxidative stress which was likely to be dependent on the extent of persulfidation induced by the donors within cells.

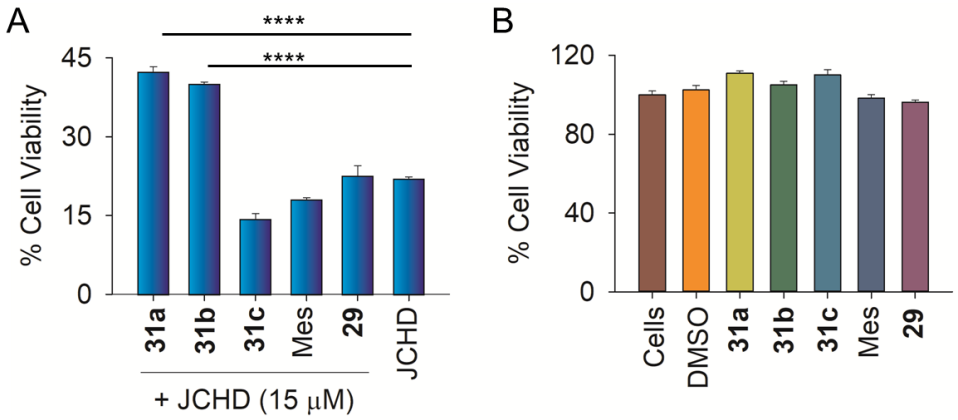

Figure 4.1.15. a) Cytoprotective effects of H_2S donors (50 μM) against JCHD (15 μM) induced stress in human colon carcinoma, DLD-1 cells. Results are expressed as mean ± SEM (n = 3). Mes represents mesalamine (50 μM). b) Cell viability using H_2S donors (50 μM) in DLD-1 cells.

4.1.2.9. Protection against JCHD induced stress in WT-MEF cells

Wild type mouse embryonic fibroblast cells have been reported to have lower expression of NQO1 enzyme.[24] Thus, in order to test the selectivity of the donors towards activation by NQO1 enzyme, the aforementioned cytoprotective effect of the H_2S donors was tested against WT-MEF cells. Cells were treated with H_2S donors along with JCHD (15 μM) for 24 h, following which the cell viability was monitored using MTT assay. As expected, no significant increase in the cell viability was observed with 50 μM concentration of the donors (Figure 4.1.16). Thus, the experiment supported the fact that the compounds reported herein were selective towards activation by NQO1 enzyme.

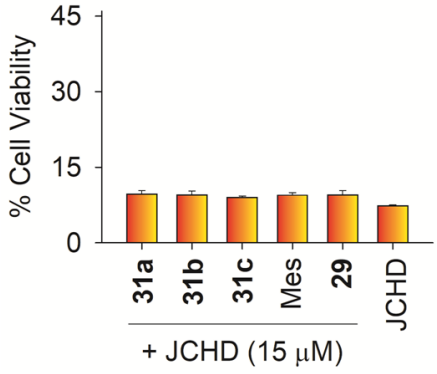

Figure 4.1.16. Cytoprotective effects of compounds against JCHD (15 μM) induced stress in wild type mouse embryonic, WT-MEF cells. Results are expressed as mean ± SEM (n = 3). Mes represents mesalamine.

The cytotoxicity profile of the donors was monitored in WT-MEF cells. Cells were incubated with varying concentrations of the compounds for 24 h and the cell viability was monitored (Figure 4.1.17). The compounds were found to be non-toxic at the reported concentrations. Collectively, the results obtained suggested that the effects observed were due to the release of H_2S via activation through NQO1 enzyme in the cells. The compounds were found to be well tolerated by cells at 50 µM concentration. Therefore, the compounds reported herein can be used as tools to study the biological implications of H_2S.

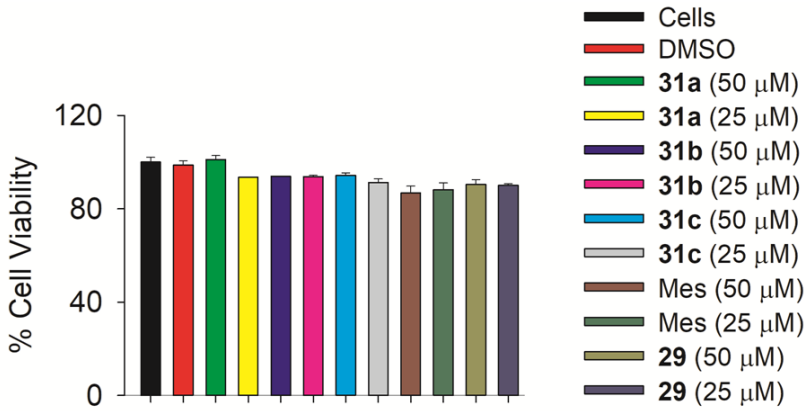

Figure 4.1.17. Cell viability of H_2S donors in WT-MEF cells.

4.1.3. Summary

NQO1 activated H_2S donors were synthesized for targeted delivery towards colon. Mesalamine (NSAID) was conjugated with H_2S to prepare H_2S-NSAID hybrid donor. The compounds were capable of generating H_2S in the presence of NQO1 enzyme. The donors prepared were stable towards hydrolysis in media and were selective towards activation by NQO1. The compounds were capable of persulfidating the cellular proteins which was shown by using improved tag switch technique. A difference in the extent of persulfidation caused by these donors was observed which was dependent on the rate of H_2S production. Compound **31c** being a slow H_2S donor showed a lower extent of persulfidation compared to **31a** and **31b**. Finally, the compounds were tested for their ability to protect the cells against JCHD (source of ROS) induced oxidative stress. Compounds **31a** and **31b** were able to mitigate the oxidative stress produced by JCHD in human colon carcinoma, DLD-1 cells. Compound **31c** showed no significant increase in the cell viability compared with **31a** and **31b** which may be due to the lower extent of persulfidation caused by this donor. Also, the donors were found to be ineffective in wild type mouse embryonic fibroblast, WT-MEF cells which has lower expression of NQO1 enzyme. Collectively, the data suggests that the

compounds reported herein are stable and selective towards activation by NQO1. Cytoprotective effects of the donors are likely to be dependent on the extent of persulfidation observed with these donors.

4.1.4. Experimental and characterization of data

4.1.4.1. Experimental Section:

Synthesis of 4-(((tert-butyldimethylsilyl)oxy)methyl)phenyl 3-methyl-3-(2,4,5-trimethyl-3,6-dioxocyclohexa-1,4-dien-1-yl)butanoate (28):

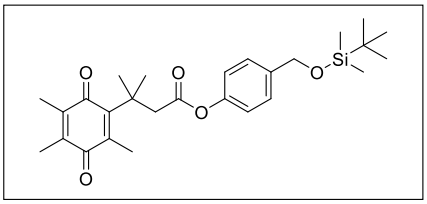

To a solution of 3-methyl-3-(2,4,5-trimethyl-3,6-dioxocyclohexa-1,4-dien-1-yl)butanoic acid (1.22 g, 4.89 mmol) and 4-(((tert-butyldimethylsilyl)oxy)methyl)phenol (0.8 g, 4.07 mmol) in dry DCM at 0 ^{o}C, EDC.HCl (1.56 g, 8.15 mmol) and DMAP (1 g, 8.15 mmol) were added. The reaction mixture was allowed to stir for 10 min. The progress of the reaction was monitored by TLC. After completion, the reaction mixture was washed with 1N HCl, organic layer was dried over Na_2SO_4 and concentrated in vacuo. The crude was purified using column chromatography to give **28** (1.36 g, 71%) as yellow oily liquid. FT-IR (ν_{max} , cm^{-1}) 1750, 1644, 1258; ^{1}H NMR (400 MHz, $CDCl_3$): δ 7.28 (d, *J* = 8.7 Hz, 2H), 6.92 (d, *J* = 8.6 Hz, 2H), 4.69 (s, 2H), 3.23 (s, 2H), 2.17 (s, 3H), 1.93-1.91 (m, 6H), 1.52 (s, 6H), 0.93(s, 9H), 0.08 (s, 6H); ^{13}C NMR (100 MHz, $CDCl_3$) δ 190.9, 187.4, 171.4, 152.0, 149.2, 142.9, 139.1, 139.0, 138.5, 127.0, 121.2, 64.4, 47.7, 38.5, 28.9, 25.9, 18.4, 14.3, 12.6, 12.1, -5.3; HRMS (ESI-TOF) for $[C_{27}H_{38}O_5Si + H]^+$: calcd. 471.2567, found 471.2570.

Synthesis of 4-(hydroxymethyl)phenyl 3-methyl-3-(2,4,5-trimethyl-3,6-dioxocyclohexa-1,4-dien-1-yl)butanoate (29):

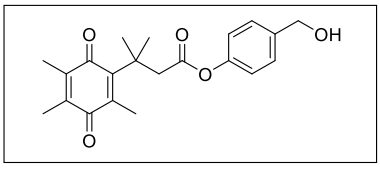

To a solution of **28** (0.69 g, 1.45 mmol) in THF (6 mL), water and acetic acid (1:1:3) were added. The progress of the reaction was monitored by TLC. After stirring the reaction mixture for 6 h, saturated $NaHCO_3$ solution was added to quench the reaction. The aqueous layer was extracted by DCM and dried over Na_2SO_4. The organic layer was concentrated under vacuo. The crude was purified by column chromatography to give **29** (0.5 g, 97%) as yellow liquid. FT-IR (ν_{max} , cm^{-1}) 3510, 1747, 1643; ^{1}H NMR (400 MHz, $CDCl_3$): δ 7.33 (d, *J* = 8.3 Hz, 2H), 6.95 (d, *J* = 8.4 Hz, 2H), 4.64 (s, 2H), 3.24 (s, 2H), 2.17 (s, 3H), 1.92-1.91 (m, 6H), 1.52 (s, 6H); ^{13}C NMR (100 MHz, $CDCl_3$) δ 190.9, 187.4, 171.4, 152.0, 149.8, 142.9, 139.1, 138.6, 138.5, 128.0, 121.6, 64.7, 47.7, 38.4, 28.9, 14.4, 12.6, 12.1; HRMS (ESI-TOF) for $[C_{21}H_{24}O_5 + H]^+$: calcd. 357.1702, found 357.1711.

Synthesis of 4-(bromomethyl)phenyl 3-methyl-3-(2,4,5-trimethyl-3,6-dioxocyclohexa-1,4-dien-1-yl)butanoate (30):

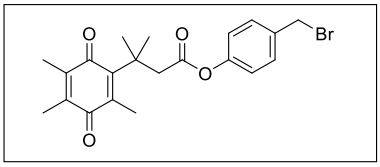

To a solution of **29** (0.51g, 1.43 mmol) in dry DCM, tribromophosphine (170 µL, 1.71 mmol) was added at 0 ^{o}C. The reaction was allowed to stir for 10 min and the progress was monitored by TLC. After completion, the reaction was quenched with saturated solution of $NaHCO_3$ and the aqueous layer was extracted by EtOAc. The combined organic layer was dried over Na_2SO_4 and concentrated under vacuo. Crude was purified by column chromatography and compound was obtained as yellow liquid with 43% yield. FT-IR (ν_{max} , cm^{-1}) 2924, 2856, 1747, 1648, 1601; ^{1}H NMR (400 MHz, $CDCl_3$): δ 7.35 (d, *J* = 8.5 Hz, 2H), 6.95 (d, *J* = 8.6 Hz, 2H), 4.45 (s, 2H), 3.24 (s, 2H), 2.17 (s, 3H) 1.93-1.92 (m, 6H), 1.52 (s, 6H); ^{13}C NMR (100 MHz, $CDCl_3$) δ 190.8, 186.7, 171.2, 151.8, 150.3, 142.8, 138.6, 138.2, 135.4, 130.2, 121.9, 47.6, 38.4, 32.6, 28.9, 14.4, 12.7, 12.1; HRMS (ESI-TOF) for $[C_{21}H_{23}BrO_4 + H]^+$: calcd. 419.0858, found 419.0836.

Synthesis of methyl 2-hydroxy-5-((((4-((3-methyl-3-(2,4,5-trimethyl-3,6-dioxocyclohexa-1,4-dien-1-yl)butanoyl)oxy)benzyl)thio)carbonyl)amino)benzoate (31a):

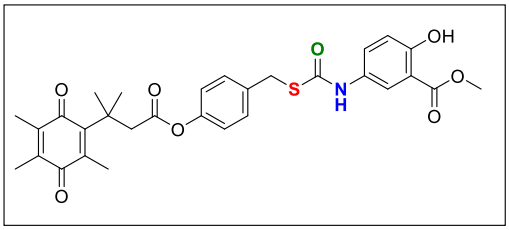

To a solution of **30** (0.26 g, 0.61 mmol) in dry THF, thiourea (0.10 g, 1.33 mmol) was added at room temperature. The reaction was allowed to stir for 12 h. After completion the solvent was removed under vacuum to obtain a yellow coloured solid. The crude was dissolved in 15 mL water and 20 mL DCM under nitrogen atmosphere. $Na_2S_2O_5$ (0.46 g, 2.43 mmol) was then added to the reaction mixture and refluxed at 60 ^{o}C for 4 h. After completion, the crude was extracted using DCM. The organic layer was dried over Na_2SO_4 and concentrated under vacuo. The product obtained is unstable and therefore was taken directly to the next step. Crude was dissolved in dry DMF (8 mL) followed by the addition of **17** (0.19 g, 0.56 mmol) and Et_3N (175 µL, 1.25 mmol). The reaction was allowed to stir for 2 h. The progress of the reaction was monitored by thin layer chromatography (TLC). After completion, the reaction was quenched by the addition of water and extracted by EtOAc (20 mL). The organic layer was washed multiple times with water to remove DMF. The crude was purified by preparative HPLC using kromasil C-18 column and water: acetonitrile as mobile phase to give **31a** (146 mg, 43 % of 2 steps) as yellow solid. FT-IR

(ν_{max} , cm^{-1}) 3330, 1745, 1681, 1643; ^1H NMR (400 MHz, $CDCl_3$): δ 10.63 (s, 1H), 7.91 (s, 1H), 7.48 (bs, 1H), 7.35 (dd, *J* = 8.9 Hz, 2.8 Hz, 1H), 7.29 (d, *J* = 8.6 Hz, 2H), 6.89 (d, *J* = 8.5 Hz, 3H), 4.13 (s, 2H), 3.90 (s, 3H), 3.23 (s, 2H), 2.15 (s, 3H), 1.91-1.90 (m, 6H), 1.51 (s, 6H); ^{13}C NMR (100 MHz, $CDCl_3$) δ 190.8, 187.4, 171.5, 170.0, 158.6, 151.9, 149.5, 142.8, 139.2, 138.6, 135.7, 130.0, 121.6, 118.1, 112.1, 52.5, 47.6, 38.4, 33.7, 28.9, 14.4, 12.7, 12.1; HRMS (ESI-TOF) for $[C_{30}H_{31}NO_8S + H]^+$: calcd. 566.1848, found 566.1848.

Synthesis of 4-((((4-methoxyphenyl)carbamoyl)thio)methyl)phenyl 3-methyl-3-(2,4,5-trimethyl-3,6-dioxocyclohexa-1,4-dien-1-yl)butanoate (31b):

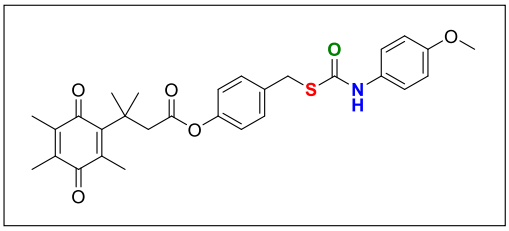

Compound **31b** was synthesized using procedure outlined for **31a**. The compound was obtained as yellow solid (241 mg, 65%). FT-IR (ν_{max} , cm^{-1}) 3336, 1745, 1644; ^1H NMR (400 MHz, $CDCl_3$): 7.33-7.26 (m, 4H), 7.01 (s, 1H), 6.90 (d, *J* = 8.5 Hz, 2H), 6.85 (d, *J* = 9 Hz, 2H), 4.15 (s, 2H), 3.78 (s, 3H), 3.22 (s, 2H), 2.17 (s, 3H), 1.92-1.91 (m, 6H), 1.53 (s, 6H); ^{13}C NMR (100 MHz, $CDCl_3$) δ 190.9, 187.4, 171.4, 151.9, 149.5, 142.9, 139.1, 138.6, 135.8, 130.0, 121.6, 114.3, 55.5, 47.7, 38.4, 33.8, 28.9, 14.4, 12.7, 12.1; HRMS (ESI-TOF) for $[C_{29}H_{31}NO_6S + H]^+$: calcd. 522.1950, found 522.1945.

Synthesis of 4-(((propylcarbamoyl)thio)methyl)phenyl 3-methyl-3-(2,4,5-trimethyl-3,6-dioxocyclohexa-1,4-dien-1-yl)butanoate (31c):

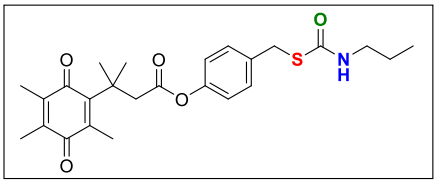

Compound **31c** was synthesized using procedure outlined for **31a**. The compound was obtained as yellow solid (110 mg, 34%). FT-IR (ν_{max} , cm^{-1}) 3373, 2926, 1744, 1647; ^1H NMR (400 MHz, $CDCl_3$): 7.28 (d, *J* = 8.5 Hz, 2H), 6.89 (d, *J* = 8.4 Hz, 2H), 5.52 (s, 1H), 4.10 (s, 2H), 3.25-3.22 (m, 4H), 2.16 (s, 3H), 1.92-1.91 (m, 6H), 1.52 (s, 8H), 0.90 (t, *J* = 7.4 Hz, 3H); ^{13}C NMR (100 MHz, $CDCl_3$) δ 190.9, 187.4, 171.4, 166.4, 152.0, 149.4, 142.9, 139.1, 138.6, 136.3, 129.9, 121.5, 47.6, 43.2, 38.4, 33.5, 28.9, 22.9, 14.3, 12.7, 12.1, 11.2; HRMS (ESI-TOF) for $[C_{25}H_{31}NO_5S + H]^+$: calcd. 458.2002, found 458.2002.

4.1.4.2. Methylene Blue method for H_2S detection:[15]

Each assay described here was done in triplicate in vials with closed lids, containing 374 µL of PBS, 4 µL of H_2S donor (10 mM stock in DMSO), 10 µL of NADH (10 mM stock), 4 µL

of NQO1 (1 mg/mL), 4 μL carbonic anhydrase (1% stock in PBS buffer) and 4 μL $Zn(OAc)_2$ (40 mM stock in H_2O) . The reaction mixture was incubated at 37 ^oC for 4 h. For the control with dicoumarol, we added 100 μM (10 mM stock in 0.1N NaOH) of the dicoumarol to the reaction mixture containing compound **31a**. After 4 h, 100 μL aliquot was removed from each reaction vial and diluted with 100 μL of $FeCl_3$ (30 mM stock in 1.2 M HCl) and 100 μL of *N*,*N*–dimethyl-p-pheneylenediamine sulfate (20 mM stock in 7.2 M HCl). The mixture was incubated at 37 ^oC for 30 min. After completion of methylene blue complex formation, aliquots were transferred to a 96 well plate (250 μL/ well) and the absorbance spectra were collected from 500 to 800 nm on a plate reader. The analysis was done by subtracting the absorbance of the control experiment. The kinetics of H_2S generation was followed using a similar protocol with H_2S donors (50 μM).

4.1.4.3. H_2S detection using an electrode ISO-H2S-100:

The 5mm H_2S sensitive microelectrode (ISO-H2S-100) was first calibrated using the manufacture's protocol using authentic Na_2S solution. The reaction was performed by incubating compound **31a** (10μL, 2.5 mM) in phosphate buffer pH 7.4 (925 μL) containing CA (5 μL, 1% stock), NADH (50 μL, 10 mM) and NQO1 (10 μL, 1 mg/mL) at 37 ^oC. The H_2S produced was detected using 5mm H_2S sensitive microelectrode (ISO-H2S-100) attached to a TBR 4100 Free Radical Analyser (WPI) and shown as picoamps current generated. The signal for current so obtained was plotted against time which signified the generation of H_2S.

4.1.4.4. HPLC analysis:

The decomposition of compound **31b** was followed by HPLC. A stock solution of H_2S donors (2.5 mM) was prepared in DMSO. The stock of NQO1 (1mg/mL) and NADH (10 mM) were prepared in phosphate buffer (pH 7.4, 10 mM). The reaction mixture consisted of compound (25 μM) in buffer containing NQO1 (10 μg/mL) and NADH (100 μM) and incubated at 37 ^oC. At predetermined time points, an aliquot of the reaction mixture was removed, filtered (0.22 micron filter) and injected (50 μL) in a high performance liquid chromatography (HPLC Agilent Technologies 1260 Infinity). The mobile phase was H_2O/ACN. The stationary phase was C-18 reverse phased column (Phenomenex, 5 μm, 4.6 x 250 mm). A multistep gradient was used with a flow rate of 1 mL/min starting with → 0 - 13 min, 50:50 to 10:90 → 13 - 16 min, 10:90 to 10:90 → 16 - 20 min, 10:90 to 50:50.

A similar protocol was used for compound **31a**. The reaction mixture consisted of compound (50 μM) in buffer containing NQO1 (10 μg/mL) and NADH (100 μM) and incubated at 37 ^{o}C. At predetermined time points, an aliquot of the reaction mixture was removed, filtered (0.22 micron filter) and injected (50 μL) in a high performance liquid chromatography (HPLC Agilent Technologies 1260 Infinity). The mobile phase was H_2O/ACN. The stationary phase was C-18 reverse phased column (Phenomenex, 5 μm, 4.6 x 250 mm). A multistep gradient was used with a flow rate of 1 mL/min starting with → 0 - 5 min, 40:60 to 25:75 → 5 - 10 min, 25:75 to 10:90 → 10 - 15 min, 10:90 to 0:100 → 15 – 17 min 0:100 to 0:100 → 17 – 20 min, 0:100 to 40:60 → 20-22 min, 40: 60.

4.1.4.5. Cell viability Assay:

The cytotoxicity effect of the H_2S donors was tested against various cell lines using a similar protocol. Human colon cancer cells, DLD-1, were seeded at a concentration of 1×10^4 cells/well overnight in a 96-well plate in complete RPMI media. Cells were exposed to varying concentrations of the test compounds prepared as a DMSO stock solution so that the final concentration of DMSO was 0.5%. The cells were incubated for 24 h at 37 ^{o}C. A solution of 3-(4, 5-dimethylthiazol-2-yl)-2, 5-diphenyl tetrazolium bromide (MTT) was prepared using 3.5 mg in 7 mL RPMI media. 100 μL of the resulting solution was added to each well. After 4 h incubation, the media was removed carefully and 100 μL of DMSO was added to each well. Spectrophotometric analysis of each well using a microplate reader (Thermo Scientific Varioskan) at 570 nm was carried out to estimate cell viability.A similar protocol was followed for wild type mouse embryonic fibroblast (WT-MEF cells).

Human breast carcinoma, MCF-7 cells were seeded at a concentration of 1 x 10^3 cells/well in a 96 well plate overnight in complete DMEM media. The cells were treated with varying concentrations of compounds for 72 h following which the cell viability was measured using MTT.

4.1.4.6. LDH assay:

Lactate Dehydrogenase (LDH) release was monitored to determine the cytotoxicity of the compounds, as a measurement of necrotic cell death using CCK036, EZCount^{TM} LDH cell assay kit from Himedia Cell culture. The manufacturer's protocol was followed to determine the cytotoxicity. Briefly, human breast carcinoma, MCF-7 cells were seeded at a concentration of 1 x 10^4 cells/well in a 96 well plate and incubated for 16 h. After the cells

were attached the media was removed and replaced with fresh media containing varying concentrations of the compound with maximum DMSO concentration of 0.5%. The cells were then allowed to incubate for another 24 h at 37 ^{o}C. After 24 h cells control was treated with 10 µL of lysis buffer and incubated for 45 min. Next, the plate was centrifuged for 15 min at 1500 rpm to settle down the cell debris. Following this, 50 µL of the media was transferred to another 96 well plate to which 50 µL of LDH reagent was added. The plate was incubated in Varioskan microtiter plate reader at 37 ^{o}C and the absorbance was measured after 25 min at 490 nm. The absorbance was plotted as a measure of cell viability with respect to the DMSO control[25].

4.1.4.7. Protection against oxidative stress:

Human colon adenocarcinoma cells DLD-1 were seeded in a 96-well plate with 10^4 cells/well in RPMI media supplemented with 10% FBS (fetal bovine serum) and 1% antibiotic solution and incubated in an atmosphere of 5% CO_2 at 37 °C for 16 h. Stock solutions of compounds were prepared in RPMI with final concentration of DMSO not exceeding 0.5%. After 16 h, the cells were co-treated with different concentrations of the compound and JCHD (15 µM). The cells were incubated for 24 h at 37 °C. The media was removed after 24 h and the cells were treated with 3-(4, 5-dimethylthiazol-2-yl)-2, 5-diphenyl tetrazolium bromide (MTT) at a concentration of 0.5 mg/mL. A stock solution of MTT was prepared by dissolving 3.5 mg in 7 mL RPMI media and 100 mL of this stock was added to each well. After incubating at 37 °C for 4 h, the media was carefully removed and 100 µL of DMSO was added to each well. Absorbance at 570 nm was recorded using a microplate reader (Thermo Scientific Varioskan) to estimate the cell viability.[22]

A similar protocol was followed for demonstrating the effects of H_2S donors against JCHD induced oxidative stress in WT-MEF cells. Cells were grown in DMEM media supplemented with 10% FBS and 1% antibiotic solution.

4.1.4.8. Persulfidation protocol:

Human colon carcinoma, DLD-1 cells were seeded in a 12 well plate at a concentration of 0.1 x 10^6 cells/well in RPMI media supplemented with 10% FBS (fetal bovine serum) and 1% antibiotic solution and incubated in an atmosphere of 5% CO_2 at 37 °C overnight. Next day, the cells were treated with H_2S donors (10 µM) and Na_2S (200 µM) for 1 h. The cells were washed twice with sterile PBS after the treatment was over. Cells were then fixed by

incubating on ice cold methanol at -20 ^{o}C for 20 min and subsequently permeabilized using ice cold acetone -20 ^{o}C for 5 min. The cells were then washed with PBS and treated with 50 mM HEPES containing triton (1%) and MSBT (10 mM) for overnight at room temperature. The cells were again washed with PBS (3 times) and further incubated with CN-BOT (25 μM) in PBS for 1 h at 37 ^{o}C. The cells were then washed 5 times with PBS and imaged using IX83 microscope from Olympus.[20]

4.1.5 Spectra:

^{1}H NMR ($CDCl_3$, 400 MHz) of compound **28**

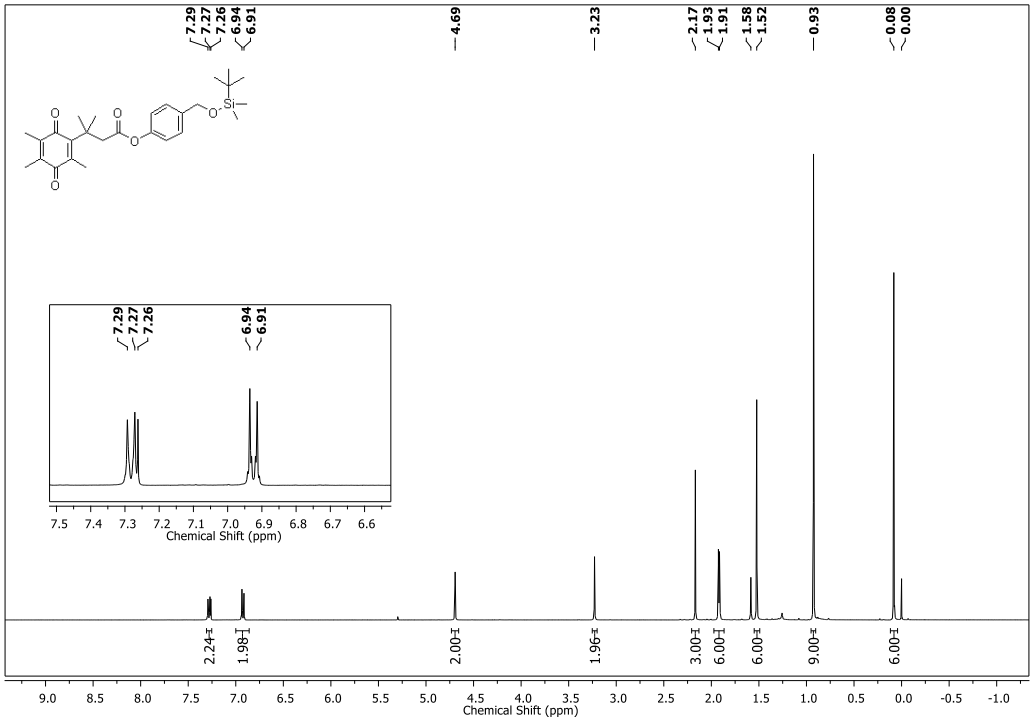

^{13}C NMR ($CDCl_3$, 100 MHz) of compound **28**

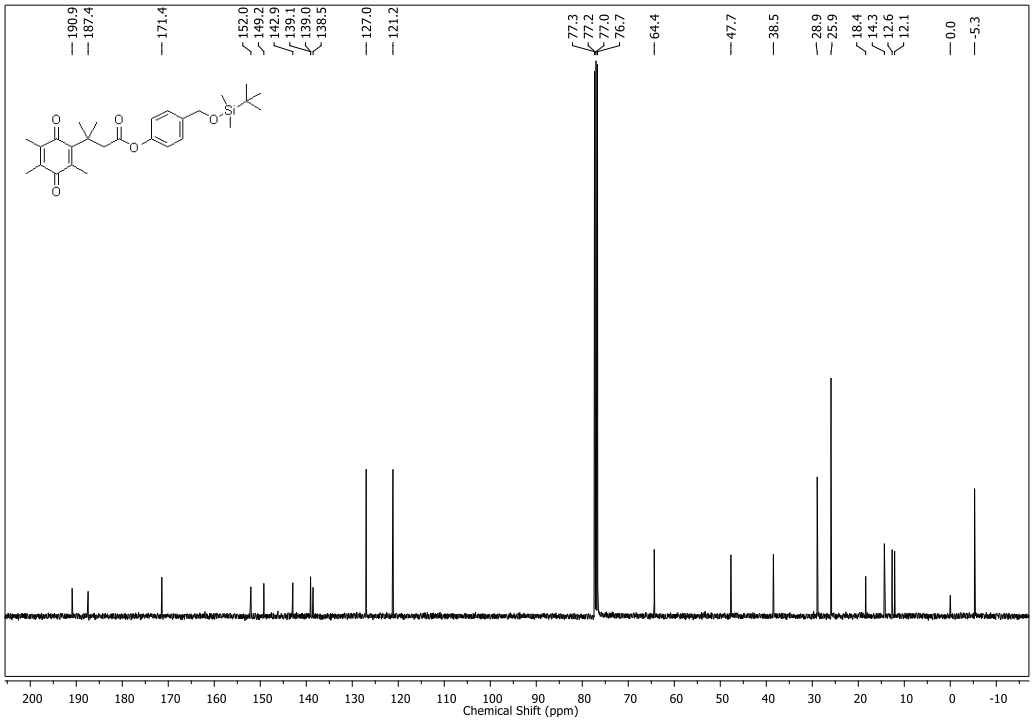

^{1}H NMR ($CDCl_3$, 400 MHz) of compound **29**

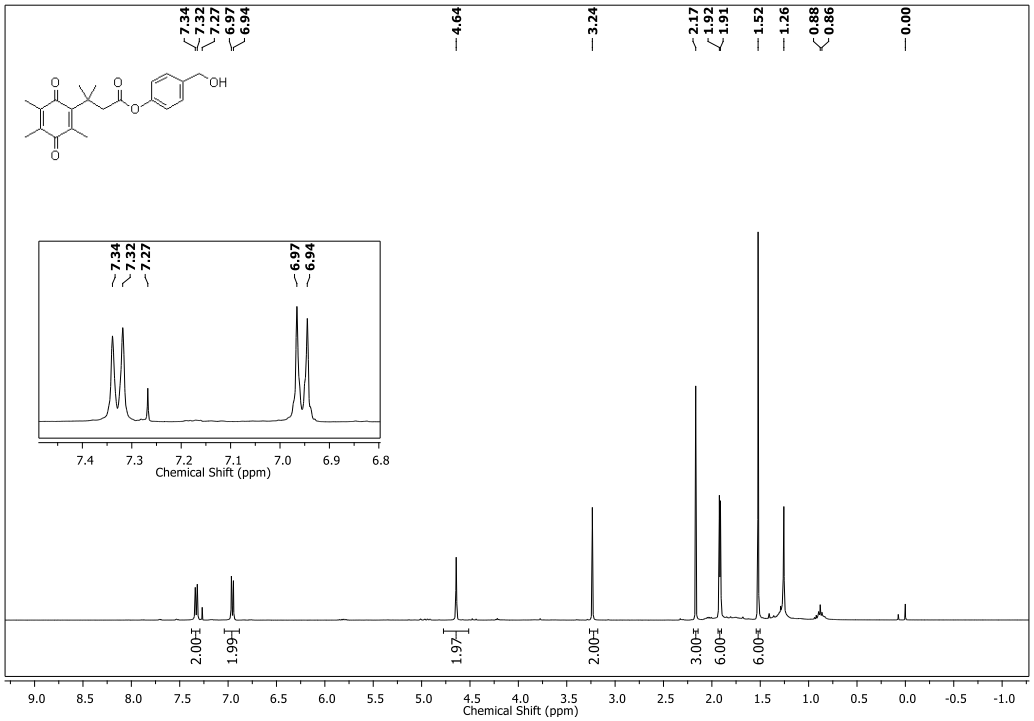

^{13}C NMR ($CDCl_3$, 100 MHz) of compound **29**

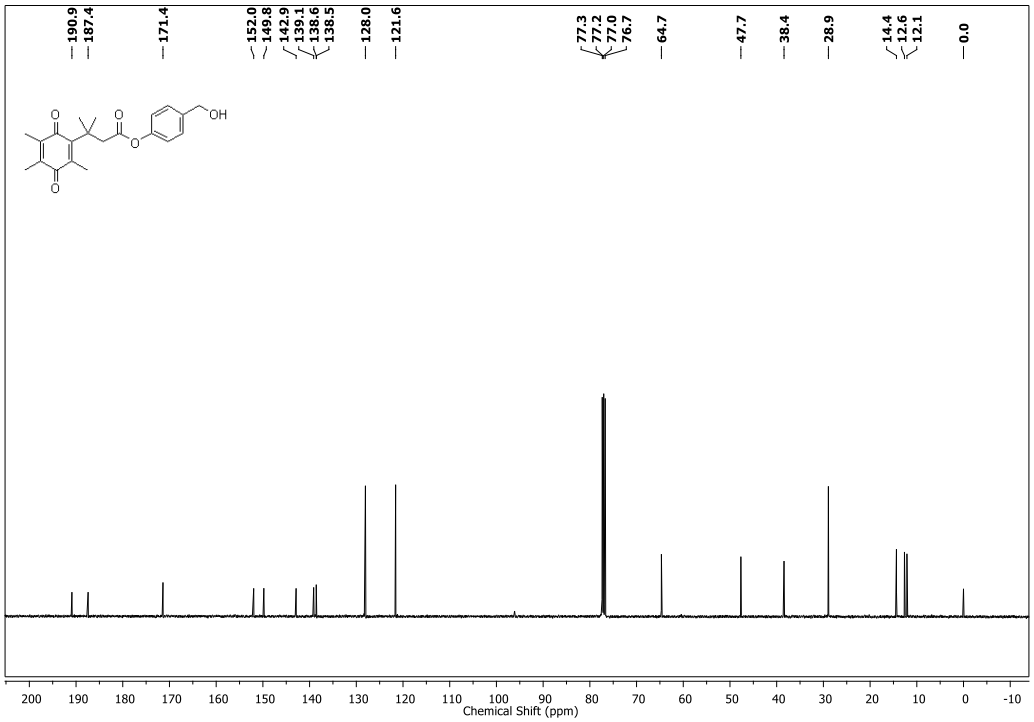

^{1}H NMR ($CDCl_3$, 400 MHz) of compound **30**

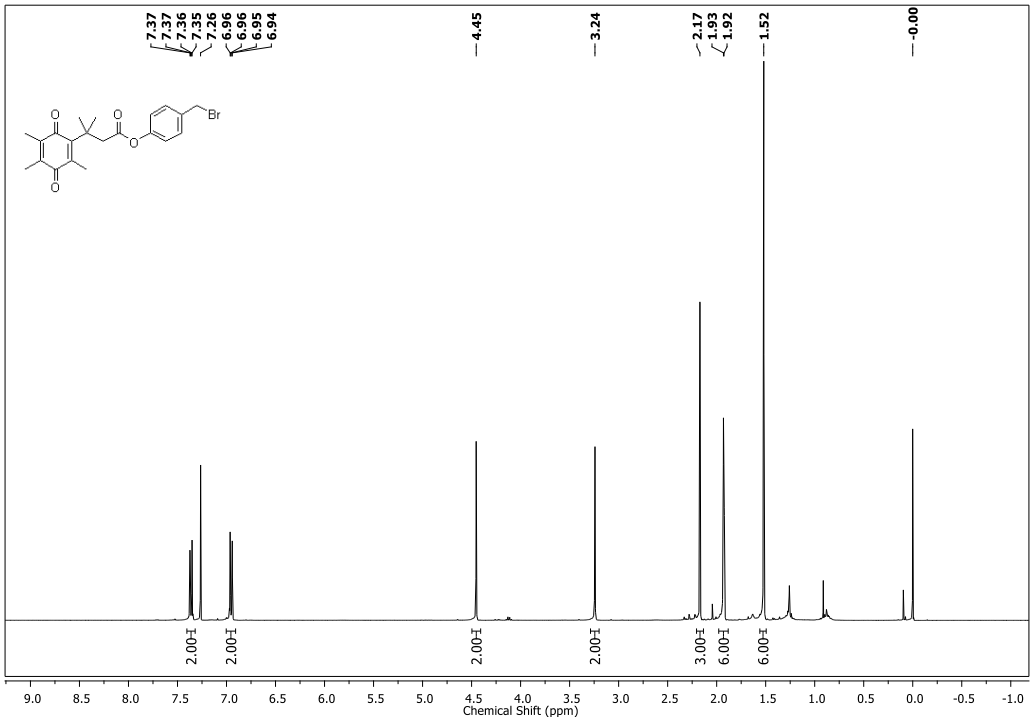

^{1}H NMR ($CDCl_3$, 400 MHz) of **30**

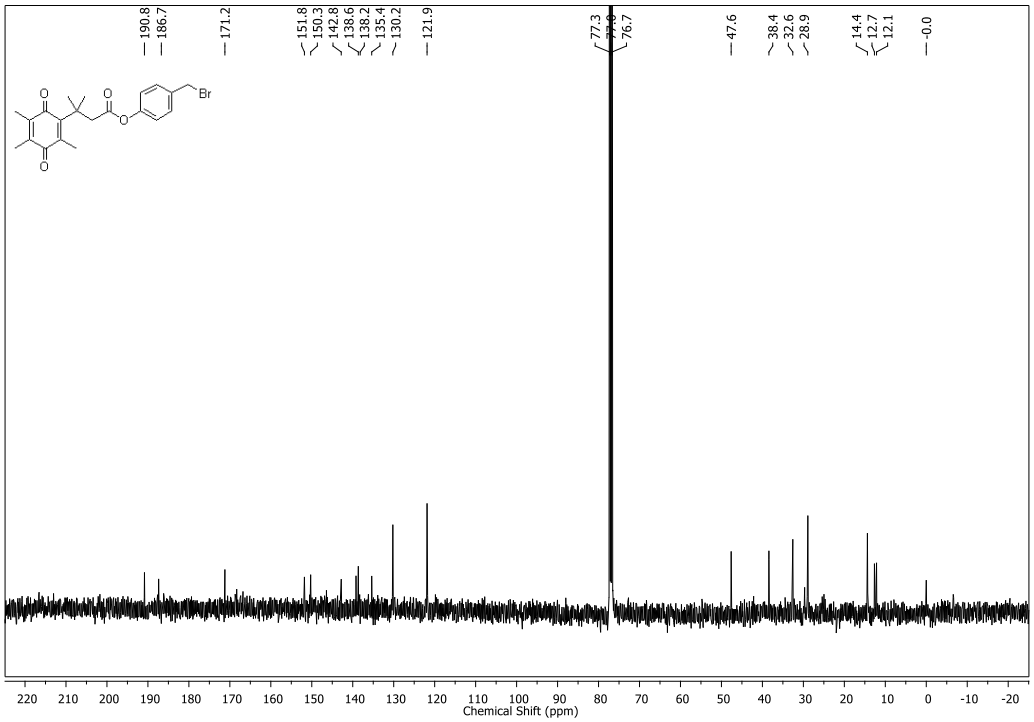

^{1}H NMR ($CDCl_3$, 400 MHz) of compound **31a**

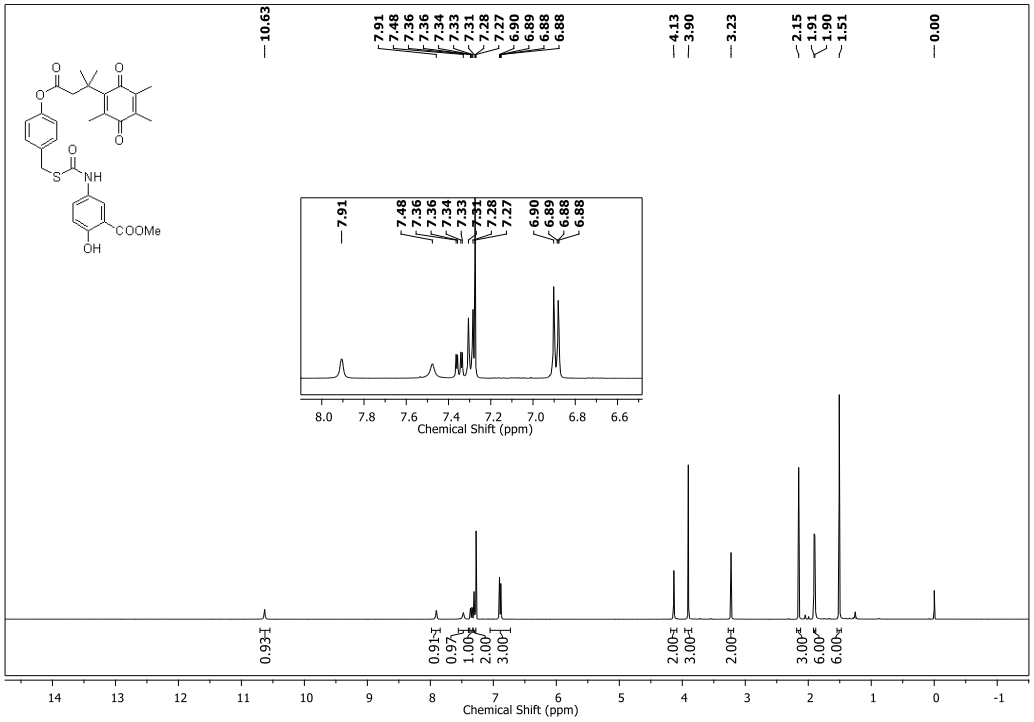

^{13}C NMR ($CDCl_3$, 100 MHz) of compound **31a**

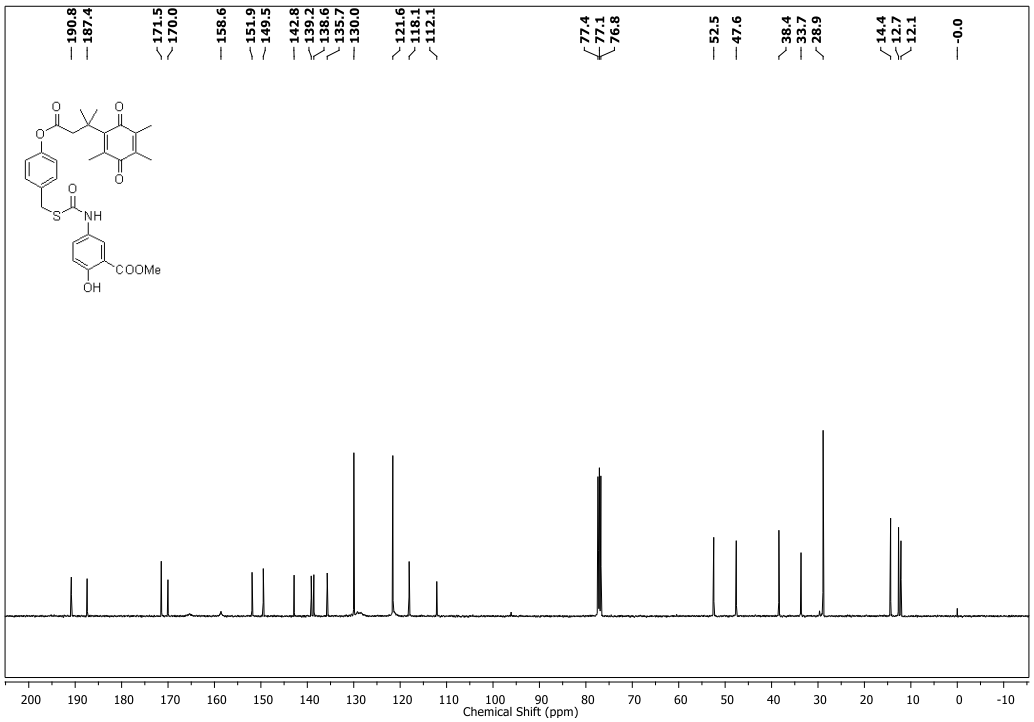

^{1}H NMR ($CDCl_3$, 400 MHz) of compound **31b**

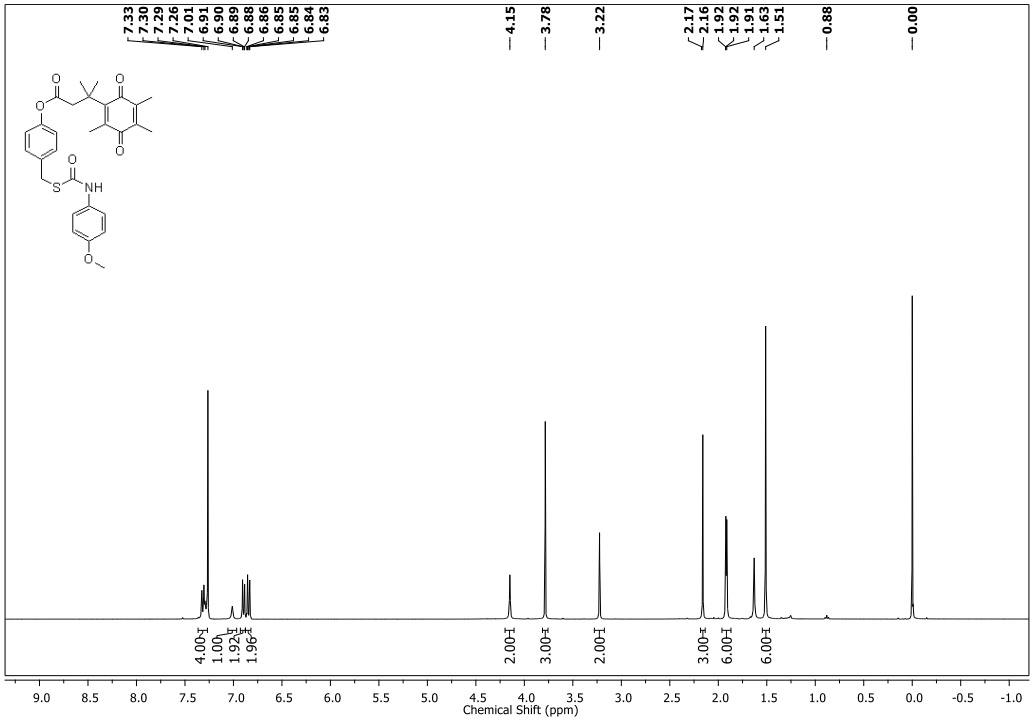

^{13}C NMR ($CDCl_3$, 100 MHz) of compound **31b**

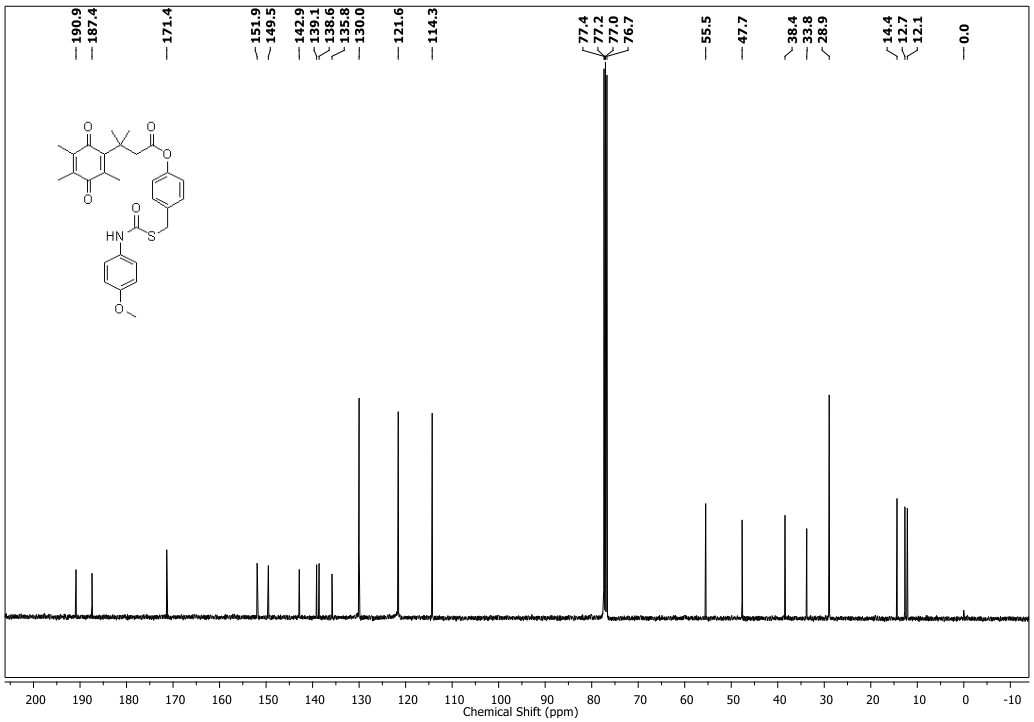

^{1}H NMR ($CDCl_3$, 400 MHz) of compound **31c**

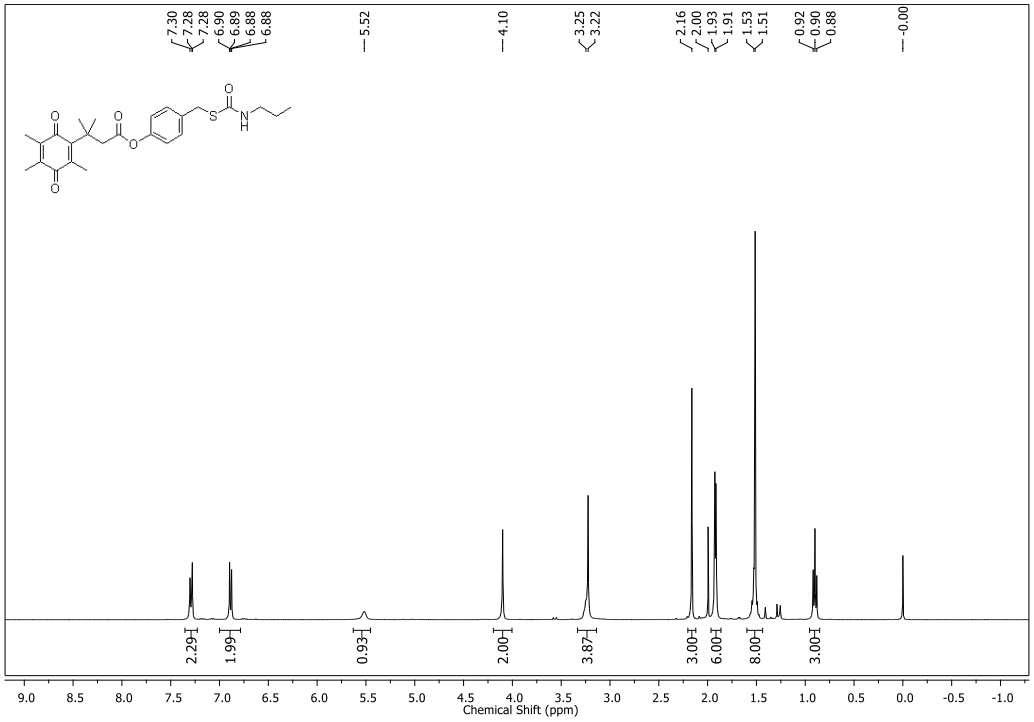

^{13}C NMR ($CDCl_3$, 100 MHz) of compound **31c**

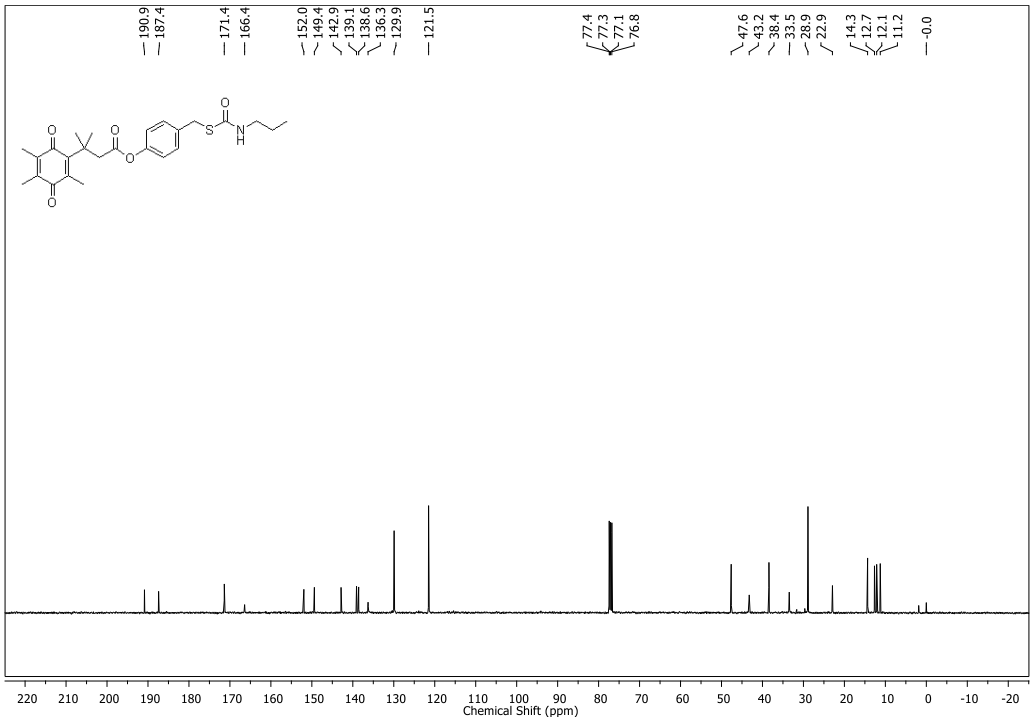

^{1}H NMR ($CDCl_3$, 400 MHz) of Thiol

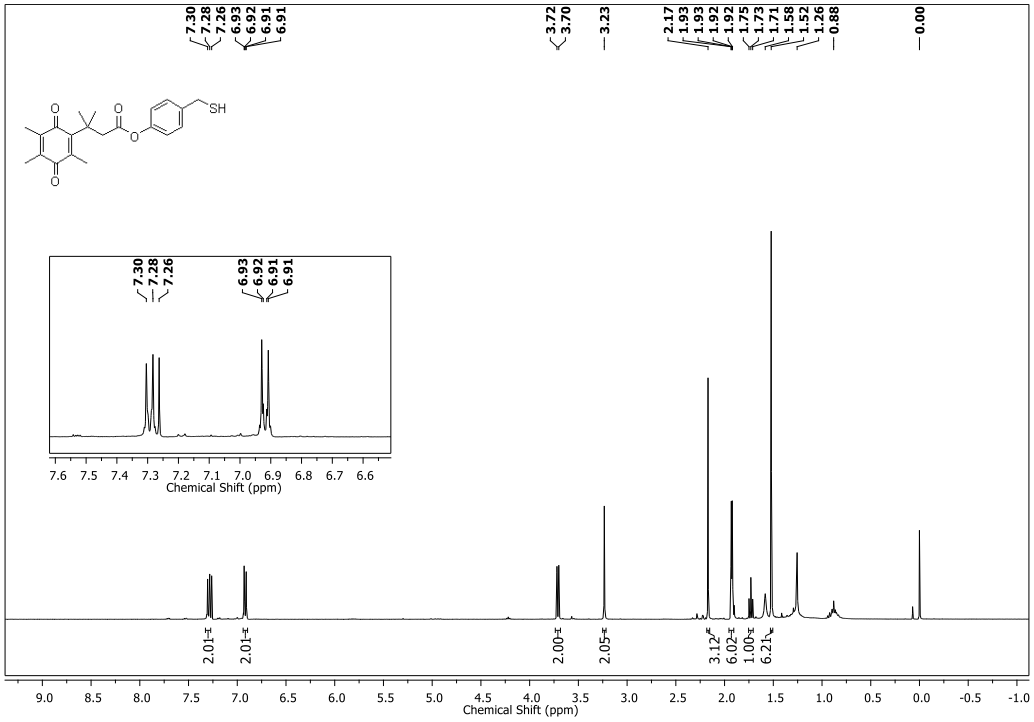

4.1.6. References

(1) Wallace, J. L.; Ferraz, J. G. P.; Muscara, M. N. *Antioxid. Redox Signal.* **2012**, *17*, 58.

(2) Zhao, Y.; Biggs, T. D.; Xian, M. *Chem. Commun.* **2014**, *50*, 11788.

(3) Fiorucci, S.; Orlandi, S.; Mencarelli, A.; Caliendo, G.; Santagada, V.; Distrutti, E.; Santucci, L.; Cirino, G.; Wallace, J. L. *Br. J. Pharmacol.* **2007**, *150*, 996.

(4) Hanauer, S. B. *Colorectal Dis.* **2006**, *8*, 20.

(5) Karagozian, R.; Burakoff, R. *Ther. Clin. Risk Manag.* **2007**, *3*, 893.

(6) Ham, M.; Moss, A. C. *Expert rev. clin. pharmacol.* **2012**, *5*, 113.

(7) Korzenik, J. R.; Podolsky, D. K. *Nat. Rev. Drug Discov.* **2006**, *5*, 197.

(8) Ross, D.; Siegel, D. *Front. Physiol.* **2017**, *8*.

(9) Ross, D.; Siegel, D.; Beall, H.; Prakash, A. S.; Mulcahy, R. T.; Gibson, N. W. *Cancer and Metastasis Rev.* **1993**, *12*, 83.

(10) Siegel, D.; Ross, D. *Free Radic. Biol. Med.* **2000**, *29*, 246.

(11) Raina, A. K.; Templeton, D. J.; deak, J. C.; Perry, G.; Smith, M. A. *Redox Rep.* **1999**, *4*, 23.

(12) Xie, T.; Jaiswal, A. K. *Biochem. Pharmacol.* **1996**, *51*, 771.

(13) Okoh, O. A.; Klahn, P. *ChemBioChem* **2018**, *19*, 1668.

(14) Danson, S.; Ward, T. H.; Butler, J.; Ranson, M. *Cancer Treat. Rev.* **2004**, *30*, 437.

(15) Powell, C. R.; Foster, J. C.; Okyere, B.; Theus, M. H.; Matson, J. B. *J. Am. Chem. Soc.* **2016**, *138*, 13477.

(16) Steiger, A. K.; Marcatti, M.; Szabo, C.; Szczesny, B.; Pluth, M. D. *ACS chem. biol.* **2017**, *12*, 2117.

(17) Filipovic, M. R.; Zivanovic, J.; Alvarez, B.; Banerjee, R. *Chem. Rev.* **2018**, *118*, 1253.

(18) Wallace, J. L.; Wang, R. *Nat. Rev. Drug. Discov.* **2015**, *14*, 329.

(19) Yang, G.; Zhao, K.; Ju, Y.; Mani, S.; Cao, Q.; Puukila, S.; Khaper, N.; Wu, L.; Wang, R. *Antioxid. Redox Signal.* **2013**, *18*, 1906.

(20) Wedmann, R.; Onderka, C.; Wei, S.; Szijártó, I. A.; Miljkovic, J. L.; Mitrovic, A.; Lange, M.; Savitsky, S.; Yadav, P. K.; Torregrossa, R.; Harrer, E. G.; Harrer, T.; Ishii, I.; Gollasch, M.; Wood, M. E.; Galardon, E.; Xian, M.; Whiteman, M.; Banerjee, R.; Filipovic, M. R. *Chem. Sci.* **2016**, *7*, 3414.

(21) Zhang, D.; Macinkovic, I.; Devarie-Baez, N. O.; Pan, J.; Park, C.-M.; Carroll, K. S.; Filipovic, M. R.; Xian, M. *Angew. Chem. Int. Ed.* **2014**, *53*, 575.

(22) Bora, P.; Chauhan, P.; Manna, S.; Chakrapani, H. *Org. Lett.* **2018**, *20*, 7916.

(23) Dharmaraja, A. T.; Chakrapani, H. *Org. Lett.* **2014**, *16*, 398.

(24) Probst, B. L.; McCauley, L.; Trevino, I.; Wigley, W. C.; Ferguson, D. A. *PLoS One.* **2015**, *10*, e0135257.

(25) Ahmad, A.; Olah, G.; Szczesny, B.; Wood, M. E.; Whiteman, M.; Szabo, C. *Shock.* **2016**, *45*, 88.

CHAPTER 4.2: NQO1 activated persulfide donors

4.2.1. Introduction:

H_2S signalling is mediated by oxidative post translational modification of cysteine residues of proteins to form protein persulfides. [1,2] Several persulfidated protein targets have been identified over the past few years with potential therapeutic outcomes.[3,4] However, the mechanism by which H_2S forms persulfides remains elusive and requires further attention. Formation of protein persulfides from H_2S requires an oxidant, as the direct reaction is not feasible due to redox constraints.[2] H_2S reacts with oxidized cysteine residues like polysulfides or sulfenic acid residues to form persulfides.[5] The formation of persulfides is required for the activity of enzymes like 3-mercaptopyruvate sulphur transferase (3-MST), rhodanese and thiosulfate sulfurtransferase (TST). A transient persulfide intermediate is formed in the active site cysteine of the enzyme which subsequently persulfidates the proteins.[6] Enzymes like CBS and CSE form low molecular weight persulfides CysSSH which are involved in the biosynthetic pathway of H_2S.[7,8] This clearly states the importance of the formation of persulfides within the cells. Thus achieving site directed delivery of persulfides would assume importance from mechanistic and therapeutic stand point.

Persulfides (RSSH) have each sulfur in its -1 oxidation state. The lower bond dissociation energy of S-H bond in perthiols (70 kcal mol^{-1}) compared to the corresponding thiol (92 kcal mol^{-1}) makes the perthiols more acidic than corresponding thiols. This reduces the pK_a of perthiols by approximately 2 units.[2] Therefore, we propose to evaluate the ability of the scaffold to release perulfides upon activation by NQO1 enzyme.

A few triggerable persulfide donors, have been reported in the past to achieve better understanding of the effects of this reactive sulfur specie (RSSH) within the cells (Figure 4.2.1).[9] Ming Xian and co-workers reported 9-fluorenylmethyl disulfide (FmSSPy-A) based persulfide donors which undergo a disulfide exchange with small molecule thiols or protein thiols to form RSS-Fm. The mixed disulfide is sensitive to base and therefore, in the presence of 1,8-Diazabicyclo[5.4.0]undec-7-ene (DBU), an amidine based base, releases persulfide.[10] Esterase sensitive persulfide donors (BW-HP-201/ BW-GP-401) have been reported in the recent years by Binghe Wang and co-workers which upon stimulation by esterase releases persulfides (GSSH also).[11,12] In order to study the potential therapeutic role of persulfides, Matson and co-workers reported ROS responsive persulfide donors (BDP-NAC) and demonstrated the cytoprotective effects of the molecule.[13] Independently, our lab has also

reported ROS sensitive persulfide donors following a 1,4 relay approach to release benzyl persulfide within cells.[14] The cytoprotective effects of persulfide donors against xenobiotic induced oxidative stress has been demonstrated.

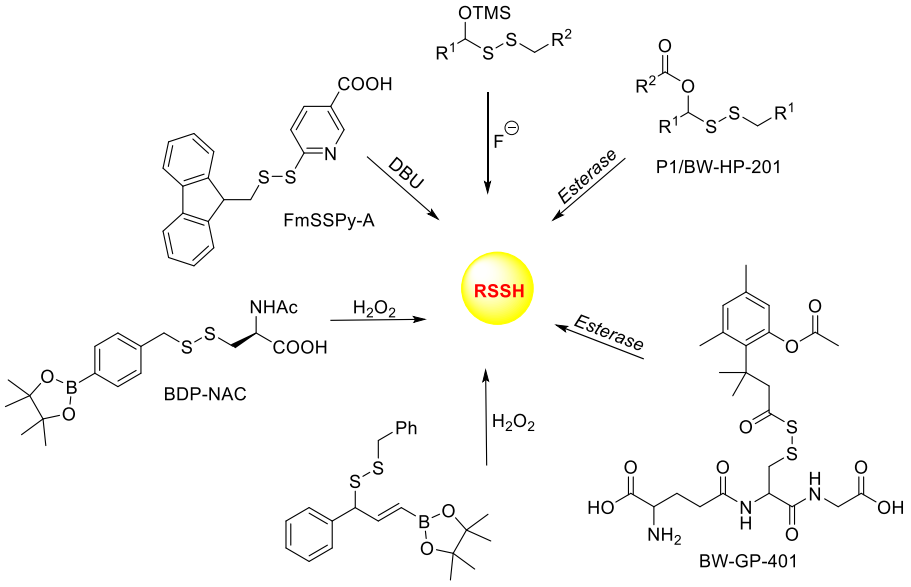

Figure 4.2.1. Triggerable persulfide donors.

Therefore, NQO1 responsive donors for colon targeted delivery of persulfides are proposed. The mechanism of perthiol release is as follows: the donors upon activation by NQO1 in cells release an intermediate which further dissociates to generate persulfides (Scheme 4.2.1).

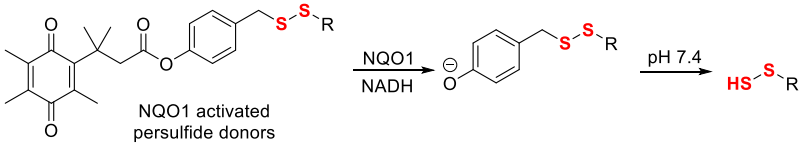

Scheme 4.2.1. NQO1 activated persulfide donor.

4.2.2. Results and Discussion

4.2.2.1. Synthesis of NQO1 responsive persulfide donors

NQO1 activated persulfide donors were synthesized in this series with *N*-acetyl cysteine (NAC) and benzyl persulfides as the leaving groups (Figure 4.2.2). First, mixed disulfide of NAC and benzyl mercaptan were prepared by reacting the thiols with 2-aldrithiol to give compound **33** in 73% yield and **34** in 95% yield respectively (Scheme 4.2.2).[13]

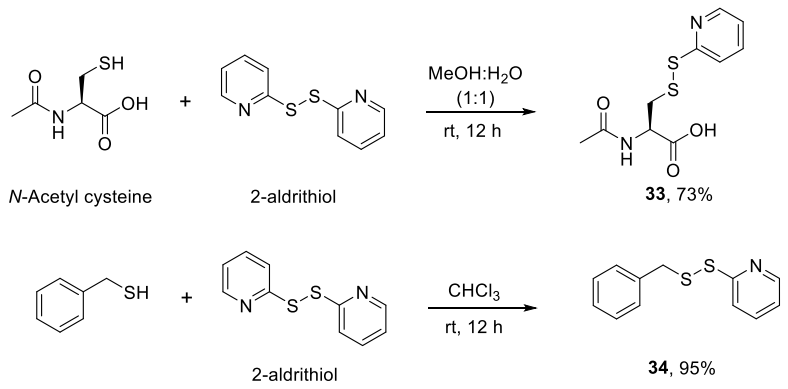

Scheme 4.2.2. Synthesis of mixed disulfides, **33** and **34**.

Compound **30** was synthesized using protocol reported in the previous chapter. Briefly, 2,3,5-trimethylbenzene-1,4-diol was reacted with 3-methylbut-2-enoic acid to give compound **26** which was then oxidized to **27** in the presence of *N*-bromosuccinimide (NBS). The acid of compound **27** was coupled with the hydroxyl group of **25** to form an ester, **28** in the presence of EDC.HCl and DMAP in 71% yield. This was followed by a deprotection of TBDMS in the presence of acetic acid in THF and water to give compound **29** in 97% yield, which was further reacted with tribromophosphine to yield compound **30** in 43% yield. Compound **30** was further reacted with thiourea to give the thiourea adduct which was hydrolysed to form thiol. The thiol so formed was extremely unstable and was readily reacted with respective mixed disulfides (**33**, **34**) to give compound **35a** in 53% yield, **35b** in 89% yield respectively (Scheme 4.2.3).

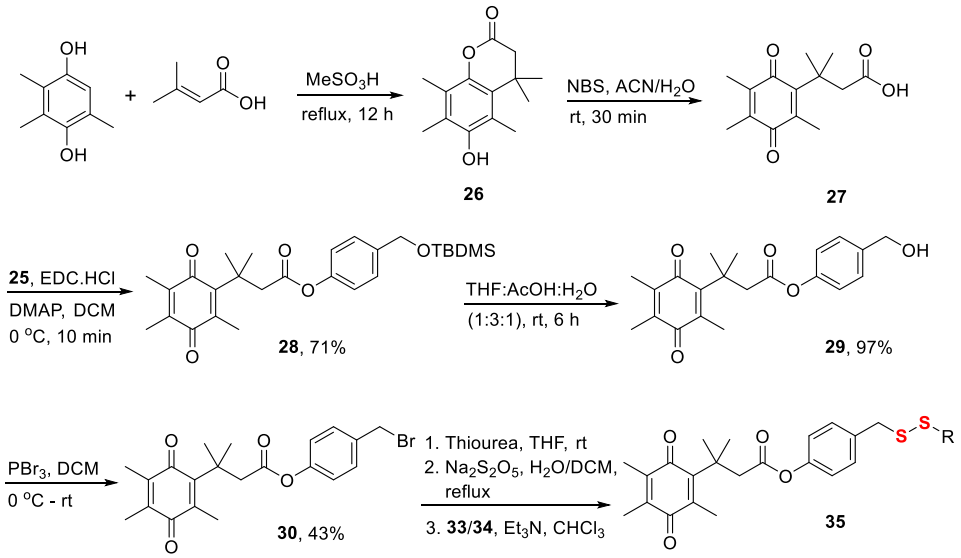

Scheme 4.2.3. Synthesis of NQO1 activated persulfide donors.

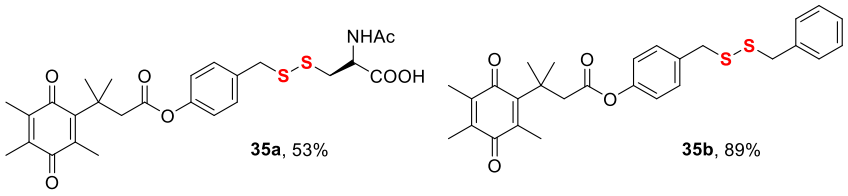

Figure 4.2.2. Structures of NQO1 responsive persulfide donors.

4.2.2.2. HPLC studies

Formation of persulfide can be monitored using a method reported by Binghe Wang and co-workers and also by our lab, wherein the persulfide generated is trapped by reacting with 1-fluoro-2,4-dinitrobenzene (FDNB) to form of an FDNB adduct, **36**. [11] Compound **35b** upon reduction with NQO1 in the presence of NADH undergoes reduction followed by lactonization to release intermediate **III**. The intermediate thus formed dissociates to release benzyl persulfide which can react with FDNB to form compound **36** that can be monitored by HPLC (Scheme 4.2.4).

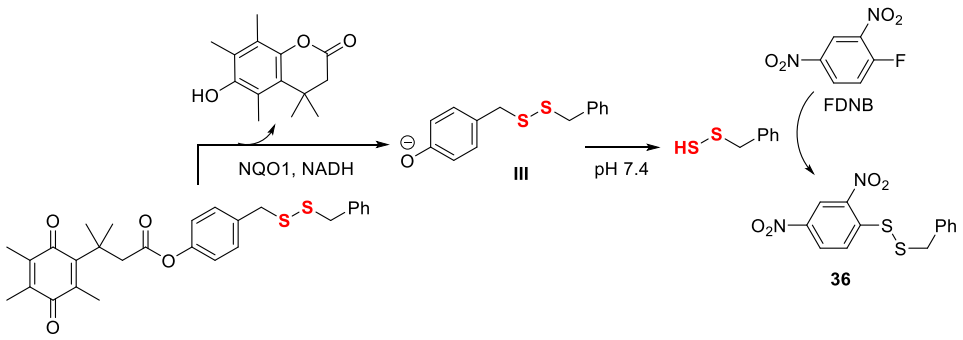

Scheme 4.2.4. Trapping of persulfide in the form of FDNB adduct.

In order to demonstrate the production of benzyl persulfide using HPLC, first compound **35b** was injected in ACN which eluted at 16.67 min. Next, the compound was incubated in buffer (pH 7.4) containing NQO1, NADH and FDNB at 37 ^{o}C and injected in HPLC at different time intervals. Peak corresponding to **35b** disappeared over a period of 1 h with concomitant formation of lactone (5.68 min). A new peak attributable to the intermediate formation was observed which remained intact even after 13 h of incubation (Figure 4.2.3). This could be due to the slow decomposition of the intermediate to form the persulfide. However no peak corresponding to the formation of **36** was observed even after 13 h of incubation. The results observed suggested that rate of decomposition of the intermediate was slow. Also, the FDNB was unstable for long duration and therefore was not found to be effective in trapping the

small amount of persulfide that might be generated in the reaction mixture. Thus persulfide formation was not observed with our scaffolds as reported by Matson and co-workers.[13]

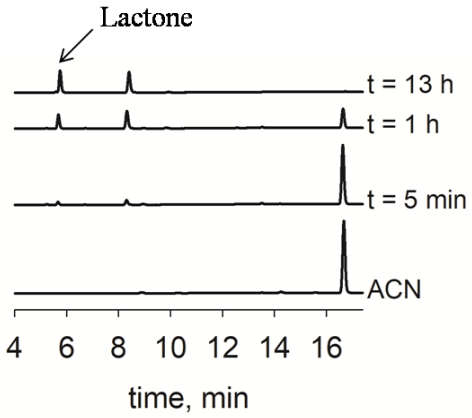

Figure 4.2.3. HPLC traces for the decomposition of compound **35b** in the presence of NQO1.

4.2.2.3. Decomposition studies in cell lysate

Next we proposed to monitor the dissociation of compound in cell lysate and observe the decomposition of the intermediate. Compound **35a** was used in this experiment due to the improved aqueous solubility of the molecule. First, compound **35a** was injected in MeOH which eluted at 16.24 min. Next, the compound was incubated in phosphate buffer (pH 7.4) in the presence of NQO1 and NADH and injected in HPLC at different time intervals. A completed disappearance of the peak corresponding to **35a** was observed after 5min of incubation indicating towards the fast activation of compound by NQO1. Two new peaks were observed which were attributable to the formation of lactone and intermediate (Figure 4.2.4). The intermediate formed was found to be intact even after 1 h of incubation in buffer.

In order to demonstrate the decomposition of compound in cells, human colorectal adenocarcinoma, DLD-1 cells were incubated with compound **35a** (50 μM) for 1 h. The media was removed and cells were washed with PBS. The cells were then lysed using MeOH and vigorous vortexing for 2 min. Finally the mixture was centrifuged and supernatant was injected in HPLC after filtration. A peak corresponding to lactone was observed in the cell lysate mixture. However, a complete disappearance of the peak corresponding to the intermediate was observed (Figure 4.2.4). This suggested that the intermediate formed was unstable in a cellular environment and readily decomposed within 1 h of incubation.

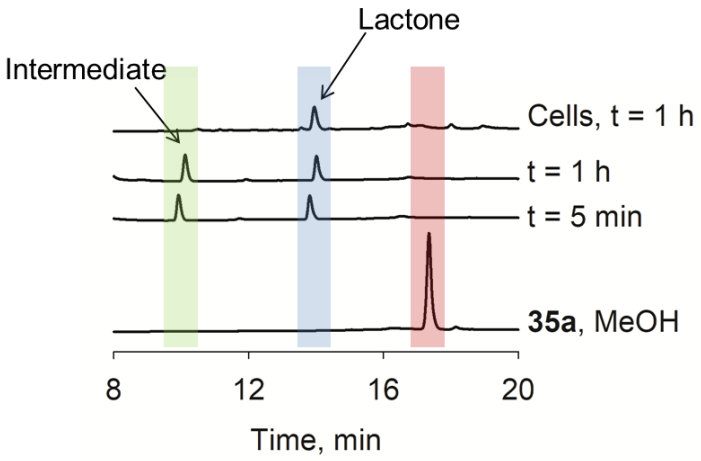

Figure 4.2.4. Representative HPLC traces for decomposition of compound **35a** in buffer and cell lysate.

4.2.2.4. Mechanism of protein persulfidation:

The general mechanism of persulfide formation using persulfide donors is as follows: Compounds upon activation of external stimulus releases persulfidating agent which undergoes a sulfhydryl exchange with proteins to induce protein persulfidation. The formation of protein persulfides can occur via two pathways: protein may form a mixed disulfide with persulfidating agent by releasing H_2S in the process. The mixed disulfide can further react with H_2S with simultaneous release of thiol to form protein persulfide. In the second possibility, proteins can directly react with perulfidating agent to form protein persulfides by releasing free thiol (Scheme 4.2.5).

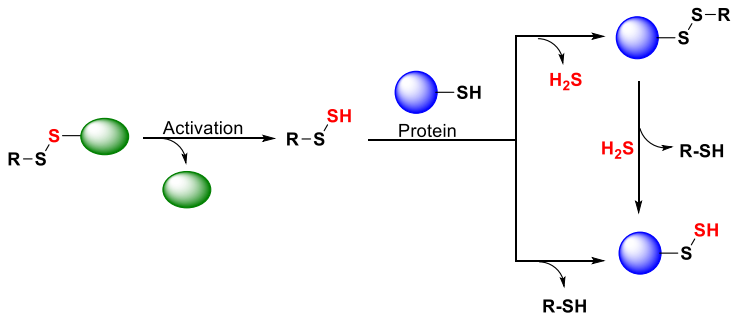

Scheme 4.2.5. Mechanism of protein persulfidation.

4.2.2.5. Cell viability assay:

Next, the toxicity of the compounds was elucidated using standard cell viability assay. DLD-1 cells were incubated with varying concentration of **35a** for 24 h following which the cell

viability was monitored using MTT. The compound was found to be well tolerated at 100 µM concentration over a period of 24 h (Figure 4.2.5).

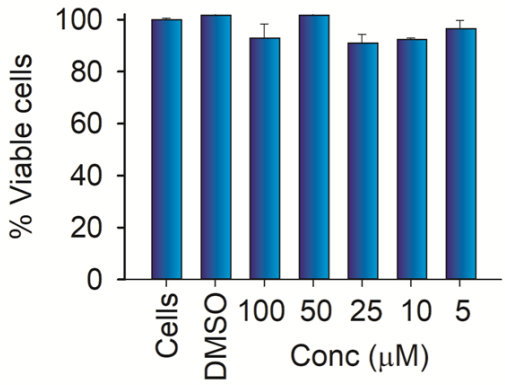

Figure 4.2.5. Cell viability assay for compound **35a** in DLD-1 cells.

4.2.2.6. Protection against JCHD induced toxicity:

Next, the cytoprotective effects of the donors were evaluated against JCHD induced toxicity. Protocol from the previous chapter was followed to test the cytoprotective effects. Briefly, DLD-1 cells were incubated with varying concentrations of compounds along with JCHD (15 µM), ROS inducing agent, for 24 h. The cell viability was monitored after 24 h of incubation using MTT. A dose dependent increase in the cell viability was observed in the case of compound **35a** (Figure 4.2.6a). Compound **35b** showed similar cytoprotective effects against JCHD induced stress, however, the extent of increase in cell viability was lower in the case of **35b** compared to **35a** (Figure 4.2.6b). Compound **29** was used as a negative control which did not show any cytoprotective effects (Figure 4.2.6c). Similarly, when *N*-acetylcysteine (NAC) was tested for its ability to protect the cells against JCHD induced toxicity, however, no significant improvement in the cell viability was observed at the reported concentrations (Figure 4.2.6d). NAC is extensively used as an antioxidant, however a higher concentration is required to observe the desired cytoprotective effects.

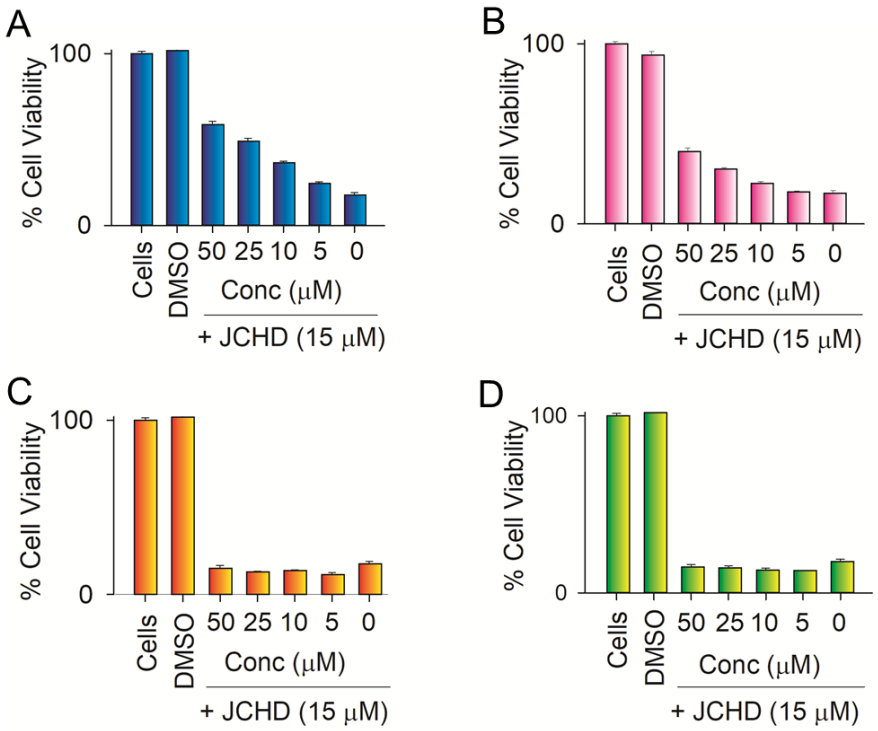

Figure 4.2.6. a) Cytoprotective effects of compound **35a** against JCHD (15 μM) induced stress in human colon carcinoma, DLD-1 cells. Results are expressed as mean ± SEM (n = 3). b) Cell viability with compound **35b** against JCHD induced stress. c) Cytoprotective effects of compound **29**, which acts as a negative control, against JCHD induced stress. d) Cytoprotective effects of compound NAC.

4.2.3. Summary

In summary, we synthesized NQO1 activated persulfide donors with NAC and benzyl persulfide as the leaving groups. The compounds were found to be stable towards hydrolysis. The rate of persulfide formation from the reported donors was found to be extremely slow. However, the donors were found to be effective in a cellular environment and showed protective effects against JCHD induced cytotoxicity.

4.2.4. Experimental Section

4.2.4.1. Synthesis and Characterization:

Compounds **33** and **34**[15] were synthesized using a reported protocol and the analytical data obtained was matching with the reported values.

Synthesis of *N*-acetyl-S-((4-((3-methyl-3-(2,4,5-trimethyl-3,6-dioxocyclohexa-1,4-dien-1-yl)butanoyl)oxy)benzyl)thio)-L-cysteine (35a):

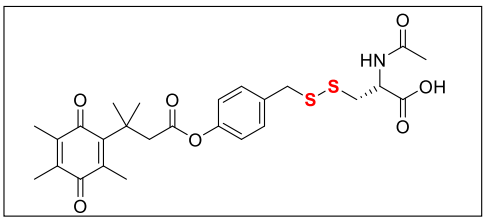

To a solution of **30** (0.25 g, 0.61 mmol) in dry THF, thiourea (0.092 g, 1.21 mmol) was added at room temperature. The reaction was allowed to stir for 12 h. After completion the solvent was removed under vacuum to obtain a yellow coloured solid. The crude was dissolved in 15 mL water and 20 mL DCM under nitrogen atmosphere. $Na_2S_2O_5$ (0.46 g, 2.43 mmol) was then added to the reaction mixture and refluxed at 60 ^oC for 4 h. After completion, the crude was extracted using DCM. The organic layer was dried over Na_2SO_4 and concentrated under vacuo. The product obtained was unstable and therefore was taken directly to the next step. Crude was dissolved in dry $CHCl_3$ (8 mL) followed by the addition of **33** (0.22 g, 0.81 mmol) and Et_3N (225 µL, 1.61 mmol). The reaction was allowed to stir for 2 h. The progress of the reaction was monitored by thin layer chromatography (TLC). After completion, the reaction was quenched by the addition of water and extracted by $CHCl_3$ (20 mL) 3 times. The crude was purified by preparative HPLC using kromasil C-18 column. The compound was obtained as yellow solid (171 mg, 53%). FT-IR (ν_{max} , cm^{-1}) 3361, 2926, 1746, 1639, 1586; ^1H NMR (400 MHz, DMSO-d6): 7.84 (s, 1H), 7.32 (d, *J* = 8.3 Hz, 2H), 6.94 (d, *J* = 8.3 Hz, 2H), 4.28 (s, 1H), 3.93 (s, 2H), 3.21(dd, *J* = 13.0 Hz, 4.2 Hz, 1H), 3.17 (s, 2H), 2.91 (dd, J = 12.8 Hz, 8.0 Hz, 1H), 2.11 (s, 3H), 1.86 (s, 9H), 1.46(s, 6H); ^{13}C NMR (100 MHz, $CDCl_3$) δ 190.2, 186.6, 170.7, 168.9, 151.5, 149.0, 142.3, 138.5, 137.9,135.3, 130.2, 121.4, 53.5, 46.7, 41.1, 38.0,28.3, 22.8, 21.6, 13.9, 12.3, 11.7; HRMS (ESI-TOF) for $[C_{26}H_{31}NO_7S_2 + Na]^+$: calcd. 556.1439, found 556.1436.

Synthesis of 4-((benzyldisulfanyl)methyl)phenyl 3-methyl-3-(2,4,5-trimethyl-3,6-dioxocyclohexa-1,4-dien-1-yl)butanoate (35b):

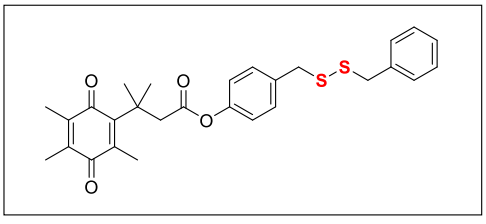

Compound **35b** was synthesized using procedure outlined for **35a**. The compound was obtained as

yellow solid (237 mg, 89%). FT-IR (ν_{max} , cm^{-1}) 2925, 1747, 1644, 1597; ^{1}H NMR (400 MHz, $CDCl_3$): 7.31-7.27 (m, 3H), 7.26-7.24 (m, 2H), 7.17 (d, *J* = 8.4 Hz, 2H), 6.91 (d, J = 8.5 Hz, 2H), 3.64 (s, 2H), 3.51 (s, 2H), 3.23(s, 2H), 2.17 (s, 3H), 1.90 (s, 6H), 1.52 (s, 6H); ^{13}C NMR (100 MHz, $CDCl_3$) δ 190.9, 187.4, 171.2, 151.9, 149.7, 142.9, 139.1, 138.1, 137.3, 134.9, 130.4, 129.4, 128.5, 127.5, 121.5, 47.7, 43.3, 42.5, 38.4, 28.9, 14.4, 12.6, 12.1; HRMS (ESI-TOF) for $[C_{28}H_{30}O_4S_2 + H]^+$: calcd. 495.1664, found 495.1654.

4.2.4.2. **HPLC analysis:**

The decomposition of compound **35b** was followed by HPLC. A stock solution of H_2S donors (2.5 mM) was prepared in DMSO. The stock of NQO1 (1mg/mL) and NADH (10 mM) were prepared in phosphate buffer (pH 7.4, 10 mM). The reaction mixture consisted of compound (50 µM) in buffer containing NQO1 (10 µg/mL) and NADH (100 µM) and incubated at 37 ^{o}C. At predetermined time points, an aliquot of the reaction mixture was removed, filtered (0.22 micron filter) and injected (50 µL) in a high performance liquid chromatography (HPLC Agilent Technologies 1260 Infinity). The mobile phase was H_2O/ACN. The stationary phase was C-18 reverse phased column (Phenomenex, 5 µm, 4.6 x 250 mm). A multistep gradient was used with a flow rate of 1 mL/min starting with → 0 - 5 min, 40:60 to 25:75 → 5 - 10 min, 25:75 to 10:90 → 10 - 15 min, 10:90 to 0:100 → 15 – 17 min 0:100 to 0:100 → 17 – 20 min, 0:100 to 40:60 → 20-22 min, 40: 60.

4.2.4.3. **HPLC studies in cell lysate:**

In order to follow the decomposition of compound **35a** we followed a different method. A similar protocol was used for compound **35a**. The reaction mixture consisted of compound (50 µM) in buffer containing NQO1 (10 µg/mL) and NADH (100 µM) and incubated at 37 ^{o}C. At predetermined time points, an aliquot of the reaction mixture was removed, filtered (0.22 micron filter) and injected (50 µL) in a high performance liquid chromatography (HPLC Agilent Technologies 1260 Infinity). The mobile phase was H_2O and MeOH with 0.02% TFA. The stationary phase was C-18 reverse phased column (Phenomenex, 5 µm, 4.6 x 250 mm). A multistep gradient was used with a flow rate of 1 mL/min starting with → 0 - 13 min, 50:50 to 10:90 → 13 - 16 min, 10:90 to 10:90 → 16 - 20 min, 10:90 to 50:50. Same method was used for monitoring the decomposition of **35a** in cells.

Human colorectal adenocarcinoma, DLD-1 cells were seeded in a 10 cm plate in RPMI media supplemented with 10% FBS (fetal bovine serum) and 1% antibiotic solution and

incubated in an atmosphere of 5% CO_2 at 37 °C. After the plate was confluent, the old media was removed and fresh media was added containing compound **35a** (50 uM). The cells were incubated with compound for 1 h at 37 ^{o}C. Next, the cells were scraped off and centrifuged to form a pellet. The pellet formed was re-dissolved in PBS (1X) and centrifuged. The pellet was re-suspended in 200 μL of MeOH and vortexed vigorously to lyse the cells. The cell lysate was again centrifuged and the supernatant was injected into HPLC after filtration.

4.2.4.4. Protection against oxidative stress:

Human colon adenocarcinoma cells DLD-1 were seeded in a 96-well plate with 10^4 cells/well in RPMI media supplemented with 10% FBS (fetal bovine serum) and 1% antibiotic solution and incubated in an atmosphere of 5% CO_2 at 37 °C for 16 h. Stock solutions of compounds were prepared in RPMI with final concentration of DMSO not exceeding 0.5%. After 16 h, the cells were co-treated with different concentrations of the compound and JCHD (15 μM). The cells were incubated for 24 h at 37 °C. The media was removed after 24 h and the cells were treated with 3-(4, 5-dimethylthiazol-2-yl)-2, 5-diphenyl tetrazolium bromide (MTT) at a concentration of 0.5 mg/mL. A stock solution of MTT was prepared by dissolving 3.5 mg in 7 mL RPMI media and 100 mL of this stock was added to each well. After incubating at 37 °C for 4 h, the media was carefully removed and 100 μL of DMSO was added to each well. Absorbance at 570 nm was recorded using a microplate reader (Thermo Scientific Varioskan) to estimate the cell viability.[14]

4.2.5. Spectra:

^{1}H NMR (DMSO-d6, 400 MHz) of compound **35a**

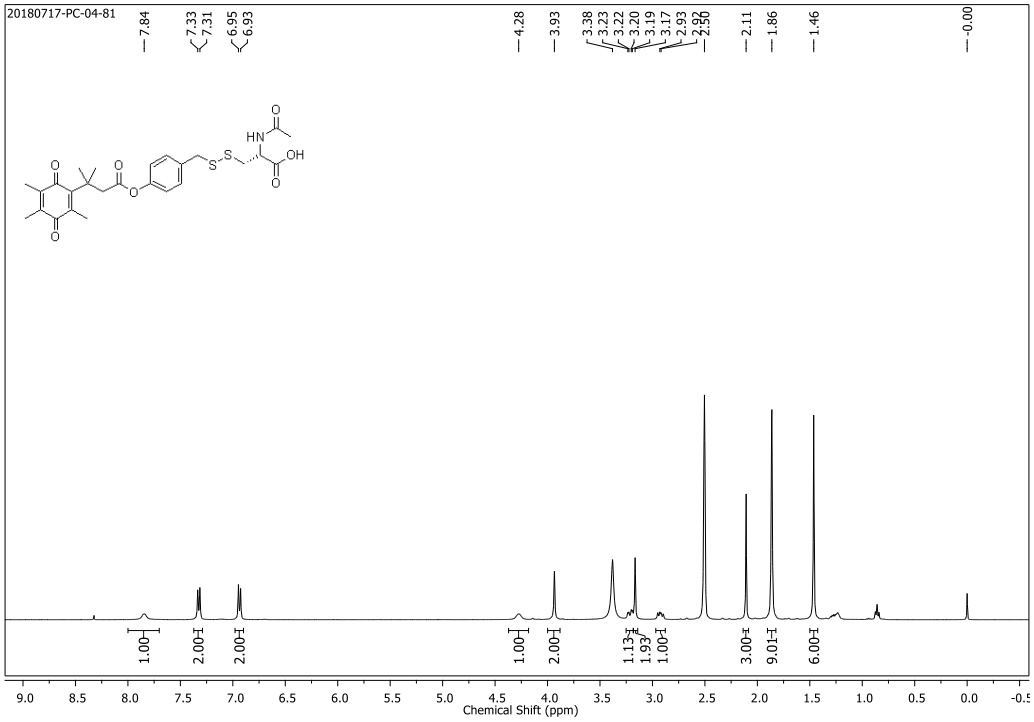

^{13}C NMR (DMSO-d6, 100 MHz) of compound **35a**

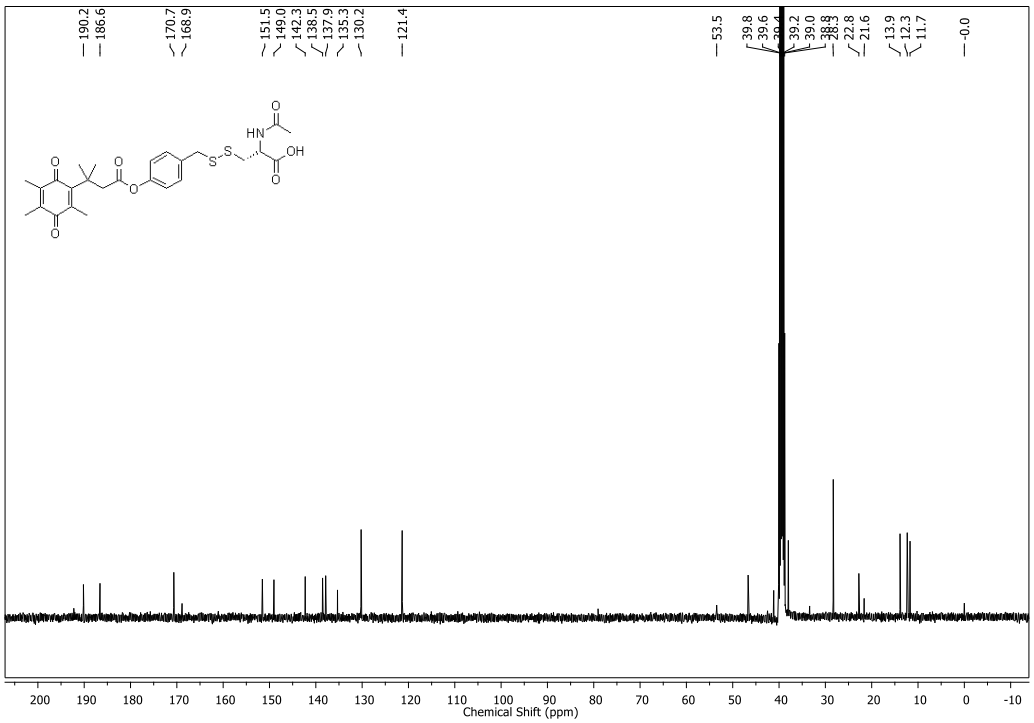

^{1}H NMR ($CDCl_3$, 400 MHz) of compound **35b**

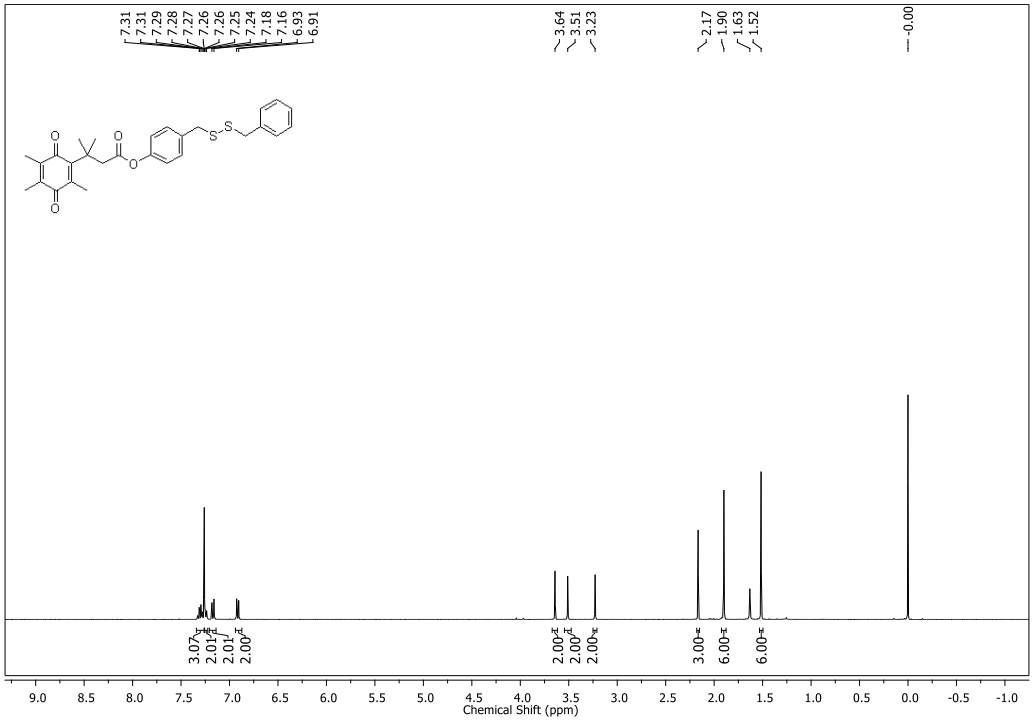

^{13}C NMR ($CDCl_3$, 100 MHz) of compound **35b**

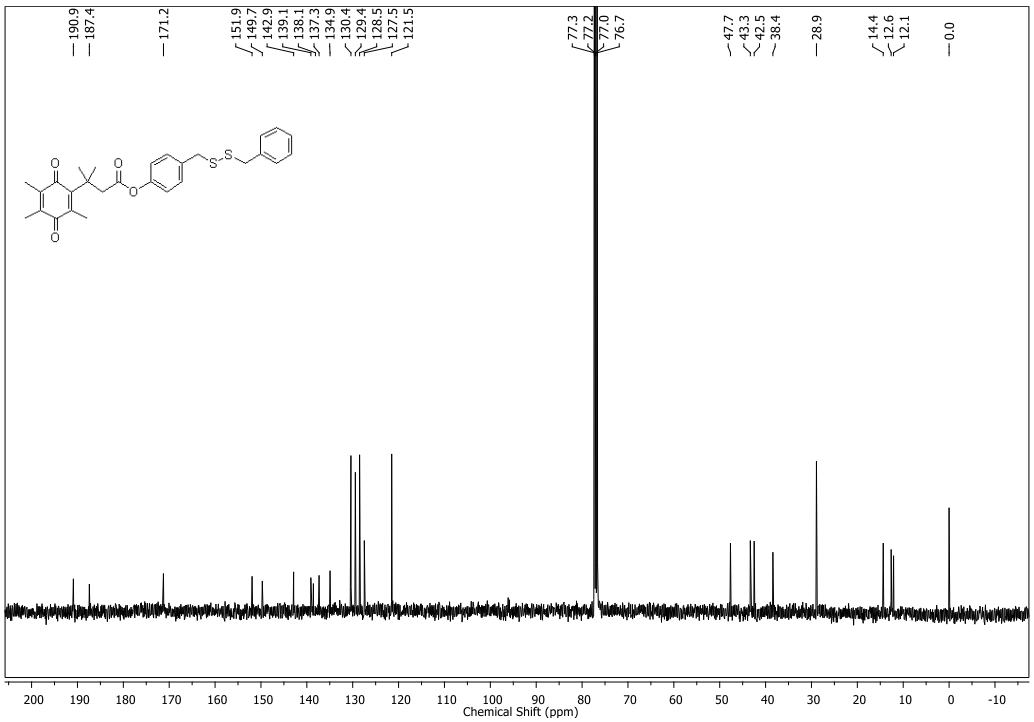

4.2.6. References:

(1) Bora, P.; Chauhan, P.; Pardeshi, K. A.; Chakrapani, H. *RSC Adv.* **2018**, *8*, 27359.

(2) Filipovic, M. R.; Zivanovic, J.; Alvarez, B.; Banerjee, R. *Chem. Rev.* **2018**, *118*, 1253.

(3) Vandiver, M. S.; Paul, B. D.; Xu, R.; Karuppagounder, S.; Rao, F.; Snowman, A. M.; Ko, H. S.; Lee, Y. I.; Dawson, V. L.; Dawson, T. M.; Sen, N.; Snyder, S. H. *Nat. Commun.* **2013**, *4*, 1626.

(4) Paul, B. D.; Snyder, S. H. *Nat. Rev. Mol. Cell Biol.* **2012**, *13*, 499.

(5) Zhang, D.; Macinkovic, I.; Devarie-Baez, N. O.; Pan, J.; Park, C.-M.; Carroll, K. S.; Filipovic, M. R.; Xian, M. *Angew. Chem. Int. Ed. Engl.* **2014**, *53*, 575.

(6) Mishanina, T. V.; Libiad, M.; Banerjee, R. *Nat. chem. biol.* **2015**, *11*, 457.

(7) Yadav, P. K.; Martinov, M.; Vitvitsky, V.; Seravalli, J.; Wedmann, R.; Filipovic, M. R.; Banerjee, R. *J. Am. Chem. Soc.* **2016**, *138*, 289.

(8) Ida, T.; Sawa, T.; Ihara, H.; Tsuchiya, Y.; Watanabe, Y.; Kumagai, Y.; Suematsu, M.; Motohashi, H.; Fujii, S.; Matsunaga, T.; Yamamoto, M.; Ono, K.; Devarie-Baez, N. O.; Xian, M.; Fukuto, J. M.; Akaike, T. *Proc. Natl. Acad. Sci. U. S. A.* **2014**, *111*, 7606.

(9) Kang, J.; Xu, S.; Radford, M. N.; Zhang, W.; Kelly, S. S.; Day, J. J.; Xian, M. *Angew. Chem. Int. Ed.* **2018**, *57*, 5893.

(10) Park, C.-M.; Johnson, B. A.; Duan, J.; Park, J.-J.; Day, J. J.; Gang, D.; Qian, W.-J.; Xian, M. *Org. Lett.* **2016**, *18*, 904.

(11) Zheng, Y.; Yu, B.; Li, Z.; Yuan, Z.; Organ, C. L.; Trivedi, R. K.; Wang, S.; Lefer, D. J.; Wang, B. *Angew. Chem. Int. Ed.* **2017**, *56*, 11749.

(12) Yuan, Z.; Zheng, Y.; Yu, B.; Wang, S.; Yang, X.; Wang, B. *Org. Lett.* **2018**, *20*, 6364.

(13) Powell, C. R.; Dillon, K. M.; Wang, Y.; Carrazzone, R. J.; Matson, J. B. *Angew. Chem. Int. Ed.* **2018**, *57*, 6324.

(14) Bora, P.; Chauhan, P.; Manna, S.; Chakrapani, H. *Org. Lett.* **2018**, *20*, 7916.

(15) Biscans, A.; Rouanet, S.; Vasseur, J.-J.; Dupouy, C.; Debart, F. *Org. Biomol. Chem.* **2016**, *14*, 7010.

Synopsis

Towards Targeted and Tunable Release of Hydrogen Sulfide

Chapter 1: Introduction

Hydrogen sulfide (H_2S) has emerged as an important gaseous signaling molecule along with nitric oxide (NO) and carbon monoxide (CO). H_2S is now known to play a critical role in human health and disease. Endogenous production of H_2S from cysteine and homocysteine, largely depends on the activity of three enzymes – cystathionine-β-synthase (CBS), cystathionine-γ-lyase (CSE) and 3-mercaptopyruvate sulfur transferase (3-MST) (Figure 1). Endogenously produced H_2S regulates the homeostasis of various physiological functions like neuronal, cardiovascular, gastrointestinal, renal etc. The increased physiological relevance of H_2S makes it a potent therapeutic agent. Both endogenous and exogenous administration of H_2S has shown protective effects against diseases like myocardial ischemia injury, neuronal or gastrointestinal disorders suggesting that modulating the levels of H_2S within cells has tremendous impact on disease biology. [1-4]

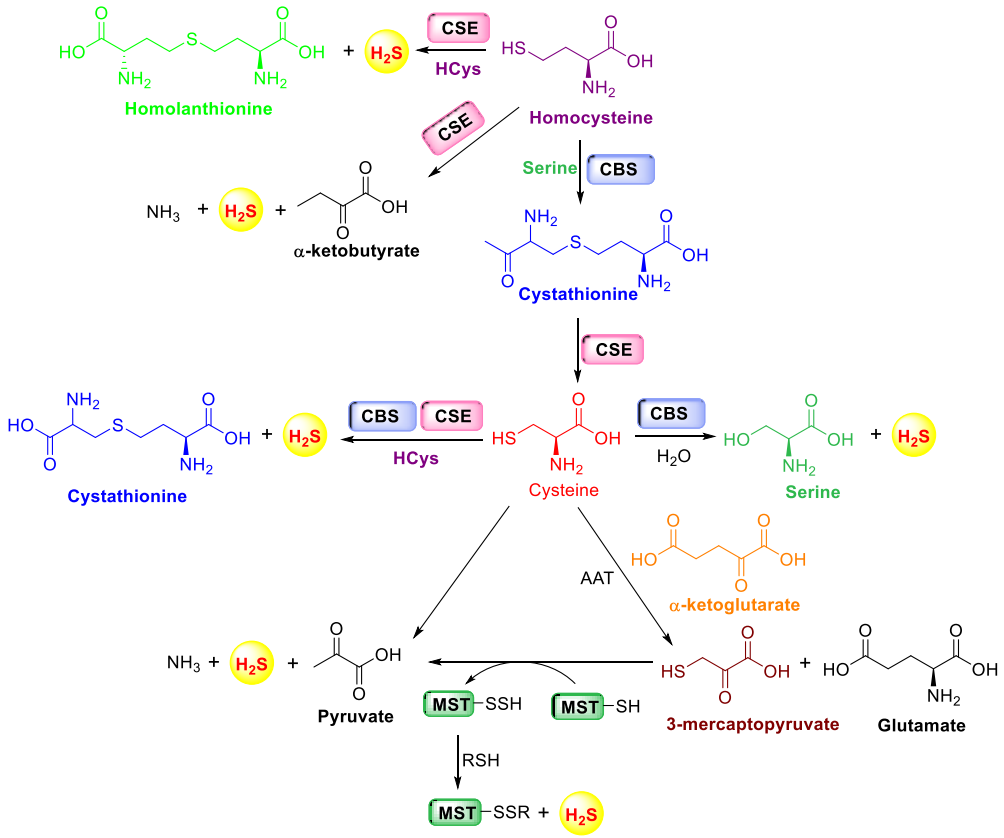

Figure 1. Biosynthesis of H_2S.

H_2S maintains the redox homeostasis of various systems in the human body which include neuronal, cardiovascular, respiratory, renal, gastrointestinal, liver and reproductive systems.[1,2] Lipid soluble nature of H_2S allows easy diffusion through the plasma membrane to reach its molecular targets either on the plasma membrane, cytosol or any intracellular organelle.[3] The ubiquitous nature of this gasotransmitter underscores a wide range of physiological roles played by H_2S (Figure 2). The vasodilatory effects of H_2S are attributable to the activation of ATP sensitive potassium (K_{ATP}) channels through persulfidation of the Cys6 and Cys26 residues of the sulfonylurea receptor 1 (SUR1) subunit of K_{ATP} channel complex.[1,5] H_2S forms a part of the anti-oxidant machinery of a cell and thus helps in maintaining the redox homeostasis. Persulfidation of Cys151 residue of Kelch-like ECH- associated protein 1 (KEAP1) initiates the dissociation of nuclear factor erythroid 2-related factor 2 (NRF2) from KEAP1. NRF2 is then translocated to the nucleus where it binds to the antioxidant response element (ARE) and increases the transcription of anti-oxidant genes such as NQO1, HO-1, or GST. This leads to an increase in the glutathione (GSH) levels which is likely responsible for the beneficial effects of H_2S.[6]

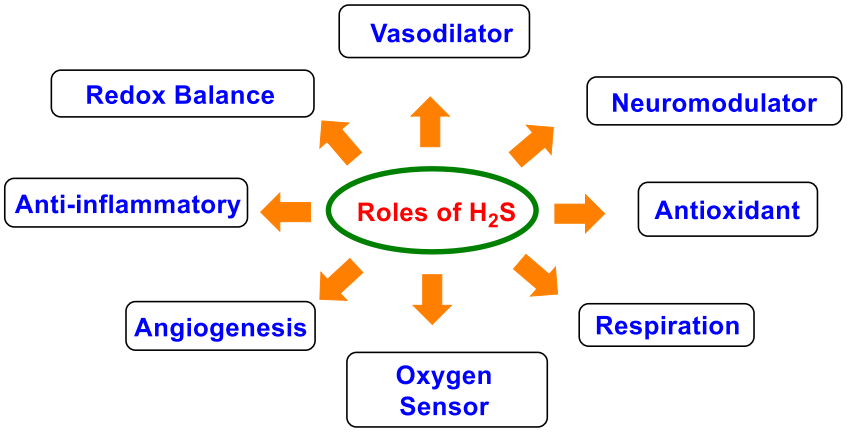

Figure 2. Physiological roles of H_2S.

H_2S has a tremendous impact on disease biology. Various diseases such as cardiovascular, endocrinal, neurodegenerative disorders, gastrointestinal diseases or liver diseases, etc are associated with an abnormal decrease in the endogenous levels of H_2S. Thus, exogenous administration of H_2S has shown beneficial effects under these conditions. For example, Parkinson's disease (PD) is a neurodegenerative disorder associated with elevated levels of reactive oxygen and nitrogen species.

Nitrosylation of cysteine residues of parkin inactivates its catalytic activity thereby leading to Parkinson's disease.[7,8] Exogenous administration of H_2S under such condition, induces persulfidation of the cysteine residues of parkin which re-instates its activity and thus acts as a neuroprotective agent (Figure 3). Beneficial roles of H_2S in rodent models of PD have also been demonstrated previously.[9-11] This forms an important example of H_2S based therapeutics.

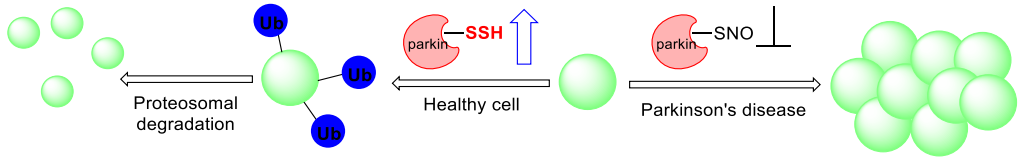

Figure 3. Persulfidation in a model of Parkinson's disease.

However, the therapeutic effects of H_2S largely depend on the concentration and the rate of release. For example, H_2S exerts both pro and anti-inflammatory effects depending on the rate of release.[12]. P.K. Moore and co-workers have demonstrated the effects of the rate of release of H_2S in a model of inflammation. NaSH, fast releasing H_2S donor, showed pro-inflammatory effects by increasing the production of pro-inflammatory cytokines. On the other GYY4137, a slow releasing H_2S donor showed opposite effects against LPS induced inflammation in RAW macrophages. The apparent discrepancy is a testament to the pro- *versus* anti-inflammatory effects of H_2S (Figure 4).[13]

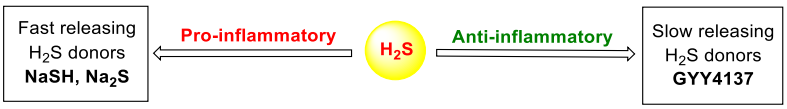

Figure 4. Pro and anti-inflammatory effects of H_2S.

The role of H_2S in diseases such as cancer is also controversial with both pro- and anti-cancer effects reported. However, Moore and co-workers have shown that treating cancer cells with relatively higher concentrations of H_2S leads to uncontrolled intracellular acidification which suppresses the growth of cancer cells and thus induces cell cycle arrest followed by apoptosis.[14,15] With growing therapeutic importance of H_2S, methodologies to achieve controlled generation and dissipation of H_2S assume utmost importance. Due to its gaseous nature, controlled and site directed delivery of H_2S is challenging. Delivery of gaseous species can be achieved by

masking them in the form of inorganic or organic compounds which dissociate to generate the gas. These molecules are known as 'H_2S donors' and can be broadly classified into three categories – naturally occurring H_2S donors, hydrolysis based H_2S donors and triggerable H_2S donors. Naturally occurring donors are organic polysulfides such as diallyl sulphide (DAS), diallyl disulfide (DADS) and diallyl trisulfide (DATS) which release H_2S upon reaction with thiols. Non-triggerable donors include NaSH, GYY4137, ADT-OH or Lawesson's reagent. Spontaneous release of H_2S from these donors and lack of appropriate negative controls limits their use. Triggerable donors include thiol activated donors, light activated donors, enzyme activated donors or pH controlled release of H_2S. However, none of the aforementioned donors are capable of achieving site directed delivery of H_2S. Also, modulating the rate of H_2S after activation by an external stimulus still remains a challenge (Figure 5).

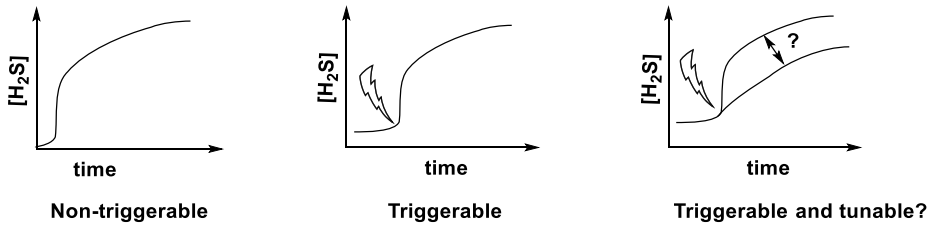

Figure 5. Categories of H_2S donors

Nitroreducatse (NTR) activated gem-dithiol based H_2S donors have been reported by our group to achieve bacteria targeted delivery of H_2S. The role of H_2S in antibiotic resistance has been studied using these donors. The nitrobenzyl group upon reduction by NTR forms an intermediate **A** which further dissociates to form geminal dithiol **B**. The gem-dithiol so formed readily hydrolysis to release 2 moles of H_2S (Scheme 1).[16]

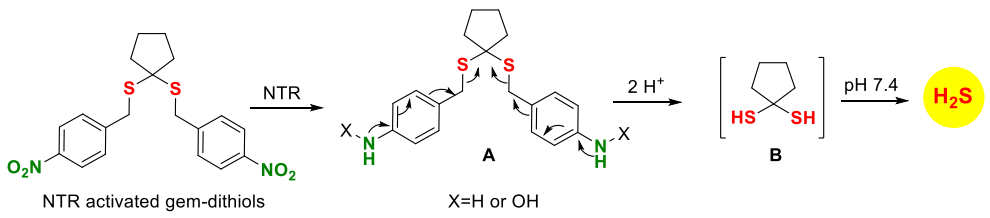

Scheme 1. Nitroreductase (NTR) activated gem-dithiol based H_2S donors

Using this strategy, we proposed to synthesize ROS activated H_2S donors by replacing nitro group with boronate ester.[17] It was hypothesised that boro-gem dithiol would

react with H_2O_2 to release an intermediate **C** which would further undergo fragmentation to release 2 moles of H_2S. However, intermediate **C** was found to be stable in buffer and no further dissociation to release H_2S was observed (Scheme 2). The stability of intermediate **C** was attributable to the poor leaving group ability of thiols due to which affects the cleavage of C-S. Also, high electronegativity of 'O' compared to 'N' might hinder the process of delocalisation of electrons to release thiol. Thus, both the reasons could contribute to the inefficient release of H_2S from boro-gem dithiol based H_2S donors.

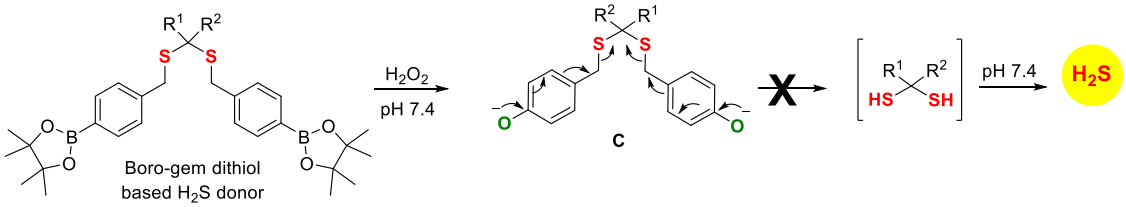

Scheme 2. ROS activated gem-dithiol based H_2S donor

Thus based on the results obtained, the strategy to release H_2S was modified. In order to facilitate the process of thiol release via cleaving of the C-S bond, we propose to decrease the pK_a of the thiol which could increase its leaving group ability. In the second approach, we propose to introduce a self immolative linker which would allow the formation of intermediate **A** and thus, enable the release of 2 moles of H_2S in the presence of ROS (Scheme 3).

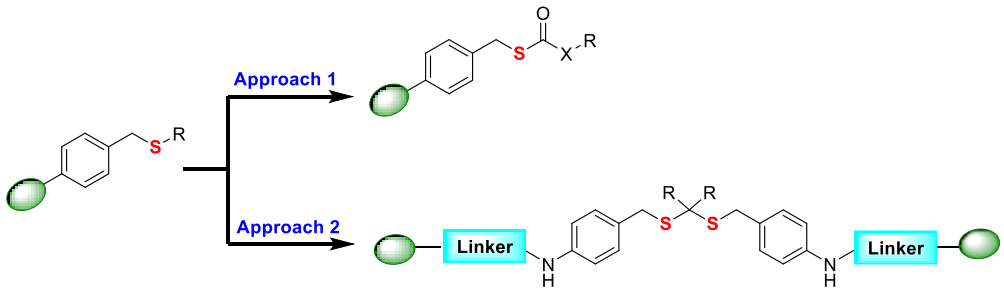

Scheme 3. Two approaches for H_2S delivery.

In approach 1, we designed scaffolds by fixating carbonyl group next to 'SH' with 'X' as a leaving group. The scaffolds are termed as carbonothioates with alcohols as leaving group(X = O) and carbamothioates (X = NH) for amines as leaving group. The proposed mechanism of H_2S release from the scaffolds is as follows: compound

upon activation by an external stimulus releases an intermediate **I** which further dissociates to release carbonyl sulfide (COS) gas and the leaving group alcohol (X = O) or amine (X = NH) (Scheme 4)**.**

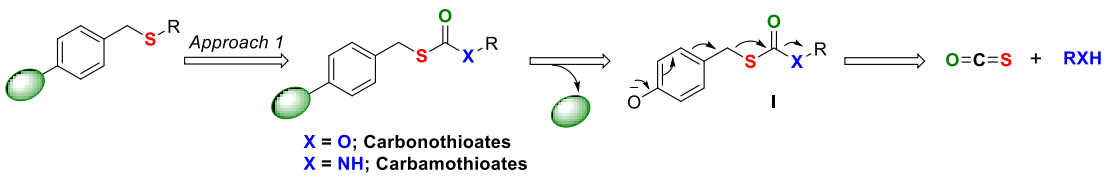

Scheme 4. Proposed mechanism of COS release from approach 1.

Carbonyl sulfide (COS) thus formed is readily hydrolysed to H_2S by the action of carbonic anhydrase (CA), a widely prevalent enzyme in a mammalian system (Scheme 5).[18] Thus, COS produced from dissociation of carbonothioates or carbamothioates can act as surrogate for H_2S release.

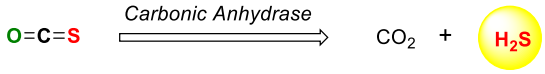

Scheme 5. COS is hydrolysed to H_2S by carbonic anhydrase.

In **chapter 2**, esterase activated carbonothioates and carbamothioates based H_2S donors are presented. Esterase is considered for the preliminary studies due to the wide occurrence of the enzyme in nearly all the cells which would be useful in understanding the biology of H_2S. Esterase cleaves the ester bond to release an intermediate which further dissociates to generate COS and a leaving group. COS produced is further hydrolysed to H_2S.The nature of the leaving group X may affect the release of COS and hence could modulate the rate of H_2S release. In **chapter 3.1**, ROS triggered COS/H_2S delivery is proposed. Amine is fixed as the leaving group in this series for modulating the release of H_2S. The versatility of the scaffold is demonstrated by conjugating it with a non-steroidal anti-inflammatory drug (NSAID) for the delivery of H_2S-NSAID hybrid donors. In **chapter 3.2**, we propose to follow approach 2 to achieve ROS triggered delivery of H_2S with increased payload of the gaseous species. The scaffold allows the release of two moles of H_2S per mole of the donor and therefore can be utilized to study the anti-cancer effects of H_2S. In **chapter 4.1**, colon targeted delivery of H_2S and H_2S-NSAID hybrid donors is proposed by using NAD(P)H quinone oxidoreductase (NQO1) as a trigger. NQO1 is a 2 e^- reducing cytosolic enzyme which reduces quinones to hydroquinones. Thus,

bioreductively activated H_2S and H_2S-mesalamine hybrid molecules for targeted delivery towards colon are prepared. Finally, in **chapter 4.2**, the effect of pK_a of thiols on their leaving group ability is further investigated. Perthiols or persulfides (RSSH) are biologically relevant reactive sulfur species containing each sulfur in -1 oxidation state. H_2S forms cysteine persulfides as a part of its signalling mechanism. The lower bond dissociation energy of S-H bond in perthiols (70 kcal mol^{-1}) compared to corresponding thiol (92 kcal mol^{-1}) makes them more acidic than their corresponding thiols. Thus, the pK_a of perthiols is approximately 2 units lower than thiols.[3] Therefore, ability of the scaffold to release persulfides is elucidated in the final chapter.

Chapter 2: Esterase activated COS/H_2S donors:

In chapter 2 esterase activated COS/H_2S donors were synthesized using approach 1. Esterase was used as a trigger for the preliminary studies to establish the release of COS from carbonothioates (X = O) and carbamothioate (X = NH) based scaffolds. The nature of leaving group X would determine the release of H_2S. Esterase hydrolysis the ester bond followed by a rapid release of formaldehyde to form intermediate **I**. The intermediate further dissociates to generate COS which is hydrolysed to produce H_2S by carbonic anhydrase (CA) (Scheme 6).

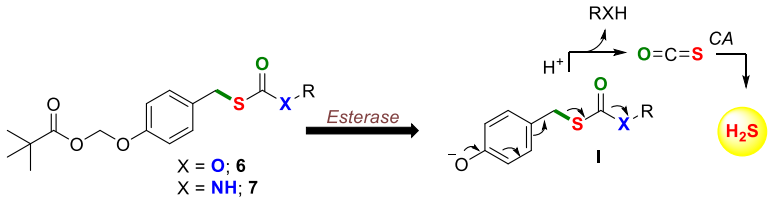

Scheme 6. Proposed mechanism for esterase activated COS/H_2S donors.

Six donors were synthesized in this series with varying pK_a values. The three carbonothioates that were synthesized had following leaving groups: compound **6a** was synthesized with *p*-nitrophenol as a leaving group; compound **6b** had phenol as a leaving group and compound **6c** had benzyl alcohol as a leaving group. In case of carbamothioates, compound **7a** had aniline as a leaving group, **7b** had *p*-anisidine as a leaving group and compound **7c** had benzyl amine as leaving group.

First the production of COS from the scaffolds was elucidated using mass spectrometry. Compound **6a** upon incubation with esterase (ES) showed a mass peak

corresponding to the protonated form of COS (Figure 6). This was in accordance with the previous reports.[19]

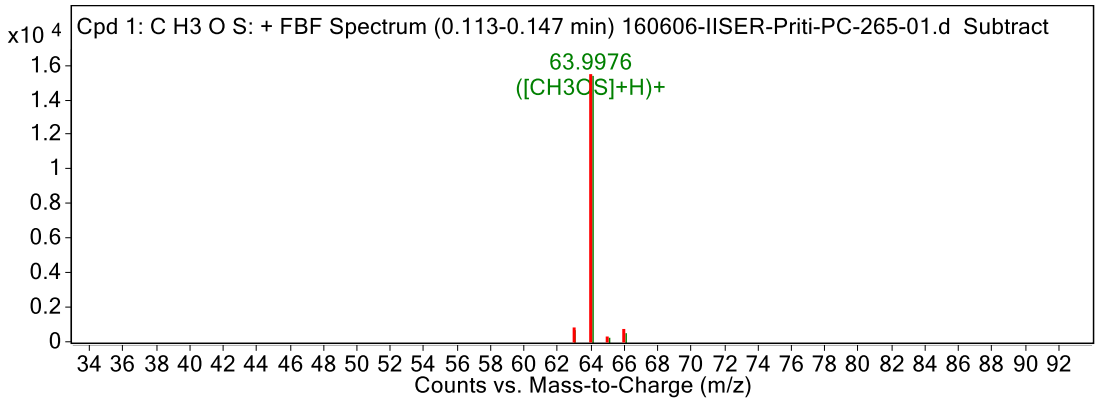

Figure 6. Detection of COS by mass spectrometry.

The compounds were tested for their ability to produce H_2S using dansyl azide as H_2S selective probe. Dansyl azide (Dn-N_3) reacts with H_2S to form dansyl amine (Dn-NH_2) which is fluorescent. All the compounds showed a signal corresponding to the formation of Dn-NH_2 (excitation 340 nm, emission 535 nm) in the presence of esterase and CA. No signal for Dn-NH_2 formation was observed with compound **4** which lacked the ability to produce COS (Figure 7).

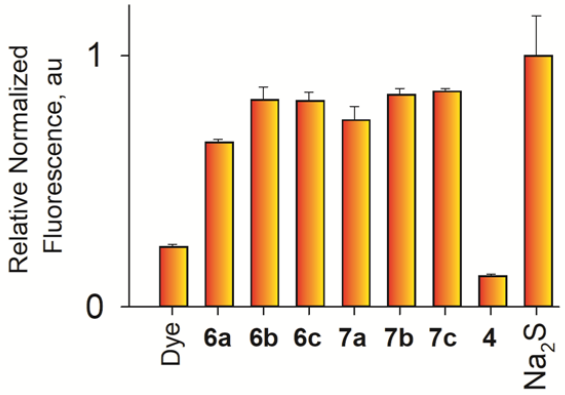

Figure 7. Detection of H_2S from esterase sensitive COS/H_2S donors using Dn-N_3.

The generation of H_2S from the reported scaffolds was also evaluated using independent techniques such as lead acetate paper test, sulfide selective electrode and methylene blue assay.

H_2S formation from compound **6a** was monitored using sulfide selective electrode. Compound **6a** was incubated with CA in buffer (pH 7.4) at 37 ^{o}C. A significant

increase in the current corresponding to the formation of H_2S was observed upon addition of ES (marked by the arrow) (Figure 8).

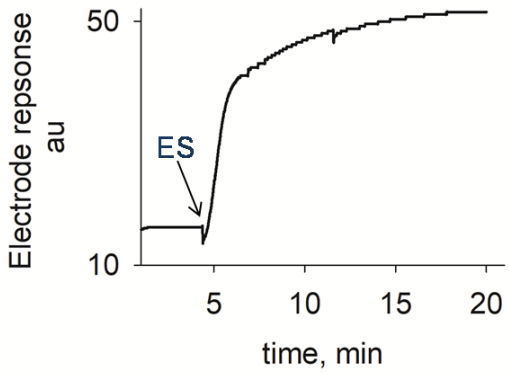

Figure 8. Detection of H_2S using sulfide selective electrode from compound **6a**.

Next, the kinetics of H_2S release from carbonothioates was monitored using Dn-N_3 based fluorescent method. Although the difference in the pK_a values of the leaving groups was significant, yet the differences in the rates of H_2S release from the carbonothioates were not found to be significant in magnitude. This was possibly because of the instability of carbonothioate core towards ES which cleaves it to give free thiol which also reduced Dn-N_3 to Dn-NH_2. Thus, carbonothioates were incapable of modulating the rate of release of H_2S.

Table 1. Rates of H_2S production from carbonothioates (**6a - 6c**) using Dn-N_3 method.

Compd	R	k, min^{-1}	Rel. Rate	pK_a
6a	4-NO_2Ph	0.042	1	7.2
6b	Ph	0.040	0.95	9.9
6c	$PhCH_2$	0.039	0.93	14.4

Next, the kinetics of H_2S release was monitored with carbamothioate scaffolds using Dn-N_3 based method. Compounds were incubated with ES, CA and Dn-N_3 in pH 7.4 buffer at 37 ^oC. The formation of Dn-NH_2 was followed at excitation 340 nm and emission 535 nm. Compounds **7a** (aniline as leaving group, pK_aH = 4.6) and **7b** (*p*-anisidine as leaving group, pK_aH = 5.2) showed a similar rate of H_2S production, however, compound **7c**, with benzyl amine as a leaving group (pK_aH = 9.1) showed a

slightly decreased rate of H_2S release (Figure 9, Table 2). This suggested that basicity of amine was playing a role in modulating the rate of generation of H_2S. This laid a strong foundation to further investigate the effect of basicity of amine on the rate of H_2S production.

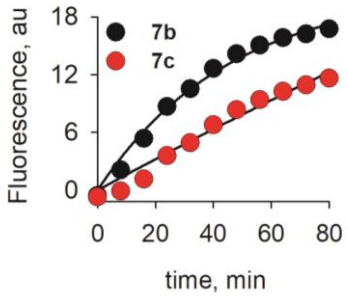

Figure 9. H_2S release profile for compounds **7b** and **7c** using Dn-N_3 probe.

Table 2. Rates of H_2S production from carbamothioates (**7a** - 7**c**) using Dn-N_3 method.

Compd	R	k, min^{-1}	Rel. Rate	pK_aH
7a	Ph	0.031	0.97	4.6
7b	4-OMePh	0.032	1	5.2
7c	$PhCH_2$	0.014	0.44	9.1

The observed difference in the rates of H_2S release from compound **7b** and **7c** were confirmed by HPLC analysis where decomposition of the intermediate formed after the reaction of compounds with ES was followed. Also, the rate of generation of H_2S from **7b** and **7c** was monitored using methylene blue assay. The formation of methylene blue complex was monitored by measuring the absorbance at 676 nm. Compounds were treated with ES and CA at 37 ^oC in buffer. An aliquot of the reaction mixture was treated with methylene blue reagents (*N*,*N*-*p*-phenylene diamine, $FeCl_3$) and the absorbance was measured at 676 nm. Compound **7b** showed a saturation of signal for H_2S released after 1 h of incubation whereas the signal for H_2S release from compound **7c** continuously increased for a period of 4 h. This clearly indicated that the rate of H_2S release can be tuned using carbamothioate based scaffolds. Also, the scaffold can be utilised for the delivery of H_2S-drug hybrids.

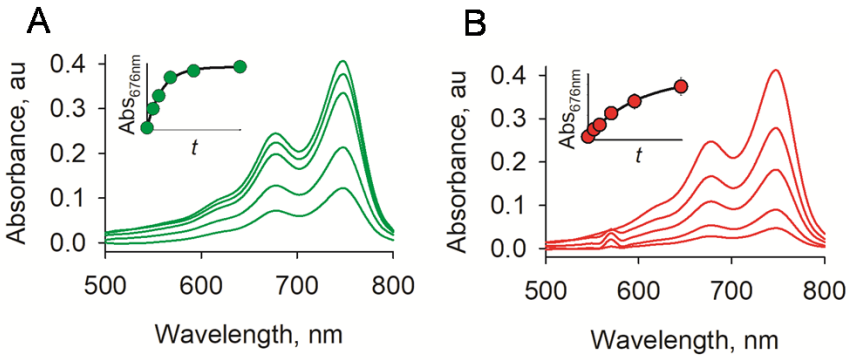

Figure 10. a) Methylene blue profile for compound **7b** obtained over a period of 4 h at different time intervals – 15 min, 30 min, 60 min, 120 min and 240 min. b) Methylene blue profile obtained for compound **7c** over a period of 4 h.

Finally, the compounds were tested for cytotoxicity in human breast cancer, MCF-7 cells for 24 h using standard MTT assay. Compounds were found to be well tolerated by cells at 50 µM concentration. Also, the ability of the donors to produce H_2S within cells was evaluated using NBD-Fluorescein, a H_2S selective probe. A dose dependent increase in the fluorescent signal corresponding to the release of H_2S was observed upon incubating MCF-7 cells with compound **7b** (Figure 11).

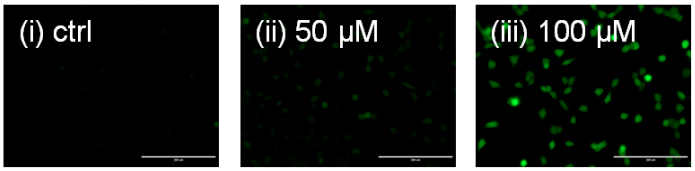

Figure 11. Cell Viability assay for cytotoxicity of H_2S donor motifs in MCF-7 cells.

CHAPTER 3.1: ROS triggered COS/H_2S donors for targeted and tunable release

Most of the diseases such as cardiovascular, neuronal, gastrointestinal or inflammation, are associated with increased levels of reactive oxygen species (ROS). H_2S is a part of the anti-oxidant machinery of a cell and therefore achieving ROS triggered delivery of H_2S may have beneficial effects.[1,4] However, the therapeutic role of H_2S largely depends on the concentration and the rate at which it is produced.[20] For example, the rate at which H_2S is released monitors the anti-inflammatory effects of H_2S. Fast releasing H_2S donor (NaSH) shows pro-inflammatory effects whereas a slow releasing H_2S donors (GYY4137) shows anti-inflammatory response.[13] Therefore, tools to understand the complex effects of H_2S on inflammatory responses are needed. In chapter 3.1, we propose to design ROS activated COS/H_2S donors with

tunable release of H_2S. Based on the results obtained in chapter 2, we propose to use carbamothioates for obtaining tunable release of H_2S. Boronate ester is used as a trigger for ROS activated delivery of H_2S. It is proposed that compounds upon activation by H_2O_2 release an intermediate which further dissociates to release COS. In this chapter we establish that the release of COS is dependent on the basicity of the amine group.

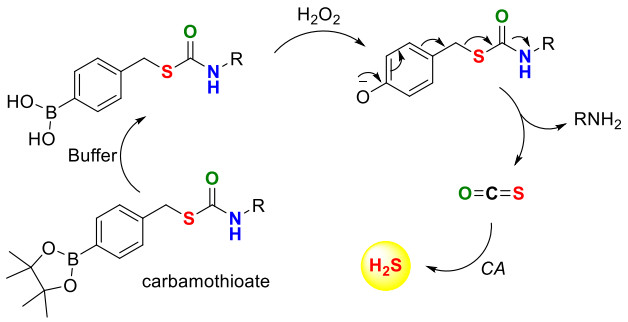

Scheme 7. ROS triggered delivery of COS/H_2S donors

ROS activated carbamothioate based COS/H_2S donors were synthesized in this series with varying pK_aH values of the amines (Figure 12).

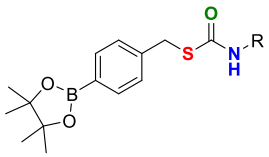

13a; R = (3-COOMe)Ph
13b; R = 4-OCH_2CH_2OHPh
13c; R = (4-OMe)Ph
13d; R = (4-NO_2)$PhCH_2$
13e; R = 4-(O-Propargyl)-$PhCH_2$
13f; R = $PhCH_2$
13g; R = $CH_3CH_2CH_2$

Figure 12. ROS activated COS/H_2S donors

Next, the kinetics of H_2S release was monitored using methylene blue assay. Compounds were incubated with H_2O_2 (10 eq) and CA in buffer (pH 7.4, 10 µM DTPA) at 37 ^oC. An aliquot of the reaction mixture was removed and treated with methylene blue reagents for 30 min followed by measuring the absorbance at 676 nm. Compound **13a** with pK_aH value of 4.75 was found to have faster rate of H_2S production compared to compound **13g** with pK_aH value of 10.53 (Figure 13).

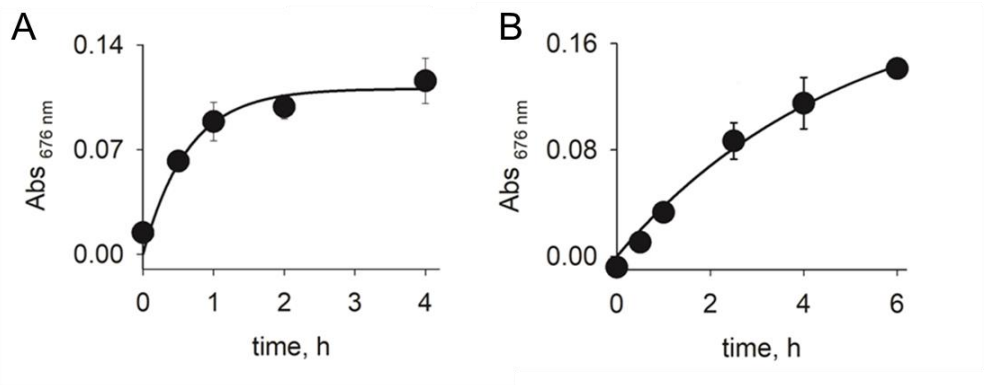

Figure 13. Representative H_2S release plots using methylene blue assay. a) H_2S release plot for compound **13a**. b) H_2S release plot for compound **13g**.

The relative rates of the H_2S generation were calculated with compound **13c** as the fastest donor (Table 3). All the aniline based donors (**13a-13c**) with lower pK_aH values were found to have faster rate of H_2S generation compared to benzyl amine based donors (**13d-13f**). Compound **13g** with propylamine as the leaving group showed lowest relative rate of H_2S generation. Thus, the compounds reported herein, can vary the half-lives of H_2S generation from 24 min to 204 min.

Table 3. Rates of H_2S generation from compounds **13a-13g**.

entry	compd	pK_aH	k, min^{-1}	$t_{1/2}$, min	relative rate
1.	**13a**	4.75	0.026	26.7	0.90
2.	**13b**	5.03	0.017	40.8	0.59
3.	**13c**	5.34	0.029	23.9	1.00
4.	**13d**	8.36	0.004	173.3	0.14
5.	**13e**	9.18	0.0045	154.0	0.16
6.	**13f**	9.34	0.0049	141.4	0.17
7.	**13g**	10.53	0.0034	203.8	0.12

A good correlation was observed when the obtained relative rates were plotted against the pK_aH values of the amines into a linear regression analysis (Figure 14). This suggested the rate of generation of H_2S from carbamothioates can be monitored by varying the basicity of the amines.

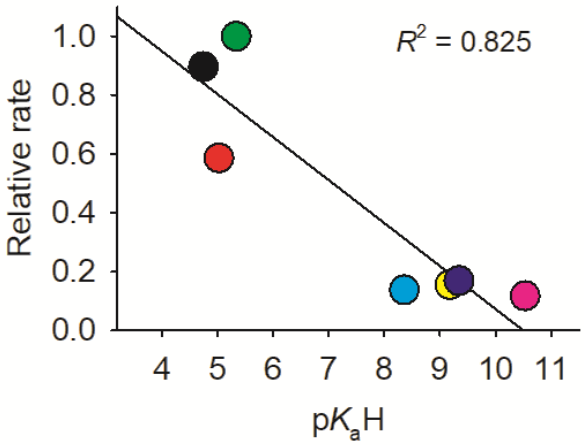

Figure 14. Linear regression analysis of pK_aH of amines v/s observed relative rates.

Next the mechanism of H_2S release from the proposed carbamothioate scaffolds was elucidated. It is assumed that compounds upon incubation in buffer is hydrolysed to form boronic acids. Boronic acids formed could react with H_2O_2 and follow two pathways for the release of COS. In pathway 1, intermediate **I** formed could further decompose to release an intermediate **II** which in turn dissociates to release COS. Another possibility is the release of COS from intermediate **I** by following a concerted pathway (Scheme 8).

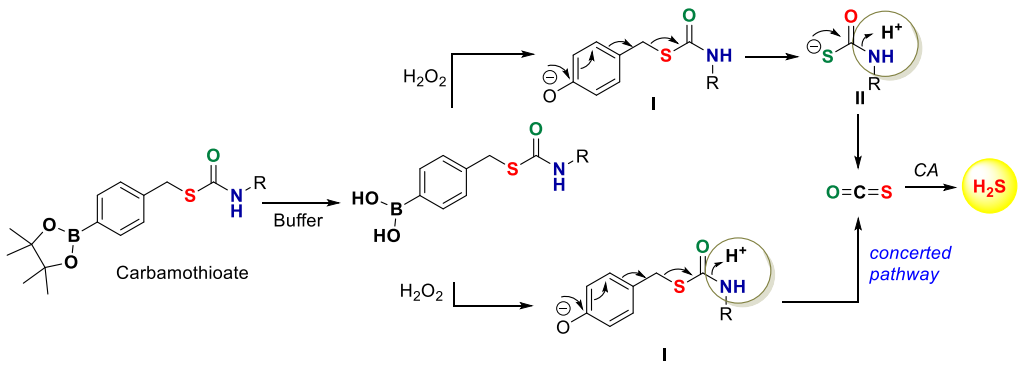

Scheme 8. Possible pathways of release of COS from ROS activated H_2S donors.

In order to differentiate between the possible pathways, we followed the decomposition of compound **13g** in DMSO:D_2O mixture in the presence of H_2O_2 using ^{1}H NMR. Compound reacted with H_2O_2 to form phenolate intermediate **I** (Scheme 9). A complete conversion to the intermediate **I** was observed within 30 min of incubation which remained intact even after 30 h of incubation. No peaks

corresponding to the formation of free *p*-hydroxybenzyl alcohol or propylamine were observed in the NMR spectrum (Figure 15).

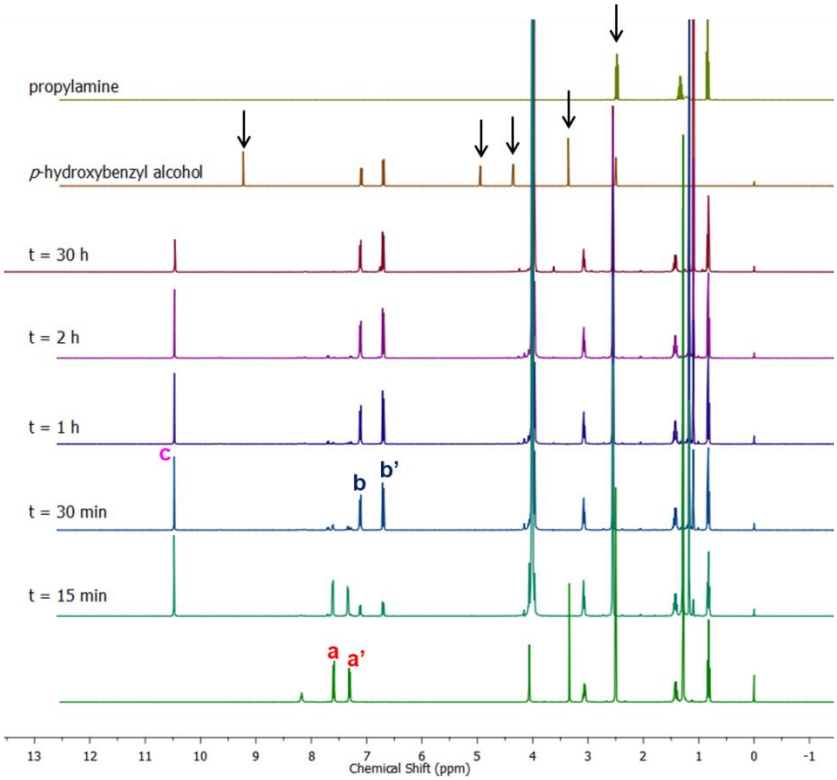

Figure 15. ^{1}H NMR experiment to follow the decomposition of compound **13g**.

This suggested that the decomposition of intermediate **I** determined the rate of H_2S release. Also, the formation and dissipation of intermediate was followed using HPLC from decomposition of compound **13g** suggesting that the intermediate has UV absorbance properties. Collectively, the data suggested that the intermediate **I** was formed after the reaction of compounds with H_2O_2 which further decomposed to release COS.

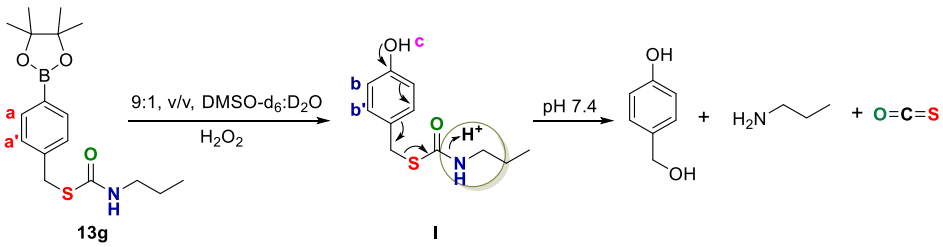

Scheme 9. Proposed mechanism of decomposition of compound **13g**.

Finally, the release of H_2S-NSAID hybrid donor was demonstrated using carbamothioate scaffold. Mesalamine is a clinically used drug for the treatment of

colitis. Therefore, the amine functionality of methyl ester derivative of mesalamine was conjugated to give ROS activated H_2S-NSAID hybrid donor, **18**. The release of H_2S from compound **18** in the presence of H_2O_2 was monitored by methylene blue assay (Figure 16). The pseudo first order rate constant of the H_2S release was calculated which was found to follow the trend of linear regression analysis.

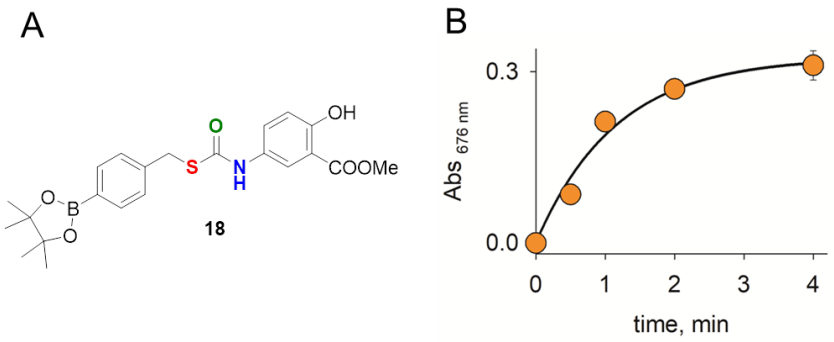

Figure 16. H_2S release from compound **18** (H_2S-NSAID hybrid donor) using methylene blue assay.

CHAPTER 3.2: ROS activated gem-dithiol based H_2S donors

In chapter 3.2, approach 2 was tested to demonstrate the release of H_2S from gem dithiol based scaffolds. The role of H_2S in cancer has been controversial with both pro and anti-cancer effects reported. However, recent reports suggest that increasing the concentration of H_2S within cells can induce apoptosis by increasing intracellular acidification. Thus, achieving cancer targeted delivery with increased payload of H_2S would be useful.

Previous experiments resulted in the hypothesis that intermediate **A** decomposes to give 2 moles of H_2S via formation of intermediate **B**. However, intermediate **C** was found to be stable under these conditions and did not produce H_2S (Scheme 10).

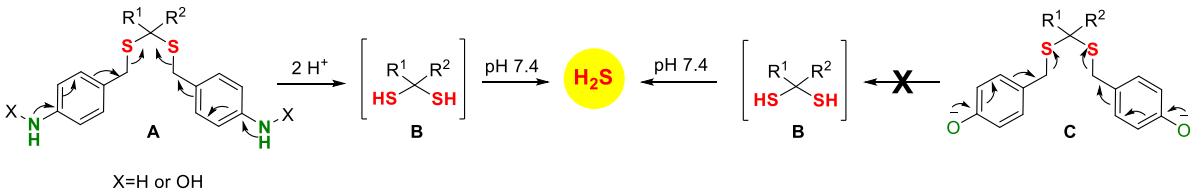

Scheme 10. Proposed mechanism of H_2S release from intermediate **A** and **C**.

Thus, based on these results, we propose to follow approach 2 to design ROS activated gem-dithiol based donor with increased payload of H_2S. It is proposed

compound **24** upon reaction with H_2O_2 forms an intermediate **D** which further decomposes to release 2 moles of H_2S (Scheme 11).

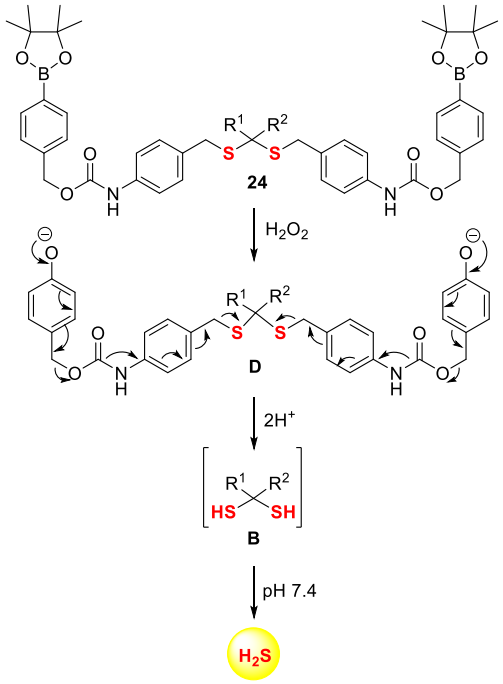

Scheme 11. Proposed mechanism of H_2S release from ROS activated gem dithiol based donor.

The release of H_2S from compound **24** in the presence of H_2O_2 was established using NBD-Fluorescein dye. Compound was incubated in pH 7.4 buffer containing H_2O_2 (10 eq) and NBD-Fluorescein at 37 ^oC. The release of fluorescein was monitored by measuring the fluorescence at excitation 490 nm and emission at 514 nm. Compound **24** showed a signal corresponding to the release of fluorescein indicating towards the release of H_2S after 21 h of incubation in buffer (Figure 17). Howevre, a slight increase in the fluorescence was also observed when dye was incubated in the presence of H_2O_2. Also, compound **15**, which served as a negative control also showed a fluorescence signal. Thus, the release of H_2S from compound **24** could not be confirmed in this experiment. The poor solubility of the compound was a major concern due to which H_2S generation from **24** could not be established through any other method. Thus, making a water soluble derivative would be useful to establish the release of H_2S from this scaffold.

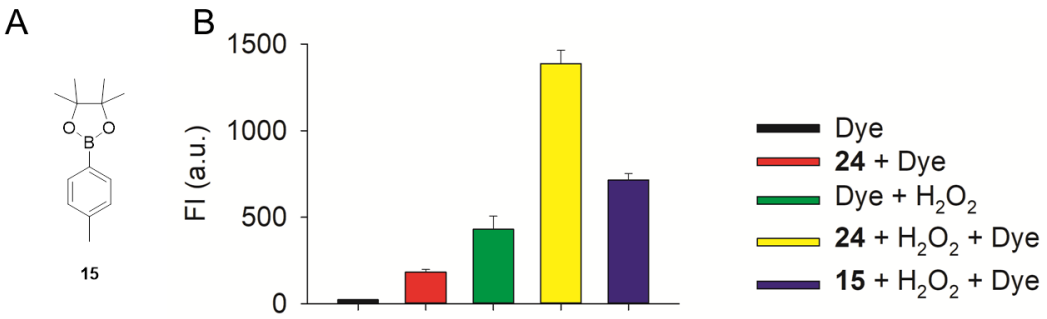

Figure 17. Detection of H_2S release from compound **24** in the presence of H_2O_2 using NBD-Fluorescein dye.

CHAPTER 4.1: NQO1 responsive COS/H_2S donors

In the chapter 4.1 we propose to design colon targeted H_2S and H_2S-NSAID hybrid donors.[21-23] Mesalamine as mentioned previously, is a clinically used non-steroidal anti-inflammatory drug (NSAID) for the treatment of ulcerative colitis. [24-26] However, the drug is effective only against mild to moderate forms of colitis and becomes ineffective against the severe forms of the disease.[27] Wallace and co-workers have reported that ATB-429, which is a H_2S-mesalamine hybrid donor, enhances the anti-inflammatory effects of the parent drug when tested against a mice model of colitis (Figure 18). Also, H_2S released shows protective effects against the tissue damage caused by the excessive usage of NSAIDs. However, the compound produces H_2S spontaneously upon hydrolysis in buffer and therefore provides limited scope of targeted delivery.[23] Also, lack of appropriate controls complicate the conclusions drawn from the experiments.

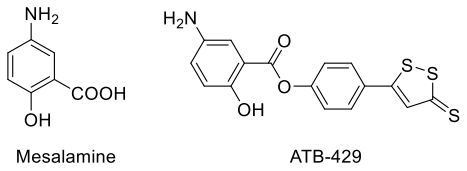

Figure 18. Structures of mesalamine and ATB-429.

NAD(P)H quinone oxidoreductase 1 (NQO1) a two electron reducing cytosolic enzyme which is known to reduce quinones to hydroquinones.[28,29] Cell specific distribution of NQO1 as detected by immunohistochemistry shows that tissues like respiratory epithelium, thyroid follicle, colonic epithelium has higher expression of NQO1 enzyme.[30] Also, the expression of NQO1 goes up under oxidative and

electrophilic stress.[31,32] Thus, this strategy was utilised for targeted delivery of H_2S and H_2S-NSAID hybrid donors to colon.

It is proposed that NQO1 in the presence of NADH reduces quinone to hydroquinones which is followed by the release of lactone to give intermediate **I**. The intermediate formed further dissociates to release COS which is hydrolysed to H_2S by CA (Scheme 12).

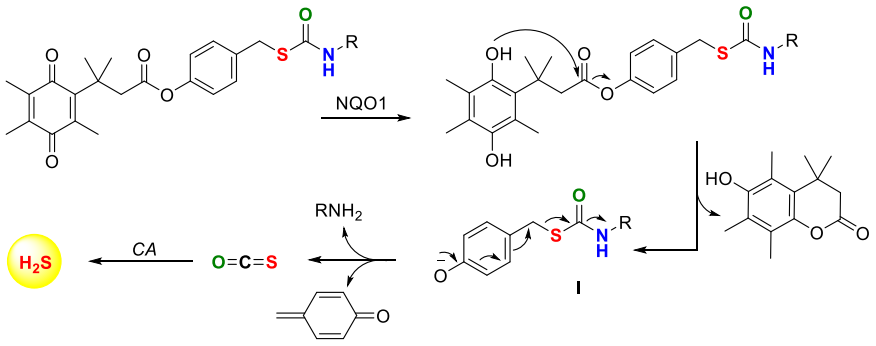

Scheme 12. NQO1 responsive COS/H_2S donors.

Three molecules were synthesized in the series of NQO1 activated COS/H_2S donors. Compound **31a** had mesalamine derivative as the leaving group. Compound **31b** with *p*-anisidine as leaving group served as a fast H_2S donor and compound **31c** with propylamine as leaving group served as slow releasing H_2S donor (Figure 19).

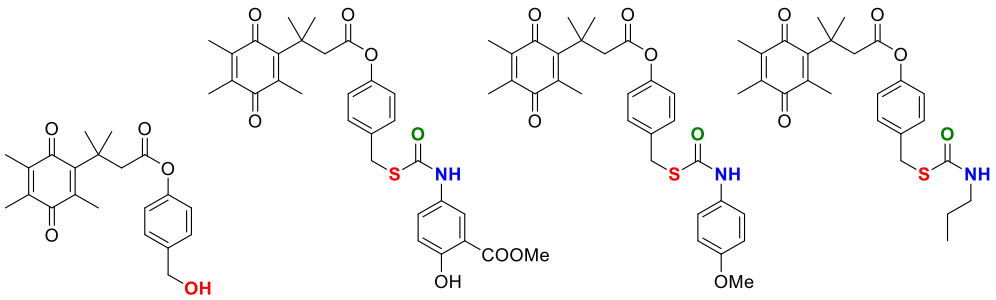

Figure 19. Structures of NQO1 activated compounds used in the study.

The release of H_2S from the scaffolds was demonstrated using methylene blue assay. Compounds were incubated in buffer containing NQO1, NADH and CA at 37 ^oC for 4 h, following which the reaction mixture was treated with methylene blue reagents. Signal corresponding to the generation of H_2S was observed from all the donors. No signal was observed with compound **29** which served as a negative control. Also, compound **31a** alone did not produce signal for H_2S generation, suggesting that the compounds were stable towards hydrolysis. Interestingly, the signal for H_2S generation was diminished in the presence of compound **32**, dicoumarol, which acts

as an inhibitor of NQO1 enzyme (Figure 20). Thus, the results obtained suggested that the compounds synthesized in the series were stable and selective towards activation by NQO1 enzyme.

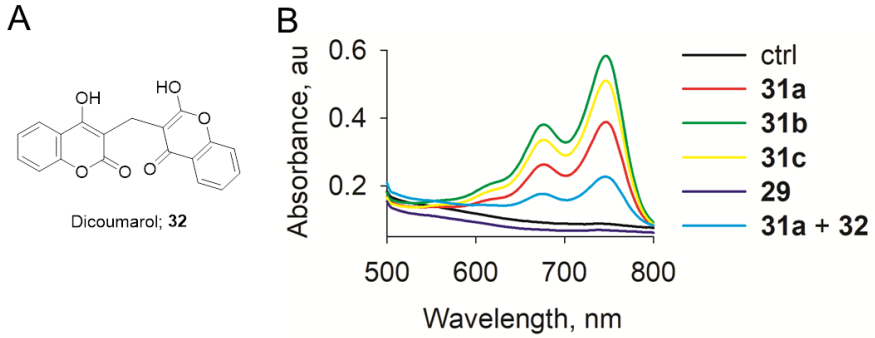

Figure 20. Detection of H_2S from NQO1 activated donors using methylene blue assay.

H_2S acts as a signalling molecule by persulfidating the cysteine residues of a protein. H_2S persulfidates the oxidized cysteine residues (Cys-SOH, Cys-SNO, Cys-SSR) of a protein to form persulfides which are highly reactive in nature. The intracellular persulfidation can be monitored using improved tag switch technique reported previously. Briefly, protein persulfides are blocked by MBST (thiol blocking reagent) to form mixed disulfide which is further reacted with CN-BOT nucleophile to form a thioether bond which is tagged with a fluorescent reporter and can be imaged.

Human colorectal adenocarcinoma, DLD-1 cells were treated with donors (10 µM) for 1 h followed by treatment with MSBT and CN-BOT. Compounds **31a** and **31b** showed enhancement in the fluorescent signal corresponding to the formation of persulfides in cells. However, compound **31c** which was slow releasing H_2S donor showed a diminished signal of persulfide formation (Figure 21). This suggested that the compounds were capable of inducing persulfidation within cells which was dependent on the rate of release of H_2S from the donors. The data obtained was quantified to show the extent of persulfidation induced by the donors (Figure 22). All the donors showed significant enhancement in the fluorescent signal corresponding to the formation of persulfides. Na_2S showed a fluorescent signal comparable to **31c**.

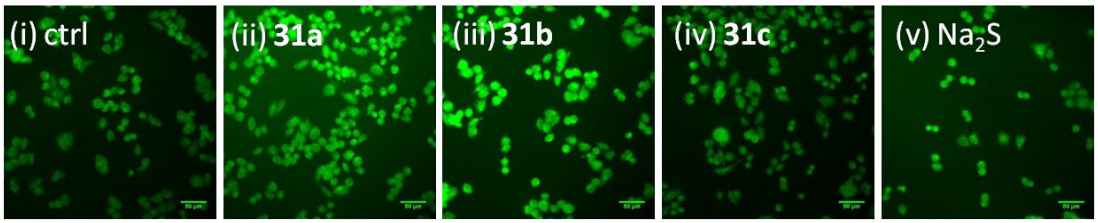

Figure 21. Detection of intracellular persulfidation induced by the donors using improved biotin tag switch technique.

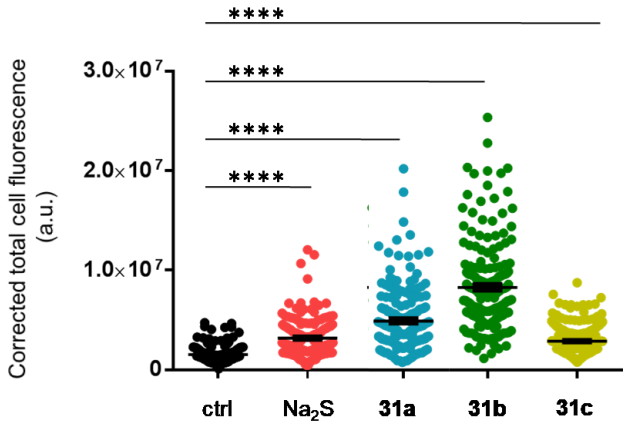

Figure 22. Corrected total cell fluorescence in DLD-1 cells. Persulfidation induced by H_2S donors (**31a**, **31b**, **31c** and Na_2S) within DLD-1 cells imaged using IX83 microscope from Olympus.

Next, the cytoprotective effects of the donors was tested against xenobiotic induced oxidative stress. JCHD, a derivative of juglone, is a superoxide generator.

DLD-1 cells were co-treated with JCHD (15 µM) and H_2S donors (50 µM) for a period of 24 h following which the cell viability was monitored using MTT assay. Compounds **31a** and **31b** showed a significant increase in the cell viability compared to JCHD control. Compound **29**, negative control and mesalamine alone were found to ineffective under these conditions. No significant increase in the cell viability was observed with compound **31c** which was a slow releasing H_2S donor (Figure 23a). This could be correlated to the lower extent of persulfidation induced by compound **31c**. No significant toxicity was observed when DLD-1 cells were treated with compounds for 24 h (Figure 23b).

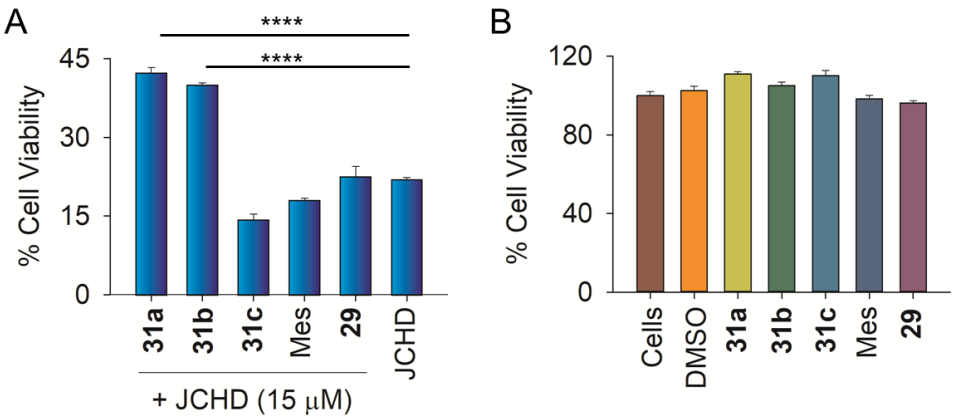

Figure 23. Cytoprotective effects of H_2S donor motifs against JCHD induced toxicity.

Finally, the cytoprotective effects of the compounds were tested in wild-type mouse embryonic fibroblast (WT-MEF) cells with lower expression of NQO1 enzyme. A similar experiment was conducted where cells were co-treated with JCHD (15 µM) and H_2S donors (50 µM) for 24 h. The cell viability was monitored after 24 h using MTT assay. No significant increase in the cell viability was observed from the donors suggesting that the compounds reported herein were selective towards activation by NQO1 enzyme (Figure 24).

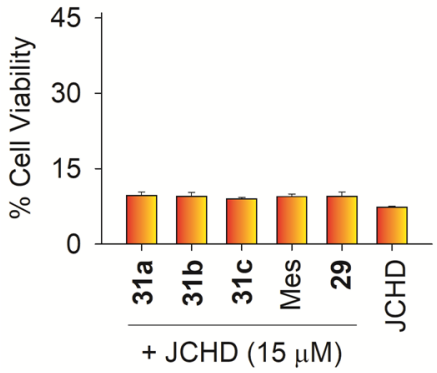

Figure 24. Cytoprotective effects of H_2S donors against JCHD induced toxicity in WT-MEF cells.

CHAPTER 4.2: NQO1 activated persulfide donors

In chapter 4.2, we propose to design NQO1 activated persulfide donors. Persulfides (RSSH) are biologically relevant reactive sulfur species which are generated upon reaction of cysteine residues of a protein by H_2S. The perthiols are more acidic than the corresponding thiol due to their lower bond dissociation energy. Thus, the pKa values of perthiols are approximately 2 units lower than the corresponding thiols.[3]

Therefore, we propose to evaluate the ability of the scaffold to release persulfides using NQO1 as a trigger (Scheme 13).

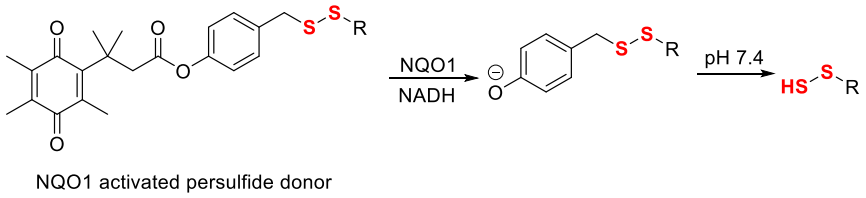

Scheme 13. Proposed mechanism of NQO1 activated persulfide release.

Two compounds were synthesized in this series. Compound **35a** was *N*-acetylcysteine (NAC) based persulfide donor and compound **35b** was benzyl persulfide donor (Figure 25).

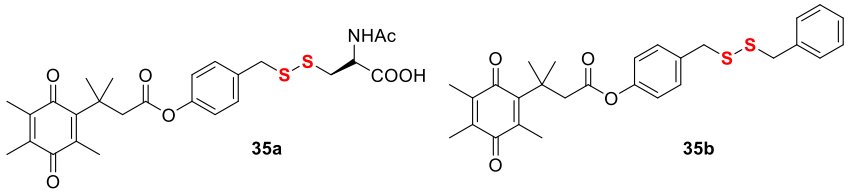

Figure 25. NQO1 activated persulfide donors.

The compounds were tested to produce persulfides in the presence of NQO1 in buffer by HPLC using a previously reported protocol. However, no persulfide formation was observed from the donors. Compound **35a** was incubated with NQO1 in buffer at 37 ^{o}C and injected in HPLC. Peak corresponding to the formation of lactone and intermediate were observed. The intermediate formed was stable even after 1 h of incubation at 37 ^{o}C. Hence, we tested the decomposition of intermediate in the cell lysate using HPLC. DLD-1 cells were incubated with compound **35a** for 1 h. Next, the cells were lysed using methanol and centrifuged. The supernatant was injected into HPLC after filtration. The intermediate was found to decompose in the cell lysate after 1 h (Figure 26). This indicated that the intermediate formed was unstable in cellular conditions and produced persulfides.

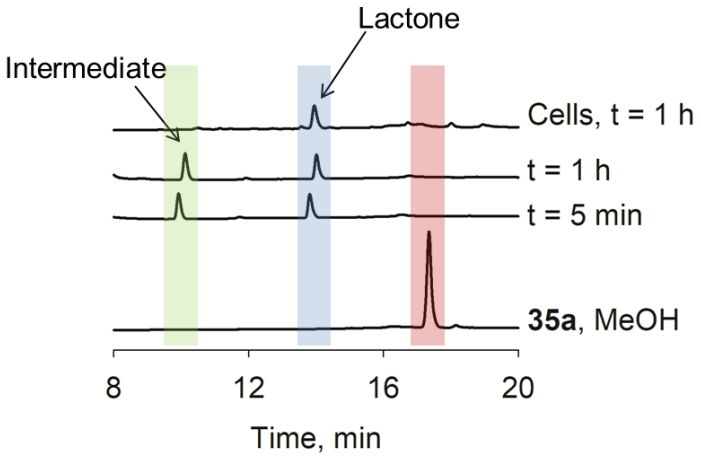

Figure 26. HPLC study to follow the decomposition of **35a** in cell lysate.

Next, the cytoprotective effects of compound **35a** was tested against JCHD induced toxicity. DLD-1 cells were co-treated with JCHD (15 µM) and varying concentrations of compounds for a period of 24 h following which the cell viability was monitored using MTT assay. A dose dependent increase in the cell viability was observed with **35a** compared to the JCHD control (Figure 27a). No cytoprotective effects were observed with **29** (Figure 27b) and NAC (Figure 27c) under these conditions. This indicated that the compound **35a** was capable of producing persulfides within cells and therefore showed cytoprotective effects.

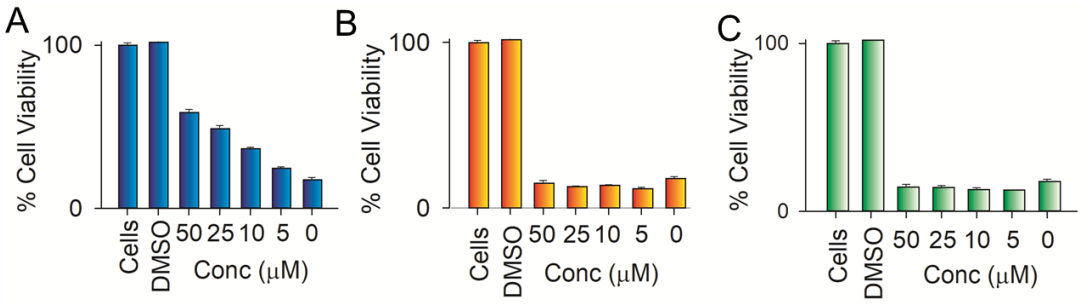

Figure 27. a) Cytoprotective effects of compound **35a** against JCHD (15 µM) induced stress in human colon carcinoma, DLD-1 cells. Results are expressed as mean ± SEM (n = 3). b) Cytoprotective effects of compound **29**, which acts as a negative control, against JCHD induced stress. d) Cytoprotective effects of compound NAC.

List of References:

(1) Wallace, J. L.; Wang, R. *Nat. Rev. Drug. Discov.* **2015**, *14*, 329.

(2) Wang, R. *Physiological Reviews* **2012**, *92*, 791.

(3) Filipovic, M. R.; Zivanovic, J.; Alvarez, B.; Banerjee, R. *Chem. Rev.* **2018**, *118*, 1253.

(4) Szabo, C. *Nat Rev Drug Discov* **2007**, *6*, 917.

(5) Jiang, B.; Tang, G.; Cao, K.; Wu, L.; Wang, R. *Antioxid. Redox Signal.* **2010**, *12*, 1167.

(6) Yang, G.; Zhao, K.; Ju, Y.; Mani, S.; Cao, Q.; Puukila, S.; Khaper, N.; Wu, L.; Wang, R. *Antioxid. Redox Signal.* **2013**, *18*, 1906.

(7) Hatano, T.; Kubo, S.-i.; Sato, S.; Hattori, N. *J. Neurochem.* **2009**, *111*, 1075.

(8) Vandiver, M. S.; Paul, B. D.; Xu, R.; Karuppagounder, S.; Rao, F.; Snowman, A. M.; Ko, H. S.; Lee, Y. I.; Dawson, V. L.; Dawson, T. M.; Sen, N.; Snyder, S. H. *Nat. Commun.* **2013**, *4*, 1626.

(9) Kida, K.; Yamada, M.; Tokuda, K.; Marutani, E.; Kakinohana, M.; Kaneki, M.; Ichinose, F. *Antioxid. redox signal.* **2011**, *15*, 343.

(10) Hu, L.-F.; Lu, M.; Tiong, C. X.; Dawe, G. S.; Hu, G.; Bian, J.-S. *Aging Cell* **2010**, *9*, 135.

(11) Lu, M.; Zhao, F.-F.; Tang, J.-J.; Su, C.-J.; Fan, Y.; Ding, J.-H.; Bian, J.-S.; Hu, G. *Antioxid. redox signal.* **2012**, *17*, 849.

(12) Li, L.; Moore, P. K. *Expert rev. clin. pharmacol.* **2013**, *6*, 593.

(13) Whiteman, M.; Li, L.; Rose, P.; Tan, C.-H.; Parkinson, D. B.; Moore, P. K. *Antioxid. Redox Signal.* **2010**, *12*, 1147.

(14) Lee, Z. W.; Teo, X. Y.; Tay, E. Y. W.; Tan, C. H.; Hagen, T.; Moore, P. K.; Deng, L. W. *Br. J. Pharmacol.* **2014**, *171*, 4322.

(15) Lee, Z. W.; Zhou, J.; Chen, C.-S.; Zhao, Y.; Tan, C.-H.; Li, L.; Moore, P. K.; Deng, L.-W. *PloS one.* **2011**, *6*, e21077.

(16) Shukla, P.; Khodade, V. S.; SharathChandra, M.; Chauhan, P.; Mishra, S.; Siddaramappa, S.; Pradeep, B. E.; Singh, A.; Chakrapani, H. *Chem. Sci.* **2017**, *8*, 4967.

(17) Miller, E. W.; Albers, A. E.; Pralle, A.; Isacoff, E. Y.; Chang, C. J. *J. Am. Chem. Soc.* **2005**, *127*, 16652.

(18) Protoschill-Krebs, G.; Wilhelm, C.; Kesselmeier, J. *Atmos. Environ.* **1996**, *30*, 3151.

(19) Tanc, M.; Carta, F.; Scozzafava, A.; Supuran, C. T. *ACS Med. Chem. Lett.* **2015**, *6*, 292.

(20) Li, L.; Whiteman, M.; Guan Yan, Y.; Neo Kay, L.; Cheng, Y.; Lee Shiau, W.; Zhao, Y.; Baskar, R.; Tan, C.-H.; Moore Philip, K. *Circulation* **2008**, *117*, 2351.

(21) Wallace, J. L.; Ferraz, J. G. P.; Muscara, M. N. *Antioxid. Redox Signal.* **2012**, *17*, 58.

(22) Zhao, Y.; Biggs, T. D.; Xian, M. *Chem. Commun.* **2014**, *50*, 11788.

(23) Fiorucci, S.; Orlandi, S.; Mencarelli, A.; Caliendo, G.; Santagada, V.; Distrutti, E.; Santucci, L.; Cirino, G.; Wallace, J. L. *Br. J. Pharmacol.* **2007**, *150*, 996.

(24) Hanauer, S. B. *Colorectal Dis.* **2006**, *8*, 20.

(25) Karagozian, R.; Burakoff, R. *Ther. Clin. Risk Manag.* **2007**, *3*, 893.

(26) Ham, M.; Moss, A. C. *Expert rev. clin. pharmacol.* **2012**, *5*, 113.

(27) Korzenik, J. R.; Podolsky, D. K. *Nat. Rev. Drug Discov.* **2006**, *5*, 197.

(28) Ross, D.; Siegel, D. *Front. Physiol.* **2017**, *8*.

(29) Ross, D.; Siegel, D.; Beall, H.; Prakash, A. S.; Mulcahy, R. T.; Gibson, N. W. *Cancer and Metastasis Rev.* **1993**, *12*, 83.

(30) Siegel, D.; Ross, D. *Free Radic. Biol. Med.* **2000**, *29*, 246.

(31) Raina, A. K.; Templeton, D. J.; deak, J. C.; Perry, G.; Smith, M. A. *Redox Rep.* **1999**, *4*, 23.

(32) Xie, T.; Jaiswal, A. K. *Biochem. Pharmacol.* **1996**, *51*, 771.

List of Figures

Results are expressed as mean ± SEM (n = 3). b) Cell viability with compound **35b** against JCHD induced stress. c) Cytoprotective effects of compound **29**, which acts as a negative control, against JCHD induced stress. d) Cytoprotective effects of compound NAC

List of Schemes

List of Tables

List of Publications

1) **Chauhan, P.**; Bora, P.; Ravikumar, G.; Jos, S.; and Chakrapani, H. Esterase Activated Carbonyl Sulfide/Hydrogen Sulfide (H_2S) Donors. *Org. Lett.*, **2017**, *19*, 62-65.

2) Shukla, P.; Khodade, V. S.; Sharath Chandra, M.; **Chauhan, P.**; Mishra, S.; Siddaramappa, S.; Pradeep, B. E.; Singh, A.; Chakrapani, H. "On Demand" Redox Buffering by H_2S contributes to antibiotic resistance revealed by a bacteria specific H_2S donor. *Chem. Sci.* **2017**, *8*, 4967.

3) Sharma, A. K.; Nair, M.; **Chauhan, P.**; Gupta, K.; Saini, D. K.; Chakrapani, H. Visible Light triggered Uncaging of Carbonyl Sulfide for H_2S release. *Org. Lett.* **2017**, *19*, 4822.

4) **Chauhan, P.**; Jos, S.; and Chakrapani, H. Reactive Oxygen Species-Triggered Tunable Hydrogen Sulfide Release. *Org. Lett.*, **2018**, *20*, 3766-3770.

5) Bora, P.; **Chauhan, P.**; Pardeshi, K.; and Chakrapani, H. Small molecule generators of biologically reactive sulfur species. *RSC Adv.*, **2018**, *8*, 27359-27374.

6) Bora, P.; **Chauhan, P.**; Manna, S.; and Chakrapani, H. A Vinyl Boronate Ester Based Persulfide Donor Controllable by Hydrogen Peroxide, a Reactive Oxygen Sulfur Species. *Org. Lett.*, **2018**, *20*, 7916–7920.

7) **Chauhan, P**., Gupta, K., Govindan, R., Saini, D. and Chakrapani, H., Carbonyl Sulfide (COS) Donor induced protein persulfidation protects against oxidative stress. *Chem. Asian J.,* **2019** (Accepted Manuscript).

Manuscripts Under Preparation

1. **Chauhan, P.**; Gupta, K.; Saini, D. K.; Chakrapani, H. NQO1 responsive persulfide donors. (Manuscript under preparation)